Sexual development of *Botrytis* species

Razak Bin Terhem

Sexual development of *Botrytis* species

Razak Bin Terhem

Thesis

submitted in fulfilment of the requirements for the degree of doctor

at Wageningen University

by the authority of the Rector Magnificus

Prof. Dr A.P.J. Mol,

in the presence of the

Thesis Committee appointed by the Academic Board

to be defended in public

on Monday 14 September 2015

at 4 p.m. in the Aula.

Contents

Chapter 1

General introduction and outline of the thesis

Introduction

The genus *Botrytis*

The genus name refers to the structure of the macroconidia, which rise and form clusters with the shape of grape bunches: 'botryose'. *Botrytis* is the asexual stage of *Botryotinia*. The *Botrytis* community has in its recent meeting (Italy, 23-28 June 2013) unanimously recommended the exclusive use of the asexual name *Botrytis* over *Botryotinia,* the name of the sexual stage, since *Botrytis* is historically the oldest name and it is commonly used by plant pathologists, breeders and growers. In line with this recommendation, a list of generic names of fungi for protection under the International Code of Nomenclature has included this genus under the name *Botrytis* and not *Botryotinia* (Kirk et al. 2013). I therefore follow this recommendation in this thesis and will exclusively use the name *Botrytis*.

Species of the genus *Botrytis* infect over 250 host species, including major greenhouse and field crops such as tomato, grape, strawberry, onion and ornamentals such as rose, lily, and tulip (Staats et al. 2005). Most *Botrytis* species are necrotrophic pathogens that are able to kill the host tissue during infection. Interestingly, an endophytic species (*B. deweyae*) has recently been discovered which under appropriate conditions can cause 'spring sickness' in ornamental *Hemerocallis* (daylily) hybrids (Grant-Downton et al. 2014). *B. cinerea* is the best-studied species within the genus (Williamson et al. 2007) and was elected as the second most important plant pathogenic fungal species (Dean et al. 2012).

In the asexual state, *Botrytis* produces different morphological structures including mycelia, macroconidia, microconidia, and sclerotia. Macroconidia have an ellipsoidal to obovoid shape and rise from conidiophore branches into botryose clusters. They are pale brown in color and range in size from 9–23 × 8–15 µm. Microconidia are more spherical and much smaller than macroconidia (about 1µm), and function as male spermatia (Groves and Loveland 1953; Faretra et al. 1988; Beever and Parkes 1993; Fukumori et al. 2004). Sclerotia are irregular hemispherical, convex structures which normally have a concave surface. They are black, with sizes ranging between 1 and 10 mm (Whetzel 1945), and function not only as survival structures during the winter but also as maternal parent in the production of apothecia.

During the sexual stage, fruiting bodies are produced which are called apothecia: a cup-shaped ascoma at the top of a stipe that acts as a platform to discharge ascospores from asci. *Botrytis* apothecia vary in size, depending on the species, between 1 and 25 mm in height and 1-6 mm in diameter (Hennebert and Groves 1963; Bergquist and Lorbeer 1972). Apothecia are brown and become dark during maturation (Hennebert and Groves 1963; Bergquist and Lorbeer 1972; Faretra and Antonacci 1987). Multiple apothecia can develop on a single sclerotium. Mature apothecia normally can be observed two months after fertilization (Faretra et al. 1988; Hennebert and Groves 1963; van Der Vlugt-Bergmans et al. 1993).

Species identification and numbers

Approximately half of the *Botrytis* species are named after the host that they infect from which they were first isolated and characterized. Table 1 lists the members of the genus *Botrytis* and shows the 16 species that have been reported to be capable of developing apothecia. One hybrid species, *B. allii* which originated from hybridization between *B. byssoidea* and *B. aclada* (Nielsen and Yohalem 2001; Martinez et al. 2003) could not be placed in the phylogenetic tree and was therefore omitted from Table 1. The genus *Botrytis* predominantly comprises narrow host range pathogens that infect a single, or a few (often related) host species. There are at least two exceptions to this rule; *B. cinerea* can infect more than 200 host species (Jarvis 1977) and *B. pseudocinerea* has been isolated from several unrelated diseased host species (Walker et al. 2011; Leroch et al. 2013).

Taxonomic classification and nomenclature of *Botrytis* species have rarely been reviewed. Morphological descriptions of most species have been published in the 19th and first half of the 20th century in separate papers, many of which are not easily accessible. The most recent taxonomic compilation of the genus is reported in a monograph by Jarvis (1977), which also lists ~25 excluded or doubtful species, and briefly describes the historical debates between mycologists, exemplifying the confusion in classification of *Botrytis* species. Morphological features were often inadequate to distinguish species and variability often observed among isolates of the same species further complicated the situation (Jarvis 1977). Recent studies have identified *B. cinerea* and *B. pseudocinerea* as species that are very similar in morphology, yet recognized as distinct taxa that diverged several million years ago (Walker

et al. 2011). Even more puzzling, the morphology and narrow host range of *B. fabae* separate this species clearly from *B. cinerea* and *B. pseudocinerea*, but phylogenetic studies revealed it to be a sister species of *B. cinerea* (see below). These examples illustrate the limitations of morphological characters for *Botrytis* species identification.

Table 1: List of members in the genus *Botrytis*

Species	Isolate	Host	Producing apothecia
Botrytis aclada	MUCL8415	*Allium spp.*	No[a]
B. byssoidea	MUCL94	*Allium spp.*	Yes
B. calthae	MUCL1089	*Caltha palustris*	Yes
B. cinerea	MUCL87	>200 species	Yes
B. caroliniana	CB15	*Rubus fruticosus*	No
B. convoluta	MUCL11595	*Iris spp.*	No
B. croci	MUCL436	*Crocus spp.*	No
B. deweyae	CBS 134649	*Hemerocallis spp.*	No
B. elliptica	BE9714	*Lilium spp.*	Yes
B. fabae	MUCL98	*Vicia spp.*	Yes
B. ficariarum	MUCL376	*Ficaria verna*	Yes
B. fabiopsis	BC-2	*Vicia faba*	No
B. galanthina	MUCL435	*Galanthus spp.*	No
B. gladiolorum	MUCL3865	*Gladiolus spp.*	Yes
B. globosa	MUCL444	*Allium ursinum*	Yes
B. hyacinthi	MUCL442	*Hyacinthus spp.*	No
B. narcissicola	MUCL2120	*Narcissus spp.*	Yes
B. paeoniae	MUCL16084	*Paeonia spp.*	No
B. pelargonii	CBS 497.50	*Pelargonium spp.*	Yes
B. polyblastis	CBS287.38	*Narcissus spp.*	Yes
B. porri	MUCL3234	*Allium spp.*	Yes
B. pseudocinerea	VD110	*Vitis vinifera*	Yes
B.ranunculi	CBS178.63	*Ranunculus spp.*	Yes
B. sinoallii	HMAS 250008	*Allium spp.*	No
B. sphaerosperma	MUCL21481	*Allium triquetrum*	Yes
B. squamosa	MUCL1107	*Allium cepa*	Yes
B. tulipae	BT9830	*Tulipa spp.*	No

[a] No: No record of apothecia in nature and no studies were done in-vitro

Molecular phylogeny

Hoist-Jensen et al. (1998) were the first to use nuclear ribosomal *ITS* sequences to infer a phylogeny of the family *Sclerotiniaceae*, including several members of the genus *Botrytis*. The relationships among *Botrytis* species could not be resolved because of the limited number of informative characters. However the study permitted the conclusion that *Botrytis* constitutes a monophyletic lineage (Holst-Jensen et al. 1998). The phylogeny of the *Sclerotiniaceae* was further refined by Andrew et al. (2012) using three protein-coding

genes: calmodulin, glyceraldehyde 3-phosphate dehydrogenase (*G3PDH*) and heat shock protein 60 (*HSP60*).

Staats et al. (2005) performed a comprehensive phylogenetic analysis of the genus *Botrytis*, at that time comprising 22 recognized species and one hybrid. Using three protein-coding genes (*G3PDH*, *HSP60* and the DNA-dependent RNA polymerase subunit II gene (*RPB2*), they corroborated the morphological and host plant-based classification of *Botrytis* species and divided the genus into two (rather widely separated) clades. Clade I contained species that only infect eudicot plants, while clade II contained species that can infect either eudicot or monocot plants. The use of the same three genes facilitated the discovery of several new species: *Botrytis sinoallii*, a new species infecting *Allium* species, and its distinction from other *Botrytis* species infecting the same hosts (Zhang et al. 2010b); *B. fabiopsis*, a new species infecting broad bean, very distant from *B. fabae* (Zhang et al. 2010a); and *B. caroliniana*, a new species infecting blackberry (Li et al. 2012).

Two genes, encoding phytotoxic proteins *NEP1* and *NEP2*, were shown to provide higher resolution in distinguishing species in the genus *Botrytis* because they seem to be subject to higher evolutionary rates than the housekeeping genes *G3PDH*, *HSP60* and *RPB2* (Staats et al. 2007b). The *NEP1* and *NEP2* genes were shown to have evolved under positive selection which suggested a role of these proteins in the infection process (Staats et al. 2007b). One might therefore infer that such genes cannot serve as neutral phylogenetic markers. Functional analysis in *B. cinerea* and *B. elliptica* using targeted knockout mutants failed to reveal a role of *NEP* genes in virulence of these two species (Staats et al. 2007b; Staats et al. 2007a; Cuesta Arenas et al. 2010), which would lend support to considering these genes as neutral markers and adequate tools in phylogeny.

The studies by Staats et al. (2005) revealed incongruence between the phylogenies of *Botrytis* species and their hosts. Species infecting the same host clustered in different (sub) clades, e.g. *B. aclada*, *B. squamosa*, *B. porri*, *B. byssoidea* and *B. sinoallii* all infecting *Allium*. Conversely, closely related species can infect very different hosts, e.g. *B. elliptica* infecting the monocotyledonous host *Lilium* and *B. ficariarum* infecting the dicotyledonous host *Ficaria* (Staats et al. 2005). More recently, similar incongruencies have been reported for

newly described species, e.g. *B. fabiopsis* infecting *Vicia faba* is very distant from *B. fabae* infecting the same host (Zhang et al. 2010a), and *B. caroliniana* infecting blackberries and strawberries is very distant from *B. cinerea* (Li et al. 2012).

Recently, Khan et al. (2013) combined data from *ITS* and *IGS* regions with the *G3PDH* gene, with the aim of improving molecular identification of *Botrytis* species that cause neck rot disease on onion. *ITS* and *IGS* regions were insufficiently informative to distinguish *B. allii* and *B. byssoidea*. The sequences of *ITS* and *IGS* for *B. allii* and *B. byssoidea* confirmed that they have a close relationship, but *G3PDH* sequences of several *B. allii* isolates were clearly distinct, some clustering with *B. aclada* and others clustering with *B. byssoidea* (Khan et al. 2013), as may be expected for a hybrid species. Sequence analysis of the *G3PDH* and β-tubulin genes amplified from herbarium specimens of *Botrytis* collected from grey mould-infected apple (deposited in 1932) enabled O'Gorman et al. (2008) to corroborate the existence of *B. mali*, a species that had been reported (Ruehle 1931), but by lack of description was considered doubtful.

Figure 1 shows a maximum-likelihood tree of *Botrytis* species, based on concatenated sequences of parts of the *G3PDH*, *HSP60* and *RPB2* genes (Staats et al. 2005; Li et al. 2012; Zhang et al., 2010a,b; Grant-Downton et al. 2014; Walker et al. 2011). Five species described after publication of the phylogeny by Staats et al. (2005), i.e. *B. caroliniana, B. deweyae, B. fabiopsis, B. pseudocinerea* and *B. sinoallii*, clearly cluster within the genus and are genuine *Botrytis* species. *Botrytis mali* could not be included in the tree due to lack of sequence information for the *HSP60* and *RPB2* genes. Based on *G3PDH* and ß-tubulin sequences it would cluster with *B. paeoniae* (O'Gorman et al. 2008). As can also be seen in Figure 1, the different *Botrytis* species differ in their capacity to reproduce sexually. In total 11 species in Clade I and 5 species in Clade II are able to produce apothecia. Below I will first discuss the sexual reproduction in Ascomycota in general and then discuss the state of the art of knowledge on the mating system in the genus *Botrytis*.
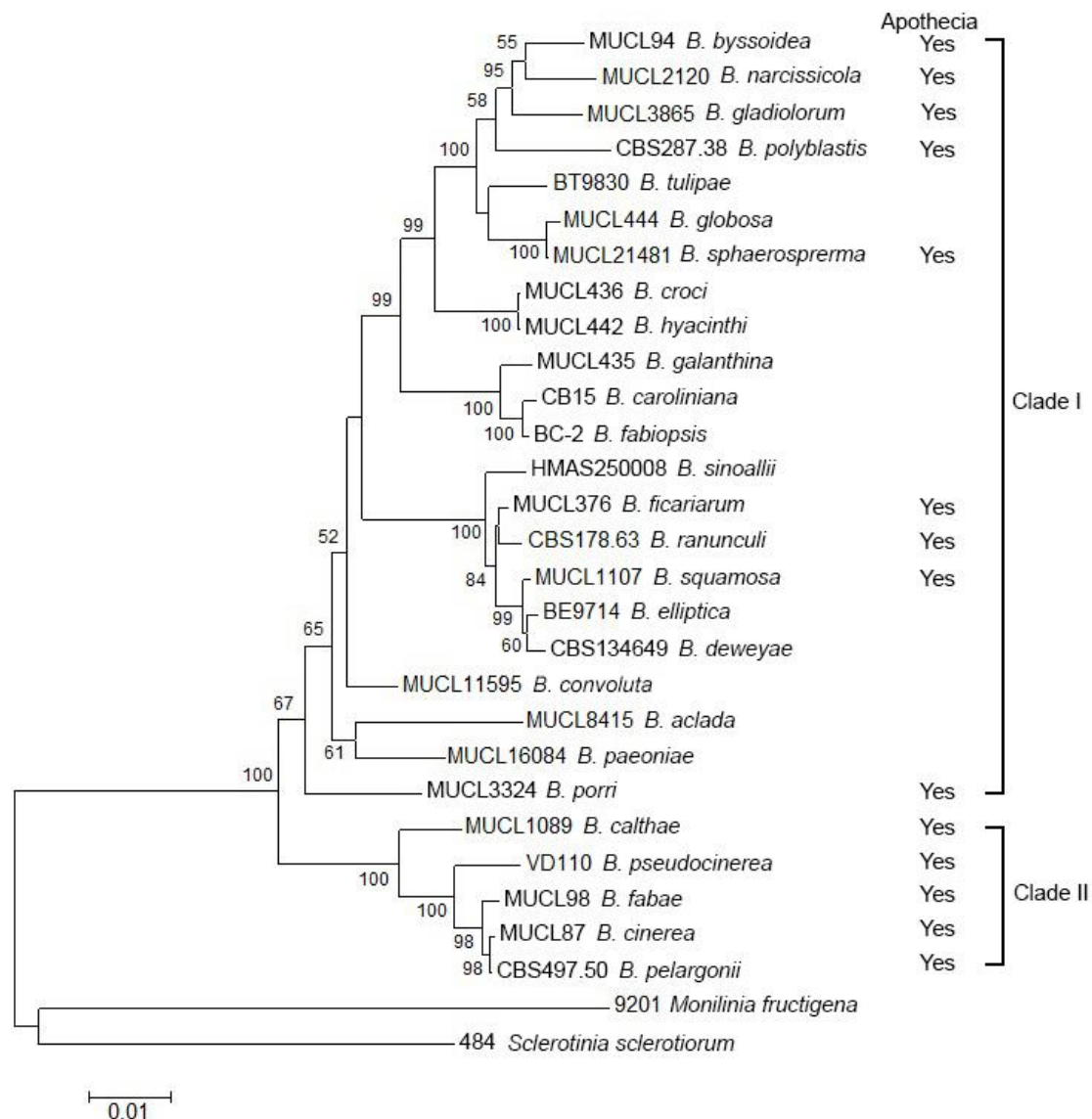
Figure 1: Phylogram generated from Maximum likelihood analysis based on combined sequences of *G3PDH*, *HSP60* and *RPB2* from 27 recognized *Botrytis* species. Bootstrap support values greater than 50 % are indicated above/below the nodes. The tree is rooted with *Monilinia fructigena* and *Sclerotinia sclerotiorum*

Mating systems in Ascomycota

Fungi can display homothallic and heterothallic mating behavior. Homothallic mating refers to the ability of an individual to complete the sexual reproduction cycle in the absence of a mating partner (self-fertile). By contrast, heterothallic mating requires the presence of two genotypes of opposite mating type to undergo sexual reproduction (out-crossing). In the phylum Ascomycota, homothallic and heterothallic mating systems can be found in different species belonging to the same genus, as reported for the genera *Aspergillus*, *Botrytis*, *Neurospora*, and *Sordaria*.

To date only two species in the genus *Botrytis* have been recorded to behave as homothallic i.e. *B. porri* and *B. globosa* (Buchwald 1953; Elliott 1964). Other species in the genus *Botrytis*, including *B. cinerea*, are reported to have a heterothallic mating behavior (Elliott 1964; Faretra et al. 1988). There are, however, a few records of heterothallic fungi that are also capable of homothallic sexual reproduction. For instance, homothallic behavior of certain *B. cinerea* isolates was first reported by Faretra and Antonacci (1987). They reported that single ascospores collected from apothecia of *B. cinerea* could be grown in culture and self-fertilised to successfully form apothecia; however, no data are available for the segregation of mating type alleles in ascospores retrieved from such apothecia. Other examples of homothallic behavior are reported for *Sordaria brevicollis* (Robertson et al., 1998) and *Ceratocystis coerulescens* (Harrington and McNew 1997), which normally have heterothallic mating systems. Two field strains of *C. coerulescens* of the *MAT1-2* mating type could form fruiting bodies in the absence of a strain of opposite mating type (Harrington and McNew 1997).

The mating type locus

The mating system in heterothallic Ascomycota is bipolar, which means that there are two alleles. The MAT alleles in different fungi have historically received different names, for instance *MAT- α* and *MAT- a* (*Saccharomyces cerevisiae*), *MAT- -* and *MAT-+* (*Podospora anserina*)*,* or *MAT1-1* and *MAT1-2* (many fungi, including *Botrytis spp.*). The two mating types can be distinguished by the DNA sequences at the mating type (*MAT*) locus and their gene products play a crucial role in regulating sexual reproduction. One peculiarity of the *MAT* locus is the lack of nucleotide sequence homology between opposite mating alleles, which were therefore historically referred to as idiomorphs (Cozijnsen and Howlett 2003; Turgeon et al. 1993; Metzenberg and Glass 1990). The MAT loci of *S. cerevisiae* were the first fungal MAT loci that were identified and sequenced (Astell et al. 1981); the *MAT-α* idiomorph contains two genes *MAT-α1* (α-domain transcription factor) *and MAT-α2* (homeodomain transcription factor) while the *MAT-a* idiomorph contains a single gene *MAT-a1* (homeodomain transcription factor) (Figure 2)*.* In most Ascomycota (but not in *S. cerevisiae*) the *MAT* locus idiomorphs are flanked by two conserved genes, *APN2* and *SLA2* (Heitman et al. 2007; Cozijnsen and Howlett 2003; Metzenberg and Glass 1990; Turgeon et

al. 1993). The conservation of the flanking regions in many Ascomycota suggests that this overall structure represents the ancestral configuration in Ascomycota (Heitman et al. 2007).

The concerted action of *MAT1-1* and *MAT1-2* loci is considered to be essential for activating the expression of genes that are involved in development of the fruiting body, meiosis and formation of asci with ascospores. By convention, the *MAT1-1* idiomorph encodes a transcription factor, containing a DNA-binding domain named alpha domain, while the *MAT1-2* idiomorph encodes a different transcription factor, containing a DNA binding high-mobility group (HMG) domain (Coppin et al. 1997). In most heterothallic Ascomycota fungi the *MAT1-1* and *MAT1-2* loci contain additional genes (Figure 2). For example, in *Neurospora crassa* and *Magnaporthe grisea*, the *MAT1-1* locus contains three genes: *MAT1-1-1* (alpha domain), *MAT1-1-2* and *MAT1-1-3* while the *MAT1-2* locus of *N. crassa* contains two genes *MAT1-2-1* (HMG domain) and *MAT1-2-2* and the *MAT1-2* locus of *M. grisea* contains two genes *MAT1-2-1* (HMG domain) and *MAT1-1-3*.

In most homothallic *Ascomycota* fungi, the *MAT1-1* and *MAT1-2* genes are located in the same location in a single genome, flanked by the *APN2* gene and the *SLA2* gene, just as in heterothallic species. For example, in the homothallic species *Gibberella zeae* the *MAT* locus has four genes at the same chromosomal location; *MAT1-1-1* (alpha domain), *MAT1-1-2*, *MAT1-1-3*, and *MAT1-2-1* (HMG domain) (Figure 2). Also the *Sclerotinia sclerotiorum MAT* locus contains *MAT1-1* and *MAT1-2* genes in a single genomic location (Amselem et al., 2011). By contrast, the homothallic species *Aspergillus nidulans* contains the *MAT1-1* and *MAT1-2* genes in a single genome, yet in different chromosomal locations, i.e. chromosomes 6 and 3 (Paoletti et al., 2007).

Orthologs of the *MAT1-1-2* gene usually can be found in *Sordariomycetes* (Debuchy et al. 2010) and encode a protein with a DNA polymerase processivity factor (DNA_PPF) domain (Kanematsu et al. 2007; Klix et al. 2010). Orthologs of the *MAT1-1-3* gene encode a protein with a HMG domain (Ferreira et al. 1996; Klix et al. 2010), but their function differs from the MAT1-2-1 protein, presumably because MAT1-1-3 lacks a sequence that is conserved at the C- terminal end of the HMG domain of MAT1-2-1 (Debuchy et al. 2010).

Individual deletion of the *MAT1-1-2* or *MAT1-1-3* gene in *N. crassa* did not affect sexual reproduction, but the deletion of both these genes resulted in a severely reduced number of asci, although the asci that were present contained eight ascospores (Ferreira et al., 1998). Deletion of the *MAT1-1-2* gene in *S. macrospora* and *P. anserina* resulted in sterility and no fruiting bodies were developed (Arnaise et al. 2001; Klix et al. 2010).

The *MAT* loci in fungal genomes appear to evolve faster than other regions, and therefore the sequences and organization of the *MAT* locus vary among species (Pöggeler 1999; Turgeon 1998). In spite of their faster evolution, the functions of genes in the *MAT* locus are well conserved among species (Coppin et al. 1997). For example, the *MAT* genes in heterothallic Ascomycota *N. crassa, Cochliobolus heterostrophus*, *A. nidulans* play the same role in fertilization events (Paoletti et al. 2007; Ferreira et al. 1998). The *MAT* genes can sometimes be functionally interchangeable between homothallic and heterothallic Ascomycota. For example, a knock out mutant in the *MAT1-2-1* gene of the heterothallic species *C. heterostrophus* became self-fertile, when the entire *MAT* locus from the homothallic species *C. luttrellii* was introduced (Yun et al., 1999). Conversely, replacement of the homothallic *MAT* locus of *C. luttrellii* by a heterothallic locus of *C. heterostrophus* (either *MAT1-1-1* or *MAT1-2-1*) switched the sexual behavior of *C. luttrellii* to heterothallic (Lu et al. 2011). Remarkably, however, transgenic *C. luttrellii* transformed with a single *C. heterostrophus MAT* allele (either *MAT1-1-1* or *MAT1-2-1*) were able to produce tiny pseudothecia with reduced number of asci, but containing normally viable ascospores (Lu et al. 2011), suggesting the ability of fruiting body development in the absence of a strain of opposite mating type.

In a study by Pöggeler et al. (1997), the *MAT* genes appeared not to be interchangeable between the closely related species *P. anserina* (heterothallic) and *S. macrospora* (homothallic). Introduction of the entire (homothallic) *MAT* locus of *S. macrospora* into *P. anserina MAT-- (MAT1-1)* or *MAT-+ (MAT1-2)* strains resulted in transformants that were able to produce a fruiting body structure which, however, completely lacked asci and ascospores (Pöggeler et al. 1997).
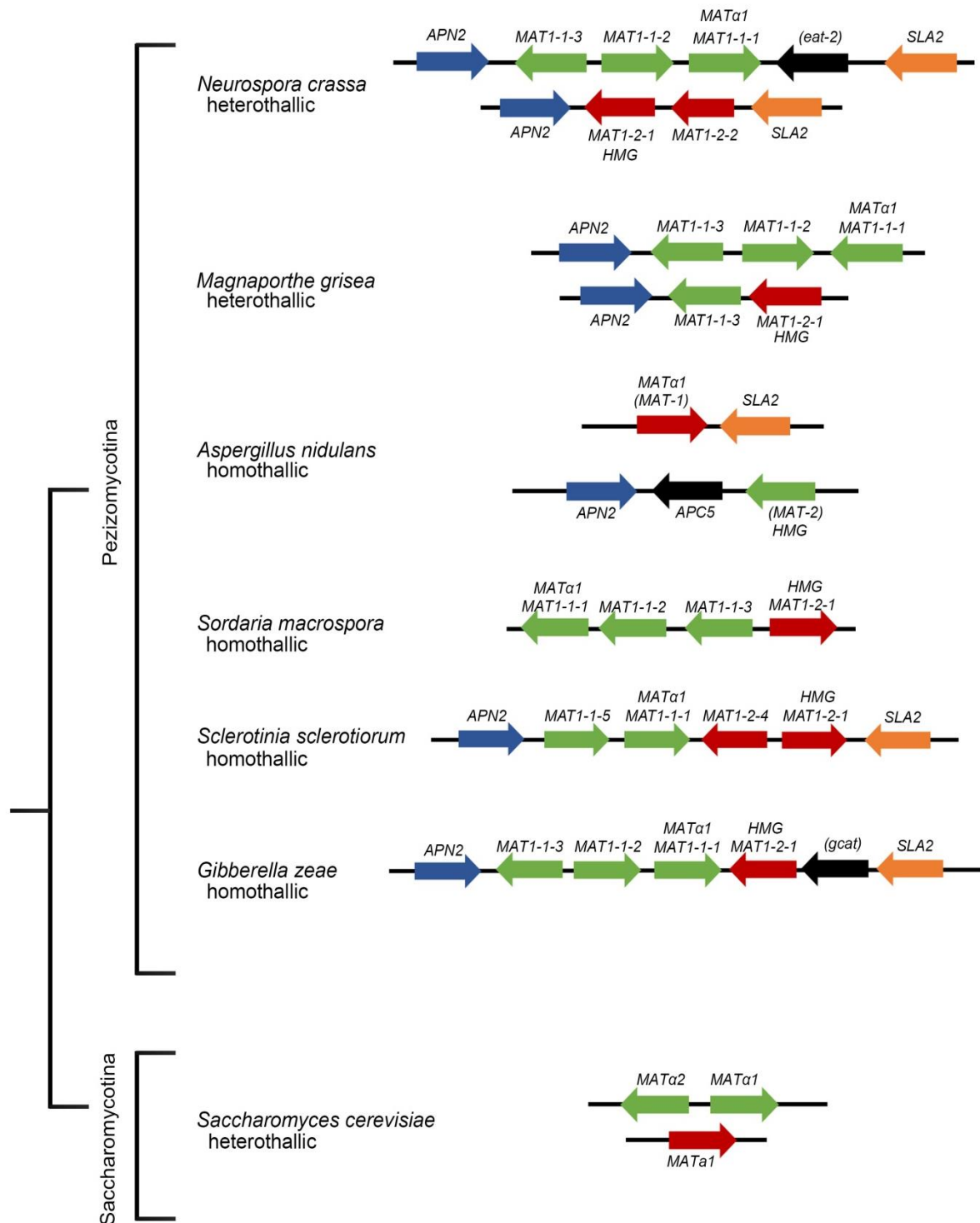
Figure 2: *MAT* loci arrangement in Pezizomycotina and Saccharomycotina adapted from Amselem et al. 2011; Heitman et al., 2007; Klix et al., 2010; Pöggeler and Kück. 2000

Mating system in *Botrytis cinerea*

B. cinerea has been classified as a fungus with a heterothallic mating system. Mating occurs between a strain carrying a *MAT1-1* locus and a strain carrying a *MAT1-2* locus. In *B. cinerea*, the *MAT1-1* locus (Figure 3) contains the *MAT1-1-1* gene, which encodes an alpha domain protein, and a gene named *MAT1-1-5* of unknown function. The *MAT1-2* locus (Figure 3) contains the *MAT-1-2-1* gene, which encodes a HMG-box protein, and the *MAT1-2-4* gene of unknown function. In the closely related homothallic species *Sclerotinia sclerotiorum,* a single *MAT* locus is present that contains four genes that are orthologous to the genes present in the *B. cinerea MAT1-1* and *MAT1-2* loci (Amselem et al. 2011). As in most Ascomycota, both *MAT* loci in *B. cinerea* are flanked by the genes *APN2* (encoding DNA lyase) and *SLA2* (encoding a cytoskeleton protein) that are convergently transcribed with respect to the *MAT* locus (Amselem et al. 2011).

Dual mater behavior in *B. cinerea*

Faretra et al. (1988), Beever and Parkes (1993), van der Vlugt-Bergmans et al. (1993), and Amselem et al. (2011) discovered unique mating behavior in *B. cinerea*, which was referred to as 'dual mater'. Approximately 5% of progeny from a cross between two heterothallic strains is a 'dual mater', which is able to mate with *MAT1-1* and *MAT1-2* reference strains (Amselem et al. 2011). For example a 'dual mater' *MAT1-2* strain is able to mate with another strain with a heterothallic *MAT1-2* background and undergo sexual development. Similar behavior has also been discovered in strains of *MAT1-1* background, which are able to mate with other strains of *MAT1-1* background and undergo sexual development. The mechanisms underlying this unusual behavior in *B. cinerea* were not unraveled. Since the first reports of dual mating in *B. cinerea*, in the 1990's, some other fungi have been reported to behave in similar ways, and in these cases the phenomenon is referred to as "unisexual reproduction" (Roach et al., 2014; Ni et al., 2013; Lin et al., 2005).
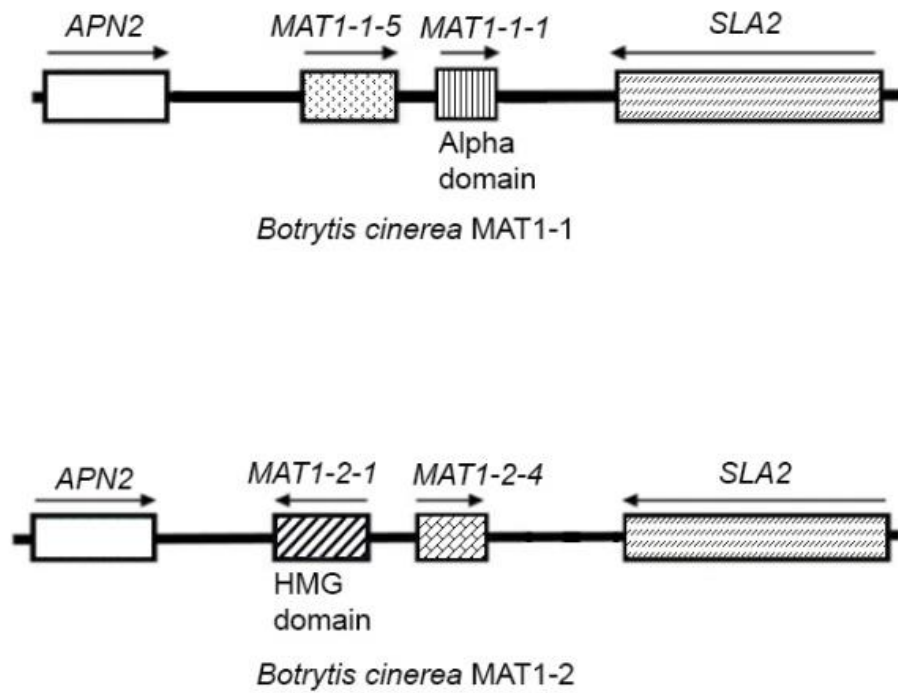
Figure 3: Arrangement of *MAT1-1* and *MAT1-2* loci in *Botrytis cinerea* (adapted from Amselem et al. 2011)

Outline of the thesis

The aims of the research described in this thesis were to study the mechanisms involved in apothecium development of *B. cinerea*, and to describe the morphology of *Botrytis* spp and their fruiting bodies.

Chapter 2 describes a genome-wide transcriptome analysis of different stages of apothecium development and a study on the function of *MAT* genes in apothecium development of *B. cinerea*. RNA-seq analysis was performed on sclerotia, apothecia in different stages of development, and ascospores. Transcriptional changes that occurred during developmental transitions were analysed by comparing the transcriptomes of successive developmental stages. Cluster analysis was performed to identify sets of genes with common transcriptional profiles over the developmental stages. Finally, the function of mating type genes was studied by generating knock out mutants, and analyzing their mating behavior.

Chapter 3 describes the functional analysis of three hydrophobin genes in sclerotium and apothecium development of *B. cinerea*. Knockout mutants with single or multiple deletions of hydrophobin genes were used to study the role of hydrophobin genes in asexual and sexual development of *B. cinerea*.

Chapter 4 describes the structure of the *MAT* locus in *B. elliptica* and the morphology of apothecia of *B. elliptica* generated in the laboratory.

Chapter 5 provides a morphological and phylogenetic description of a novel *Botrytis* species, named *Botrytis deweyae*, which is the only species within the genus that behaves as an endophyte. Under certain conditions, *B. deweyae* can cause 'spring sickness' disease in hybrid *Hemerocallis* cultivars.

Chapter 6 presents a general discussion of the results presented in Chapter 2-5 and puts them in a broader perspective. In addition experiments aimed at understanding the genetic basis of dual mater behavior are discussed.

References

Amselem J, Cuomo CA, van Kan JAL, Viaud M, Benito EP, Couloux A, Coutinho PM, de Vries RP, Dyer PS, Fillinger S, Fournier E, Gout L, Hahn M, Kohn L, Lapalu N, Plummer KM, Pradier J-M, Quévillon E, Sharon A, Simon A, ten Have A, Tudzynski B, Tudzynski P, Wincker P, Andrew M, Anthouard V, Beever RE, Beffa R, Benoit I, Bouzid O, Brault B, Chen Z, Choquer M, Collémare J, Cotton P, Danchin EG, Da Silva C, Gautier A, Giraud C, Giraud T, Gonzalez C, Grossetete S, Güldener U, Henrissat B, Howlett BJ, Kodira C, Kretschmer M, Lappartient A, Leroch M, Levis C, Mauceli E, Neuvéglise C, Oeser B, Pearson M, Poulain J, Poussereau N, Quesneville H, Rascle C, Schumacher J, Ségurens B, Sexton A, Silva E, Sirven C, Soanes DM, Talbot NJ, Templeton M, Yandava C, Yarden O, Zeng Q, Rollins JA, Lebrun M-H, Dickman M (2011) Genomic analysis of the necrotrophic fungal pathogens *Sclerotinia sclerotiorum* and *Botrytis cinerea*. PLoS Genetics 7 (8):e1002230.

Andrew M, Barua R, Short SM, Kohn LM (2012) Evidence for a common toolbox based on necrotrophy in a fungal lineage spanning necrotrophs, biotrophs, endophytes, host generalists and specialists. PLoS ONE 7 (1):e29943.

Arnaise S, Zickler D, Le Bilcot S, Poisier C, Debuchy R (2001) Mutations in mating-type genes of the heterothallic fungus *Podospora anserina* lead to self-fertility. Genetics 159 (2):545-556.

Astell CR, Ahlstrom-Jonasson L, Smith M, Tatchell K, Nasmyth KA, and Hall BD (1981) The Sequence of the DNAs coding for the mating-type loci of *Saccharomyces cerevisiae*. Cell 27:15-23.

Beever RE, Parkes SL (1993) Mating behaviour and genetics of fungicide resistance of *Botrytis cinerea* in New Zealand. New Zealand Journal of Crop and Horticultural Science 21(4):303-310.

Bergquist RR, Lorbeer JW (1972) Apothecial production, compatibility and sex in *Botryotinia squamosa*. Mycologia 64 (6):1270-1281.

Buchwald N (1953) *Botryotinia* (*Sclerotinia*) globosa sp. on *Allium ursinum*, the perfect stage of *Botrytis globosa* Raabe. Phytopathologische Zeitschrift 20 (3):241-254.

Coppin E, Debuchy R, Arnaise S, Picard M (1997) Mating types and sexual development in filamentous ascomycetes. Microbiology and Molecular Biology Reviews 61 (4):411-428.

Cozijnsen A, Howlett B (2003) Characterisation of the mating-type locus of the plant pathogenic ascomycete *Leptosphaeria maculans*. Current Genetics 43 (5):351-357.

Cuesta Arenas Y, Kalkman ERIC, Schouten A, Dieho M, Vredenbregt P, Uwumukiza B, Osés Ruiz M, van Kan JAL (2010) Functional analysis and mode of action of phytotoxic Nep1-like proteins of *Botrytis cinerea*. Physiological and Molecular Plant Pathology 74 (5–6):376-386.

Dean R, Van Kan JAL, Pretorius ZA, Hammond-Kosack KE, Di Pietro A, Spanu PD, Rudd JJ, Dickman M, Kahmann R, Ellis J, Foster GD (2012) The Top 10 fungal pathogens in molecular plant pathology. Molecular Plant Pathology 13 (4):414-430.

Debuchy R, Berteaux-Lecellier V and Silar P (2010). Mating systems and sexual morphogenesis in ascomycetes. In: Borkovich KA and Ebbole DJ, eds. Cellular and molecular biology of filamentous fungi, (pp. 501-535). ASM Press, Washington.

Elliott ME (1964) Self-fertility in *Botryotinia porri*. Canadian Journal of Botany 42 (10):1393-1395.

Faretra F, Antonacci E (1987) Production of apothecia of *Botryotinia fuckeliana* (de Bary) Whetz. under controlled environmental conditions. Phytopathologia Mediterranea 26:29-35.

Faretra F, Antonacci E, Pollastro S (1988) Sexual behaviour and mating system of *Botryotinia fuckeliana*, teleomorph of *Botrytis cinerea*. Journal of General Microbiology 134 (9):2543-2550.

Ferreira AB, Saupe S, Glass NL (1996) Transcriptional analysis of the mtA idiomorph of *Neurospora crassa* identifies two genes in addition to mtA-1. Molecular Genetics and Genomics. 250:767-774.

Ferreira AV-B, An Z, Metzenberg RL, Glass NL (1998) Characterization of mat A-2, mat A-3 and ΔmatA mating-type mutants of *Neurospora crassa*. Genetics 148 (3):1069-1079.

Fukumori Y, Nakajima M, Akutsu K (2004) Microconidia act the role as spermatia in the sexual reproduction of *Botrytis cinerea*. Journal of General Plant Pathology 70 (5):256-260.

Grant-Downton RT, Terhem RB, Kapralov MV, Mehdi S, Rodriguez-Enriquez MJ, Gurr SJ, van Kan JAL, Dewey FM (2014) A novel *Botrytis* species is associated with a newly emergent foliar disease in cultivated *Hemerocallis*. PLoS ONE 9 (6):e89272.

Groves JW, Loveland CA (1953) The connection between *Botryotinia fuckeliana* and *Botrytis cinerea*. Mycologia 45 (3):415-425.

Heitman J, Kronstad JW, Taylor JW, Casselton LA, eds. 2007. Sex in fungi: Molecular Determination and Evolutionary Implications. Washington DC: ASM Press.

Chapter 1

Harrington T, McNew D (1997) Self-fertility and uni-directional mating-type switching in *Ceratocystis coerulescens*, a filamentous ascomycete. Current Genetics 32 (1):52-59.

Hennebert G, Groves J (1963) Three new species of *Botryotinia* on Ranunculaceae. Canadian Journal of Botany 41 (3):341-370.

Holst-Jensen A, Vaage M, Schumacher T (1998) An approximation to the phylogeny of *Sclerotinia* and related genera. Nordic Journal of Botany 18 (6):705-719.

Jarvis WR (1977) *Botryotinia* and *Botrytis* species: taxonomy, physiology, and pathogenicity: a guide to the literature. Monograph 15, Research Branch, Can Depart Agric.

Kanematsu S, Adachi Y, Ito T (2007) Mating-type loci of heterothallic *Diaporthe* spp.: homologous genes are present in opposite mating-types. Current Genetics 52 (1):11-22.

Khan MI, Marroni V, Keenan S, Scott IW, Viljanen-Rollinson SH, Bulman S (2013) Enhanced molecular identification of *Botrytis* spp. from New Zealand onions. European Journal of Plant Pathology 136 (3):495-507.

Kirk PM, Stalpers JA, Braun U, Crous PW, Hansen K, Hawksworth DL, Hyde KD, Lücking R, Lumbsch TH, Rossman AY, Seifert KA, Stadler M (2013) A without-prejudice list of generic names of fungi for protection under the International Code of Nomenclature for algae, fungi, and plants. IMA Fungus 4 (2):381-443.

Klix V, Nowrousian M, Ringelberg C, Loros JJ, Dunlap JC, Pöggeler S (2010) Functional characterization of MAT1-1-specific mating-type genes in the homothallic Ascomycete *Sordaria macrospora* provides new insights into essential and nonessential sexual regulators. Eukaryotic Cell 9 (6):894-905.

Leroch M, Plesken C, Weber RWS, Kauff F, Scalliet G, Hahn M (2013) Gray mold populations in German strawberry fields are resistant to multiple fungicides and dominated by a novel clade closely related to *Botrytis cinerea*. Applied and Environmental Microbiology 79 (1):159-167.

Li X, Kerrigan J, Chai W, Schnabel G (2012) *Botrytis caroliniana*, a new species isolated from blackberry in South Carolina. Mycologia 104 (3):650-658.

Lin X, Hull CM, Heitman J (2005) Sexual reproduction between partners of the same mating type in *Cryptococcus neoformans*. Nature 434 (7036):1017-1021.

Lu S-W, Yun S-H, Lee T, Turgeon BG (2011) Altering sexual reproductive mode by interspecific exchange of MAT loci. Fungal Genetics and Biology 48 (7):714-724.

Martinez F, Blancard D, Lecomte P, Levis C, Dubos B, Fermaud M (2003) Phenotypic differences between vacuma and transposa subpopulations of *Botrytis cinerea*. European Journal of Plant Pathology 109 (5):479-488.

Metzenberg RL, Glass NL (1990) Mating type and mating strategies in *Neurospora*. Bioessays 12 (2):53-59.

Nielsen K, Yohalem DS (2001) Origin of a polyploid *Botrytis* pathogen through interspecific hybridization between *Botrytis aclada* and *B. byssoidea*. Mycologia 93 (6):1064-1071.

Ni M, Feretzaki M, Li W, Floyd-Averette A, Mieczkowski P, Dietrich FS, Heitman J (2013) Unisexual and heterosexual meiotic reproduction generate aneuploidy and phenotypic diversity *De Novo* in the yeast *Cryptococcus neoformans*. PLoS Biololgy 11 (9):e1001653.

O'Gorman DT, Sholberg PL, Stokes SC, Ginns J (2008) DNA sequence analysis of herbarium specimens facilitates the revival of *Botrytis mali*, a postharvest pathogen of apple. Mycologia 100 (2):227-235.

Paoletti M, Seymour FA, Alcocer MJC, Kaur N, Calvo AM, Archer DB, Dyer PS (2007) Mating type and the Genetic Basis of Self-Fertility in the Model Fungus *Aspergillus nidulans*. Current Biology 17 (16):1384-1389.

Pöggeler S (1999) Phylogenetic relationships between mating-type sequences from homothallic and heterothallic ascomycetes. Current Genetics 36 (4):222-231.

Pöggeler S, Kück U (2000) Comparative analysis of the mating-type loci from *Neurospora crassa* and *Sordaria macrospora*: identification of novel transcribed ORFs. Molecular and General Genetics 263 (2):292-301.

Poggeler S, Risch S, Kuck U, Osiewacz HD (1997) Mating-type genes from the homothallic fungus *Sordaria Macrospora* are functionally expressed in a heterothallic Ascomycete. Genetics 147 (2):567-580.

Roach KC, Heitman J (2014) Unisexual reproduction reverses Muller's Ratchet. Genetics 198 (3):1059-1069.

Robertson SJ, Bond DJ, Read ND (1998) Homothallism and heterothallism in *Sordaria brevicollis*. Mycological Research 102 (10):1215-1223.

Ruehle GD (1931) New apple-rot fungi from Washington.Phytopathology 21:1141–1152.

Staats M, Van Baarlen P, Schouten A, Van Kan JAL (2007a) Functional analysis of NLP genes from *Botrytis elliptica*. Molecular Plant Pathology 8 (2):209-214.

Staats M, van Baarlen P, Schouten A, van Kan JAL, Bakker FT (2007b) Positive selection in phytotoxic protein-encoding genes of *Botrytis* species. Fungal Genetics and Biology 44 (1):52-63.

Staats M, van Baarlen P, van Kan JAL (2005) Molecular phylogeny of the plant pathogenic genus *Botrytis* and the evolution of host specificity. Molecular Biology and Evolution 22 (2):333-346.

Turgeon B (1998) Application of mating type gene technology to problems in fungal biology. Annual Review of Phytopathology 36 (1):115-137.

Turgeon B, Bohlmann H, Ciuffetti L, Christiansen S, Yang G, Schäfer W, Yoder OC (1993) Cloning and analysis of the mating type genes from *Cochliobolus heterostrophus*. Molecular Genetics and Genomics. 238 (1-2):270-284.

van Der Vlugt-Bergmans CJB, Brandwagt BF, Vant't Klooster JW, Wagemakers CAM, Van Kan JAL (1993) Genetic variation and segregation of DNA polymorphisms in *Botrytis cinerea*. Mycological Research 97 (10):1193-1200.

Walker A-S, Gautier A, Confais J, Martinho D, Viaud M, Le Pêcheur P, Dupont J, Fournier E (2011) *Botrytis pseudocinerea*, a new cryptic species causing gray mold in French vineyards in sympatry with *Botrytis cinerea* (Phytopathology). Phytopathology 101 (12):1433-1445.

Whetzel HH (1945) A synopsis of the genera and species of the Sclerotiniaceae, a family of stromatic inoperculate Discomycetes. Mycologia 37 (6):648-714.

Williamson B, Tudzynski B, Tudzynski P, Van Kan JAL (2007) *Botrytis cinerea*: the cause of grey mould disease. Molecular Plant Pathology 8 (5):561-580.

Yun S-H, Berbee ML, Yoder OC, Turgeon BG (1999) Evolution of the fungal self-fertile reproductive life style from self-sterile ancestors. Proceedings of the National Academy of Sciences 96 (10):5592-5597.

Zhang J, Wu M-D, Li G-Q, Yang L, Yu L, Jiang D-H, Huang H-C, Zhuang W-Y (2010a) *Botrytis fabiopsis*, a new species causing chocolate spot of broad bean in central China. Mycologia 102 (5):1114-1126.

Zhang J, Zhang L, Li G-Q, Yang L, Jiang D-H, Zhuang W-Y, Huang H-C (2010b) *Botrytis sinoallii*: a new species of the grey mould pathogen on *Allium* crops in China. Mycoscience 51 (6):421-431.

Chapter 2

Transcriptome and functional analysis of fruiting body development in *Botrytis cinerea*

Terhem RB, Rodenburg YA, Stassen JHM, and van Kan JAL

Abstract

Botrytis cinerea is an ascomycetous plant pathogen producing apothecia as sexual fruiting bodies. Not much is known about reprogramming of gene expression during apothecium development. In this study we analysed genome-wide expression profiles of sclerotia, three stages of apothecium development (primordia, full grown stipe, apothecial disk), and ascospores. In addition we studied the role of mating type (*MAT*) genes in apothecium development. RNA-sequencing was performed on different tissue types, and the reads were mapped on gene models in the *B. cinerea* genome. The expression profiles were analysed in different ways. First, the transcript levels of *B. cinerea* orthologs of *Aspergillus nidulans* and *Sordaria macrospora* genes known to be involved in sexual development were examined. Secondly, transcriptional changes between   successive developmental stages were analysed. Strikingly, more than 5000 genes appeared to be differentially expressed in ascospores as compared to mature apothecial disks. Among the genes that were upregulated in ascospores are several genes encoding virulence factors, which indicates that ascospores are primed for infection of host plants. Thirdly, cluster analysis identified five sets of genes with common transcriptional profiles over the developmental stages. Interestingly, ~60% of the genes that were specifically expressed in mature apothecial disks were of unknown function, were either *Botrytis*-specific, or had homologs only in closely related taxa.

In order to study the function of mating type genes, single gene deletion mutants were generated in both genes present in the *MAT1-1* locus or both genes present in the *MAT1-2* locus. All four mutants were crossed with a wild type strain or knockout mutant strain of opposite mating type, in all possible combinations. Knockout mutants in the *MAT1-1-1* or *MAT1-2-1* gene were sterile. By contrast, mutants in the *MAT1-1-5* or *MAT1-2-4* gene developed into stipes but never into an apothecial disk. The *MAT1-1-5* and *MAT1-2-4* mutants showed identical phenotypes, suggesting that both genes control the transition from stipe to apothecial disk, probably by acting as transcriptional regulators. Comparative gene expression profiling between the *MAT1-1-5*-deficient mutant blocked at the transition from stipes to apothecial disk formation and wild type apothecial disks identified 114 genes that were downregulated in the mutant. These genes might be under (direct or indirect) control of the *MAT1-1-5* and *MAT1-2-4* genes.

Introduction

Botrytis cinerea is a heterothallic Ascomycota classified in the class of Leotiomycetes, order Helotiales, family Sclerotiniaceae. As member of the Helotiales, *B. cinerea* develops a fruiting body with an exposed hymenium on top of a stipe, called an apothecium. Apothecia are generally carpogenic from sclerotia, and the sclerotium serves as a source of nutrients during apothecium development (Li et al. 2011). Apothecia function as a platform to discharge ascospores (Pöggeler et al. 2006) which serve as the primary inoculum for plant infection (Jurick et al. 2004), especially in early spring when *B. cinerea* conidia are scarce.

Species within the Sclerotiniaceae can either have heterothallic or homothallic sexual reproduction systems. In a heterothallic species, mating occurs between two isolates with opposite mating types. The opposite *MAT* loci of Ascomycota are generally present at the same chromosomal location and therefore genetically allelic, but they lack sequence similarity and are called idiomorphs rather than alleles (Metzenberg and Glass 1990). Each idiomorph contains at least one gene encoding a transcription factor. By convention, the *MAT1-1* idiomorph encodes a protein with an α domain, while *MAT1-2* encodes a protein with a high mobility group box (HMG-box) (Martin et al. 2011). In *B. cinerea*, the *MAT* loci are designated as *MAT1-1* and *MAT1-2*. The *MAT1-1* locus contains two genes: *MAT1-1-1* encoding the α domain protein (with a length of 354aa), and *MAT1-1-5* of unknown function (377aa). The *MAT1-2* locus also contains two genes: *MAT-1-2-1*, encoding the HMG-box protein (with a length of 376aa), and *MAT1-2-4* of unknown function (197aa). Both *MAT* loci in *B. cinerea* are flanked by the *APN2* gene (an ortholog of the *Saccharomyces cerevisiae* gene encoding DNA lyase) and the *SLA2* gene (an ortholog of the *S. cerevisiae* gene encoding a cytoskeletal protein) which are convergently transcribed toward the *MAT* loci (Amselem et al. 2011). In many Ascomycota with heterothallic reproductive life styles, the *MAT* loci are also surrounded by *APN2* and *SLA2* genes, suggesting that this represents the ancestral configuration in all Ascomycota (Heitman 2007).

Heterothallic Ascomycota usually carry a single mating type gene in one nucleus, while homothallic Ascomycota carry both mating type genes (*MAT1-1* and *MAT1-2*) in one genome (Glass and Smith 1994; Yun et al. 1999; Yun et al. 2000; Amselem et al. 2011). For example, the homothallic species *Sclerotinia sclerotiorum* carries four linked *MAT* genes (*MAT1-1-1*, *MAT1-1-5*, *MAT1-2-1* and *MAT1-2-4*), which are equivalent to the heterothallic *MAT1-1* and *MAT1-2* loci in *B. cinerea* (Amselem et al., 2011). Another example is the homothallic species *Sordaria macrospora* which carries four linked MAT genes (*MAT1-1-1*, *MAT1-1-2*, *MAT1-1-3* and *MAT1-2-1*), equivalent to both idiomorphs of the heterothallic species *Neurospora crassa* (Pöggeler and Kück 2000; Pöggeler et al. 1997). Several studies have focussed on unravelling the function(s) of mating type genes in Ascomycota. Table 1 shows the results of functional analyses of *MAT* genes in the model fungi *Neurospora crassa*, *Podospora anserina* and *Sordaria macrospora* but there are numerous other fungi for which studies of *MAT* genes have been conducted. So far, the functions of the four genes in the *B. cinerea MAT* locus in general and more specifically in apothecium development have not been studied. The availability of genome sequences and gene annotations of *B. cinerea* (Amselem et al., 2011; van Kan et al., unpublished) enabled molecular dissection of apothecium development in *B. cinerea*, both at the transcriptional and functional level.

Table 1: Role of mating type genes in sexual development of model ascomycetous fungi

Fungal species	Reproductive system	Gene	Phenotype[a]	Reference
Neurospora crassa	Heterothallic	*MAT1-1-1*	Sterile	Ferreira et al., (1998)
		MAT1-1-2	Decreased fertility	Ferreira et al., (1998)
		MAT1-1-3	Decreased fertility	Ferreira et al., (1998)
		MAT1-2-1	Not determined	
		MAT1-2-2	Not determined	
Podospora anserina	Heterothallic	*MAT1-1-1*	Fertile	Arnaise et al., (2001)
		MAT1-1-2	Sterile	Arnaise et al., (2001)
		MAT1-1-3	Fertile	Arnaise et al., (2001)
		MAT1-2-1	Fertile	Arnaise et al., (2001)
				Arnaise et al., (2001)
Sordaria macrospora	Homothallic	*MAT1-1-1*	Fertile	Klix et al., (2010)
		MAT1-1-2	Sterile	Klix et al., (2010)
		MAT1-1-3	Fertile	Klix et al., (2010)
		MAT1-2-1	Not determined	

[a] phenotype of targeted knockout mutants

Large scale gene expression analyses in fungi have previously been performed using microarrays (Breakspear and Momany 2007; Koch et al. 2005; Kerr et al. 2000). In recent years, transcriptome analyses have shifted towards the use of RNA-sequencing, which provides a higher level of sensitivity and accuracy to quantify expression levels (Soanes et al. 2012; Fu et al. 2009; Marioni et al. 2008) and has become increasingly affordable. Therefore, genome-wide expression profile analysis by RNA-sequencing is being carried out in a rapidly increasing number of filamentous fungi, including *Aspergillus niger* (Delmas et al. 2012), *P. anserina* (Bidard et al. 2011), *Sclerotinia homoeocarpa* (Orshinsky et al. 2012), *Trichoderma harzianum* (Steindorff et al. 2014), *Metarhizium anisopliae* (Wang et al. 2014a), *Magnaporthe oryzae* (Soanes et al. 2012; Kawahara et al. 2012) and *B. cinerea* (Zhang et al. 2014). The aims of this study were to perform a genome-wide transcriptome analysis during different stages of apothecium development in *B. cinerea* using RNA-sequencing, and to identify the functions of the *B. cinerea MAT* genes in apothecium development by targeted deletion.

Materials and Methods

Strains

The wild type strains SAS56 (reference *MAT1-1* strain) and SAS405 (reference *MAT1-2* strain) were used in this study (Faretra and Antonacci 1987; Faretra et al. 1988), as well as strain B05.10 (*MAT1-1*), for which the genome sequence was determined (Amselem et al., 2011; van Kan et al., unpublished). Strains were plated on malt extract agar (MEA). For obtaining sclerotia, cultures were grown at 15 ˚C in darkness. For obtaining sporulation, the cultures were grown at 20˚C. Two-to three-day-old plates were exposed to near-UV light to enhance sporulation. Conidia were maintained in 20% glycerol and stored at -80°C.

Sexual crosses

Sexual crosses were performed using three wild type strains (SAS56, SAS405 and B05.10) and four mutants: *ΔMAT1-1-1*, *ΔMAT1-1-5*, *ΔMAT1-2-1* and *ΔMAT1-2-4*. Crosses were performed using the described protocols (Faretra et al. 1988;van der Vlugt-Bergmans et al. 1993). Sclerotia (incubated at 0 ˚C for one month) were sampled from MEA plates and the surfaces were cleaned with a soft toothbrush. Three to five sclerotia of ~1 cm in size were put in

single wells in a six-well microtiter plate. Suspensions of microconidia were prepared by pouring sterile (autoclaved) MilliQ water onto the plate from which sclerotia were removed, followed by gentle rubbing with a plastic spatula. Sclerotia in the microtiter plate were fertilized with 3 ml of this microconidia suspension per well of the microtiter plate that was subsequently sealed with parafilm and incubated at 12°C in candescent light with a 12 h photoperiod.

DNA extraction

Freeze-dried mycelium was used for genomic DNA extraction, using a Gentra Puregene DNA purification kit (Qiagen, Venlo, the Netherlands), following the manufacturer's instructions.

RNA extraction and RNA-sequencing

Samples from apothecia and ascospores were freeze-dried and total RNA was isolated using the Nucleospin RNA plant kit (Macherey Nagel, Düren, Germany), according to the manufacturer's instructions. For isolation of RNA from sclerotia, freeze-dried sclerotia were frozen in liquid nitrogen and ground with a mortar and pestle. Total RNA was isolated with TRIzol Reagent (Life Technologies, Grand Island, NY, USA) in combination with a Nucleospin RNA plant kit (Macherey Nagel, Düren, Germany), used according to the manufacturer's instructions.

The integrity of RNA was monitored by agarose gel electrophoresis and the concentration was determined using a NanoDrop 2000 spectrophotometer (Thermo Scientific, Wilmington, DE, USA). A total of 20 µg of RNA from each sample was used by Beijing Genome Institute (Hongkong) for library construction (300-700 nt insert sizes) and sequenced using Illumina HiSeq™ 2000. The paired-end RNA-Seq reads with a length of 90 nucleotides were assessed for quality using FastQC software v0.10.1 (Babraham Institute, http://www.bioinformatics.babraham.ac.uk/projects/fastqc). The reads were trimmed to 80, using FASTX-Toolkit v0.0.13.2 (http://hannonlab.cshl.edu/fastx_toolkit). The quality of the RNA libraries was checked by mapping them to the *B. cinerea* reference genome (strain B05.10; van Kan et al., unpublished). The mapping efficiency ranged from 84.2 to 96.9%. The reads mapping on the 11,701 gene models were counted and normalised.

cDNA synthesis and quantitative RT-PCR

First strand cDNA was synthesized from 1 µg total RNA with M-MLV Reverse Transcriptase (Promega, Leiden, The Netherlands) according to the manufacturer's instructions. Quantitative-Real Time-PCR (qRT-PCR) was performed using an ABI7300 PCR machine in combination with the qPCR SensiMix kit, with primers as listed in Table 2. qRT-PCR conditions were as follows: an initial 95°C denaturation step for 10 min, followed by denaturation for 15 s at 95°C and annealing/extension for 1 min at 60°C, for 40 cycles. The data were analyzed on the 7300 System SDS software and calculated according to the $2^{-\Delta\Delta Ct}$ method (Livak and Schmittgen 2001). The gene expression values were normalized to the constitutively expressed *B. cinerea* tubulin gene, *BctubA* (Benito et al. 1998).

Read mapping and differential expression

The trimmed reads were mapped on the genome of B05.10 (van Kan et al., unpublished) using the spliced aligner software Tophat v2.0.8b (Kim et al. 2013). Gene expression values were measured using two different software packages and methods: DESeq2 and Cuffdiff. DESeq2 (Anders et al. 2014; Anders and Huber 2010) was used with default settings for four pairwise statistical differential expression tests between the five stages (2 biological replicates each) in the sexual reproduction of *B. cinerea*. DESeq2 gives a p-adjusted value (Benjamini and Hochberg 1995), indicating the significant differentially expressed genes, corrected for multiple testing. Differentially expressed genes were considered significant for p-adjusted value <0.05. Cuffdiff (v2.1.1) was used with default parameters (Trapnell et al. 2013). The significant differentially expressed genes were selected on q-value <0.05 for both methods, and for each pairwise test. For each pair, the genes that were tested significant (p-adjusted or q-value <0.05) for differential expression with both methods were considered high confidence differentially expressed genes.

Clustering gene expression patterns

In order to cluster and identify co-expressed genes at different stages the R package Mfuzz was used (Futschik and Carlisle 2005). Prior to clustering, three groups of expression patterns were filtered out: (I) genes which showed expression in only one of the biological replicates, (II) genes that showed <=10 read counts over all 5 conditions and (III) genes that showed >10-fold difference in counts between the biological replicates. To determine gene

expression variation between stages, the coefficient of variance (c_v) was calculated for all genes, using the formula $c_v = \sigma \mu^{-1}$.

The 500 genes with the highest c_v were selected ('Top500'), these displayed the most strongly fluctuating expression patterns (over the five samples), relative to their average expression level. The mean expression of the biological replicates of the Top500 genes was then used for further analyses.

Enrichment tests

Fisher's exact tests were performed to test for enriched GO terms. Four subsets for each differentially expressed gene set (identified both by DEseq2 and Cufddiff), were analyzed for enriched GO terms, using a Fisher's exact test from the Blast2GO suite.

Deletion of mating type genes

The *MAT1-1-1*, *MAT1-1-5*, *MAT1-2-1* and *MAT1-2-4* genes were individually targeted for mutagenesis. *MAT1-1-1* and *MAT1-1-5* genes were deleted in SAS56, whereas the *MAT1-2-1* and *MAT1-2-4* genes were deleted in SAS405. In addition, the *MAT1-1-5* gene was also deleted in B05.10. The gene knockout strategies for generating *B. cinerea* deletion constructs, *B. cinerea* protoplast transformation and PCR-based screening of transformants were as described by Kars et al. (2005b). Table 2 shows the list of primers that were used for amplification of gene deletion fragments. The hygromycin resistance (*HPH*) cassette, amplified from vector pLOB7 (Zhang et al. 2011) with primer pair Cassette-5/Cassette-3 was used as selection marker. Genomic DNA of transformants was analyzed for the presence/absence of the wild-type target gene by amplifying the target genes *MAT1-1-1*, *MAT1-1-5*, *MAT1-2-1* and *MAT1-2-4* using primer combinations MAT111-5.1/MAT111-3.1, MAT115-5.1/MAT115-3.1, MAT121-5.1/MAT121-3.1 and MAT124-5.1/MAT124-3.1 respectively.

Table 2: Primers used in this study

Target gene	Primer name	Primer sequence 5'-3'	Reference
Gene knock out			
	MAT111-5.1	GAGGAAGTTCCTTAGCTCGT	This study
MAT 1-1-1	MAT111-5.2	CTCACCTTCGCATGTCTTGA	This study
	MAT111-5.3	GGGTACCGAGCTCGAATTCACACTGAGGATAGCAGACT	This study
	MAT111-3.1	ACCTAACATCGCCAACTATC	This study
	MAT111-3.2	CACAGAGAGGGAGAGAATTTG	This study
	MAT111-3.3	CTCGGCGCGCCGAAGCTTGCTATTGCTTACACTCCTCCC	This study
MAT 1-1-5	MAT115-5.1	TGTAGGAATTCGAATATGGGTAGG	This study
	MAT115-5.2	GTCGATTTCGTGGACTACGGGTC	This study
	MAT115-5.3	GGGTACCGAGCTCGAATTCGATACTGAACTATCTCCCGTTCCC	This study
	MAT115-3.1	CCAGGACGAGCAGATGGAAAGCAC	This study
	MAT115-3.2	GTCTCCGGCCTGTCTCCAGTC	This study
	MAT115-3.3	CTCGGCGCGCCGAAGCTTGGCTTCGTTGAACAGCTTCTG	This study
MAT 1-2-1	MAT121-5.1	CTCTCTCCTCTCTCCGACTA	This study
	MAT121-5.2	CGGCACTGTCCTCGAAACGC	This study
	MAT121-5.3	GGGTACCGAGCTCGAATTCGATCTTTGGCTTGAGACCAG	This study
	MAT121-3.1	GTGAATGGTGATGGCTAGCAT	This study
	MAT121-3.2	ATGGTGTGTCATCGAAGGCACA	This study
	MAT121-3.3	CTCGGCGCGCCGAAGCTTCTAGAGCAACAGCTTCAGCC	This study
MAT 1-2-4	MAT124-5.1	GCGTTTCGAGGACAGTGCCG	This study
	MAT124-5.2	TAGTCGGAGAGAGGAGAGAG	This study
	MAT124-5.3	GGGTACCGAGCTCGAATTCACAGCTGAGAACATGCGCTG	This study
	MAT124-3.1	CTTGAGTGCCACAAAAGGTG	This study
	MAT124-3.2	AGAGAGTTCTGGCGATGTGT	This study
	MAT124-3.3	CTCGGCGCGCCGAAGCTTGAACCATGACTCAAGCAGAG	This study
hph selection marker cassette	Cassette-5	GAATTCGAGCTCGGTACCCGGGGA	Zhang et al., (2011)
	Cassette-3	CAAGCTTCGGCGCGCCGAG	Zhang et al., (2011)
	Screen-3	GTAACCATGCATGGTTGCCT	
	Screen-5	GGGTACCGAGCTCGAATTC	
Quantitative-RT-PCR			
MAT1-1-1	QForMAT111	CACGTTGCAATGAATGAGAGAC	This study
	QRevMAT111	CCAAGCACCGTCAAAATCATGT	This study
MAT1-1-5	QForMAT115	TACAGTCGTTTCAATGCAGGAG	This study
	QRevMAT115	AACAGTCTGTGACAAGGGCAT	This study
MAT1-2-1	QForMAT121	AGTATTGGAACTCCAGAACGTC	This study
	QRevMAT121	GGAGCAAGGAACATTCTGTTGA	This study
MAT1-2-4	QForMAT124	GGACGAGGTTCAGCATCATTTA	This study
	QRevMAT124	TTTCACCAGTCCCAAATCAGCT	This study
Tubulin A	TubulinAfor	GCGTTCGTGCATTGGTATGT	Benito et al., (1998)
	TubulinArev	CACGGGCCTCAGAGAATTCA	Benito et al., (1998)

Results

Samples representing five different stages of sexual development were used for RNA extraction (Figure 1). The first sample was taken from 4-week-old sclerotia of strain SAS405 (*MAT1-2*), which had been incubated at 0^0C for one month and were ready for fertilization with microconidia of opposite mating type. The second sample was taken from stipe primordia emerging from sclerotia ~30 days after they had been fertilized with microconidia of strain SAS56 (*MAT1-1*); primordia of stages 1 (size 1-2 mm) and 2 (size 2-4 mm) were combined to form this sample. The third sample was taken from a combination of stipes of stages 3 (>5 mm, stipes elongated but not swollen at the tip) and 4 (stipes fully extended to ~1 cm, swollen at the tip and showing initiation of apothecial disk development). The fourth sample was taken from a combination of apothecial disks of stages 5 (immature disk with diameter <5 mm, partially expanded) and 6 (mature disks fully expanded to ~1 cm, filled with asci containing 8 ascospores). The fifth and last sample was taken from ascospores obtained from mature apothecia by gently crushing the apothecial disks in sterile water and filtering the suspension over glasswool to separate hymenium tissue and large debris from the ascospores (in the flow-through). These five samples were used for RNA extraction and were designated, respectively, as Scl (sclerotia), Apo12 (primordia of stages 1 and 2), Apo34 (stipes of stages 3 and 4), Apo56 (apothecial disks, stages 5 and 6) and Asc (mature ascospores). All samples were processed and prepared for cDNA synthesis and RNA sequencing.
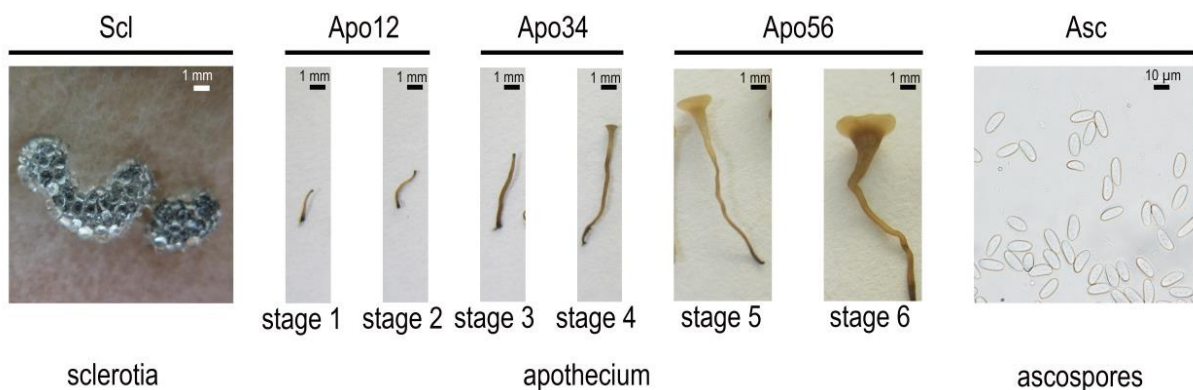

Figure 1: Tissues and stages of apothecium development used in this study. For explanations see text. Scale bars indicate the sizes in mm or µm (ascospores).

Expression of mating type genes during development of apothecia of *B. cinerea*

Figure 2 shows a qRT-PCR analysis of the transcript levels of the *MAT1-1-1*, *MAT1-1-5*, *MAT1-2-1* and *MAT1-2-4* genes over the three stages of apothecium development (Apo12, Apo34 and Apo56), relative to the internal, constitutively expressed reference gene *Bctub*A (Benito et al., 1998). Transcript levels of all four genes were lowest in primordia (Apo12), slightly increased in stipes (Apo34) and peaked in apothecial disks (Apo56).
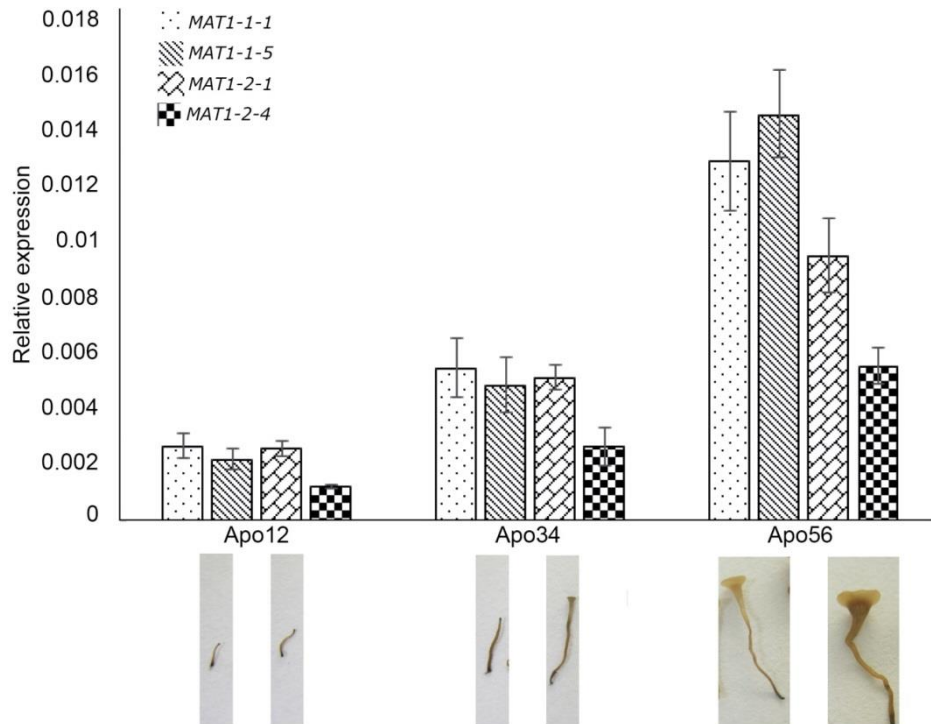
Figure 2: Transcript levels of *MAT1-1-1*, *MAT1-1-5*, *MAT1-2-1* and *MAT1-2-4* genes in different apothecial developmental stages, relative to the internal standard *Bctub*A (average of two biological replicates).

Whole-genome transcriptome analysis of *B. cinerea* during development of apothecia

RNA-sequencing was performed on the five samples described above, in two biological replicates, except for the sclerotia which were sequenced once because of difficulties in obtaining RNA of sufficient quality due to their high melanin content. Sequencing thus yielded datasets for nine RNA samples. The library size and mapping efficiency of the reads on the *B. cinerea* genome are listed in Table 3. More than 91% of gene models in the *B. cinerea* genome were represented by at least one read; in every sample, at least 75% of all genes had FPKM values ≥1. The expression profile of sample Apo56 was the most diverse, with >90% of gene models displaying an FPKM value ≥1.

Table 3: Mapping efficiency of RNA sequencing reads from different samples on the *B. cinerea* genome

Tissue type	Library size	Mapped reads	% mapped	#genes with FPKM ≥1
Sclerotium	12853250	12455209	96.9	8855 (75.6%)
Apo12A	12853250	12106317	94.2	9698 (82.8%)
Apo12B	12141566	10281723	84.7	
Apo34A	13416227	12637059	94.2	10171 (86.9%)
Apo34B	11376181	9734272	85.6	
Apo56A	13883171	13075867	94.2	10584 (90.5%)
Apo56B	11762996	10054934	85.5	
Asc-A	13184680	12471413	94.6	8873 (75.8%)
Asc-B	11958139	10953912	91.6	

Expression of *B. cinerea* genes with orthologs involved in sexual development of model fungi

The transcript levels were examined of *B. cinerea* orthologs of genes in *Aspergillus nidulans* (Dyer and O'Gorman, 2012) and *Sordaria macrospora* (Teichert et al., 2014) known to act as activators or repressors of sexual development. *B. cinerea* orthologs could be identified for 67 of these genes (Supplementary Table 1). Expression for most of these *B. cinerea* genes was detectable in nearly all samples tested, with FPKM values ranging from 1 to 3437 (Supplementary Table 1). Supplementary Figures 1-5 show the abundance in the five RNA samples of transcripts of *B. cinerea* genes orthologous to *A. nidulans* genes involved in perception of environmental signals (Figure S1), mating processes and signal transduction (Figure S2), transcription factors (Figure S3), endogenous physiological processes (Figure S4) and ascospore production and maturation (Figure S5) according to the grouping by Dyer and O'Gorman (2012). Figure 3 shows the expression profiles of a selection of genes in the entire set, which will be discussed in more detail. The *B. cinerea white collar* 2 gene (Bcin05g05530) and the *VelA* gene (Bcin15g03390) both are putative positive regulators of sexual reproduction and their transcript levels increased 2-3 fold in *B. cinerea* primordia and mature stipes, as compared to sclerotia and ascospores. On the other hand, transcripts of the *B. cinerea white collar 1* and *VelB* genes were less abundant and barely changed during sexual development (Figure S1). The *B. cinerea* ortholog to an amino acid sensing bZIP protein (AN3675), considered to be a negative regulator of sexual reproduction in *A. nidulans*, showed a 4-fold reduction in transcript levels in apothecial tissues as compared to

sclerotia and ascospores. Genes encoding components of the *B. cinerea* heterotrimeric G-protein complex (Gα1, Gβ and Gγ) all showed slight increases in transcript levels in apothecial tissues as compared to sclerotia and ascospores. The thioredoxin gene Bcin12g04280 showed an extremely high transcript level (FPKM=3437) in primordia and it was 2.5-fold higher than in sclerotia, mature apothecial discs and ascospores. The transcript level of the gene encoding ATP citrate lyase subunit ACL1 increased 3-fold in the transition from sclerotia to primordial stipes, remained constant in apothecia and futher increased up to 9-fold in ascospores. The expression profiles of *B. cinerea* genes orthologous to several *S. macrospora* genes required for sexual development were also examined, and were found to be expressed most abundantly in ascospores (pro4) or in all three stages of apothecial development, but not in sclerotia and ascospores (pro41).
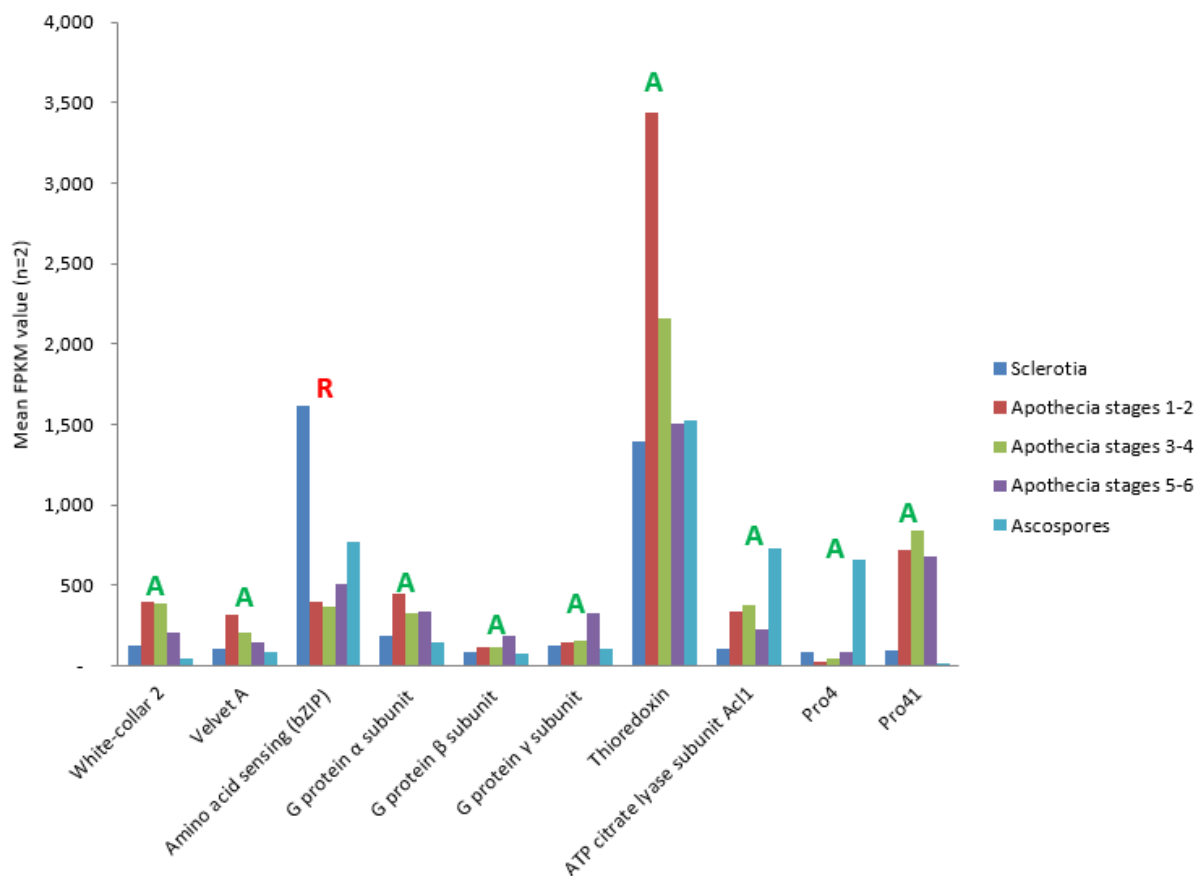

Figure 3: Expression profiles in sclerotia, three stages of apothecial development and ascospores for a subset of *B. cinerea* genes that are orthologous to *Aspergillus nidulans* and *Sordaria macrospora* genes known to act as activators or repressors of sexual development. A: activator of sexual development, R: repressor of sexual development

Genes differentially expressed between different stages of apothecial development

Changes in gene expression correlated with transitions between stages of apothecial development (Scl-Apo12; Apo12-Apo34; Apo34-Apo56; Apo56-Asc) were analysed using DESeq2 and Cuffdiff. The sets of differentially expressed genes detected by each of the two methods were compared for each of the four pairwise tested stages of apothecial development. The Venn diagrams in Figure 4 show that DESeq2 and Cuffdiff exhibit different levels of sensitivity and specificity, giving rise to the identification of distinct sets of differentially expressed genes, with a significant overlap between both methods. The genes for which differential expression was detected by both methods were considered as high confidence differentials, and these were further analysed.
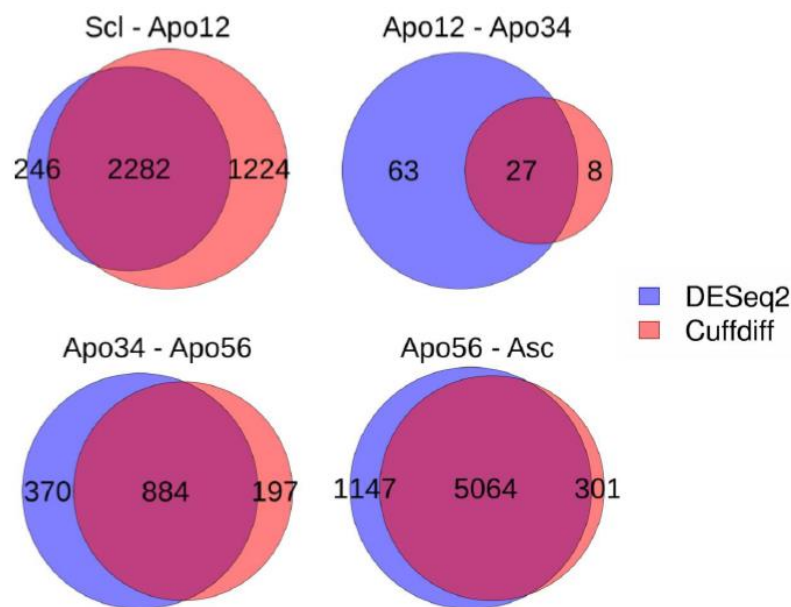
Figure 4: The numbers of differentially expressed genes between different stages of apothecial development as identified by DESeq2 (blue circle) and Cuffdiff (red circle). Four Venn diagrams are depicted, one for each pairwise comparison (indicated on top of each diagram). The numbers on the left in each Venn diagram represent the number of differentially expressed genes only detected by DESeq2, while the numbers on the right represent the numbers of differentially expressed genes only detected by Cuffdiff. The numbers within the overlapping area represent the number of differentially expressed genes identified by both methods.

Table 4 provides a more detailed overview of the differentially expressed genes detected by both methods. The most pronounced changes in transcript levels were detected between apothecial disks (Apo56) and ascospores (Asc), with over 5000 high confidence differentials, as well as during the transition from sclerotia to primordia (stage Apo12; 2282 high

confidence differentials). By contrast, only 27 genes were differentially expressed between primordia (Apo12) and stipes (Apo34), whereas between stipes (Apo34) and apothecial disks (Apo56), the number of differentially expressed genes was 884. Features of these sets of high confidence differentials are discussed below.

Table 4: Differentially expressed genes detected by the DESeq2 and Cuffdiff method

Pairwise test	Concordant by DESeq2 and Cuffdiff	Upregulated	Downregulated
Scl – Apo12	2282	1307	975
Apo12 – Apo34	27	0	27
Apo34 – Apo56	884	428	456
Apo56 – Asc	5064	2504	2560

Differentially expressed genes in the transition from sclerotia to primordia

The transition from sclerotia to primordia (Apo12) resulted in 1307 upregulated and 975 downregulated genes (Table 4). The upregulated genes showed an overrepresentation of the GO terms "cell division related processes", "fatty acid biosynthetic process", "double strand break repair via break-induced replication" and "protein import into peroxisome matrix", "docking", "DNA strand elongation involved in DNA replication", "positive regulation of asexual sporulation resulting in formation of cellular spore". GO terms that were overrepresented in the down-regulated genes mostly related to the assimilation, dissimilation and transport of carbohydrates, for example "glycolysis" and "gluconeogenesis".

Differentially expressed genes in the transition from primordia to stipes

The transition from primordia (Apo12) to stipes (Apo34) resulted in 27 differentially expressed genes that were all down-regulated (Table 4). Among these were genes encoding the oxaloacetate hydrolase *BcOAH1* required for biosynthesis of oxalic acid (Han et al. 2007), an MFS transporter with unknown substrate specificity, as well as several genes in a cluster of secondary metabolite genes including the polyketide synthase gene *BcPKS15*, of which the product is unknown. In view of the small number of differentials, GO enrichment analysis did not detect any significant enrichment.

Differentially expressed genes in the transition from stipes to apothecial disks

The transition from stipes (Apo34) to apothecial disks (Apo56) resulted in 428 upregulated and 456 downregulated genes. The upregulated genes showed an overrepresentation of GO terms related to nutrient transport and cell-wall related processes. "Carbohydrate transport" was the most significantly overrepresented GO term, but this transition also showed an overrepresentation of the GO term "G2/M transition of mitotic cell cycle" and terms related to post-translational modification of proteins. Overrepresented GO terms in the downregulated genes in this set included "peroxisome processes", many oxidation-reduction processes and the term "negative regulation of sexual sporulation resulting in formation of cellular spore".

Differentially expressed genes in the transition from apothecial disks to ascospores

Between the apothecial disks (Apo56) and the ascospore sample, >5000 genes were differentially expressed, of which half were upregulated and half were downregulated (Table 4). GO enrichment analysis on the upregulated genes revealed overrepresentation of the terms "isoleucine/valine/leucine biosynthetic process", "mycelium development" and "ribosome synthesis". The less related terms "pre-replicative complex assembly involved in nuclear cell cycle DNA replication" and other DNA-replication oriented processes were also overrepresented. Down-regulated genes showed an overrepresentation of GO terms related to "carbohydrate transport", "hydrogen peroxide transport", "defense response", "proteolysis" and "reciprocal meiotic recombination".

Cluster analysis of expression profiles

A set of genes with the highest (relative) variance in gene expression levels over the five samples was selected and designated as "Top500" genes. Soft clustering of the expression patterns of the "Top500" genes resulted in 6 clusters, containing a minimum of 2 genes and a maximum of 246 genes for clusters 2 and 6, respectively (Figure 5). The clusters represent expression patterns showing almost exclusive peaks at one of the five different stages tested. Clusters 4 and 5 both show transcript peaks in the apothecial disk stage (Apo56), but the genes assigned to cluster 4 showed some rise in transcript levels already in stipes (Apo34), while genes in cluster 5 did not show this early rise.
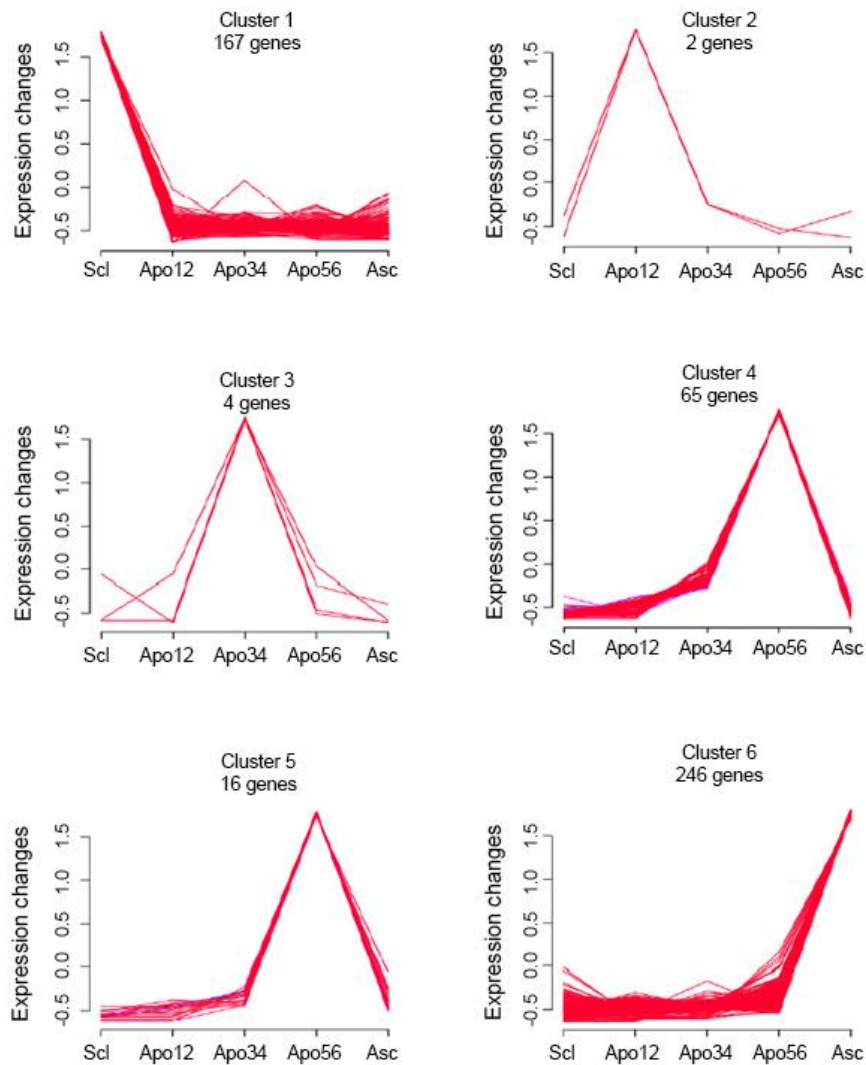

Figure 5: Soft clustering of the "Top500" genes with relatively most variable gene expression patterns

A hierarchical clustering (Figure 6) ordered the "Top500" genes into five groups, clearly distinguished in the dendrogram by deep splits between branches. The groups represent sets of genes that are predominantly expressed in only one of the five stages of apothecial development, as demonstrated by clear colour boundaries between groups in the heat map (Figure 6). The coloured bar at the right hand side of the gene dendrogram (left of the heat map) shows the correspondence between the hierarchical clustering and the grouping derived from the soft cluster method. The coloured bars are often continuous for multiple genes, indicating they are assigned to the same cluster by both methods, with the exception of the pink and blue bars. These genes were assigned to clusters 4 and 5 by the soft clustering method, but appear to be mingled by the hierarchical clustering. Other than this minor discrepancy, the two methods yielded very concordant results and provide support for the existence of five types of expression profiles within the "Top500" genes. The composition of the clusters will be discussed below.
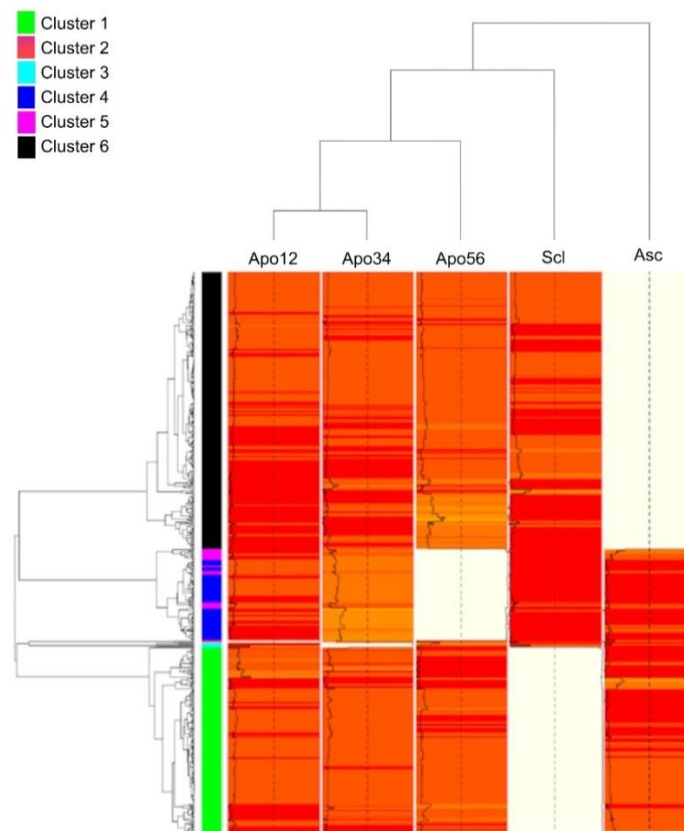
Figure 6: Heat map created with a k-means hard clustering method. On the vertical axis is a hierarchical tree depicting the clustering of expression patterns of individual genes. The horizontal axis shows a clustering of the samples based on expression patterns of the genes together. The sample labels are shown at the top of the columns. Lines within the plot show the standardized expression levels of genes. The coloured vertical bars indicate to which Mfuzz cluster the gene was assigned. The colour code of these clusters is provided in the left top corner.

Sclerotium-specific expression (Soft Cluster 1)

Cluster 1 (Supplementary Table 2) comprises 167 genes that are expressed predominantly in sclerotia and barely in any of the other four stages tested. Among these are four cytochrome P450 encoding genes, seven MFS transporter encoding genes, four HET domain containing genes, several taurine and carnosine metabolism genes, one mannitol dehydrogenase encoding gene and the polyketide synthase gene *BcPKS19*. Strikingly, the set of 167 genes contains six clusters of at least three (up to seven) consecutive genes that are all predominantly expressed in sclerotia. However, the function of most of these 26 genes remains unknown because they have no functional annotation.

Primordia-specific expression (Soft Cluster 2)

Cluster 2 (Supplementary Table 3) comprises only two genes that are specifically expressed in stage Apo12. One of these genes (Bc04g02570) encodes a small secreted protein (length of the mature protein 86aa) containing 13 cysteine residues in a pattern reminiscent of hydrophobins. The second member of this cluster is the polyketide synthase gene Bc05g06220 (*BcPKS15*), which is located in a secondary metabolite cluster on chromosome 5 that also contains genes encoding a methyltransferase, an alcohol dehydrogenase and two transcription factors (one Zn2Cys6 type and one C2H2 type). Closer inspection revealed that these genes show similar expression as *BcPKS15*, but their absolute transcript levels were too low to be included in the list of "Top500" genes (not shown).

Stipe-specific expression (Soft Cluster 3)

Cluster 3 (Supplementary Table 4) comprises four genes of which three have functional annotations, i.e. a putative ornithine decarboxylase, a secreted tannase and a secreted feruloyl esterase B precursor.

Apothecial disk-specific expression (Soft Clusters 4 and 5)

Clusters 4 and 5 (Supplementary Tables 5 and 6) both contain genes that are predominantly expressed in apothecial disks (Apo56). The distinction between the clusters is that the 65 genes in cluster 4 already show a slight transcript increase in stage Apo34 and peak in stage Apo56, whereas the 16 genes in cluster 5 do not show a similar early increase in Apo34. Of the 65 genes in cluster 4, 45 genes are of unknown function and unique to *Botrytis,* to

Sclerotiniaceae or to *Helotiales*, while 5 genes encode proteins of unknown function that are conserved in many filamentous fungi. Of the 15 genes in this cluster with a functional description, there are two genes encoding Zn2Cys6 transcription factors, and other genes encoding an MFS hexose transporter, a putative aquaporin, a homolog of the SNF2 chromatin remodelling protein, a WD-domain containing protein and a CAZY GH76 α-mannanase. Of the 16 genes in cluster 5, six encode secreted proteins (of which one is a predicted glutaminase and one a predicted tannase), one is an MFS transporter encoding gene, and one a calpain family cysteine proteinase encoding gene. Half of the 16 genes have no homologs outside the *Helotiales*.

Ascospore-specific expression (Soft Cluster 6)

Cluster 6 (Supplementary Table 7) is especially rich in transporter genes, with 17 members of the MFS transporter family, including predicted sugar, phosphate and carboxylic acid transporters as well as three ABC transporter genes, including *Bcatr*B and *Bcatr*D which have been implicated in resistance to fungicides and plant defense compounds (Schoonbeek et al. 2003; Schoonbeek et al. 2002; Hayashi et al. 2002; Schoonbeek et al. 2001). Moreover cluster 6 contains a number of genes encoding plant cell wall degrading enzymes, such as *BcPG2* (Kars et al. 2005a), *BcPME2* (Kars et al. 2005b) and a pectin lyase gene. Furthermore, this cluster comprises two aspartyl proteinase genes, *BcAP4* and *BcAP14* (ten Have et al. 2010).

Targeted deletion of the *MAT1-1-1*, *MAT1-1-5*, *MAT1-2-1* and *MAT1-2-4* genes

In order to study the function of mating type genes *MAT1-1-1*, *MAT1-1-5*, *MAT1-2-1* and *MAT1-2-4* in apothecium development, deletion mutants were generated by replacing the coding region of each gene by the hygromycin phosphotransferase gene (*HPH*) in wild type strains of *B. cinerea*, SAS56 and SAS405 (Supplementary Figure 6). In addition, the *MAT1-1-5* gene was deleted in the genetic background of strain B05.10 (not shown). Between three and six independent deletion mutants were obtained for each of the *MAT* genes. The growth rate and morphology of asexual structures (mycelium, sclerotia, macroconidia, microconidia) of all *ΔMAT1-1-1*, *ΔMAT1-1-5*, *ΔMAT1-2-1* and *ΔMAT1-2-4* deletion mutants were indistinguishable from those of the wild type (not shown).

Reciprocal crosses were set up, using two wild type strains, SAS56 and SAS405, and four single gene mutant strains (*ΔMAT1-1-1*, *ΔMAT1-1-5*, *ΔMAT1-2-1* or *ΔMAT1-2-4*) in all relevant combinations, the results of which are shown in Table 5. All crosses were carried out with three independent deletion mutants for each gene and results were similar for independent mutants (not shown). In the control cross of wild type sclerotia (maternal parent) fertilized with wild type microconidia (paternal parent), apothecia developed as described by Faretra et al. (1988) and Whetzel (1945). By contrast, no apothecia developed and there was no sign of outgrowth of primordia when crosses were performed between wild type strain SAS405 and mutant *ΔMAT1-1-1*, or between wild type strain SAS56 and mutant *ΔMAT1-2-1* (Figure 7). The lack of development of sexual structures was also observed in reciprocal crosses, indicating that the *MAT1-1-1* and *MAT1-2-1* genes are essential for the initiation of sexual development, both in maternal and paternal tissues.

Different results were observed for *ΔMAT1-1-5* and *ΔMAT1-2-4* deletion mutants. An aberrant development of apothecia was observed in crosses between wild type strain SAS405 and the *ΔMAT1-1-5* knockout mutant, as well as in crosses between wild type strain SAS56 and the *ΔMAT1-2-4* knockout mutant (Figure 7). The initial stages of primordium emergence and stipe development were similar to those in wild type apothecia, but the stipes remained blocked at the transition to disk development. The stipes did swell at the tip similar to wild type, but failed to expand laterally, even after several weeks of extended incubation. The stipes developed lobed, indented structures at the top (Figure 8), in which asci and ascospores were never observed (not shown).

The failure of *ΔMAT1-1-5* and *ΔMAT1-2-4* deletion mutants to make the switch from stipes to disks occurred in both reciprocal crosses irrespective whether the mutant was used in a cross as maternal parent (sclerotia) or as paternal parent (microconidia). Crosses between a *ΔMAT1-1-5* mutant and a *ΔMAT1-2-4* mutant yielded an identical, defective phenotype as crosses between either single mutant and their corresponding wild type mating partner (Figure 7), suggesting that these two genes jointly control the transition from stipe to disk development.

Table 5: Summary of crosses performed between *B. cinerea* deletion mutants in *MAT* genes.

Type of cross	Sclerotia (maternal parent)	Microconidia (paternal parent)	Fertility	Primordia	Stipe	Apothecial disk	Asci and ascospores
WT[+] x WT	SAS56	SAS405	Yes	Yes	Yes	Yes	Yes
WT x WT	SAS405	SAS56	Yes	Yes	Yes	Yes	Yes
WT x Δ*	SAS56	*ΔMAT1-2-1*[a]	No	No	No	No	No
WT x Δ	SAS56	*ΔMAT1-2-4*[a]	Yes	Yes	Yes	No	No
WT x Δ	SAS405	*ΔMAT1-1-1*[b]	No	No	No	No	No
WT x Δ	SAS405	*ΔMAT1-1-5*[b]	Yes	Yes	Yes	No	No
Δ x WT	*ΔMAT1-2-1*[a]	SAS56	No	No	No	No	No
Δ x WT	*ΔMAT1-2-4*[a]	SAS56	Yes	Yes	Yes	No	No
Δ x WT	*ΔMAT1-1-1*[b]	SAS405	No	No	No	No	No
Δ x WT	*ΔMAT1-1-5*[b]	SAS405	Yes	Yes	Yes	No	No
Δ x Δ	*ΔMAT1-2-1*[a]	*ΔMAT1-1-1*[b]	No	No	No	No	No
Δ x Δ	*ΔMAT1-2-1*[a]	*ΔMAT1-1-5*[b]	No	No	No	No	No
Δ x Δ	*ΔMAT1-2-4*[a]	*ΔMAT1-1-1*[b]	No	No	No	No	No
Δ x Δ	*ΔMAT1-2-4*[a]	*ΔMAT1-1-5*[b]	Yes	Yes	Yes	No	No
Δ x Δ	*ΔMAT1-1-1*[b]	*ΔMAT1-2-1*[a]	No	No	No	No	No
Δ x Δ	*ΔMAT1-1-1*[b]	*ΔMAT1-2-4*[a]	No	No	No	No	No
Δ x Δ	*ΔMAT1-1-5*[b]	*ΔMAT1-2-1*[a]	No	No	No	No	No
Δ x Δ	*ΔMAT1-1-5*[b]	*ΔMAT1-2-4*[a]	Yes	Yes	Yes	No	No
Control	*ΔMAT1-2-1*[a]	SMW[c]	No	No	No	No	No
Control	*ΔMAT1-2-4*[a]	SMW[c]	No	No	No	No	No
Control	*ΔMAT1-1-1*[b]	SMW[c]	No	No	No	No	No
Control	*ΔMAT1-1-5*[b]	SMW[c]	No	No	No	No	No
Control	SAS56	SMW[c]	No	No	No	No	No
Control	SAS405	SMW[c]	No	No	No	No	No

[a] mutant created in genetic background of SAS405

[b] mutant created in genetic background of SAS56

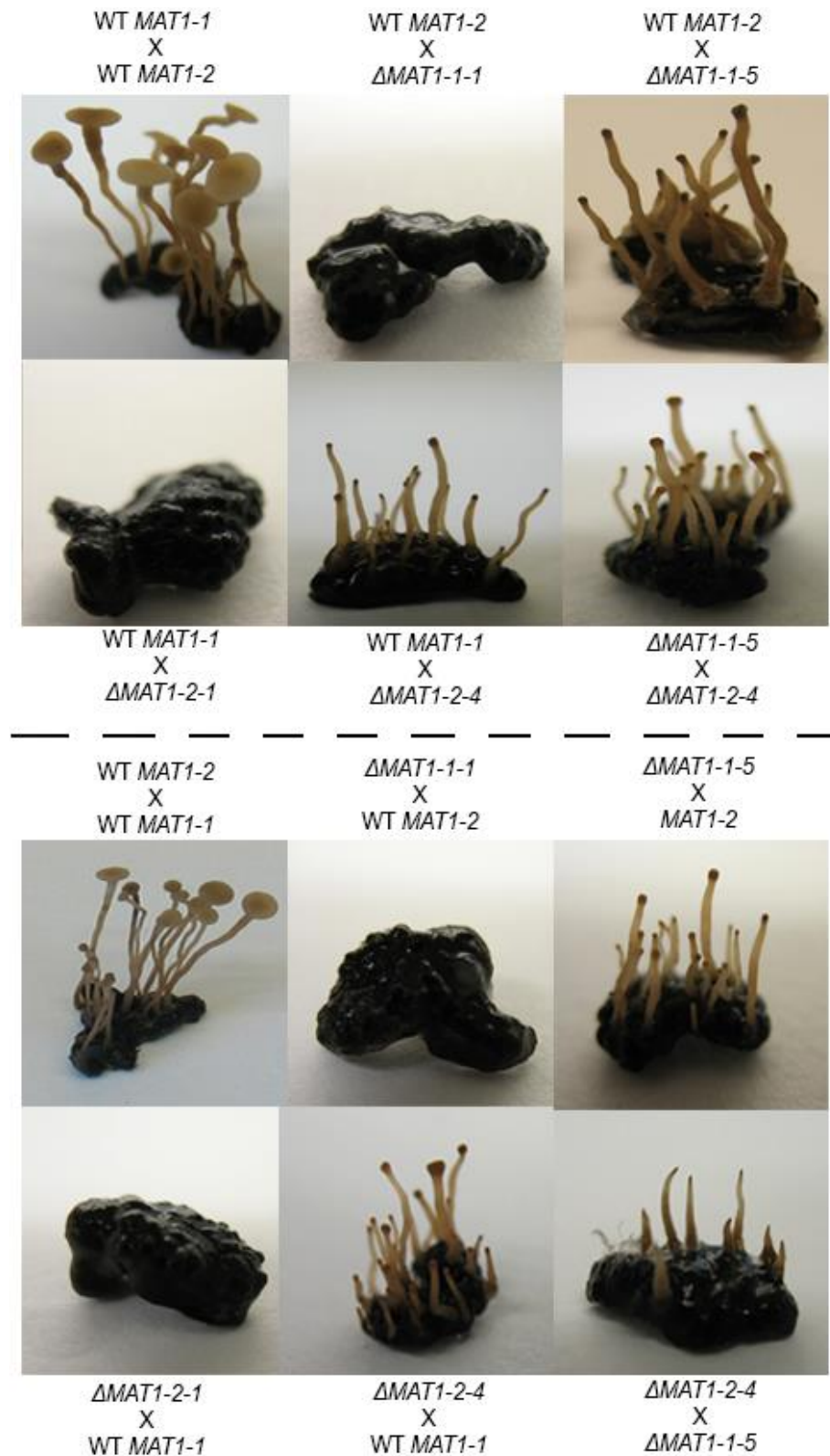[c] Sterile MilliQ Water

[+] WT wild type

* Δ mutant

Figure 7: Phenotypes of different crosses between wild type and mutants, as indicated. The maternal parent (sclerotia) is always mentioned first and the paternal parent (microconidia) is mentioned second. For each mutant, results of one deletion mutant are shown; similar results were obtained with two additional, independent deletion mutants.

Figure 8: Close-up of the phenotype resulting from a cross between wild type strain SAS405 (sclerotia) and *ΔMAT1-1-5* microconidia. The stipe is blocked in transition to the apothecial disk and forms only a lobed, indented structure at the tip of the stipe.

Gene expression in stipes blocked in transition to the apothecial disk

qRT-PCR was performed on *MAT* genes (*MAT1-1-1*, *MAT1-1-5*, *MAT1-2-1* and *MAT1-2-4*) in the *ΔMAT1-1-5* and *ΔMAT1-2-4* stipes and compared to wild type stipes at the same stage (Figure 9). In the *ΔMAT1-1-5* stipes, the transcript of the *MAT1-1-5* gene was undetectable as expected, but also the transcript level of the *MAT1-1-1* and *MAT1-2-1* genes was lower than in the wild type stipes. In the *ΔMAT1-2-4* stipes, the transcript of the *MAT1-2-4* gene was undetectable as expected, but also the transcript levels of the other three *MAT* genes were lower than in the wild type (Figure 9).
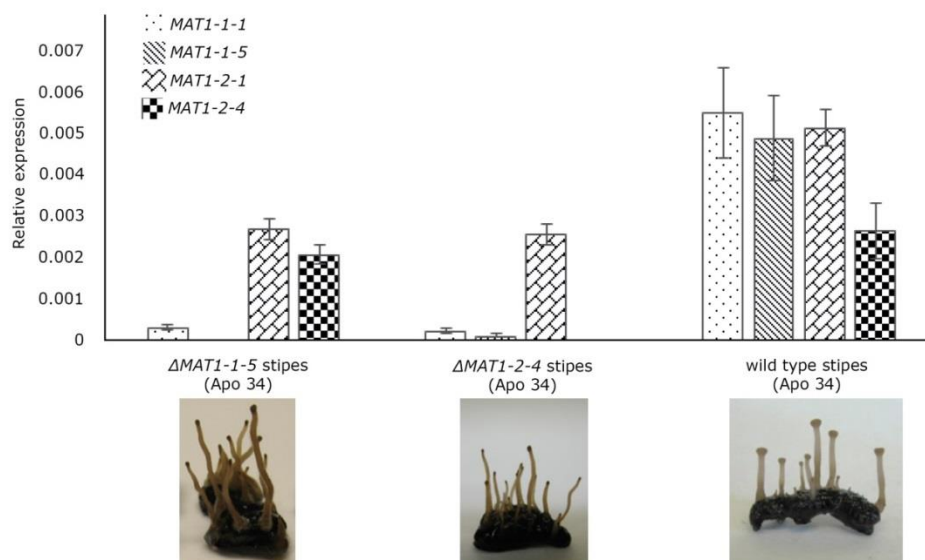
Figure 9: Relative expression of *MAT1-1-1*, *MAT1-1-5*, *MAT1-2-1* and *MAT1-2-4* genes in mutant stipes, blocked in transition to apothecial disks, as compared to stipes from a cross between two wild type isolates (competent for apothecial disk development) in the same stage. The left panel shows results for *ΔMAT1-1-5* mutant stipes, the middle panel shows results for *ΔMAT1-2-4* stipes, and the right panel shows results for wild type stipes. The data presented are the average of two biological replicates, with error bars indicating the standard deviation.

Fully elongated stipes with a swelling at the tip (blocked in transition to apothecial disk development, see Figure 8), were sampled from a cross between the wild type strain SAS405 and the *ΔMAT1-1-5* deletion mutant, made in the genetic background of strain B05.10 and from a control cross between two wild type strains at the same stage. Several stipes of mutant and wild type apothecia were pooled and RNA was isolated for transcriptome analysis. RNA sequencing reads were mapped on the genome of *B. cinerea* B05.10 and normalized read counts on gene models were determined.

A total of 6441704 and 6419648 read pairs were obtained from wild type and defective *ΔMAT1-1-5* stipes (Apo34), respectively, of which 94% (for both samples) could be mapped to the *B. cinerea* genome. A total of 33 genes with FPKM value >20 were exclusively expressed in wild type stipes (Apo34) (Supplementary Table 8). Another 81 genes with FPKM >20 were at least 50-fold downregulated in the mutant stipes (Supplementary Table 8). Conversely, a single gene with FPKM > 20 was exclusively expressed in the mutant stipes but not detectable in the wild type; moreover, 11 genes showed >20-fold higher transcript level in mutant stipes as compared to wild type (Supplementary Table 8). Most of these 12 genes had no functional annotation, and five of them were physically clustered (Supplementary Table 8).

Among the genes that were downregulated in the *ΔMAT1-1-5* mutant stipes (Apo34), three encoded RNA binding-domain containing proteins, two encoded transcription factors (Zn2Cys6 and C2H2), one an ortholog of histone H3 acetyltransferase protein GCN5/NGF1, one a FK506 suppressor gene Sfk1, one a high affinity glucose transporter, one a non-ribosomal peptide synthase (NRPS4), as well as dozens of genes that encoded proteins either specific to *Botrytis* or to *Sclerotiniaceae*.

Among the 114 genes that were downregulated in the mutant stipes, 11 were present in the "Top500" clusters 4 and 5 (genes specifically expressed in apothecial disks). Of these only two genes were functionally annotated, as a Zn2Cys6 transcription factor and the FK506 suppressor Sfk1. The remaining 9 genes are unique to *Botrytis* or have homologs only in the *Sclerotiniaceae*. There was also an overlap of 41 genes between the set of 114 genes downregulated in the *ΔMAT1-1-5* mutant stipes and the genes that are differentially

expressed in wild type apothecia between stages Apo34 and Apo56. These 41 genes encode, among others, a MHYT-domain signalling protein, the FK506 suppressor Sfk1, the putative calcium homeostasis protein regucalcin, the Zn2Cys6 transcription factor mentioned above, the protein kinase CBK1, a glucose transporter, an elongation factor 2 kinase, the non-ribosomal peptide synthase BcNRPS4, the histone acetyltransferase GCN5/NGF1 and a protein tyrosine phosphatase. Other genes in this set of 41 genes have no functional annotation and are mostly unique to *Botrytis* or have homologs only in the *Sclerotiniaceae*.

Discussion

***B. cinerea* apothecium development**

Using apothecia as a resource for transcriptome analysis to study sexual development within the Ascomycota is attractive as compared to other ascocarps such as cleistothecia, perithecia and pseudothecia because it is feasible to obtain tissues from distinct developmental stages fairly easily. Apothecia of *Sclerotiniaceae* germinate carpogenically from sclerotia in an aqueous environment minimizing contamination with hyphal tissue derived from the parents. Once the sclerotia rupture to give rise to the emergence of primordia, the apothecia develop over a period of several weeks. Although different developmental stages can be harvested, >100 primordia (1-3 mm in height) were required to obtain sufficient RNA for sequencing. The samples are clean and distinct, and the use of laser microdissection to obtain pure ascocarp tissues, as reported for *Sordaria macrospora* (Teichert et al. 2012), was not required for *B. cinerea.*

We carried out a detailed transcriptome analysis of sexual development of *B. cinerea*, starting with the sclerotia, through three stages of apothecial development and finally the ascospores that were released from mature apothecia. This study presents, to our knowledge, the first whole genome transcriptional analysis of sexual development within the *Helotiales*, and the first study on gene expression in ascospores of any filamentous Ascomycota species. Apothecial disks (stages 5-6, Figure 1) contain the greatest diversity of cell types, since they are composed of cell layers of excipulum and hymenium, of dikaryotic cells, diploid cells undergoing meiosis as well as asci and ascospores in different stages of development and maturity. This diversity in tissue types was reflected in the high number of

genes expressed in the apothecial disk sample: more than 98.5% of the gene models in the *B. cinerea* genome were represented by at least one read, and >90% of the gene models displayed an FPKM value ≥1. By contrast, sclerotia and ascospore samples, which represented more homogeneous tissue, displayed FPKM values ≥1 for only 75% of the gene models.

Transcriptome analysis of *B. cinerea* sclerotia, apothecia and ascospores

The RNA sequencing data were analysed in different ways. Firstly, the transcript levels were analysed for *B. cinerea* orthologs of genes from *Aspergillus nidulans* and *Sordaria macrospora*, which are known to regulate sexual development. Many *B. cinerea* orthologs were expressed to different levels during the consecutive stages of apothecium development, no unusual expression patterns could be distinguished. *B. cinerea* genes that, based on functions described in *A. nidulans*, likely act as positive regulators of sexual development, in several cases showed a high transcript level in early stages of apothecium development, which dropped in mature apothecial disks and ascospores. Conversely, some *B. cinerea* genes that, based on functions described in *A. nidulans*, likely act as negative regulators of sexual development displayed high transcript levels in sclerotia and primordia, which dropped in later stages of apothecium development and ascospores. Such patterns were, however, not consistently observed for all *B. cinerea* genes that presumably act as positive or negative regulators in sexual development, based on functions described in *A. nidulans*. In several cases the expression level was fairly constant, or showed a distinct pattern (Figures S1-5). It should be kept in mind that the role of any particular gene as a positive or negative regulator of sexual development, does not necessarily imply that this gene itself is differentially transcribed in distinct stages of sexual development.

The second type of analysis identified genes which displayed significant changes in transcript levels between two consecutive stages of sexual development. The biggest changes were observed in the transition from sclerotia to primordia (with >2000 differentially expressed genes), and even more so in the transition from mature disks to ascospores (with >5000 differentially expressed genes). Both these transitions reflect a dramatic morphological and physiological change. It is thus not surprising that these transitions showed the largest shifts in gene expression, but the fact that almost half of the genes in the genome are differentially

expressed in the transition from apothecial disks to ascospores (with equal proportions up- and down-regulated) was surprising. The transitions from primordia to stipes and from stipes to disks resulted in substantially lower numbers of differentially expressed genes. Especially the primordia and stipes are morphologically similar to each other. There is a continuous tissue elongation, eventually swelling at the tip when the stipe has emerged from the water and reached a height of about 1 cm. It was thus no surprise that only 27 genes were differentially expressed between these stages, however, these genes were all down-regulated. We anticipated that the upregulation of genes required for the swelling and transition to disk development might have been detected, however, no upregulated genes were identified. There were 884 genes differentially expressed between stages Apo34 and Apo56, and GO enrichment analysis showed that some terms related to sexual development were enriched in the dataset. Specifically, the upregulated genes displayed, amongst others, an overrepresentation of the term "G2/M transition of mitotic cell cycle" while the term "negative regulation of sexual sporulation resulting in formation of cellular spore" was overrepresented in the downregulated genes at this transition.

Soft and hierarchical clustering were applied to identify genes with a stage-specific expression pattern. The results of both methods were largely congruent for both methods, with the only difference that soft clustering divided the genes with high expression levels in apothecial disks into two clusters, which differed in the extent to which transcript levels started to increase in stipes. The hierarchical clustering, however, did not support this division. Overall the clustering methods identified five distinct clusters, each typified by genes with a very high transcript level in one stage and extremely low levels in the four other stages.

167 genes were exclusively expressed in sclerotia among which four HET-domain proteins, whose physiological function in *B. cinerea* remains unknown. Also several genes involved in taurine and carnosine metabolism were highly expressed in sclerotia, possibly because of the function of these compounds as antioxidants. Also mannitol dehydrogenase might function to generate mannitol as a scavenger of reactive oxygen species. Polyketide synthase *BcPKS19* was specifically expressed in sclerotia, but its product is unknown yet. The *BcPKS19* gene is flanked by a glutathione S-transferase encoding gene, but for the remainder it is

surrounded on both sides by >10 kb repetitive sequences, separated from other genes that are normally present in secondary metabolite gene clusters.

There were very few genes with primordia-specific expression, one of which encodes a small secreted protein, with 13 cysteine residues in a pattern that very much resembles the cysteine spacing present in hydrophobins. The reason for not annotating this protein as a hydrophobin might be the large (and uneven) number of cysteine residues. Also specifically expressed in primordia was a group of five physically clustered genes encoding the polyketide synthase *BcPKS15*, whose product is unknown, an alcohol dehydrogenase, a methyltransferase, and two transcription factors. Stipes showed a specific expression of genes encoding a secreted tannase, a feruloyl esterase and an ornithine decarboxylase, indicating that stipes may produce putrescine.

Among the 81 genes almost exclusively expressed in the apothecial disks, two genes encoded Zn2Cys6-type transcription factors, three encoded putative transporters, and three were single genes encoding a secreted glutaminase, a calpain family cysteine proteinase, a homolog of the SNF2 chromatin remodelling protein, and a WD-domain protein (ortholog of *S. cerevisiae* Cdc20p which is part of the APC complex involved in meiosis; Pan and Chen 2004).

Mature ascospores displayed an expression profile remarkably distinct from apothecial disks. More than 5000 genes were differentially expressed between apothecial disks and the ascospores, representing almost half the genes present in the *B. cinerea* genome. Among the 2500 upregulated genes were many that likely function in plant infection, including genes encoding pectinases (an exo- and endopolygalacturonase, pectin methylesterase), aspartic proteinases, as well as putative sugar, phosphate and carboxylic acid transporters (member of the MFS superfamily) and ABC transporters known to be involved in efflux of plant defence compounds. This observation suggests that ascospores are primed, at least at the transcriptional level, for the production of virulence factors prior to contact with a host plant. Whether the transcripts are actually translated into functional enzymes is uncertain.

The development of an apothecium is a paraphyletic trait

Both the cluster analysis and differential expression analysis between two consecutive developmental stages identified a large number of genes that lack known protein domains and are unique to *B. cinerea*, or restricted to fungi in the family *Sclerotiniaceae.* More than 60% of the genes that were identified by cluster analysis as being expressed in the three stages of apothecium development (primordia, stipes, disks) have no homologues in fungi producing other types of fruiting bodies (perithecia, cleistothecia, pseudothecia). Traeger et al. (2013) reported a similar observation for *Pyrenoma confluens*, a basal Pezizomycete fungus that also produces apothecia and contains in its genome >5700 "orphan" genes, of which >20% were upregulated during sexual development. There was no homology, however, between the *B. cinerea* genes and *P. confluens* genes that are specifically expressed in apothecia. Gargas and Taylor (1995) inferred from SSU rDNA sequences that Ascomycota species that are capable of producing apothecia can be found in four different orders and therefore do not represent a monophyletic lineage. This indicates that the development of an apothecium is a paraphyletic trait. *Blumeria graminis* is the closest relative to *B. cinerea* and *S. sclerotiorum* of which the genome was sequenced (Spanu et al., 2010) and this species produces cleistothecia as fruiting bodies. The apothecium of *Sclerotiniaceae* may be a recent invention that evolved after their divergence from the *Erisyphales.*

Mating type genes *MAT1-1-5* and *MAT1-2-4* jointly act as dimeric transcriptional regulators

Single gene deletion mutants in the *B. cinerea MAT1-1* or *MAT1-2* locus were strongly compromised in apothecium development. Deletion of the *MAT1-1-1* gene or the *MAT1-2-1* gene, both of which are highly conserved among Ascomycota, rendered *B. cinerea* entirely sterile, as in other Ascomycota fungi (Ferreira et al. 1998). Even the emergence of primordia was blocked, suggesting that sexual fertility was affected in a very early stage. The precise defect in sexual development was not further investigated since it is unknown when and where in the *B. cinerea* sclerotium the fertilization process occurs during the weeks after adding microconidia of the paternal parent to the sclerotia. In any case, the *MAT1-1-1* and *MAT1-2-1* genes are essential to initiate apothecium development in *B. cinerea*.

On the other hand, the *MAT1-1-5* and *MAT1-2-4* genes are only required in later stages of apothecium development. Deletion of the *MAT1-1-5* or the *MAT1-2-4* gene still resulted in formation of stipes which were, however, blocked in the transition to an apothecial disk. We never observed asci or ascospores in these mutant stipes. The same phenotype was observed in crosses using *ΔMAT1-1-5* or *ΔMAT1-2-4* mutants with a wild type strain of opposite mating type, and the defect occurred in reciprocal crosses alike. Also a cross between a *ΔMAT1-1-5* and a *ΔMAT1-2-4* mutant resulted in the same phenotype, demonstrating that the *MAT1-1-5* and *MAT1-2-4* genes display a genetic interaction.

The transition from stipe to apothecial disk is typified by the formation of crozier cells in which karyogamy occurs (Malagnac et al., 1997; Coppin et al. 2012) and the resulting diploid nuclei subsequently enter meiosis to eventually form 8 ascospores in an ascus. We propose that *MAT1-1-5* and *MAT1-2-4* act as dimeric transcriptional regulators that directly or indirectly control the formation of crozier cells, and the absence of either of these proteins results in failure to proceed to karyogamy which blocks further downstream processes such as apothecial disk expansion. It remains to be demonstrated whether MAT1-1-5 and MAT1-2-4 proteins indeed physically interact to perform a complex with DNA binding properties, and to which sequence elements they might bind. To obtain a first glance of genes controlled by the *MAT1-1-5* gene, RNA sequencing was performed to reveal which genes were differentially expressed in *ΔMAT1-1-5* stipes that were blocked in transition to disks, as compared to wild type apothecia. Among the 114 genes that were entirely switched off or >50-fold down-regulated in the mutant stipes were three genes encoding RNA binding-domain containing proteins, two genes encoding transcription factors (Zn2Cys6-type and C2H2-type), and the ortholog of the histone H3 acetyltransferase protein GCN5. The transcription factors might be important in regulating the expression of downstream genes, whereas the histone H3 acetyltransferase GCN5 might be involved in epigenetic regulation of gene expression, or in facilitating meiotic recombination. Yamada et al. (2004) reported that *Schizosaccharomyces pombe* double mutants in which the histone acetyltransferase Gcn5 and the Swi2-like chromatin remodeling factor Snf22 were both deleted, showed abolished chromatin remodeling and significant reduction of meiotic recombination in a recombination hotspot.

There is as yet no evidence for epigenetic regulation of sexual development in filamentous Ascomycota, but the expression pattern of the histone acetyltransferase GCN5 and its lack of expression in *ΔMAT1-1-5* mutant stipes might suggest that this gene is involved in regulating apothecium disk development. Expression data in the present *B. cinerea* dataset provide (indirect) hints for epigenetic regulation in certain stages. Several examples were observed of physically clustered genes that are co-regulated during developmental transitions. The most striking example was in the set of genes with a sclerotium-specific expression pattern: of the 167 genes in this set, 26 genes (all with unknown function) are located in clusters of three to seven consecutive genes. Future studies need to resolve whether the co-expression of such physically clustered genes is mediated by common transcription factor binding sites in their promoter regions, or by epigenetic regulation of chromatin architecture.

The present study has revealed that *MAT1-1-5* and *MAT1-2-4* are important (transcriptional) regulators of *B. cinerea* apothecium development, and has provided insight into genes and processes that they control. The downstream pathways regulated by *MAT1-1-5* and *MAT1-2-4* will be subject of future studies.

Supporting information

Supplementary Figure 1, Supplementary Figure 2, Supplementary Figure 3, Supplementary Figure 4, Supplementary Figure 5, Supplementary Figure 6, Supplementary Table 1, Supplementary Table 2, Supplementary Table 3, Supplementary Table 4, Supplementary Table 5, Supplementary Table 6, Supplementary Table 7 and Supplementary Table 8.

References

Amselem J, Cuomo CA, van Kan JAL, Viaud M, Benito EP, Couloux A, Coutinho PM, de Vries RP, Dyer PS, Fillinger S, Fournier E, Gout L, Hahn M, Kohn L, Lapalu N, Plummer KM, Pradier J-M, Quévillon E, Sharon A, Simon A, ten Have A, Tudzynski B, Tudzynski P, Wincker P, Andrew M, Anthouard V, Beever RE, Beffa R, Benoit I, Bouzid O, Brault B, Chen Z, Choquer M, Collémare J, Cotton P, Danchin EG, Da Silva C, Gautier A, Giraud C, Giraud T, Gonzalez C, Grossetete S, Güldener U, Henrissat B, Howlett BJ, Kodira C, Kretschmer M, Lappartient A, Leroch M, Levis C, Mauceli E, Neuvéglise C, Oeser B, Pearson M, Poulain J, Poussereau N, Quesneville H, Rascle C, Schumacher J, Ségurens B, Sexton A, Silva E, Sirven C, Soanes DM, Talbot NJ, Templeton M, Yandava C, Yarden O, Zeng Q, Rollins JA, Lebrun M-H, Dickman M (2011) Genomic analysis of the necrotrophic fungal pathogens *Sclerotinia sclerotiorum* and *Botrytis cinerea*. PLoS Genetics 7 (8):e1002230.

Anders S, Huber W (2010) Differential expression analysis for sequence count data. Genome Biology 11 (10):R106

Anders S, Pyl PT, Huber W (2014) HTSeq–A Python framework to work with high-throughput sequencing data. Bioinformatics:btu638

Arnaise S, Zickler D, Le Bilcot S, Poisier C, Debuchy R (2001) Mutations in mating-type genes of the heterothallic fungus *Podospora anserina* lead to self-fertility. Genetics 159 (2):545-556.

Benito E, ten Have A, van 't Klooster J, van Kan JL (1998) Fungal and plant gene expression during synchronized infection of tomato leaves by *Botrytis cinerea*. European Journal of Plant Pathology 104 (2):207-220.

Benjamini Y, Hochberg Y (1995) Controlling the false discovery rate: A practical and powerful approach to multiple testing. Journal of the Royal Statistical Society Series B. Methodological 57 (1):289-300.

Bidard F, Aït Benkhali J, Coppin E, Imbeaud S, Grognet P, Delacroix H, Debuchy R (2011) Genome-wide gene expression profiling of fertilization competent mycelium in opposite mating types in the heterothallic fungus *Podospora anserina*. PLoS ONE 6 (6):e21476.

Breakspear A, Momany M (2007) The first fifty microarray studies in filamentous fungi. Microbiology 153 (1):7-15.

Coppin E, Berteaux-Lecellier V, Bidard F, Brun S, Ruprich-Robert G, Espagne E, Aït-Benkhali J, Goarin A, Nesseir A, Planamente S, Debuchy R, Silar P (2012) Systematic Deletion of Homeobox Genes in *Podospora anserina* Uncovers Their Roles in Shaping the Fruiting Body. PLoS ONE 7 (5):e37488.

Delmas S, Pullan ST, Gaddipati S, Kokolski M, Malla S, Blythe MJ, Ibbett R, Campbell M, Liddell S, Aboobaker A, Tucker GA, Archer DB (2012) Uncovering the genome-wide transcriptional responses of the filamentous fungus *Aspergillus niger* to lignocellulose using RNA sequencing. PLoS Genetics 8 (8):e1002875.

Dyer PS, O'Gorman CM (2012) Sexual development and cryptic sexuality in fungi: insights from *Aspergillus species*. FEMS microbiology reviews 36 (1):165-192.

Faretra F, Antonacci E (1987) Production of apothecia of *Botryotinia fuckeliana* (de Bary) Whetz. under controlled environmental conditions. Phytopathologia Mediterranea 26:29–35.

Faretra F, Antonacci E, Pollastro S (1988) Sexual behaviour and mating system of *Botryotinia fuckeliana*, teleomorph of *Botrytis cinerea*. Journal of General Microbiology 134 (9):2543-2550.

Ferreira AV-B, An Z, Metzenberg RL, Glass NL (1998) Characterization of mat A-2, mat A-3 and ΔmatA Mating-Type Mutants of *Neurospora crassa*. Genetics 148 (3):1069-1079.

Fu X, Fu N, Guo S, Yan Z, Xu Y, Hu H, Menzel C, Chen W, Li Y, Zeng R, Khaitovich P (2009) Estimating accuracy of RNA-Seq and microarrays with proteomics. BMC Genomics 10 (1):161.

Futschik ME, Carlisle B (2005) Noise-robust soft clustering of gene expression time-course data. Journal of Bioinformatics and Computational Biology 3 (04):965-988.

Gargas A, Taylor JW (1995) Phylogeny of Discomycetes and early radiations of the apothecial Ascomycotina inferred from SSU rDNA sequence data. Experimental Mycology 19 (1):7-15.

Glass NL, Smith ML (1994) Structure and function of a mating-type gene from the homothallic species *Neurospora africana*. Molecular and General Genetics 244 (4):401-409.

Han Y, Joosten H-J, Niu W, Zhao Z, Mariano PS, McCalman M, Van Kan J, Schaap PJ, Dunaway-Mariano D (2007) Oxaloacetate hydrolase, the C–C bond lyase of oxalate secreting fungi. Journal of Biological Chemistry 282 (13):9581-9590.

Hayashi K, Schoonbeek HJ, De Waard MA (2002) Expression of the ABC transporter BcatrD from *Botrytis cinerea* reduces sensitivity to sterol demethylation inhibitor fungicides. Pesticide Biochemistry and Physiology 73 (2):110-121.

Heitman J (2007) Sex in fungi : molecular determination and evolutionary implications. ASM Press, Washington, D.C.

Jurick WM, Dickman MB, Rollins JA (2004) Characterization and functional analysis of a cAMP-dependent protein kinase A catalytic subunit gene (pka1) in *Sclerotinia sclerotiorum*. Physiological and Molecular Plant Pathology 64 (3):155-163.

Kars I, Krooshof GH, Wagemakers L, Joosten R, Benen JAE, van Kan JAL (2005a) Necrotizing activity of five *Botrytis cinerea* endopolygalacturonases produced in *Pichia pastoris*. Plant Journal 43 (2):213-225.

Kars I, McCalman M, Wagemakers L, van Kan JA (2005b) Functional analysis of *Botrytis cinerea* pectin methylesterase genes by PCR-based targeted mutagenesis: Bcpme1 and Bcpme2 are dispensable for virulence of strain B05. 10. Molecular Plant Pathology 6 (6):641-652.

Kawahara Y, Oono Y, Kanamori H, Matsumoto T, Itoh T, Minami E (2012) Simultaneous RNA-seq analysis of a mixed transcriptome of rice and blast fungus interaction. PLoS ONE 7 (11):e49423.

Kerr MK, Martin M, Churchill GA (2000) Analysis of variance for gene expression microarray data. Journal of Computational Biology 7 (6):819-837.

Kim D, Pertea G, Trapnell C, Pimentel H, Kelley R, Salzberg SL (2013) TopHat2: accurate alignment of transcriptomes in the presence of insertions, deletions and gene fusions. Genome Biololgy 14 (4):R36.

Klix V, Nowrousian M, Ringelberg C, Loros J, Dunlap J, Pöggeler S (2010) Functional characterization of MAT1-1 specific mating-type genes in the homothallic ascomycete *Sordaria macrospora* provides new insights into essential and nonessential sexual regulators. Eukaryotic cell 9 (6):894-905.

Koch CA, Li PCH, Utkhede RS (2005) Evaluation of thin films of agarose on glass for hybridization of DNA to identify plant pathogens with microarray technology. Analytical Biochemistry 342 (1):93-102.

Li M, Liang X, Rollins JA (2011) Sclerotinia sclerotiorum γ-Glutamyl Transpeptidase (Ss-Ggt1) Is Required for Regulating Glutathione Accumulation and Development of Sclerotia and Compound Appressoria Molecular Plant-Microbe Interactions. Molecular plant-microbe interactions 25 (3):412-420.

Livak KJ, Schmittgen TD (2001) Analysis of relative gene expression data using Real-Time Quantitative PCR and the $2^{-\Delta\Delta CT}$ Method. Methods 25 (4):402-408.

Malagnac F, Wendel B, Goyon C, Faugeron G, Zickler D, Rossignol J-L, Noyer-Weidner M, Vollmayr P, Trautner TA, Walter J (1997) A gene essential for de novo methylation and development in *Ascobolus* reveals a new type of eukaryotic DNA methyltransferase structure. Cell 91: 281-290.

Marioni JC, Mason CE, Mane SM, Stephens M, Gilad Y (2008) RNA-seq: an assessment of technical reproducibility and comparison with gene expression arrays. Genome Research 18 (9):1509-1517.

Martin SH, Wingfield BD, Wingfield MJ, Steenkamp ET (2011) Structure and evolution of the *Fusarium* mating type locus: New insights from the *Gibberella fujikuroi* complex. Fungal Genetics and Biology 48 (7):731-740.

Metzenberg RL, Glass NL (1990) Mating type and mating strategies in *Neurospora*. Bioessays 12 (2):53-59.

Orshinsky AM, Hu J, Opiyo SO, Reddyvari-Channarayappa V, Mitchell TK, Boehm MJ (2012) RNA-Seq Analysis of the *Sclerotinia homoeocarpa* – Creeping Bentgrass Pathosystem. PLoS ONE 7 (8):e41150.

Ostapenko D, Gileadi O (2000) Rad25p, a DNA helicase subunit of yeast transcription factor TFIIH, is required for promoter escape in vivo. Gene 245 (1):109-117.

Pan J, Chen RH (2004) Spindle checkpoint regulates Cdc20p stability in *Saccharomyces cerevisiae*. Genes and Development 18 (12):1439-1451.

Pöggeler S, Kück U (2000) Comparative analysis of the mating-type loci from *Neurospora crassa* and *Sordaria macrospora*: identification of novel transcribed ORFs. Molecular and General Genetics 263 (2):292-301.

Pöggeler S, Nowrousian M, Kück U (2006) Fruiting-body development in ascomycetes. The Mycota I. In Kües U, Fischer R, Pöggeler S, Nowrousian M, & U. Kück (Eds.), *Growth, Differentiation and sexuality* (pp. 325–355). Berlin Heidelberg: Springer.

Pöggeler S, Risch S, Kück U, Osiewacz HD (1997) Mating-type genes from the homothallic fungus *Sordaria Macrospora* are functionally expressed in a heterothallic Ascomycete. Genetics 147 (2):567-580.

Schoonbeek HJ, Raaijmakers JM, De Waard MA (2002) Fungal ABC transporters and microbial interactions in natural environments. Molecular Plant-Microbe Interactions 15 (11):1165-1172.

Schoonbeek H, Del Sorbo G, De Waard MA (2001) The ABC transporter BcatrB affects the sensitivity of *Botrytis cinerea* to the phytoalexin resveratrol and the fungicide fenpiclonil. Molecular Plant-Microbe Interactions 14 (4):562-571.

Schoonbeek HJ, van Nistelrooy JGM, de Waard MA (2003) Functional analysis of ABC transporter genes from *Botrytis cinerea* identifies BcatrB as a transporter of eugenol. European Journal of Plant Pathology 109 (9):1003-1011.

Spanu PD, Abbott JC, Amselem J, Burgis TA, Soanes DM, Stüber K, van Themaat EVL, Brown JK, Butcher SA, Gurr SJ (2010) Genome expansion and gene loss in powdery mildew fungi reveal tradeoffs in extreme parasitism. Science 330 (6010):1543-1546.

Soanes DM, Chakrabarti A, Paszkiewicz KH, Dawe AL, Talbot NJ (2012) Genome-wide transcriptional profiling of appressorium development by the rice blast fungus *Magnaporthe oryzae*. PLoS pathogens 8 (2):e1002514.

Steindorff A, Ramada MH, Coelho AS, Miller RN, Pappas G, Ulhoa C, Noronha E (2014) Identification of mycoparasitism-related genes against the phytopathogen *Sclerotinia sclerotiorum* through transcriptome and expression profile analysis in *Trichoderma harzianum*. BMC Genomics 15 (1):204

Teichert I, Nowrousian M, Pöggeler S, Kück U (2014) The filamentous fungus *Sordaria macrospora* as a genetic model to study fruiting body development. Advances in Genetics 87:199-244.

Teichert I, Wolff G, Kück U, Nowrousian M (2012) Combining laser microdissection and RNA-seq to chart the transcriptional landscape of fungal development. BMC Genomics 13 (1):511.

ten Have A, Espino JJ, Dekkers E, Van Sluyter SC, Brito N, Kay J, González C, van Kan JA (2010) The *Botrytis cinerea* aspartic proteinase family. Fungal Genetics and Biology 47 (1):53-65.

Traeger S, Altegoer F, Freitag M, Gabaldon T, Kempken F, Kumar A, Marcet-Houben M, Pöggeler S, Stajich JE, Nowrousian M (2013) The genome and development-dependent transcriptomes of *Pyronema confluens* : A window into fungal evolution. PLoS Genetics 9 (9):e1003820.

Trapnell C, Hendrickson DG, Sauvageau M, Goff L, Rinn JL, Pachter L (2013) Differential analysis of gene regulation at transcript resolution with RNA-seq. 31 (1):46-53.

van der Vlugt-Bergmans CJB, Brandwagt BF, Vant't Klooster JW, Wagemakers CAM, Van Kan JAL (1993) Genetic variation and segregation of DNA polymorphisms in *Botrytis cinerea*. Mycological Research 97 (10):1193-1200.

Velculescu VE, Zhang L, Vogelstein B, Kinzler KW (1995) Serial analysis of gene expression. Science 270 (5235):484-487.

Wang Z-X, Zhou X-Z, Meng H-M, Liu Y-J, Zhou Q, Huang B (2014a) Comparative transcriptomic analysis of the heat stress response in the filamentous fungus *Metarhizium anisopliae* using RNA-Seq. Applied microbiology and biotechnology 98 (12):5589-5597.

Wang Z, Lopez-Giraldez F, Lehr N, Farré M, Common R, Trail F, Townsend JP (2014b) Global gene expression and focused knockout analysis reveals genes associated with fungal fruiting body development in *Neurospora crassa*. Eukaryotic Cell 13 (1):154-169.

Whetzel HH (1945) A synopsis of the genera and species of the Sclerotiniaceae, a family of stromatic inoperculate Discomycetes. Mycologia 37 (6):648-714.

Yamada T, Mizuno K, Hirota K, Kon N, Wahls WP, Hartsuiker E, Murofushi H, Shibata T, Ohta K (2004) Roles of histone acetylation and chromatin remodeling factor in a meiotic recombination hotspot. EMBO Journal 23(8):1792-803.

Yun S-H, Arie T, Kaneko I, Yoder OC, Turgeon BG (2000) Molecular organization of mating type loci in heterothallic, homothallic, and asexual *Gibberella/Fusarium* Species. Fungal Genetics and Biology 31 (1):7-20.

Yun S-H, Berbee ML, Yoder OC, Turgeon BG (1999) Evolution of the fungal self-fertile reproductive life style from self-sterile ancestors. Proceedings of the National Academy of Sciences 96 (10):5592-5597.

Zhang L, Hua C, Stassen JH, Chatterjee S, Cornelissen M, van Kan JAL (2014) Genome-wide analysis of pectate-induced gene expression in *Botrytis cinerea*: identification and functional analysis of putative D-galacturonate transporters. Fungal Genetics and Biology 72:182-191.

Zhang L, Thiewes H, van Kan JAL (2011) The D-galacturonic acid catabolic pathway in *Botrytis cinerea*. Fungal Genetics and Biology 48 (10):990-997.

Supplementary Figure 1

Transcript levels of *B.cinerea* genes orthologous to *A. nidulans* genes involved in perception of environmental signals during sexual development (according to Dyer and O'Gorman, 2012).

Tissue samples analysed are *B. cinerea* sclerotia, apothecial primordia, stipes, disks, as well as ascospores.

Transcript levels are presented as average FPKM values of two independent biological replicates, with the exception of the sclerotia, which represent a single sample. A: activator of sexual development, R: repressor of sexual development
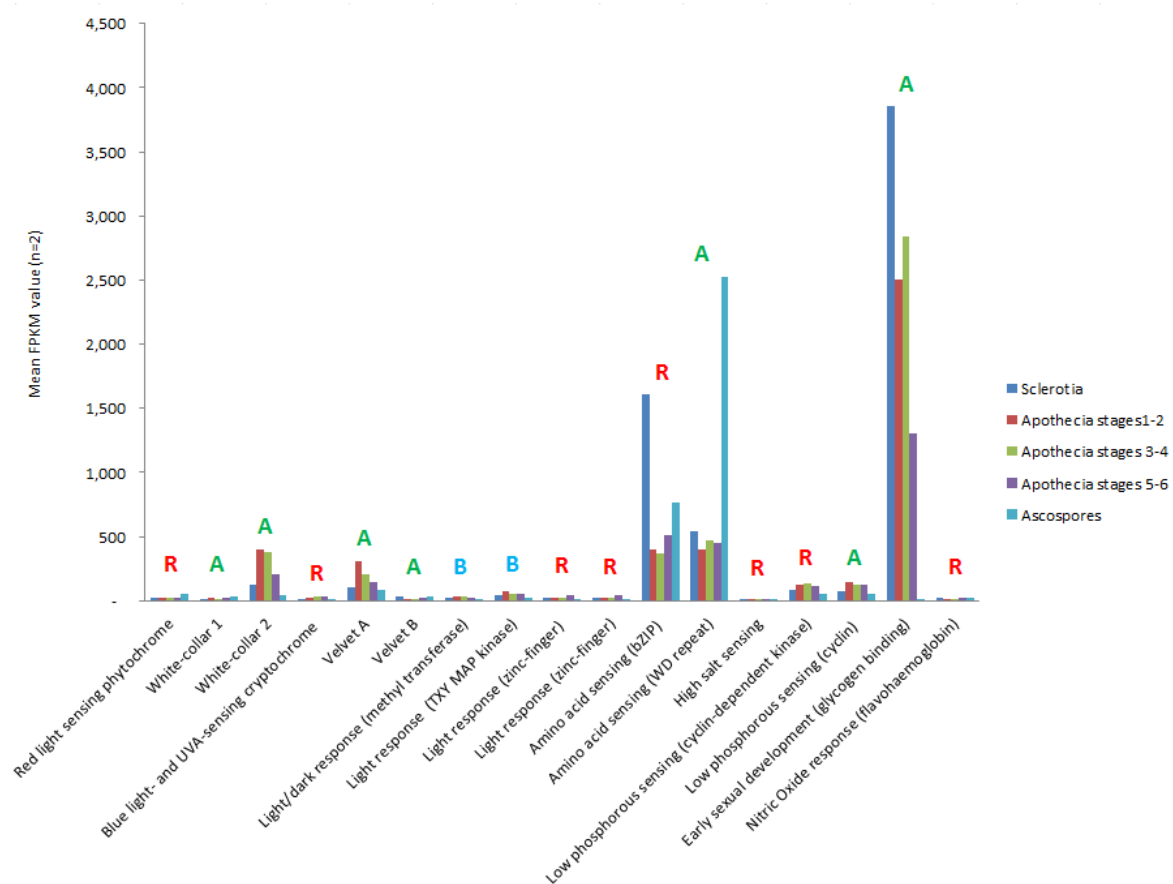
Supplementary Figure 2

Transcript levels of *B. cinerea* genes orthologous to *A. nidulans* genes involved in mating processes and signal transduction during sexual development (according to Dyer and O'Gorman, 2012).

Tissue samples analysed are *B. cinerea* sclerotia, apothecial primordia, stipes, disks, as well as ascospores.

Transcript levels are presented as average FPKM values of two independent biological replicates, with the exception of the sclerotia, which represent a single sample. A: activator of sexual development, R: repressor of sexual development

Supplementary Figure 3
Transcript levels of *B. cinerea* genes orthologous to *A. nidulans* genes encoding transcription factors and regulatory proteins involved in sexual development (according to Dyer and O'Gorman, 2012).

Tissue samples analysed are *B. cinerea* sclerotia, apothecial primordia, stipes, disks, as well as ascospores.

Transcript levels are presented as average FPKM values of two independent biological replicates, with the exception of the sclerotia, which represent a single sample. A: activator of sexual development, R: repressor of sexual development

Supplementary Figure 4

Transcript levels of *B. cinerea* genes orthologous to *A. nidulans* genes involved in endogenous physiological processes during sexual development (according to Dyer and O'Gorman, 2012).

Tissue samples analysed are *B. cinerea* sclerotia, apothecial primordia, stipes, disks, as well as ascospores.

Transcript levels are presented as average FPKM values of two independent biological replicates, with the exception of the sclerotia, which represent a single sample. A: activator of sexual development, R: repressor of sexual development
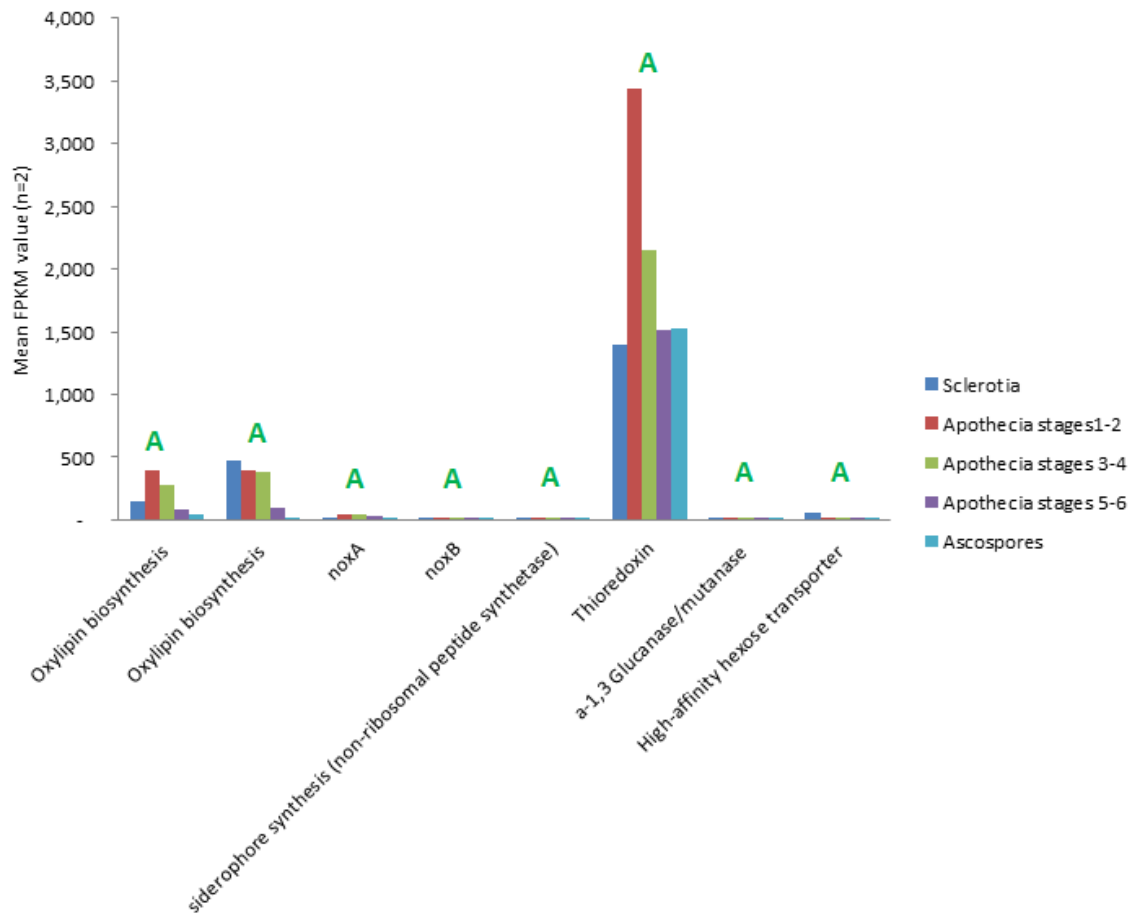
Supplementary Figure 5

Transcript levels of *B. cinerea* genes orthologous to *A. nidulans* genes involved in ascospore production and maturation during sexual development (according to Dyer and O'Gorman, 2012).

Tissue samples analysed are *B. cinerea* sclerotia, apothecial primordia, stipes, disks, as well as ascospores.

Transcript levels are presented as average FPKM values of two independent biological replicates, with the exception of the sclerotia, which represent a single sample. A: activator of sexual development, R: repressor of sexual development
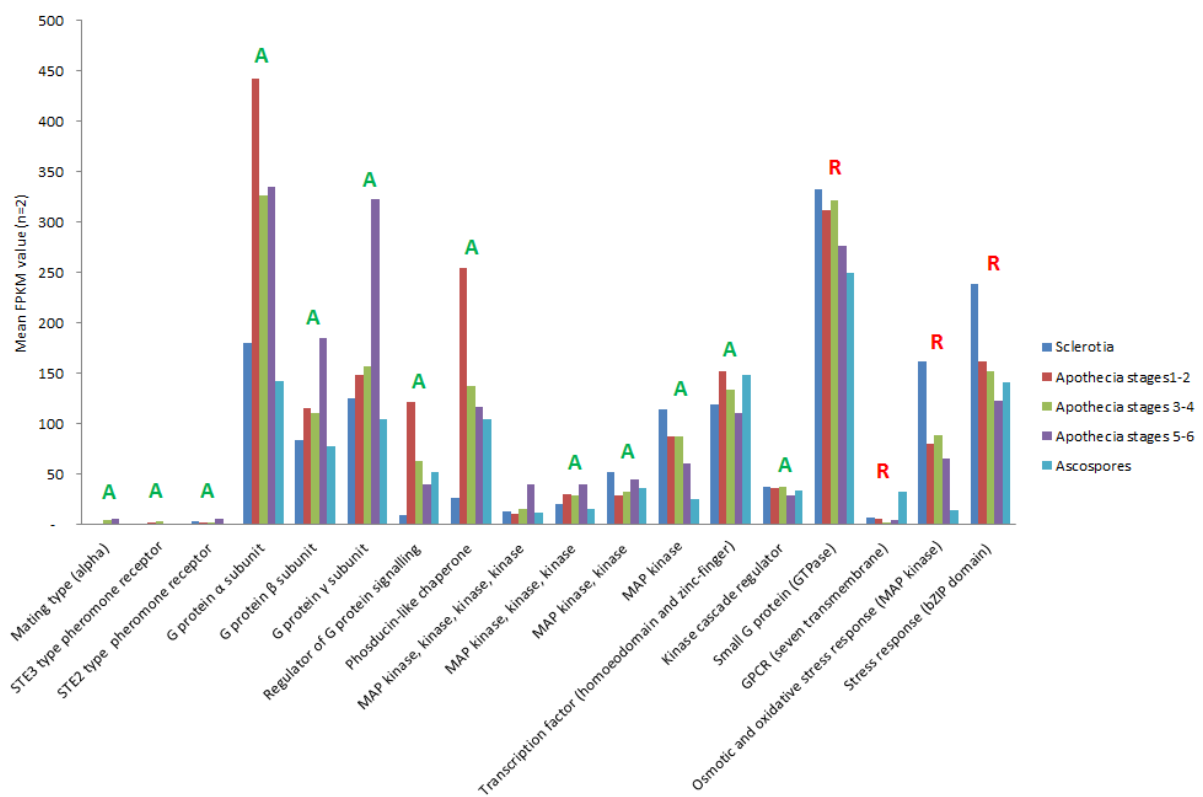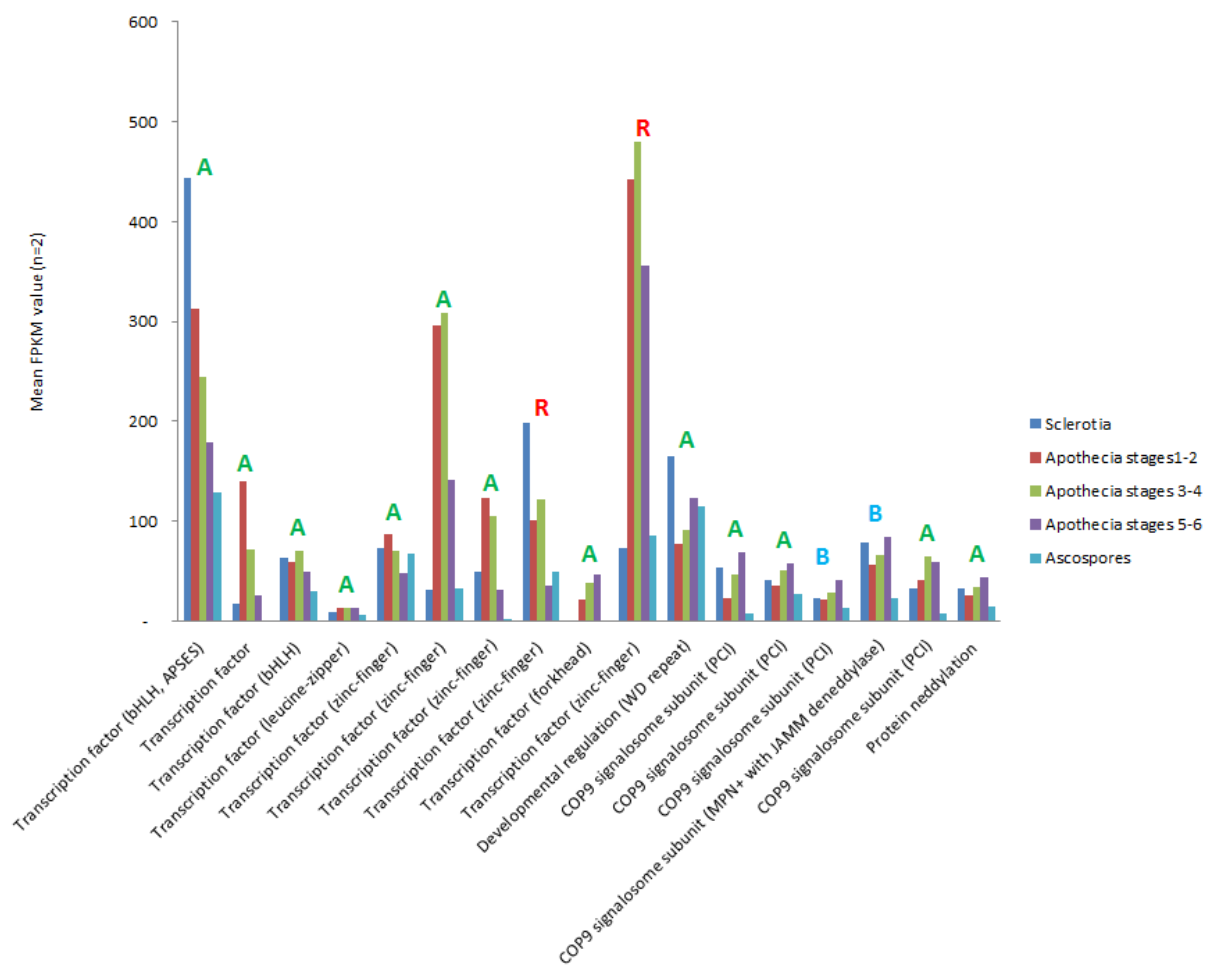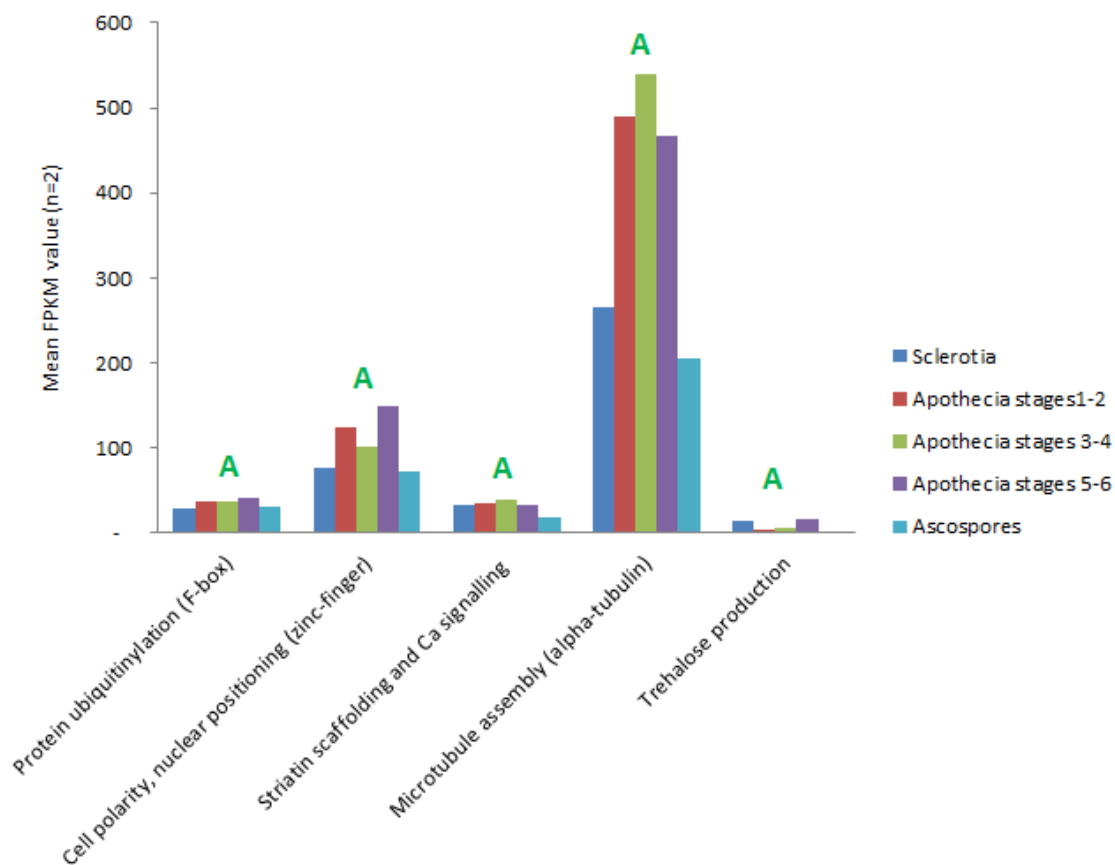
Supplementary Figure 6

Schematic representation of strategy for targeted deletion of *MAT* genes.

Knockout of *BcMAT1-1-1*, *BcMAT1-1-5*, *BcMAT1-2-1* and *BcMAT1-2-4* by targeted gene replacement. Organization of *BcMAT1-1-1*, *BcMAT1-1-5*, *BcMAT1-2-1* and *BcMAT1-2-4* locus before and after homologous recombination. Orentation of the target gene and *HPH* are indicated by white and grey arrows, respectively. Upstream and downstream flanks of target genes are shown with open boxes. Polymerase chain reaction (PCR) analysis of wild-type strain SAS56, SAS405 and knockout mutant strains. The genomic DNA of each strain was used to verify 5' and 3' homologous recombination and absence of targeted genes in corresponding knockout mutants, respectively.
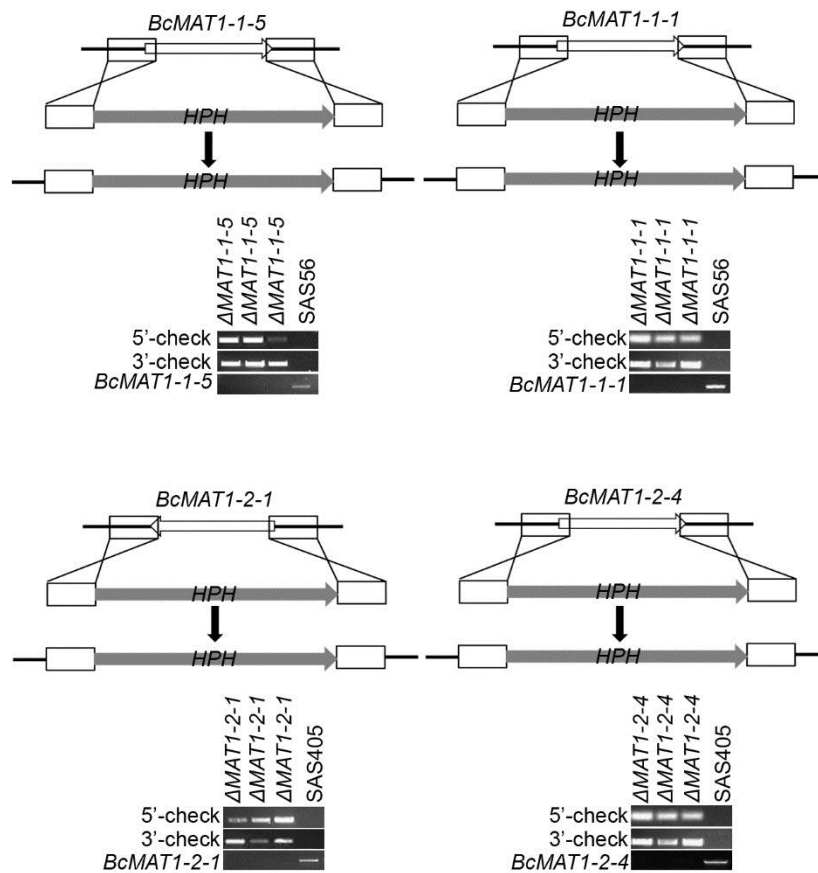
Supplementary Table 1

Transcript levels of *B.cinerea* genes orthologous to *A. nidulans* genes involved in perception of environmental signals during sexual development (according to Dyer and O'Gorman, 2012).

Gene	Protein function (domain)	Sex effect	Locus	Reference	Botrytis ID	Score	E value	Scl	Apo12	Apo34	Apo56	Asc
fphA	Red light sensing phytochrome	Repressor	AN9008	Blumenstein et al 2005	Bcin13g04690.1 gene=Bcin13g04690	1093	0	21.11	21.48	19.34	26.68	50.98
					Bcin01g09230.1 gene=Bcin01g09230	835	0	26.85	33.98	52.37	42.41	11.20
					Bcin06g01290.1 gene=Bcin06g01290	753	0	13.46	2.31	2.07	2.20	1.04
lreA	Blue light–sensing white-collar (LOV, PAS, zinc-finger)	Activator	AN3435	Purschwitz et al. (2008)	Bcin02g07400.2 gene=Bcin02g07400	481	e-136	15.48	20.46	15.05	18.83	30.07
lreB	Blue light–sensing white-collar (PAS, zinc-finger)	Activator	AN3607	Purschwitz et al. (2008)	Bcin05g05530.1 gene=Bcin05g05530	201	4E-52	124.62	399.26	383.46	207.85	40.34
cryA	Blue light- and UVA-sensing cryptochrome (PHR)	Repressor	AN0387	Bayram et al. (2008a)	Bcin05g08060.1 gene=Bcin05g08060	647	0	7.12	23.59	32.96	34.12	2.74
veA	Light/dark response (velvet complex)	Activator	AN1052	Kim et al. (2002)	Bcin15g03390.1 gene=Bcin15g03390	286	1E-77	101.63	312.97	205.45	140.88	88.29
velB	Light/dark response (velvet complex)	Activator	AN0363	Bayram et al. (2008b)	Bcin01g02730.1 gene=Bcin01g02730	305	2E-83	34.66	15.88	14.78	27.30	36.82
laeA	Light/dark response (methyl transferase)	Bimodal‡	AN0807	Sarikaya Bayram et al. (2010)	Bcin05g01210.1 gene=Bcin05g01210	246	8E-66	26.77	34.49	29.98	22.31	5.21
					Bcin09g04500.1 gene=Bcin09g04500	177	6E-45	13.23	55.88	47.02	8.63	0.42
					Bcin06g07480.1 gene=Bcin06g07480	173	7E-44	7.43	10.19	12.93	34.59	18.97
imeB	Light response, low glucose sensing (?) (TXY MAP kinase)	Bimodal	AN6243	Bayram et al. (2009)	Bcin14g03860.1 gene=Bcin14g03860	852	0	47.75	77.72	52.95	50.00	19.45
silA	Light response (zinc-finger)	Repressor	AN1893	Han et al. (2008c)	Bcin08g04710.1 gene=Bcin08g04710	300	1E-81	19.75	22.41	21.56	40.77	16.08
silG	Light response (zinc-finger)	Repressor	AN0709	Han et al. (2005)	Bcin13g04470.1 gene=Bcin13g04470	307	8E-84	19.75	22.41	21.56	40.77	16.08
cpcA	Amino acid sensing (bZIP)	Repressor	AN3675	Hoffmann et al. (2000)	Bcin01g10810.1 gene=Bcin01g10810	80	6E-16	1,612.95	401.60	370.17	511.16	767.67
cpcB	Amino acid sensing (WD repeat)	Activator	AN4163	Hoffmann et al. (2000)	Bcin14g03010.1 gene=Bcin14g03010	606	e-174	540.58	395.95	471.09	452.63	2,528.10
lsdA	High salt sensing	Repressor	AN2330	Lee et al. (2001)	Bcin10g01510.1 gene=Bcin10g01510	192	2E-49	2.78	1.67	3.19	6.18	4.27
phoA	Low phosphorous sensing (cyclin-dependent kinase)	Repressor	AN8261	Bussink & Osmani (1998)	Bcin10g01320.1 gene=Bcin10g01320	535	e-153	89.42	123.94	132.20	118.97	59.04
An-pho80	Low phosphorous sensing (cyclin)	Activator	AN5156	Wu et al. (2004)	Bcin04g04020.1 gene=Bcin04g04020	251	3E-67	76.57	148.14	126.11	121.53	51.78
esdC	Early sexual development (glycogen binding domain)	Activator	AN9121	Han et al. (2008b)	Bcin14g02070.1 gene=Bcin14g02070	274	2E-74	3,854.57	2,503.40	2,838.79	1,301.20	12.49
fhbA	NO response (flavohaemoglobin)	Repressor	AN7169	Baidya et al. (2011)	Bcin04g06230.1 gene=Bcin04g06230	419	e-118	20.56	7.42	12.81	24.52	19.91

Transcript levels of *B. cinerea* genes orthologous to *A. nidulans* genes involved in mating processes and signal transduction during sexual development (according to Dyer and O'Gorman, 2012).

Gene	Protein function (domain)	Sex effect	Locus	Reference	Botrytis ID	Score	E value	Scl	Apo12	Apo34	Apo56	Asc
MAT1	Mating type (alpha)	Activator	AN2755	Paoletti et al. (2007)	Bcin01g02150.1 gene=Bcin01g02150	88	4E-18	0.21	1.70	5.17	6.06	0.27
ppgA	Pheromone precursor (a-type)	Activator	AN5791	Paoletti et al. (2007)	Bcin01g07500.1 gene=Bcin01g07500	36	0.003	2.05	10.51	2.56	1.12	5.32
preA/gprB	a-Type pheromone receptor (GPCR seven transmembrane)	Activator	AN7743	Dyer et al. (2003), Seo et al. (2004)	Bcin10g00700.1 gene=Bcin10g00700	105	2E-23	0.46	0.76	2.56	3.96	0.09
fadA	G protein α subunit	Activator	AN0651	Rose´n et al. (1999)	Bcin05g06770.1 gene=Bcin05g06770	669	0	180.61	442.59	326.15	335.63	142.15
					Bcin15g03610.1 gene=Bcin15g03610	339	7E-94	96.54	53.45	49.91	52.39	29.81
					Bcin14g01730.1 gene=Bcin14g01730	324	3E-89	196.04	305.07	267.35	236.55	104.77
sfaD	G protein β subunit	Activator	AN0081	Rose´n et al. (1999)	Bcin08g01420.1 gene=Bcin08g01420	610	e-175	83.52	115.54	110.39	185.04	78.49
gpgA	G protein γ subunit	Activator	AN2742	Seo et al. (2005)	Bcin10g03840.1 gene=Bcin10g03840	114	4E-27	124.96	148.33	156.76	322.60	105.04
flbA	Regulator of G protein signalling	Activator	AN5893	Han et al. (2001)	Bcin07g04430.1 gene=Bcin07g04430	642	0	9.79	122.32	63.73	40.42	52.26
phnA	Phosducin-like chaperone	Activator	AN0082	Seo & Yu (2006)	Bcin08g01410.1 gene=Bcin08g01410	160	3E-40	27.25	254.91	137.89	116.40	104.65
STE20	MAP kinase, kinase, kinase, kinase	N/A	AN5674	Dyer et al. (2003)	Bcin01g09870.1 gene=Bcin01g09870	627	e-180	13.05	10.60	15.88	40.23	11.63
					Bcin02g02370.1 gene=Bcin02g02370	341	5E-94	13.05	10.60	15.88	40.23	11.63
					Bcin13g03980.1 gene=Bcin13g03980	195	3E-50	44.94	26.70	26.67	29.92	13.54
steC/steB	MAP kinase, kinase, kinase	Activator	AN2269	Wei et al. (2003)	Bcin03g02630.1 gene=Bcin03g02630	830	0	20.27	30.22	29.46	40.14	15.96
					Bcin02g06590.1 gene=Bcin02g06590	221	1E-57	15.05	13.47	12.38	11.05	10.85
					Bcin04g00630.1 gene=Bcin04g00630	200	1E-51	11.91	12.22	12.97	28.88	12.29
STE7	MAP kinase, kinase	Activator¶	AN3422	Paoletti et al. (2007)	Bcin04g05630.1 gene=Bcin04g05630	495	e-140	52.91	29.21	33.37	45.17	36.54
					Bcin03g07190.1 gene=Bcin03g07190	187	9E-48	51.91	51.17	50.15	42.34	54.49
					Bcin09g06900.1 gene=Bcin09g06900	186	1E-47	86.66	66.60	67.20	40.73	58.63
mpkB	MAP kinase	Activator	AN3719	Paoletti et al. (2007)	Bcin02g08170.2 gene=Bcin02g08170	670	0	114.22	88.20	87.45	60.98	24.95
					Bcin02g08170.1 gene=Bcin02g08170	670	0	114.22	88.20	87.45	60.98	24.95
					Bcin09g02390.1 gene=Bcin09g02390	349	7E-97	143.53	40.14	58.89	100.57	36.16
steA	Transcription factor (homoeodomain & zinc-finger)	Activator	AN2290	Vallim et al. (2000)	Bcin10g05560.1 gene=Bcin10g05560	785	0	118.97	152.35	134.13	110.39	148.81

ste50	Kinase cascade regulator	Activator	AN7252	Paoletti et al. (2007)	Bcin08g03660.1 gene=Bcin08g03660	423	e-119	37.76	35.99	37.22	29.40	34.05
rasA	Small G protein (GTPase)	Repressor	AN0182	Hoffmann et al. (2000	Bcin12g05760.1 gene=Bcin12g05760	355	4E-99	332.61	311.85	321.32	276.94	250.40
gprD	GPCR (seven transmembrane)	Repressor	AN3387	Han et al. (2004)	Bcin10g01660.1 gene=Bcin10g01660	198	2E-51	6.79	6.23	1.94	4.54	33.19
sakA/hogA	Osmotic and oxidative stress response (MAP kinase)	Repressor	AN1017	Kawasaki et al. (2002)	Bcin15g03580.2 gene=Bcin15g03580	589	e-169	162.02	80.15	89.19	66.30	14.37
atfA	Stress response (bZIP domain)	Repressor	AN2911	Lara-Rojas et al. (2011)	Bcin09g00920.1 gene=Bcin09g00920	176	1E-44	239.32	162.16	152.42	122.77	140.86

Transcript levels of *B. cinerea* genes orthologous to *A. nidulans* genes encoding transcription factors and regulatory proteins involved in sexual development (according to Dyer and O'Gorman, 2012).

Gene	Protein function (domain)	Sex effect	Locus	Reference	Botrytis ID	Score	E value	Scl	Apo12	Apo34	Apo56	Asc
stuA	Transcription factor (bHLH, APSES)	Activator	AN5836	Wu & Miller (1997)	Bcin04g00280.1 gene=Bcin04g00280	503	e-143	443.11	313.31	244.56	178.79	128.96
medA	Transcription factor	Activator	AN6230	Busby et al. (1996)	Bcin12g00460.1 gene=Bcin12g00460	390	e-108	16.84	139.54	71.61	26.24	1.06
devR	Transcription factor (bHLH)	Activator	AN7553	Tü¨ncher et al. (2004)	Bcin07g02960.1 gene=Bcin07g02960	186	2E-47	62.91	59.06	70.11	49.34	29.40
dopA	Transcription factor (leucine-zipper)	Activator	AN2094	Pascon & Miller (2000)	Bcin06g05770.1 gene=Bcin06g05770	1517	0	9.74	13.10	12.89	13.04	5.72
nsdC	Transcription factor (zinc-finger)	Activator	AN4263	Kim et al. (2009)	Bcin01g02800.1 gene=Bcin01g02800	344	6E-95	73.55	87.64	70.01	48.19	67.18
nsdD	Transcription factor (zinc-finger)	Activator	AN3152	Han et al. (2001)	Bcin14g03930.1 gene=Bcin14g03930	219	1E-57	31.57	295.52	308.84	141.42	32.29
nosA	Transcription factor (zinc-finger)	Activator	AN1848	Vienken & Fischer (2006)	Bcin01g10880.1 gene=Bcin01g10880	550	e-157	49.27	122.79	105.02	31.14	2.33
rosA	Transcription factor (zinc-finger)	Repressor	AN5170	Vienken et al. (2005)	Bcin01g10880.1 gene=Bcin01g10880	429	e-120	49.27	122.79	105.02	31.14	2.33
flbC	Transcription factor (zinc-finger)	Repressor	AN2421	Kwon et al. (2010a)	Bcin06g05800.2 gene=Bcin06g05800	260	4E-70	197.85	100.61	121.98	36.10	49.73
fhpA	Transcription factor (forkhead)	Activator	AN4521	Lee et al. (2005)	Bcin05g02510.1 gene=Bcin05g02510	109	2E-24	1.05	21.85	38.31	46.84	0.56
nrdA/msnA	Transcription factor (zinc-finger)	Repressor	AN1652	Jeon et al. (2009)	Bcin01g05160.1 gene=Bcin01g05160	360	e-100	73.83	442.10	480.07	355.81	85.79
rcoA	Developmental regulation (WD repeat)	Activator	AN6505	Todd et al. (2006)	Bcin16g04710.1 gene=Bcin16g04710	712	0	165.60	77.99	91.72	123.94	114.65
csnA	COP9 signalosome subunit (PCI)	Activator	AN1491	Busch et al. (2007)	Bcin10g03920.1 gene=Bcin10g03920	412	e-115	53.02	22.71	46.72	68.91	7.04
csnB	COP9 signalosome subunit (PCI)	Activator	AN4783	Busch et al. (2007)	Bcin06g04360.1 gene=Bcin06g04360	684	0	40.49	35.91	50.41	57.43	26.68
csnD	COP9 signalosome subunit (PCI)	Bimodal	AN1539	Busch et al. (2003, 2007)	Bcin02g03980.1 gene=Bcin02g03980	385	e-107	23.22	20.95	29.04	41.28	12.97
csnE	COP9 signalosome subunit (MPN+ with JAMM deneddylase)	Bimodal	AN2129	Busch et al. (2007) Nahlik et al. (2010)	Bcin08g02520.1 gene=Bcin08g02520	446	e-126	78.27	56.53	66.65	84.94	23.47
csnG/acoB	COP9 signalosome subunit (PCI)	Activator	AN3623	Lewis & Champe (1995) Busch et al. (2007)	Bcin05g06150.1 gene=Bcin05g06150	193	7E-50	33.30	41.57	64.96	59.37	7.30
candA-C	Protein neddylation	Activator	AN2458	Helmstaedt et al. (2011)	Bcin03g07250.1 gene=Bcin03g07250	911	0	32.24	26.19	33.81	43.88	14.51

Transcript levels of *B. cinerea* genes orthologous to *A. nidulans* genes involved in endogenous physiological processes during sexual development (according to Dyer and O'Gorman, 2012).

Gene	Protein function (domain)	Sex effect	Locus	Reference	Botrytis ID	Score	E value	Scl	Apo12	Apo34	Apo56	Asc
ppoA	Oxylipin biosynthesis (dioxygenase)	Activator	AN1967	Tsitsigiannis et al. (2004)	Bcin02g03060.1 gene=Bcin02g03060	922	0	145.68	397.82	282.64	77.17	38.13
ppoB	Oxylipin biosynthesis	Activator	AN6320	Tsitsigiannis et al. (2005)	Bcin04g05000.1 gene=Bcin04g05000	603	e-172	467.23	395.10	383.54	101.70	0.62
					Bcin02g03060.1 gene=Bcin02g03060	504	e-143	145.68	397.82	282.64	77.17	38.13
ppoC	Oxylipin biosynthesis	Repressor	AN5028	Tsitsigiannis et al. (2005)	Bcin04g05000.1 gene=Bcin04g05000	1088	0	467.23	395.10	383.54	101.70	0.62
noxA	Generation of reactive oxygen species (NADPH oxidase)	Activator	AN5457	Lara-Ortí´z et al. (2003)	Bcin05g00350.1 gene=Bcin05g00350	837	0	16.78	39.52	46.60	27.65	5.56
					Bcin02g04930.1 gene=Bcin02g04930	359	1E-99	11.31	21.93	22.52	12.53	4.05
sidC	Intracellular siderophore synthesis (non-ribosomal peptide synthetase)	Activator	AN0607	Eisendle et al. (2006)	Bcin16g03570.1 gene=Bcin16g03570	3150	0	3.20	7.51	7.15	7.92	0.60
					Bcin12g00690.1 gene=Bcin12g00690	786	0	6.70	11.73	8.57	20.93	2.39
					Bcin14g01300.1 gene=Bcin14g01300	650	0	6.70	11.73	8.57	20.93	2.39
trxA	Regulation of cellular redox state (thioredoxin system)	Activator	AN0170	Thön et al. (2007)	Bcin12g04280.1 gene=Bcin12g04280	110	2E-25	1,393.77	3,436.65	2,155.43	1,507.37	1,521.71
mutA	a-1,3 Glucanase/mutanase	Activator	AN7349	Wei et al. (2001)	Bcin07g02670.1 gene=Bcin07g02670	574	e-164	1.29	4.45	8.93	19.29	0.68
					Bcin02g08970.1 gene=Bcin02g08970	307	5E-84	0.30	0.11	0.15	0.72	0.03
hxtA	High-affinity hexose transporter	Activator	AN6923	Wei et al. (2004)	Bcin01g08950.1 gene=Bcin01g08950	629	0	51.81	2.10	2.74	5.11	0.49
					Bcin08g00740.1 gene=Bcin08g00740	429	e-120	2.23	10.95	23.99	149.20	165.92
					Bcin11g05510.1 gene=Bcin11g05510	330	5E-91	0.92	0.36	0.98	1.60	1.92

Transcript levels of *B. cinerea* genes orthologous to *A. nidulans* genes involved in ascospore production and maturation during sexual development (according to Dyer and O'Gorman, 2012).

Gene	Protein function (domain)	Sex effect	Locus	Reference	Botrytis ID	Score	E value	Scl	Apo12	Apo34	Apo56	Asc
grrA	Protein ubiquitinylation (F-box)	Activator	AN10516	Krappmann et al. (2006)	Bcin10g01220.1 gene=Bcin10g01220	575	e-164	28.79	37.57	37.07	41.54	31.17
samB	Cell polarity, nuclear positioning (zinc-finger)	Activator	AN0078	Kuger & Fischer (1998)	Bcin08g05880.1 gene=Bcin08g05880	644	0	77.09	123.82	100.75	150.22	73.06
strA	Striatin scaffolding and Ca signalling	Activator	AN8071	Wang et al. (2010)	Bcin07g02300.1 gene=Bcin07g02300	823	0	32.55	34.55	38.65	33.12	17.82
tubB	Microtubule assembly (alpha-tubulin)	Activator	AN0316	Kirk & Morris (1991)	Bcin02g00900.1 gene=Bcin02g00900	862	0	266.38	489.90	538.99	467.66	206.10
					Bcin02g01790.1 gene=Bcin02g01790	679	0	104.62	227.26	263.06	216.15	298.57
					Bcin01g08040.1 gene=Bcin01g08040	363	e-101	306.12	467.64	546.83	462.17	403.92
vosA	Trehalose production	Activator	AN1959	Ni & Yu (2007)	Bcin03g06410.1 gene=Bcin03g06410	164	4E-41	14.06	3.69	5.60	15.76	1.10
					Bcin15g03390.1 gene=Bcin15g03390	107	6E-24	101.63	312.97	205.45	140.88	88.29

Supplementary Table 2

Soft cluster 1: genes specifically expressed in sclerotia
Bc01g01330.1 Botrytis-specific protein
Bc01g02430.1 conserved fungal protein
Bc01g03270.1 conserved fungal protein
Bc01g03510.1 cytochrome P450
Bc01g03870.1 heterokaryon incompatibility protein
Bc01g03890.1 conserved fungal protein
Bc01g04670.1 Botrytis/Sclerotinia-specific protein
Bc01g07150.1 Botrytis-specific protein
Bc01g07640.1 Botrytis-specific protein
Bc01g08140.1 Botrytis/Sclerotinia-specific protein
Bc01g10790.1 conserved fungal protein
Bc02g00270.1 conserved fungal protein
Bc02g01470.1 ankyrin repeat protein
Bc02g01480.1 HET domain protein
Bc02g01710.1 MFS transporter
Bc02g01730.1 conserved fungal protein
Bc02g04380.1 salicylate hydroxylase
Bc02g04800.1 carboxypeptidase A
Bc02g05770.1 ankyrin repeat protein
Bc02g06300.1 conserved fungal protein
Bc02g06320.1 MFS transporter
Bc02g07810.1 UMTA methyltransferase family protein
Bc02g07820.1 conserved fungal protein
Bc02g07830.1 conserved fungal protein
Bc02g09370.1 C2 domain-containing protein
Bc03g00010.1 conserved fungal protein
Bc03g00960.1 GTP cyclohydrolase I
Bc03g01240.1 short-glycine-rich protein
Bc03g01280.1 conserved fungal protein
Bc03g01290.1 Botrytis/Sclerotinia-specific protein
Bc03g01300.1 Botrytis/Sclerotinia-specific protein
Bc03g01310.1 conserved fungal protein
Bc03g01320.1 conserved fungal protein
Bc03g01450.1 acetyltransferase
Bc03g04780.1 alpha-ketoglutarate-dependent taurine dioxygenase
Bc03g06670.1 putative carnosine synthase
Bc04g00660.1 kinesin light chain
Bc04g00670.1 conserved fungal protein
Bc04g00830.1 NACHT and WD40 domain protein
Bc04g00840.1 conserved fungal protein
Bc04g00850.1 small Botrytis-specific protein
Bc04g00870.1 conserved fungal protein
Bc04g00880.1 conserved fungal protein
Bc04g00930.1 HET domain protein
Bc04g00950.1 ankyrin repeat protein
Bc04g02330.1 Botrytis-specific protein
Bc04g02380.1 amidohydrolase
Bc04g02680.1 MFS transporter

Bc04g03990.1 phosphate permease
Bc04g04920.1 BcNMT1 thiamine synthase
Bc05g00100.1 small secreted Botrytis-specific protein
Bc05g01530.1 conserved fungal protein
Bc05g05300.1 conserved fungal protein
Bc05g06500.1 Botrytis/Sclerotinia-specific protein
Bc06g01480.1 Botrytis-specific protein
Bc06g01560.1 Botrytis-specific protein
Bc06g01730.1 conserved fungal protein
Bc06g03370.1 mitochondrial phosphate carrier protein 2
Bc06g05580.1 conserved fungal protein
Bc06g05780.1 Botrytis-specific protein
Bc06g05790.1 conserved fungal protein
Bc06g06420.1 MFS transporter
Bc06g07030.1 Botrytis-specific protein
Bc06g07590.1 CAZY GH71 family protein alpha-1,3-glucanase
Bc07g00950.1 short-chain dehydrogenase/reductase
Bc07g00980.1 MFS transporter
Bc07g00990.1 O-methyltransferase
Bc07g01570.1 conserved fungal protein
Bc07g04230.1 conserved fungal protein
Bc07g04990.1 BcABA4, short-chain dehydrogenase/reductase
Bc07g05420.1 conserved fungal protein
Bc07g05560.1 Botrytis/Sclerotinia-specific protein
Bc07g06010.1 thiazole biosynthetic enzyme, mitochondrial
Bc08g00290.1 BcPKS19
Bc08g00300.1 glutathione S-transferase
Bc08g00340.1 MFS transporter for polyketide
Bc08g00970.1 conserved fungal protein
Bc08g01290.1 secreted protein
Bc08g01760.1 taurine catabolism dioxygenase TauD
Bc08g01770.1 putative taurine catabolism dioxygenase protein
Bc08g02700.1 conserved alpha/beta hydrolase family protein
Bc08g03080.1 putative helix-loop-helix DNA-binding domain-containing protein
Bc08g03590.1 cytochrome P450
Bc08g04060.1 ferric/cupric reductase transmembrane component
Bc08g04070.1 conserved fungal GPI-anchored protein
Bc08g05820.1 conserved fungal protein
Bc08g05870.1 CAZY GH95 family protein, alpha-fucosidase
Bc08g07130.1 Asp-hemolysin family protein
Bc08g07150.1 Botrytis-specific protein
Bc08g07160.1 Botrytis-specific protein
Bc09g00010.1 Botrytis-specific protein
Bc09g00500.1 conserved fungal protein
Bc09g00520.1 conserved fungal protein
Bc09g01120.1 Botrytis-specific protein
Bc09g01770.1 conserved fungal protein
Bc09g03310.1 CCCH zinc finger DNA binding protein
Bc09g03670.1 GABA permease
Bc09g04140.1 heterokaryon incompatibility protein
Bc09g04570.1 GMC oxidoreductase, choline or cellobiose dehydrogenase

Bc09g05670.1 dienelactone hydrolase family protein
Bc09g07100.1 conserved fungal protein
Bc09g07110.1 alpha-N-arabinofuranosidase 2
Bc09g07120.1 conserved fungal protein
Bc10g00050.1 Botrytis-specific protein
Bc10g01210.1 Botrytis-specific protein
Bc10g01350.1 short-chain dehydrogenase/reductase
Bc10g02050.1 dynamin family protein
Bc10g05620.1 pectate lyase
Bc11g01680.1 putative modin protein
Bc11g02020.1 Botrytis/Sclerotinia-specific protein
Bc11g02170.1 tyrosinase
Bc11g02450.1 ankyrin repeat protein
Bc11g03710.1 MFS sugar transporter
Bc11g03900.1 Botrytis-specific protein
Bc11g05450.1 alpha/beta hydrolase fold family protein
Bc11g05460.1 Botrytis/Sclerotinia-specific protein
Bc11g05970.1 fatty acid hydroxylase, sterol desaturase
Bc11g06510.1 Botrytis-specific protein
Bc11g06520.1 cytochrome P450
Bc11g06530.1 Botrytis/Sclerotinia-specific protein
Bc12g00140.1 N-terminal amidase
Bc12g00590.1 conserved fungal protein
Bc12g00630.1 conserved fungal protein
Bc12g00860.1 putative 2-heptaprenyl-1,4-naphthoquinone methyltransferase
Bc12g01010.1 putative peptidase inhibitor i9
Bc12g02880.1 serine/threonine-protein kinase nrc-2
Bc12g03230.1 Botrytis-specific protein
Bc12g04300.1 mitochondrial S-adenosylmethionine transporter
Bc12g05860.1 glucose dehydrogenase
Bc12g06750.1 Botrytis-specific protein
Bc13g00040.1 Botrytis-specific protein
Bc13g01540.1 conserved fungal protein
Bc13g01550.1 C-terminal part of conserved protein
Bc13g02170.1 cytochrome P450
Bc13g02820.1 conserved fungal protein
Bc13g03780.1 conserved fungal protein
Bc13g04200.1 conserved fungal protein
Bc13g05320.1 Botrytis-specific protein
Bc13g05330.1 conserved fungal protein
Bc14g00090.1 thermophilic desulfurizing enzyme family protein
Bc14g03020.1 conserved fungal protein
Bc14g03270.1 conserved fungal protein
Bc14g03670.1 tetrahydrofolylpolyglutamate synthase
Bc14g04030.1 Botrytis-specific protein
Bc14g04530.1 2,3-diketo-5-methylthio-1-phosphopentane phosphatase
Bc14g04670.1 unknown
Bc14g04680.1 conserved fungal protein
Bc14g05530.1 conserved fungal protein
Bc14g05540.1 putative zinc transporter
Bc14g05560.1 epoxide hydrolase
Bc15g00290.1 conserved fungal protein

Bc15g00560.1 Botrytis/Sclerotinia-specific protein
Bc15g03060.1 conserved fungal protein
Bc15g03870.1 Botrytis/Sclerotinia-specific protein
Bc15g03940.1 conserved fungal protein
Bc15g03960.1 tyrosinase
Bc15g03970.1 conserved fungal protein
Bc15g03980.1 Botrytis-specific protein
Bc15g03990.1 Botrytis-specific protein
Bc15g04000.1 unknown protein with poor homology to other fungi
Bc15g04010.1 Botrytis-specific protein
Bc15g04640.1 Botrytis/Sclerotinia-specific protein
Bc15g05670.1 potassium/sodium efflux P-type ATPase
Bc16g00780.1 Botrytis/Sclerotinia-specific protein
Bc16g01410.1 cytochrome P450
Bc16g02740.1 Botrytis-specific protein
Bc16g03380.1 mannitol dehydrogenase

Supplementary Table 3

Soft cluster 2: genes specifically expressed in primordia (Apo12)

Bc05g06220.1 Polyketide synthase BcPKS15
Bc04g02570.1 small secreted hydrophobin-like protein

Supplementary Table 4

Soft cluster 3: genes specifically expressed in stipes (Apo34)

Bc06g02830.1 putative ornithine decarboxylase
Bc06g07000.1 secreted tannase
Bc07g00030.1 putative feruloyl esterase B precursor
Bc10g04740.1 unknown

Supplementary Table 5

Soft cluster 4: genes specifically expressed in stage Apo56 (disks) with some increase in Apo34

Bc12g00470.1 = Botrytis/Sclerotinia-specific protein
Bc12g04400.1 = Botrytis-specific protein
Bc07g04190.1 = putative transcription factor Zn2Cys6
Bc01g03280.1 = putative ubiquitin-conjugating enzyme E2
Bc12g02100.1 = conserved fungal protein
Bc11g01110.1 = Botrytis-specific protein
Bc16g01930.1 = putative transcription factor Zn2Cys6
Bc13g02810.1 = Helotiales-specific protein
Bc07g05010.1 = Botrytis/Sclerotinia-specific protein
Bc02g05350.1 = Botrytis/Sclerotinia-specific protein
Bc06g04430.1 = protein kinase domain-containing protein
Bc03g07270.1 = Botrytis/Sclerotinia-specific protein
Bc11g01850.1 = Botrytis-specific protein

Bc14g00450.1 = Botrytis-specific protein
Bc05g06780.1 = Botrytis/Sclerotinia-specific protein
Bc16g02400.1 = secreted Botrytis/Sclerotinia-specific protein
Bc06g06850.1 = Aminoglycoside 3'-phosphotransferase (APH) Choline Kinase (ChoK) family protein
Bc06g02180.1 = Botrytis/Sclerotinia-specific protein
Bc03g09200.1 = conserved fungal protein
Bc03g01600.1 = conserved fungal protein
Bc02g02560.1 = Botrytis/Sclerotinia-specific protein
Bc01g09820.1 = Botrytis/Sclerotinia-specific protein
Bc06g02440.1 = Botrytis/Sclerotinia-specific protein
Bc16g00460.1 = conserved fungal protein
Bc07g05370.1 = Botrytis-specific protein
Bc02g00590.1 = Botrytis/Sclerotinia-specific protein
Bc10g02310.1 = Botrytis/Sclerotinia-specific protein
Bc12g02500.1 = Botrytis-specific protein
Bc10g01370.1 = Botrytis/Sclerotinia-specific protein
Bc14g01470.1 = Botrytis-specific protein
Bc02g03220.1 = aquaporin-like protein (MIP superfamily)
Bc11g02860.1 = Botrytis/Sclerotinia-specific protein
Bc07g02230.1 = Botrytis-specific protein
Bc09g03300.1 = Botrytis/Sclerotinia-specific protein
Bc06g04570.1 = Botrytis-specific protein
Bc04g04620.1 = WD-domain containing protein
Bc14g02040.1 = Botrytis-specific protein
Bc03g01510.1 = Botrytis-specific protein
Bc04g02450.1 = Botrytis-specific protein
Bc02g09080.1 = Botrytis/Sclerotinia-specific protein
Bc09g02120.1 = Botrytis/Sclerotinia-specific protein
Bc02g00370.1 = CAZY GH76 protein, putative alpha-mannanase
Bc02g03720.1 = Botrytis-specific protein
Bc14g03350.1 = Botrytis/Sclerotinia-specific protein
Bc08g06360.1 = Botrytis-specific protein
Bc15g04800.1 = thioesterase-like superfamily protein
Bc05g01070.1 = Botrytis-specific protein
Bc15g04230.1 = Botrytis/Sclerotinia-specific protein
Bc09g02880.1 = Botrytis/Sclerotinia-specific protein
Bc06g06180.1 = MFS hexose transporter
Bc07g03870.1 = Botrytis-specific protein
Bc04g06970.1 = putative cytochrome P450 oxidoreductase
Bc06g01660.1 = Botrytis-specific protein
Bc10g03360.1 = conserved fungal domain-containing protein
Bc05g03480.1 = similar to FK506 suppressor Sfk1
Bc06g00300.1 = Botrytis-specific protein
Bc13g05540.1 = threonine aspartase
Bc03g08580.1 = SNF2 helicase superfamily protein
Bc01g06000.1 = Botrytis/Sclerotinia-specific protein
Bc14g04280.1 = Botrytis/Sclerotinia-specific protein
Bc12g00370.1 = phospholipase/carboxylesterase superfamily protein
Bc10g05300.1 = Helotiales-specific protein
Bc09g03290.1 = Botrytis-specific protein
Bc04g06440.1 = Botrytis-specific protein
Bc16g02350.1 = Botrytis-specific protein

Supplementary Table 6

Soft cluster 5: genes specifically expressed in stage Apo56 (apothecial disks)

Bc10g02890.1 = secreted Botrytis/Sclerotinia-specific protein
Bc13g02200.1 = secreted Botrytis-specific protein
Bc05g00310.1 = secreted glutaminase
Bc02g09010.1 = conserved fungal protein
Bc15g04520.1 = CFEM domain containing protein
Bc14g01760.1 = MFS transporter
Bc12g00580.1 = secreted protein Botrytis-specific
Bc08g00940.1 = secreted protein CFEM domain (cysteine-rich)
Bc05g06950.1 = Helotiales-specific protein
Bc12g00150.1 = putative serine/threonine kinase
Bc04g04570.1 = Botrytis-specific protein
Bc16g03330.1 = predicted protein
Bc05g02530.1 = secreted tannase/feruloyl esterase family protein
Bc02g05390.1 = Botrytis/Sclerotinia-specific protein
Bc10g01910.1 = putative calpain family cysteine protease
Bc01g10190.1 = Botrytis-specific protein

Supplementary Table 7

Soft cluster 6: genes specifically expressed in ascospores

Bc01g00160.1:short-chain dehydrogenase, NADB-Rossmann family protein
Bc01g00790.1:conserved fungal protein
Bc01g00910.1:Botrytis-specific protein
Bc01g01400.1:alpha/beta hydrolase superfamily protein
Bc01g01410.1:aspartate aminotransferase
Bc01g01430.1:MFS transporter family protein
Bc01g01500.1:FAD dependent oxidoreductase
Bc01g01760.1:CAZY GH18 family protein, putative chitinase
Bc01g02520.1:CAZY GT2 family protein, chitin synthase class III
Bc01g02530.1:similar to nuclear pore protein
Bc01g03710.1:siderophore acetyltransferase
Bc01g04230.1:phosphoadenosine phosphosulfate reductase
Bc01g04340.1:sulfate adenylyltransferase
Bc01g05050.1:Botrytis-specific protein
Bc01g06040.1:methylammonium permease 1 MeaA
Bc01g06950.1:conserved fungal protein
Bc01g08010.1:hypoxanthine guanine phosphoribosyltransferase
Bc01g08220.1:medium chain dehydrogenase/reductase
Bc01g09270.1:PQ-loop repeat protein
Bc01g09360.1:ascorbate peroxidase
Bc01g09710.1:conserved fungal protein
Bc01g10270.1:CAZY GT31 family protein
Bc01g10680.1:MFS transporter, putative vitamin B6 transporter BSU1
Bc01g11030.1:putative 3-hydroxyacyl- NAD binding protein
Bc01g11480.1:abhydrolase6 domain-contain protein, Botrytis-specific

Bc01g11550.1:putative O-methyltransferase
Bc02g00240.1:cytochrome P450 monooxygenase
Bc02g00720.1:Botrytis-specific protein
Bc02g01180.1:unknown protein
Bc02g01230.1:conserved fungal protein
Bc02g01580.1:acyl-CoA-transferase family III
Bc02g01660.1:putative amino acid transporter
Bc02g03270.1:pyridoxal phosphate (PLP)-dependent aspartate aminotransferase superfamily.
Bc02g03330.1:C4-dicarboxylate transporter/malic acid transporter
Bc02g03560.1:putative MFS phosphate transporter
Bc02g05250.1:Botrytis-specific protein
Bc02g05300.1:Major royal jelly protein
Bc02g05740.1:allantoinase, metallo-dependent hydrolase
Bc02g05800.1:NADB-Rossmann superfamily protein
Bc02g05870.1:NADP-dependent leukotriene B4 12-hydroxydehydrogenase
Bc02g07320.1:RTA1 domain-containing protein
Bc02g07330.1:HeLo domain-containing protein
Bc02g07490.1:conserved fungal protein
Bc02g09380.1:putative lactonohydrolase, gluconolactonase
Bc02g09410.1:conserved fungal protein
Bc03g00510.1:Botrytis-specific protein
Bc03g01840.1:C6 zinc finger protein, fungal-specific TF domain
Bc03g01990.1:2oxuglutarate-Fe(II) oxygenase family oxidoreductase
Bc03g02760.1:aspartic proteinase BcAP4
Bc03g03630.1:CAZY GH12 protein, endoglucanase, xyloglucan hydrolase
Bc03g03790.1:putative GPI anchored cell wall protein
Bc03g03830.1:pectin methylesterase BcPME2
Bc03g05130.1:pyridine nucleotide-disulphide oxidoreductase AMID-like
Bc03g05980.1:conserved fungal protein
Bc03g06110.1:putative cyclopropane-fatty-acyl-phospholipid synthase, SAM-dependent methyltransferase
Bc03g07360.1:CAZY PL1 family protein, pectin lyase
Bc03g07670.1:putative NAD-specific glutamate dehydrogenase
Bc03g08820.1:ankyrin repeat protein
Bc04g00180.1:aspartate aminotransferase superfamily protein
Bc04g01070.1:conserved fungal protein
Bc04g01520.1:putative branched-chain-amino-acid aminotransferase
Bc04g01690.1:ATP-dependent RNA helicase DBP3
Bc04g02240.1:2-hydroxyacid dehydrogenase
Bc04g02860.1:Botrytis-specific protein
Bc04g03000.1:putative 3'-5' exonuclease
Bc04g03100.1:ketol-acid reductoisomerase, mitochondrial precursor
Bc04g03290.1:HSP70-family protein, actin-like ATPase
Bc04g03300.1:conserved fungal protein
Bc04g03360.1:conserved fungal protein
Bc04g04490.1:asparagine synthetase
Bc04g04580.1:MFS transporter
Bc04g06040.1:CAZY GT2 family protein, chitin synthase
Bc04g06510.1:short chain dehydrogenase
Bc04g06890.1:carbonic anhydrase
Bc05g00550.1:no Blast hit
Bc05g00650.1:allantoicase

Bc05g01390.1:MFS transporter
Bc05g01660.1:CAZY GH5 family protein
Bc05g01800.1:PhosphatidylEthanolamine-Binding Protein (PEBP)
Bc05g02290.1:glucose-inducible SAM-dependent methyltransferase Rrg1
Bc05g02620.1:isocitrate lyase superfamily protein
Bc05g03370.1:CAZY GT69 family protein, alpha-1,3-mannosyltransferase
Bc05g03800.1:similar to transcription factor Zn, C2H2
Bc05g04170.1:ribosome assembly protein Noc2
Bc05g05450.1:short-chain dehydrogenase/reductase
Bc05g06260.1:Botrytis-specific protein
Bc05g06280.1:medium chain reductase/dehydrogenase
Bc05g06560.1:conserved fungal protein
Bc05g07520.1:MFS sugar transporter
Bc06g00540.1:Botrytis/Sclerotinia-specific protein
Bc06g00660.1:Major Royal Jelly protein
Bc06g00820.1:MFS sugar transporter
Bc06g01140.1:short chain dehydrogenase/reductase
Bc06g01340.1: NAD(P)-binding Rossmann-fold containing protein
Bc06g01350.1:Botrytis/Sclerotinia-specific protein
Bc06g01590.1:C4-dicarboxylate transporter/malic acid transport protein
Bc06g01620.1:conserved fungal protein
Bc06g03100.1:conserved fungal protein
Bc06g05270.1:CAZY GT71 family protein, mannosyltransferase
Bc06g05360.1:Dihydrodipicolinate synthase family
Bc07g00040.1:PI-PLC-like phosphodiesterases superfamily protein
Bc07g00090.1:NAD dependent epimerase/dehydratase family protein
Bc07g00340.1:arginase
Bc07g02180.1:MFS transporter
Bc07g02850.1:glutamine amidotransferase-like protein, putative GMP synthase
Bc07g02980.1:NADPH dehydrogenase
Bc07g04500.1:putative FKBP-type peptidyl-prolyl cis-trans isomerase
Bc07g04510.1:Type 1 glutamine amidotransferase (GATase1)-like protein
Bc07g05070.1:ribosome biogenesis protein BRX1
Bc07g06750.1:similar to transcription factor Zn, C2H2
Bc07g07100.1:MFS sugar transporter
Bc07g07120.1:acyltransferase condensation domain-containing protein
Bc07g07130.1:cytochrome P450 monooxygenase
Bc08g00720.1:BcAP14
Bc08g01870.1:MIP transporter family protein, aquaporin-like protein
Bc08g03320.1:secreted GPI-anchored protein
Bc08g03490.1:similar to arrestin
Bc08g04720.1:Botrytis-specific protein
Bc08g05890.1:putative rRNA-processing protein EBP2
Bc08g05970.1:amino acid permease
Bc08g06710.1:Botrytis/Sclerotinia-specific protein
Bc09g00150.1:MFS sugar transporter
Bc09g00320.1:conserved fungal protein
Bc09g00360.1:Botrytis-specific protein
Bc09g00570.1:conserved fungal protein
Bc09g00770.1:gluconolactonase
Bc09g00880.1:conserved fungal protein

Bc09g00890.1:Botrytis-specific protein
Bc09g01040.1:L-asparaginase
Bc09g03630.1:Rossmann-fold NAD(P)(+)-binding proteins
Bc09g03950.1:regulator of G protein signaling domain-containing protein
Bc09g05210.1:putative bZIP transcription factor protein
Bc09g06320.1:Botrytis-specific protein
Bc09g06360.1:similar to polyketide synthase
Bc09g06680.1:cytochrome P450 monoxygenase
Bc09g06840.1:conserved fungal protein
Bc10g00140.1:Rossmann-fold NAD(P)(+)-binding proteins
Bc10g00150.1:ketoreductase/ oxidoreductase
Bc10g00950.1:acyl-CoA transferase family III protein
Bc10g01500.1:ATP synthase protein 9
Bc10g01590.1:autophagy-related protein ATG22, MFS transporter
Bc10g02270.1:glutathione S-transferase
Bc10g03690.1:conserved fungal protein
Bc10g04810.1:MFS transporter, putative fucose permease
Bc10g05310.1:3-isopropylmalate dehydrogenase
Bc11g00010.1:CAZY GH1 family protein, beta-glucosidase
Bc11g00780.1:small conserved fungal peptide
Bc11g00970.1:branched-chain-amino-acid aminotransferase
Bc11g01310.1:Abhydrolase 4 domain-containing protein
Bc11g03330.1:amino acid permease
Bc11g03790.1:similar to transcription factor MADS
Bc11g04150.1:ribosome biogenesis protein erb1
Bc11g04380.1:bZIP domain-containing protein
Bc11g04460.1:ABC transporter AtrF
Bc11g04900.1:amino acid permease
Bc11g05020.1:conserved fungal protein
Bc11g05330.1:MFS transporter domain protein
Bc12g00850.1:conserved fungal protein
Bc12g01180.1:conserved fungal protein
Bc12g02050.1:medium chain dehydrogenases/reductase
Bc12g02120.1:tannase/feruloyl esterase family protein
Bc12g02300.1:MFS sugar transporter BC1G_03115
Bc12g02390.1:GMC oxidoreductase
Bc12g02650.1:conserved fungal protein
Bc12g02860.1:Botrytis/Sclerotinia-specific protein
Bc12g03430.1:putative lipase precursor
Bc12g03640.1:MFS monocarboxylate transporter
Bc12g03650.1:aldo/keto reductase similar to norsorolinic acid reductase
Bc12g04620.1:Botrytis-specific protein
Bc12g04860.1:aspartate carbamoyltransferase pyrABCN
Bc12g05120.1:conserved fungal protein wrongly annotated as pepsin domain-containing protein
Bc12g05130.1:Botrytis-specific protein
Bc12g05260.1:Botrytis/Sclerotinia-specific protein
Bc12g05690.1:putative glutathione S-transferase
Bc12g05850.1:Botrytis-specific protein
Bc12g06250.1:Botrytis-specific protein
Bc12g06270.1:Botrytis-specific protein
Bc12g06350.1:MFS sugar transporter
Bc12g06580.1:putative glutathione-dependent formaldehyde-activating protein

Bc12g06770.1:conserved fungal protein
Bc13g00050.1:conserved fungal protein
Bc13g00130.1:short-chain dehydrogenase/reductase
Bc13g00140.1:zinc-binding oxidoreductase
Bc13g00710.1:ABC transporter BcatrB
Bc13g01700.1:unknown short protein, check RNAseq reads
Bc13g02670.1:phosphoglycerate mutase family protein
Bc13g02720.1:ABC transporter BcatrD
Bc13g03100.1:cinnamyl-alcohol dehydrogenase family protein
Bc13g03110.1:Rossmann-fold NAD(P)(+)-binding protein
Bc13g03130.1:conserved fungal protein
Bc13g03160.1:secreted small putatively O-glycosylated protein
Bc13g03170.1:putative lysophospholipase PLB1
Bc13g03410.1:peptidase S9, abhydrolase 5 family protein
Bc13g03450.1:putative sulfite reductase
Bc13g04990.1:Botrytis-specific protein
Bc13g05140.1:cytochrome P450 monooxygenase
Bc13g05260.1:Zn(2)-C6 fungal-type DNA-binding domain, TF Zn2Cys6
Bc13g05300.1:alpha-1,2-mannosyltransferase Mnn2
Bc14g00210.1:NADH oxidase
Bc14g00240.1:tannase and feruloyl esterase
Bc14g00610.1:endopolygalacturonase BcPG2
Bc14g01360.1:indoleamine 2,3-dioxygenase gamma type
Bc14g01420.1:unknown protein
Bc14g01430.1:small conserved fungal protein
Bc14g01580.1:zinc-binding alcohol dehydrogenase
Bc14g01660.1:short-chain dehydrogenase/reductase
Bc14g01670.1:conserved fungal protein
Bc14g01680.1:short-chain dehydrogenase reductase
Bc14g01850.1:Botrytis/Sclerotinia-specific protein
Bc14g02580.1:zinc knuckle domain containing protein
Bc14g02750.1:MFS transporter
Bc14g04010.1:zinc-binding oxidoreductase CipB
Bc14g04320.1:indoleamine 2,3-dioxygenase, Trp catabolism
Bc15g00070.1:NMT1/THI5-like
Bc15g00100.1:conserved fungal protein
Bc15g00110.1:unknown short peptide
Bc15g00630.1:Botrytis/Sclerotinia-specific protein
Bc15g01620.1:putative tetrahydrofolate dehydrogenase/cyclohydrolase
Bc15g02580.1:secreted CFEM-domain containing protein
Bc15g03000.1:secreted protein with low complexity Pro-rich repeat
Bc15g03720.1:conserved fungal protein
Bc15g04080.1:Botrytis/Sclerotinia-specific protein
Bc15g04810.1:MFS transporter
Bc15g05220.1:secreted Botrytis/Sclerotinia-specific protein
Bc15g05440.1:6-phosphogluconate dehydrogenase
Bc16g00220.1:conserved fungal protein
Bc16g00230.1:aldo-ketoreductase
Bc16g00240.1:Rossmann-fold NAD(P)(+)-binding protein, short chain dehydrogenase
Bc16g00250.1:aldo-ketoreductase
Bc16g00470.1:amidase

Bc16g00930.1:calcineurin-dependent gene CND3
Bc16g01890.1:Zn2Cys6 fungal-specific transcription factor
Bc16g02000.1:unknown protein
Bc16g02480.1:conserved fungal protein
Bc16g02490.1:conserved fungal protein
Bc16g02770.1:deuterolysin metalloprotease
Bc16g03420.1:succinate/fumarate mitochondrial transporter
Bc16g03500.1:cystathionine beta-synthase
Bc16g03870.1:medium chain dehydrogenase/reductase
Bc16g04050.1:NADP-specific glutamate dehydrogenase
Bc16g05190.1:zinc-binding alcohol dehydrogenase

Supplementary Table 8

Genes downregulated in the *ΔMAT1-1-5* stipes

Gene ID	wild type	ΔMAT1-1-5	Ratio wt/mutant	Description
Bcin01g01660	54,3	0	∞	Botrytis/Sclerotinia-specific protein
Bcin01g01670	24,6	0	∞	Botrytis/Sclerotinia-specific protein
Bcin01g03450	20,0	0	∞	conserved fungal protein
Bcin01g05500	22,3	0	∞	Botrytis/Sclerotinia-specific protein
Bcin01g11090	48,6	0	∞	Botrytis/Sclerotinia-specific protein
Bcin02g03740	31,3	0	∞	Botrytis/Sclerotinia-specific protein
Bcin03g00600	71,1	0	∞	Botrytis-specific protein
Bcin04g01810	42,0	0	∞	Botrytis/Sclerotinia-specific protein
Bcin04g02450	41,2	0	∞	Botrytis-specific protein
Bcin05g04590	202,2	0	∞	Botrytis/Sclerotinia-specific protein
Bcin05g06570	30,0	0	∞	conserved fungal protein
Bcin05g07950	23,7	0	∞	Helotiales specific protein
Bcin05g08300	24,1	0	∞	Helotiales specific protein
Bcin06g00300	32,7	0	∞	Botrytis-specific protein
Bcin06g00570	64,4	0	∞	Botrytis/Sclerotinia-specific protein
Bcin06g03730	24,5	0	∞	Botrytis-specific protein
Bcin07g03700	59,6	0	∞	Botrytis-specific protein
Bcin07g04190	42,8	0	∞	transcription factor Zn2Cys6
Bcin07g06020	65,4	0	∞	Botrytis-specific protein
Bcin07g06760	38,8	0	∞	Botrytis/Sclerotinia-specific protein
Bcin08g06130	23,3	0	∞	Botrytis-specific protein
Bcin10g00090	22,6	0	∞	Botrytis-specific protein
Bcin10g01430	22,2	0	∞	Botrytis/Sclerotinia-specific protein
Bcin10g02110	20,7	0	∞	Botrytis-specific protein
Bcin10g06120	25,5	0	∞	Botrytis-specific protein
Bcin12g00400	50,4	0	∞	Botrytis-specific protein
Bcin12g01010	62,9	0	∞	putative peptidase inhibitor I9
Bcin12g01210	41,9	0	∞	Botrytis-specific protein
Bcin13g01220	31,6	0	∞	Botrytis/Sclerotinia-specific protein
Bcin13g03380	113,4	0	∞	Botrytis/Sclerotinia-specific protein
Bcin14g02630	149,5	0	∞	unknown protein
Bcin14g03560	32,7	0	∞	unknown protein
Bcin15g01750	52,1	0	∞	Botrytis/Sclerotinia-specific protein
Bcin16g02780	243,6	0,2	1535	Botrytis/Sclerotinia-specific protein
Bcin04g02460	253,2	0,3	822	acid phosphatase PhoA
Bcin05g02060	178,2	0,2	796	Botrytis-specific protein
Bcin09g06010	157,5	0,2	718	conserved fungal protein
Bcin08g01380	77,1	0,1	554	Helotiales specific protein
Bcin04g02440	62,3	0,1	440	Botrytis/Sclerotinia-specific protein
Bcin03g04490	482,0	1,1	420	Botrytis/Sclerotinia-specific protein
Bcin01g06180	51,8	0,2	331	Botrytis/Sclerotinia-specific protein
Bcin03g08720	193,0	0,6	324	Botrytis-specific protein
Bcin15g00750	240,8	0,8	299	protein tyrosine phosphatase
Bcin11g06360	427,3	1,5	294	conserved fungal protein

Bcin08g00450	27,2	0,1	293	Botrytis/Sclerotinia-specific protein
Bcin07g01730	89,1	0,3	286	Botrytis/Sclerotinia-specific protein
Bcin15g04070	33,4	0,1	258	Botrytis/Sclerotinia-specific protein
Bcin12g06570	85,2	0,4	242	unknown protein
Bcin07g05020	33,6	0,1	241	Botrytis/Sclerotinia-specific protein
Bcin09g06000	31,7	0,1	236	conserved fungal protein
Bcin02g05760	117,8	0,6	205	Botrytis-specific protein
Bcin06g06120	107,5	0,6	194	conserved fungal protein
Bcin01g02080	166,4	0,9	192	RNA-binding protein
Bcin07g04490	117,0	0,6	190	protein kinase CBK1
Bcin11g01540	73,3	0,4	179	Botrytis-specific protein
Bcin03g06310	124,9	0,7	177	RNA-binding domain RRM2 protein
Bcin12g05070	48,6	0,3	171	putative NRPS-like enzyme
Bcin05g07960	31,8	0,2	169	calcium homeostasis protein regucalcin
Bcin11g01520	94,9	0,6	168	Botrytis-specific protein
Bcin04g01530	80,1	0,5	162	Helotiales specific protein
Bcin10g02780	25,6	0,2	158	Botrytis/Sclerotinia-specific protein
Bcin14g00040	62,7	0,4	155	Botrytis-specific protein
Bcin12g01200	140,3	0,9	153	Botrytis-specific protein
Bcin10g01360	39,5	0,3	151	Botrytis/Sclerotinia-specific protein
Bcin14g00030	39,5	0,3	143	unknown protein
Bcin06g03390	435,8	3,1	138	nucleoside-diphosphate-sugar epimerase
Bcin12g03170	299,6	2,2	138	meiotic RNA-binding protein MSSP2
Bcin12g06500	70,2	0,5	132	ubiquitin carboxyl-terminal hydrolase
Bcin04g00190	28,5	0,2	132	Botrytis/Sclerotinia-specific protein
Bcin02g05200	251,8	2,0	127	Botrytis-specific protein
Bcin06g01570	29,5	0,2	125	conserved fungal protein
Bcin14g01470	63,3	0,5	123	Botrytis-specific protein
Bcin04g06800	33,6	0,3	121	conserved fungal protein
Bcin09g04810	46,7	0,4	119	Botrytis/Sclerotinia-specific protein
Bcin03g02690	52,6	0,5	115	Botrytis/Sclerotinia-specific protein
Bcin08g04580	94,2	0,8	111	transcription factor Zn, C2H2
Bcin03g04580	331,5	3,2	103	Botrytis/Sclerotinia-specific protein
Bcin12g01430	76,0	0,8	98	Botrytis-specific protein
Bcin11g00920	31,5	0,3	97	Botrytis/Sclerotinia-specific protein
Bcin08g00740	48,5	0,5	92	high affinity glucose transporter
Bcin13g01660	33,9	0,4	89	histone acetyltransferase GCN5/NGF1
Bcin15g04900	40,8	0,5	89	Botrytis/Sclerotinia-specific protein
Bcin15g01540	147,3	1,7	87	Botrytis/Sclerotinia-specific protein
Bcin02g00550	26,7	0,3	86	Botrytis/Sclerotinia-specific protein
Bcin14g02950	314,2	3,7	86	putative zinc knuckle transcription factor
Bcin06g01480	20,6	0,3	81	Botrytis-specific protein
Bcin05g06620	42,8	0,5	81	Botrytis-specific protein
Bcin01g09070	26,3	0,3	80	putative F-box domain protein
Bcin13g02810	75,6	1,0	72	conserved fungal protein
Bcin11g05000	109,2	1,6	68	elongation factor 2 kinase
Bcin12g03130	352,0	5,2	67	GMC oxidoreductase
Bcin06g05310	108,7	1,7	65	conserved fungal protein,
Bcin01g04410	268,6	4,2	64	DEAD box RNA helicase DED1
Bcin04g04850	56,8	0,9	64	MHYT domain signaling protein

Bcin10g02080	67,3	1,1	62	conserved fungal protein
Bcin07g00910	43,4	0,7	62	Botrytis/Sclerotinia-specific protein
Bcin11g00760	50,9	0,8	60	conserved fungal protein
Bcin12g01740	24,3	0,4	60	Botrytis-specific protein
Bcin06g00110	44,6	0,7	60	conserved fungal protein
Bcin16g02350	157,3	2,6	60	Botrytis-specific protein
Bcin08g05340	24,5	0,4	59	Botrytis-specific protein
Bcin14g03870	94,6	1,6	59	Botrytis/Sclerotinia-specific protein
Bcin02g03710	14,1	0,2	58	Botrytis/Sclerotinia-specific protein
Bcin11g01510	127,8	2,2	57	Botrytis-specific protein
Bcin12g05230	29,7	0,5	57	Botrytis/Sclerotinia-specific protein
Bcin15g03000	736,8	13,0	57	Botrytis/Sclerotinia-specific protein
Bcin08g05330	64,2	1,1	56	Botrytis/Sclerotinia-specific protein
Bcin11g02140	226,0	4,1	55	conserved fungal protein
Bcin08g03000	48,1	0,9	54	conserved fungal protein
Bcin14g03570	25,1	0,5	54	Leotiomycetes-specific protein
Bcin09g02120	52,1	1,0	53	Botrytis/Sclerotinia-specific protein
Bcin05g03590	99,5	1,9	52	Botrytis/Sclerotinia-specific protein
Bcin05g03480	57,8	1,1	51	FK506 suppressor Sfk1
Bcin08g01500	34,8	0,7	50	conserved fungal protein

Supplementary Table 8

Genes upregulated in the *ΔMAT1-1-5* stipes

Gene ID	wild type	*ΔMAT1-1-5*	Ratio wt/mutant	Description
Bcin02g00003	0	26	0	Botrytis-specific protein
Bcin03g01280	0,7	57	82	LEA-domain protein (late abundant embryogenesis)
Bcin03g01290	3,7	280	76	Botrytis/Sclerotinia-specific protein
Bcin03g01320	11,2	552	49	conserved fungal protein
Bcin08g00110	0,2	11	49	similar to microsomal epoxide hydrolase
Bcin03g01300	35,2	1159	33	Botrytis/Sclerotinia-specific protein
Bcin07g02980	2,1	67	31	NADPH dehydrogenase
Bcin03g01240	31,6	893	28	small Helotiales-specific glycine rich protein
Bcin03g01310	1,2	28	24	conserved fungal protein
Bcin09g05490	0,6	13	23	conserved fungal protein
Bcin02g00530	6,9	148	21	cytochrome P450-domain containing protein
Bcin14g04530	18,5	379	20	2,3-diketo-5-methylthio-1-phosphopentane phosphatase

Chapter 3

Functional analysis of hydrophobin genes in sexual development of *Botrytis cinerea*

This chapter is published as:

Abstract

Hydrophobins are small secreted fungal proteins that play roles in growth and development of filamentous fungi, i.e. in the formation of aerial structures and the attachment of hyphae to hydrophobic surfaces. In *Botrytis cinerea*, three hydrophobin genes have been identified. Studies by Mosbach et al. (2011) showed that hydrophobins are neither involved in conferring surface hydrophobicity to conidia and aerial hyphae of *B. cinerea*, nor are they required for virulence. The present study investigated the role of hydrophobins in sclerotium and apothecium development. Expression analysis revealed high expression of the *Bhp1* gene during different stages of apothecium development. Two *Bhp1* splice variants were detected that differ by an internal stretch of 13 amino acid residues. Seven different mutants in which either a single, two or three hydrophobin genes were knocked out, as well as two wild type strains of opposite mating types, were characterized for sclerotium and apothecium development. No aberrant morphology was observed in sclerotium development when single deletion mutants in hydrophobin genes were analyzed. Sclerotia of double knock out mutant *ΔBhp1/ΔBhp3* and the triple knock out mutant, however, showed easily wettable phenotypes. For analyzing apothecium development, a reciprocal crossing scheme was setup. Morphological aberrations were observed in crosses with two hydrophobin mutants. When the double knock out mutant *ΔBhp1/ΔBhp2* and the triple knock out mutant were used as the maternal parent (sclerotia), and fertilized with wild type microconidia, the resulting apothecia were swollen, dark brown in color and had a blotched surface. After initially growing upwards toward the light source, the apothecia in many cases collapsed due to loss of structural integrity. Aberrant apothecium development was not observed in the reciprocal cross, when these same mutants were used as the paternal parent (microconidia). These results indicate that the presence of hydrophobins in maternal tissue is important for normal development of apothecia of *B. cinerea*.

Introduction

Botrytis cinerea is a haploid necrotrophic pathogen of over 200 plant species including agronomical and ornamental crops of economic importance. *B. cinerea* produces different structures in order to complete its life cycle including macroconidia, microconidia, sclerotia and fruiting bodies called apothecia. Macroconidia and sclerotia are asexual stages while apothecia are the sexual stage. The sclerotium serves as a multicellular resting structure and a source of nutrients during apothecium development (Li and Rollins, 2009). As a heterothallic fungus, *B. cinerea* needs two isolates of opposite mating types to initiate apothecium development. Apothecia of *B. cinerea* have the shape of a cup, are light brown in color, normally 10 mm in height (Whetzel, 1945), and they contain asci with eight ascospores resulting from meiosis. Individual apothecia can produce millions of ascospores that are discharged to the environment to serve as a source of inoculum for disease development, especially in early spring. The macroscopic morphology of apothecia of *B. cinerea* closely resembles that of *Sclerotinia sclerotiorum* and *Sclerotinia minor*.   In *S. minor*, the apothecium development was divided into 4 stages (Bullock et al., 1983), whereas in *S. sclerotiorum* 7 stages are distinguished (http://www.sclerotia.org/lifecycle/apothecia).

Hydrophobins are small, surface-active proteins of about 10 kDa with eight cysteine residues in conserved positions. Hydrophobins were originally described by Wessels et al., (1991a) and Wessels et al., (1991b) and have been studied for more than two decades (Zampieri et al., 2010). These proteins can only be found in filamentous Ascomycota and Basidiomycota fungi and they are important in the formation of an amphipathic membrane at a hydrophobic–hydrophilic interface (Sunde et al., 2008; Wösten and de Vocht, 2000). In *Ophiostoma ulmi*, hydrophobins show high expression levels, of about 25% of the total mRNA or 10% of total protein content (Zhang et al., 1994). Hydrophobins can form solid hydrophobic aggregates on the surface by self-assembling activity and thereby coat the surface of conidia, mycelia or fruiting bodies of many fungi (Linder, 2009; Macindoe et al., 2012; Wessels, 1996; Wösten, 2001; Wösten et al., 1993).

Hydrophobins have various functions in supporting fungal growth and development. For example, in *Agaricus bisporus* and *Schizophyllum commune*, secreted hydrophobins help reduce the surface tension and enable the fruiting body to penetrate the water or soil surface (van Wetter et al., 2000; Wessels et al., 1991a; Wösten, 2001; Wösten et al., 1994b). Besides that, hydrophobins were shown to be involved in conidiogenesis or in the triggering of appressorium formation for penetration of host surfaces by *Magnaporthe grisea* (Talbot et al., 1996). They are also believed to be involved in the establishment of lichen symbiosis (Dyer, 2002) and the interaction between the ectomycorrhizal fungus *Tricholoma terreum* and its host trees (Mankel et al., 2002). In addition, hydrophobins are involved in microsclerotia development in *Verticillium dahliae* (Klimes and Dobinson, 2006).

Hydrophobins are divided into two classes based on hydrophobicity, amino acid arrangement and their ability to form layers (Wessels, 1994; Wösten et al., 1994a; Wösten et al., 1994b). Class I hydrophobins are commonly found in Ascomycota and Basidiomycota species, while class II hydrophobins are restricted to Ascomycota. Class I hydrophobins are generally longer than class II hydrophobins, with size ranges of 100–125 residues (class I) versus 50–100 residues (class II), respectively. The class I hydrophobins usually are able to form a stable structure of fibrillar 'basket-weave' polymer film, called rodlet layer (Beever et al., 1979; Del Sol et al., 2007), 10–25 nm in width and 35–240 nm in length (Dempsey and Beever, 1979; Gardner et al., 1983; Wu-Yuan and Hashimoto, 1977). Rodlets can be observed on the surface of conidia of *Aspergillus nidulans* (Doss et al., 1997) *Neurospora crassa* (Beever and Dempsey, 1978; Beever et al., 1979; Dempsey and Beever, 1979; Doss et al., 1997) and the fruiting body of *S. commune* (van Wetter et al., 2000). Class I hydrophobins are insoluble in water and can only be dissolved with trifluoroacetic acid (TFA) or formic acid (FA) (Bayry et al., 2012; Hektor and Scholtmeijer, 2005; Linder, 2009; Wösten, 2001; Wösten et al., 1993). Class II hydrophobins do not form rodlet layers but rather form smooth surfaces, and they are soluble in hot sodium dodecyl sulfate (SDS) or 60% ethanol (Hektor and Scholtmeijer, 2005; Linder, 2009; Paananen et al., 2003; Torkkeli et al., 2002; Wösten, 2001). Studies on the surface of *B. cinerea* conidia and hyphae have failed to provide evidence for the production of rodlet layers (Doss et al., 1997; Mosbach et al., 2011).

Various numbers of hydrophobin genes are present in genomes of different fungi, ranging between two and seven genes per species, with *Coprinopsis cinerea* as an exception, containing 33 hydrophobin genes (Bayry et al., 2012; Stajich et al., 2010). In *B. cinerea*, three bona fide hydrophobin genes have been identified which were designated *Botrytis-hydrophobin-1* (*Bhp1*; class I), *Botrytis-hydrophobin-2* (*Bhp2*; class II) and *Botrytis-hydrophobin-3* (*Bhp3*; class II) as well as several genes encoding *hydrophobin-like* proteins such as *Bhl1* (Mosbach et al., 2011). Previous studies revealed that hydrophobin genes in *B. cinerea* are not required for asexual development or for virulence (Mosbach et al., 2011). The aim of the present study was to investigate the roles of class I and class II hydrophobins in the development of sclerotia and apothecia of *B. cinerea*.

Materials and methods

Strains used

Seven hydrophobin mutants with a *MAT1-1* background (Mosbach et al., 2011), and the *MAT1-2* reference strain SAS405 (Faretra et al., 1988) were used (Table 1).

Sclerotium development and sexual crosess

The wild type and hydrophobin mutant strains were grown on malt extract agar (MEA, Oxoid, Basingstoke, UK) and incubated at 15 °C in darkness to promote sclerotium development (Faretra et al., 1988). After 4 weeks incubation, observations were made of the number of sclerotia per plate, as well as their size, shape and morphology. A protocol described by Faretra et al. (1988) and van der Vlugt-Bergmans et al. (1993) was used to generate apothecia. Crosses were setup using hydrophobin mutants (all carrying the *MAT1-1* locus) and wild type strain SAS405 (carrying the *MAT1-2* locus). All crosses were setup reciprocally, using the mutants either as the maternal parent (sclerotia) or paternal parent (microconidia). As a control, apothecia were generated from a cross between the wild type recipient strain (*MAT1-1*) and SAS405 (*MAT1-2*). Table 2 shows the full scheme of crosses that were performed.

Table 1: Hydrophobin mutants and wild type strains used in this study

Type	Strain	Hydrophobin class	Mating type
Mutants	Single knock out		
	ΔBhp1	I	*MAT1-1*
	ΔBhp2	II	*MAT1-1*
	ΔBhp3	II	*MAT1-1*
	Double knock out		
	ΔBhp2/ΔBhp3	II	*MAT1-1*
	ΔBhp1/ΔBhp2	I and II	*MAT1-1*
	ΔBhp1/ΔBhp3	I and II	*MAT1-1*
	Triple knock out		
	ΔBhp1/ΔBhp2/ΔBhp3	I and II	*MAT1-1*
Wild type	B05.10		*MAT1-1*
	SAS405		*MAT1-2*

Table 2: Sexual crosses performed in this study

Sclerotia	Microconidia	Setup	Replicates[a]	# Experiments[b]
SAS405	B05.10	Wild type	3	4
B05.10	SAS405	*x* wild type	3	4
SAS405	*ΔBhp1*		3	4
ΔBhp1	SAS405		3	4
SAS405	*ΔBhp2*	Wild type *x* single mutant	3	4
ΔBhp2	SAS405		3	4
SAS405	*ΔBhp3*		3	4
ΔBhp3	SAS405		3	4
SAS405	*ΔBhp2/ΔBhp3*		3	4
ΔBhp2/ΔBhp3	SAS405		3	4
SAS405	*ΔBhp1/ΔBhp2*	Wild type *x* double mutant	3	4
ΔBhp1/ΔBhp2	SAS405		3	4
SAS405	*ΔBhp1/ΔBhp3*		3	4
ΔBhp1/ΔBhp3	SAS405		3	4
SAS405	*ΔBhp1/ΔBhp2/ ΔBhp3*	Wild type	3	4
ΔBhp1/ΔBhp2/ΔBhp3	SAS405	*x* triple mutant	3	4
ΔBhp1	Water		1	4
ΔBhp2	Water		1	4
ΔBhp3	Water		1	4
ΔBhp2/ΔBhp3	Water	Unfertilized control	1	4
ΔBhp1/ΔBhp2	Water		1	4
ΔBhp1/ΔBhp3	Water		1	4
ΔBhp1/ΔBhp2/ΔBhp3	Water		1	4

[a] number of biological replicates within an experiment

[b] number of experiments

Apothecium development was monitored 2–3 times per week for up to 90 days after fertilization. *B. cinerea* apothecium development was divided into 6 stages (Figure 1) defined as follows; stage 1: initials 1-2 mm in height; stage 2: stipes 2–4 mm in height; stage 3: stipes >5 mm in height (stipes elongated but not swollen at the tip); stage 4: stipes fully extended to ~1 cm, swollen at the tip and showing initiation of apothecial disk development; stage 5: immature disk with diameter <5 mm, partially expanded; stage 6: mature disks fully expanded to ~1 cm, filled with asci containing 8 ascospores. A preparation of ascospores was obtained from mature apothecia by gently crushing an apothecial disk in water, and filtering the resulting suspension over a plug of glasswool. The flow-through mainly contained a suspension of single ascospores released from asci, with minor contamination of intact asci or fragments of the hymenium.
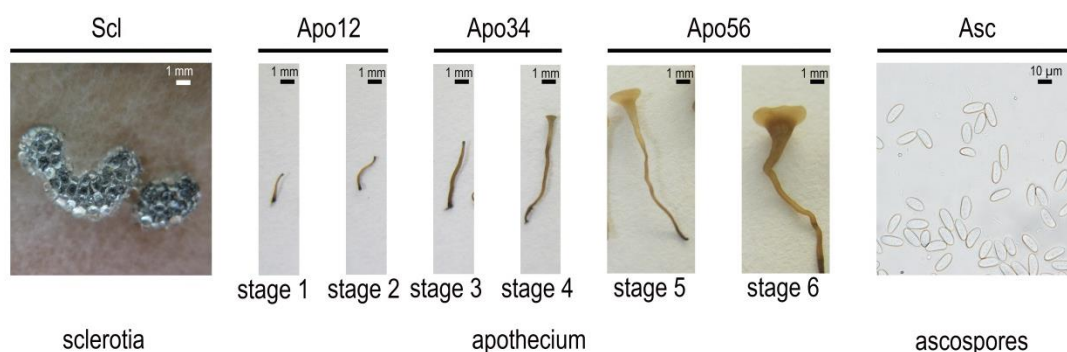
Figure 1: Tissues and stages of apothecium development used in this study. Scale bars indicate the sizes in mm or µm

RNA extraction, quantitative-real time-PCR and reverse transcriptase-PCR

Nine tissue types were sampled for RNA extraction: 1-week-old mycelia, 2-week-old mycelia, 3-week-old sclerotia, 4-week-old sclerotia grown on MEA at 15°C in darkness; 8-week-old sclerotia grown for 4 weeks at 15°C and then incubated for 4 weeks at 0°C; apothecia harvested in three stages of development: combined stages 1–2, combined stages 3–4, and combined stages 5–6; ascospores collected from mature apothecia. The specimens were freeze-dried and total RNA was isolated using the Nucleospin RNA plant kit (Macherey Nagel, Düren, Germany), according to the manufacturer's instructions. RNA was isolated from at least two biological replicates for each sample.

Five types of RNA samples were sequenced on an Illumina HiSeq 2000 platform by Beijing Genome Institute (Hongkong, China): 8-week-old sclerotia; apothecia combined stages 1–2; apothecia combined stages 3–4; apothecia combined stages 5–6; ascospores. Two biological replicates were sequenced of each sample, with the exception of the sclerotia. Reads were mapped on the *B. cinerea* B05.10 version 2 genome assembly (Staats and van Kan, 2012) using Tophat v2.0.8b (Kim et al., 2013). This constitutes the RNAseq data.

As template for Reverse Transcriptase PCR (RT-PCR), first strand cDNA was synthesized from 1 μg total RNA with M-MLV Reverse Transcriptase (Promega, Leiden, The Netherlands) according to the manufacturer's instructions. RT-PCR was performed to assess the existence of splice variants of *Bhp1*. The primer pair Bhp1Fvar1 and Bhp1Rvar1 (Table 3) was used to amplify splice variant 1, while primer pair Bhp1Fvar1 and Bhp1Rvar2 (Table 3) was used to amplify splice variant 2.   PCR conditions were as follows: 95 °C for 5 min, then 35 cycles of 94 °C for 30 s, 58 °C for 30 s and 72 °C for 30 s, followed by a final extension of 72 °C for 5 min. PCR products were visualized following electrophoresis on a 2.5% agarose gel. All experiments were performed in two biological replicates.

Quantitative-Real Time-PCR (qRT-PCR) was performed using an ABI7300 PCR machine in combination with the qPCR SensiMix kit with primers listed in Table 3. All qRT-PCR reactions were performed in three technical replicates using samples from at least two biological replicates. In order to quantify relative DNA contents of *Bhp1*, *Bhp2*, *Bhp3* and *Hph* genes, primer pairs Bhp1For6683/NewBhp1Rev, Bhp2For4417/NewBhp2Rev, Bhp3For5460/Bhp3Rev5460 and NewHphFor/NewHphRev were used, respectively. The relative DNA content values were normalized to the *Bcpg1* gene (Zhang and Van Kan, 2013). To quantify the levels of *Bhp1*, *Bhp2* and *Bhp3* transcripts, the primer pairs Bhp1For6683/Bhp1Rev6683, Bhp2For4417/Bhp2Rev4417, and Bhp3For5460/Bhp3Rev5460 were used, respectively. Gene expression values were normalized to the expression of the constitutively expressed *BctubA* gene, Genbank accession Z69263.2 (Benito et al., 1998).

qRT-PCR conditions were as follows: an initial 95 °C denaturation step for 10 min followed by denaturation for 15 s at 95 °C and annealing/extension for 1 min at 60 °C for 40 cycles. The data were analyzed on the 7300 System SDS software and calculated according to the $2^{-\Delta\Delta Ct}$ method (Livak and Schmittgen, 2001).

Table 3: List of primers used in this study.

Gene	Primer Name	Sequence	Reference
Bhp1	Bhp1For6683	GGTCGTTGCTATTCCCACTAC	This study
Bhp1	Bhp1Rev6683	TTGGGATCGGGATTTCGGCG	This study
Bhp1	NewBhp1Rev	TGCCTAGAATGCCATCACCTC	This study
Bhp1	Bhp1Fvar1	GGGCAATCTATTGGGTTTGAATTGCG	This study
Bhp1	Bhp1Rvar1	GAACATTAATCCCTCCCTGTG	This study
Bhp1	Bhp1Rvar2	GAACATTAATCCCTCCCACTG	This study
Bhp2	Bhp2For4417	CCTCGCAATGCCTACAACCC	This study
Bhp2	Bhp2Rev4417	CATCGGCGCAGACATCACTG	This study
Bhp2	NewBhp2Rev	CCTCGCAGTCTAGATCAGCTA	This study
Bhp3	Bhp3For5460	CTTCGGCTATTGACACAGCCA	This study
Bhp3	Bhp3Rev5460	TAGGTGTGATGGCAGCTTTCAA	This study
Hph	NewHphFor	CAAGCAAGGTAAGTGGACGAC	This study
Hph	NewHphRev	ACGCTGTCGAACTTTTCGATCA	This study
BctubA	TubulinAfor	GCGTTCGTGCATTGGTATGT	Benito et al., (1998)
BctubA	TubulinArev	CACGGGCCTCAGAGAATTCA	Benito et al., (1998)
Bcpg1	Bcpg1 F	CTGCCAACGGTGTCCGTATC	Zhang and van Kan (2013)
Bcgp1	Bcpg1 R	GAACGACAACACCGTAGGATG	Zhang and van Kan (2013)

Light microscopy

Transverse sections of apothecia were mounted on slides with water. Observations were made with a Nikon Eclipse 90i (Nikon Instruments, Badhoevedorp, The Netherlands) compound microscope with a Nikon DS-5MC camera attached. Measurements were performed using N.I.S. Elements AR 2.30 software (Nikon Instruments).

Scanning electron microscopy

Three to four sclerotia with sizes of 4–6 mm were collected randomly from MEA plates. Four-week-old sclerotia incubated in darkness at 15°C were used. Apothecia were harvested 60–90 days after fertilization. One to three apothecia per sclerotium were cut off using a scalpel and handled by forceps. The sclerotia and apothecia were fixed in 4% glutaraldehyde in 0.1 M potassium phosphate buffer pH 7.2. The fixation was done under vacuum for 10 min at room temperature, followed by overnight incubation at 4°C. Then, the samples were washed using 0.1 M potassium phosphate buffer pH 7.2 at 4°C (3 × 20 min) followed by post-fixation with 1% OsO4 in 0.1 M potassium phosphate buffer pH 7.2, 1 h at room temperature. The dehydration was done in ethanol (70%, 95% and 100%) for 30 min each

and finally transferred to 100% acetone for 30 min. The apothecia and sclerotia were subsequently critical point dried with carbon dioxide (CPD 030, BalTec, Liechtenstein). The samples were sputter-coated with 15 nm iridium (Leica EM SCD 500) and analyzed at 2 kV at room temperature in a field emission scanning electron microscope (Magellan 400, FEI, Eindhoven, the Netherlands). Digital images were contrast-optimized with Photoshop CS 5.

Results

Gene expression

In a previous study by Mosbach et al. (2011), expression analyses revealed low or undetectable expression of hydrophobin genes *Bhp*1 (class I), *Bhp*2 (class II), *Bhp*3 (class II) in conidia or mycelia. Only *Bhp*1 showed increased expression in sclerotia or apothecia (Mosbach et al., 2011). We performed more detailed analyses to study the expression of hydrophobin genes in sclerotia and during different stages of apothecium development. RNA samples were isolated from sclerotia in different stages of development and from apothecia in stages 1–2, 3–4, and 5–6, as well as from a fraction enriched for ascospores (Figure 1). Transcript levels of *Bhp*1, *Bhp*2 and *Bhp*3 were analyzed by RNA sequencing (five samples, Table 4) and by qRT-PCR (all samples except for the ascospore fraction, Figure 2).

In RNA-seq data, the number of reads derived from *Bhp*1 was by far the highest of the three hydrophobin genes, especially in stages 3–4, while the number of reads derived from *Bhp*2 and *Bhp*3 was extremely low (Table 4). The RNA-seq read mapping revealed a minor splice variant of the *Bhp*1 mRNA (Supplementary Figure S1a), in which an alternative splice acceptor site of the second intron led to an internal insertion of 13 amino acid residues (Supplementary Figure S2). Based on the read coverage, the abundance of the minor splice variant is ~5% of the total. Reverse Transcriptase-PCR was used to confirm the occurrence of both splice variants in all stages of apothecium development (Supplementary Figure S1b).

Figure 2 shows expression profiles of hydrophobin genes as determined by qRT-PCR relative to ß-tubulin. High levels of *Bhp*1 transcript were detected in 3-week-old sclerotia while transcript levels of *Bhp*2 and*Bhp*3 at this time were low. In 4-week-old sclerotia, transcript levels of *Bhp*2 and *Bhp*3 increased while *Bhp*1 decreased. In 8-week-old sclerotia (4 weeks at

15°C and then incubated for 4 weeks at 0°C), *Bhp*1, *Bhp*2, and *Bhp*3 transcripts were undetectable (data not shown). This indicated that the hydrophobin genes were expressed at low levels in early stages of sclerotium development.

During apothecium development, the transcript level of *Bhp*1 was high in all stages while the transcript levels of *Bhp*2 and *Bhp*3 were extremely low in all stages (Figure 2). Overall, transcription patterns of hydrophobin genes were similar for both methods, RNA sequencing and qRT-PCR.

Table 4: Number of RNA-seq reads of *Bhp* genes in different tissue types and developmental stages of apothecia.

Gene	Sclerotia	Apothecia stages 1-2	Apothecia stages 3-4	Apothecia stages 5-6	Ascospores
*Bhp*1	70 (n=1)	17358 ± 354 (n=2)[*]	28724 ± 2558 (n=2)[*]	12377 ± 1043 (n=2)[*]	419 ± 122 (n=2)[*]
*Bhp*2	13 (n=1)	16 ± 4 (n=2)[*]	6 ± 2 (n=2)[*]	7 ± 2 (n=2)[*]	3 ± 1 (n=2)[*]
*Bhp*3	0 (n=1)	1 ± 0 (n =2)[*]	1 ± 1 (n =2)[*]	26 ± 6 (n=2)[*]	5 ± 4 (n=2)[*]
#reads/ sample	10978094	9485388[*]	9757285[*]	9988141[*]	10183343[*]

[*] , given number of reads is the average for two biological replicates
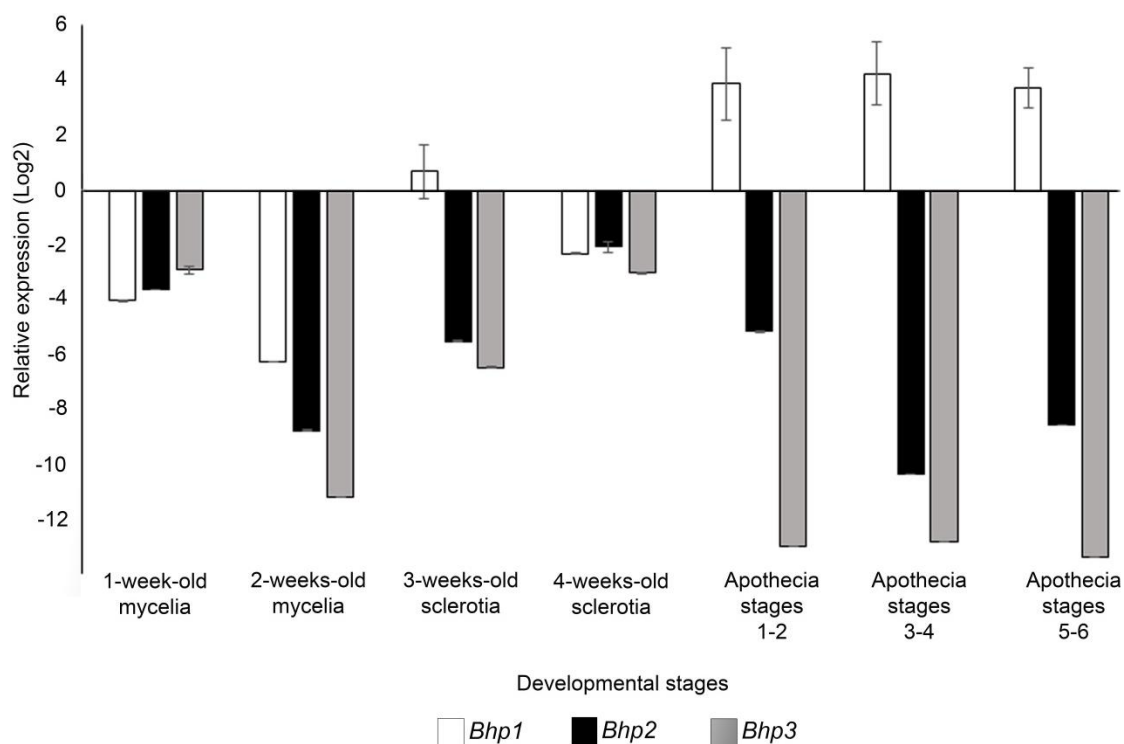
Figure 2: Transcript levels of *Bhp1*, *Bhp2* and *Bhp3* mRNA in mycelium and developing sclerotia (grown in MEA in darkness) and in different stages of apothecium development, measured by qRT-PCR. Transcript levels were normalized to the level of ß-tubulin mRNA.

Sclerotium development in hydrophobin mutants

To study the effect of the deletion of hydrophobin genes on sclerotium development, seven hydrophobin mutants and the wild type strain (Table 1) were used. The morphological appearance of sclerotia of the single Δ*Bhp*1 (class I hydrophobin) knock out mutant and two single Δ*Bhp*2 and Δ*Bhp*3 (class II hydrophobins) knock out mutants was similar to the wild type strains. The sclerotia had a silvery, shiny appearance with water droplets remaining on the surface (Figure 3, panels a and d). SEM images revealed the presence of a rough fibrillar layer on the surface of the wild type sclerotia (Figure 3, panels g and j). In double knock out mutants Δ*Bhp*1/Δ*Bhp*2 and Δ*Bhp*2/Δ*Bhp*3, the morphological appearance of the sclerotia was similar to the wild type. By contrast, sclerotia of the double knock out mutant Δ*Bhp*1/Δ*Bhp*3 and the triple knock out mutant were black and showed an easily wettable phenotype, i.e. water droplets applied on the surface easily dissipated (Figure 3, panels b, c, e and f). SEM showed that these mutant sclerotia lack a rough fibrillar layer, but instead have a smooth surface (Figure 3, panels h, i, k and l).

Apothecium development

To study the effect of the deletion of hydrophobin genes on apothecium development, reciprocal crosses were setup between hydrophobin mutants (made in a strain with *MAT1-1* identity) with wild type strain SAS405 (of *MAT1-2* identity). Sexual crosses of the wild type recipient and SAS405 were used as control. Observations were made 2–3 times a week over a period of at least 12 weeks after fertilization, until apothecia in control crosses were mature. In the crosses using the wild type recipient and the hydrophobin mutants as maternal parent, the primordia ruptured from sclerotia at 21 to 33 days after fertilization. Most of the primordia developed from the center of the sclerotia, scattered on the surface and sometimes at the edge of sclerotia (Figure 4, panel a). Within the first day after emerging, the primordia size was approximately 0.2 mm and growth was up to 1 mm in two days. The primordia continued to grow erected toward the light source and formed stipes (Figure 4, panel c), generally with a cylindrical appearance, common for the genus *Botrytis* (Whetzel, 1945). The apothecial disk began to expand between 14 and 20 days after emergence of the stipe and formed a cup-shaped structure which became flat and mature 30–60 days post emergence (60–90 days after fertilization) (Figure 4, panel g)
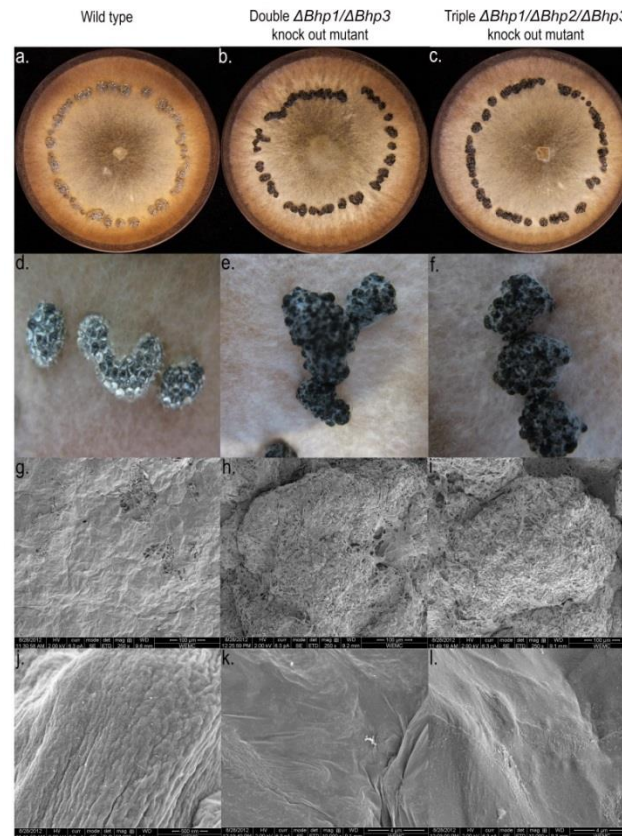
Figure 3: Morphology and wettability of sclerotia. (a and d) Wild type sclerotia had a silvery, shiny appearance with water droplets remaining on the surface; (g) a fibrillar layer is present on the surface of wild type sclerotia; (j) in high magnification the layer appears to have a rough surface; (b, c, e and f) sclerotia of the *ΔBhp1/ΔBhp3* double knock out mutant and the triple knock out mutant were black and showed an easily wettable phenotype; (h, i, k, l) in the *ΔBhp1/ΔBhp3* double knock out mutant and the triple knock out mutant, sclerotia contain a smooth external layer instead of the rough fibrillar structure.
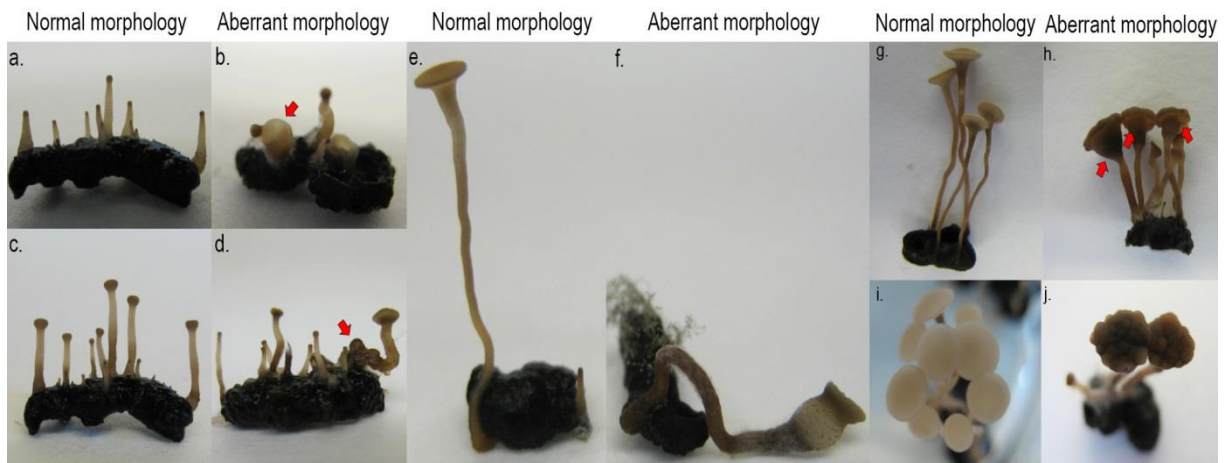
Figure 4: Aberrant apothecium development in crosses with hydrophobin mutants. Aberrant features are highlighted with a red arrow. (a) Primordia, (b) swollen primordia, (c) stipes, (d) swollen stipes, (e) apothecium developing from SAS405 as the maternal parent, normal morphology, (f) apothecium developing from triple knock out mutant as the maternal parent, collapsed during outgrowth, (g) mature wild type apothecia, (h) swollen cup of apothecia developing from triple knock out mutant, (i) flat apothecium surface, light brown in color, (j) blotched apothecium surface, dark brown in color.

Table 5: Morphological appearance of apothecium structures in different crosses

Sclerotia	Microconidia	Primordia and stipes	Saucer-cup	Apothecia surface	Color	Asci and ascospores
ΔBhp1	SAS405	WT	WT	WT	WT	WT
ΔBhp2	SAS405	WT	WT	WT	WT	WT
ΔBhp3	SAS405	WT	WT	WT	WT	WT
ΔBhp1/ΔBhp2	SAS405	Ab	Ab	Ab	Ab	WT
ΔBhp1/ΔBhp3	SAS405	WT	WT	WT	WT	WT
ΔBhp2/ΔBhp3	SAS405	WT	WT	WT	WT	WT
ΔBhp1/ΔBhp2/ΔBhp3	SAS405	Ab	Ab	Ab	Ab	WT
SAS405	*ΔBhp1*	WT	WT	WT	WT	WT
SAS405	*ΔBhp2*	WT	WT	WT	WT	WT
SAS405	*ΔBhp3*	WT	WT	WT	WT	WT
SAS405	*ΔBhp1/ΔBhp2*	WT	WT	WT	WT	WT
SAS405	*ΔBhp1/ΔBhp3*	WT	WT	WT	WT	WT
SAS405	*ΔBhp2/ΔBhp3*	WT	WT	WT	WT	WT
SAS405	*ΔBhp1/ΔBhp2/ΔBhp3*	WT	WT	WT	WT	WT

WT, normal morphological appearance; Ab, aberrant appearance.

Apothecia with normal morphological appearance were obtained in all crosses in which sclerotia of wild type strain SAS405 were fertilized with microconidia of hydrophobin mutants, and in most of the crosses in which a hydrophobin mutant was used as the maternal parent (Table 5). Aberrant development was observed in crosses using the double knock out mutant ΔBhp1/ΔBhp2 or the triple knock out mutant as the maternal parent (Figure 4). In these crosses, instead of developing cylindrical stipes, some of the primordia and stipes became swollen (Figure 4, panels b and d). Figure 4 shows two individual mature apothecia developed from the wild type (panel e) and the triple knock out mutant (panel f) as maternal parent. Both stipes had initially developed similarly, however, the apothecium derived from the triple knock out mutant as maternal parent collapsed during disk development in stage 4 (Figure, panel f). Moreover, swelling of the cup occurred before the expansion of the apothecial disk and clearly could be observed in mature apothecia in crosses in which the double knock out mutant ΔBhp1/ΔBhp2 or the triple knock out mutant served as the maternal parent. A typical example of a swollen cup is provided in Figure 4 (panel h). In addition, apothecia developing from double knock out mutant ΔBhp1/ΔBhp2 or the triple knock out mutant as the maternal parent had a blotched surface with dark brown color (Figure 4, panel j), whereas apothecia derived from the reciprocal cross had a flat, light brown surface (Figure 4, panel i).

SEM images revealed structural and morphological differences between apothecia derived from the triple knock out mutant (used as maternal parent), and those derived from two wild type parents, or apothecia derived from the triple knock out mutant used as paternal parent. Apothecia derived from the triple knock out mutant (used as maternal parent) appear to lack a smooth ectal excipulum (Figure 5, panel b). Instead the surface was covered with filamentous hyphae that do not form a continuous layer (Figure 4, panel d). In wild type apothecia (Figure 5, panel a), the cup is covered by a smooth layer and individual hyphae are not visible (Figure 5, panel c).
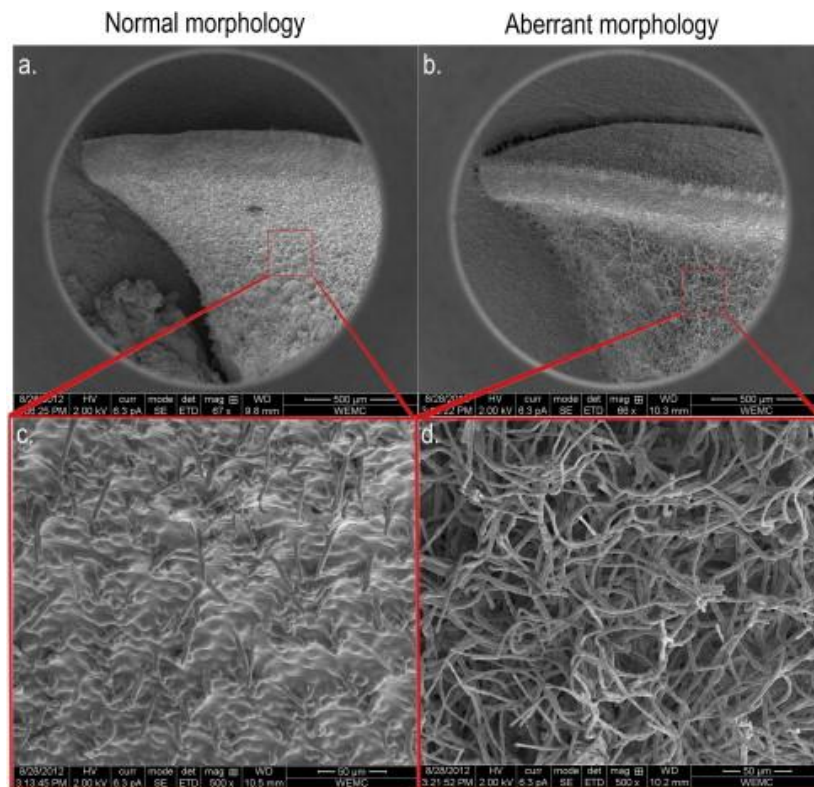
Figure 5: Scanning electron microscopy of cup stage. (a) Lower side of the cup of a wild type apothecium, (b) lower side of the cup of an apothecium developing on sclerotia of the triple knockout mutant, (c) close up of panel a, the tissue is covered with a smooth ectal excipulum, (d) close up of panel b, ectal excipulum is absent, filamentous hyphae do not appear to form a continuous layer

Asci and ascospores

Apothecia from all crosses were dissected and transverse sections were prepared and mounted on slides. No defects or aberrant phenotypes were observed in asci and ascospores of the apothecia produced using the hydrophobin mutants or wild type strain as maternal parent (not shown). The asci were on average 309 ± 36 µm ($n = 50$) in length and 16 ± 2 µm ($n = 50$) in width, while the ascospores were 11.3 ± 1.4 µm ($n = 50$) in length and 4.9 ± 0.1 µm ($n = 50$) in width. Asci are cylindrical and hyaline in color with an apical tip. Ascospores are oblong, hyaline, and there were always eight ascospores present in each ascus. No differences were observed in asci or ascospores from any crosses tested.

Gene dosage effects in crosses with knockout mutants

The aberrant apothecium development of mutants lacking both the *Bhp*1 and *Bhp*2 gene appears to be maternally controlled, and occurs even though the paternal mating partner is a wild type strain (SAS405), carrying all three functional hydrophobin genes. It should be considered that a developing apothecium is predominantly composed of maternal tissue, and contains only a limited proportion of dikaryotic cells, in which the paternal nucleus is present (Zickler, 2006). Thus the dosage (and concomitantly the transcript levels) of paternal genes is expected to be substantially lower than that of maternal genes. To examine gene dosage effects, qRT-PCR was performed to compare the DNA and mRNA levels of hydrophobin genes between reciprocal crosses of the double mutants (Δ*Bhp*1/Δ*Bhp*2 or Δ*Bhp*1/Δ*Bhp*3) or the triple knock out mutant with SAS405, using the mutant either as maternal parent (sclerotia) or paternal parent (microconidia). In apothecia from crosses with the triple knock out mutant as maternal parent, the amount of DNA of the three *Bhp* genes was 100-fold lower (Figure 6a) than in the reciprocal cross in which the same mutant served as paternal parent. In the same stage, the amount of *Bhp*1 mRNA was 60–250 fold lower than in reciprocal crosses in which the mutant served as paternal parent (Figure 6b). For *Bhp*2 and *Bhp*3, transcript levels were too low to calculate a ratio between samples.
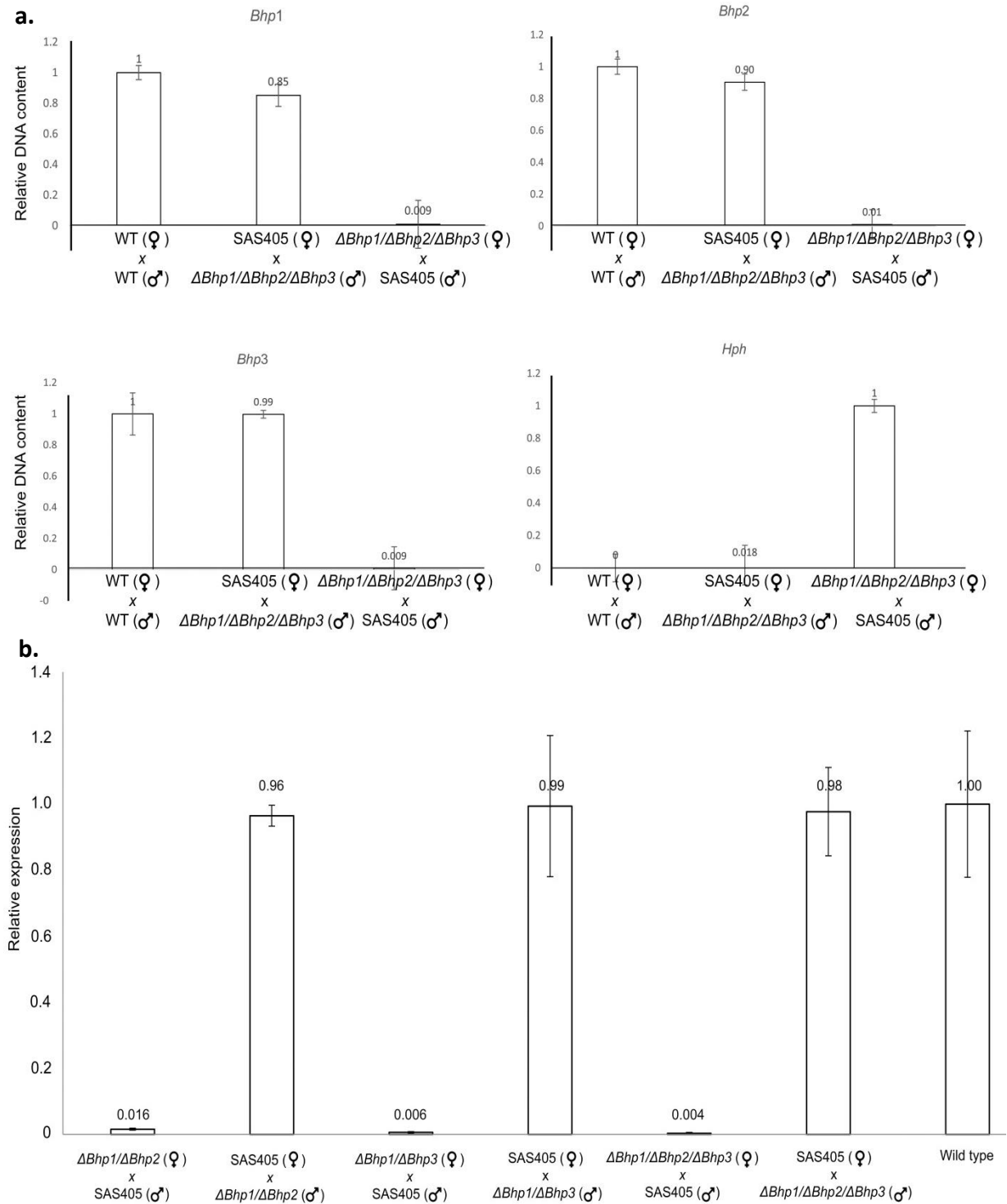
Figure 6: Panel a: Relative DNA content of *Bhp* genes and the hygromycin phosphotransferase (*Hph*) gene in apothecia derived from reciprocal crosses between wild type SAS405 and the triple knockout mutant. DNA content was normalized to the *B. cinerea Bcpg*1 gene. Panel b: Relative expression of *Bhp*1 in apothecia derived from reciprocal crosses between wild type SAS405 and double and triple knockout mutants. Transcript levels were normalized to the *B. cinerea* ß-tubulin gene *Bctub*A

Discussion

Hydrophobins are required for normal sclerotium and apothecium development in *B. cinerea*. Based on expression, one would predict that *Bhp*1 is the major component required for both structures because *Bhp*2 and *Bhp*3 are expressed only to low levels in these tissues. However, the single *Bhp*1 knock out mutant is fully functional both in sclerotium and apothecium development. A combination of the class I hydrophobin *Bhp*1 with one of the two class II hydrophobins is essential for proper development. Specifically, deletion of both *Bhp*1 (class I) and *Bhp*3 (class II) reduced surface hydrophobicity of sclerotia, and deletion of both *Bhp*1 and *Bhp*2 affected apothecium development. Aberrant apothecium development was observed only when the double knock out mutant Δ*Bhp*1/Δ*Bhp*2 (or the triple knock out mutant) served as the maternal parent but not when wild type strain SAS405 served as the maternal parent.

The maternal control of aberrant apothecium development can be explained by a gene dosage effect: based on DNA measurements, the proportion of dikaryotic cells is only 1% of the total. At this level, nuclei from the paternal parent do not contribute sufficient hydrophobin transcript to produce an adequate amount of protein. Furthermore, the dikaryotic cells containing paternal nuclei are located in the inner part of the developing stipe whereas hydrophobins must function on the surface of the emerging structure. The ectal excipulum of emerging stipes is purely of maternal origin and thus devoid of hydrophobins in the mutants.

The absence of hydrophobins caused the surface of apothecia to be discontinuous, with hyphae exposed to the outer environment without any visible external matrix. The smooth layer covering the apothecial surface in wild type apothecia therefore is proposed to be composed, at least in part, of hydrophobins possibly interacting with other surface proteins or polysaccharides. This is in agreement with the high expression level of hydrophobin *Bhp*1 during apothecium development and suggests their function in the formation of a protective coating for fungal structures that are exposed to air.

RNA-seq analysis revealed the occurrence of alternative splicing in *Bhp*1 transcripts, which results in an internal insertion of 13 amino acid residues that contains one additional

cysteine residue. Upon aligning the amino acid sequences of the resulting two Bhp1 protein variants with their orthologs in *S. sclerotiorum* and *Sclerotinia borealis* (Supplementary Figure S2), it was striking that the *S. sclerotiorum* ortholog lacks the 13 amino acids stretch insert, whereas *S. borealis* appears to contain the insert. Alignment of the nucleotide sequences of the *B. cinerea, S. sclerotiorum* and *S. borealis Bhp1* genes demonstrated that both alternative splice acceptor sites are present in all three genomes (not shown). It is tempting to propose that the alternative splicing event also occurs in *S. sclerotiorum* and *S. borealis* and possibly in other *Sclerotiniaceae*.

The implication of an insert with an additional cysteine residue for the folding of the hydrophobin is unclear. According to structural models of de Vocht et al. (2000), the eight cysteine residues are involved in disulfide bridge formation, with four couples of cysteine residues (always two consecutive residues in the primary sequence) pairing. The short *Bhp1* variant has eight cysteine residues, while the long variant has nine. This raises the question whether in the long variant protein, Cys^7 will form a disulfide bond with either Cys^8 or Cys^9, leaving a free cysteine available for interaction with other proteins. The functional role of producing splice variants of the Bhp1 protein of *B. cinerea* remains unknown. Alternative splicing appears widespread in fungi, occurring in ~1.5% of genes in *Fusarium graminearum* (Zhao et al., 2013), *Aspergillus flavus* and *M. grisea* (McGuire et al., 2008). Also in *B. cinerea*, alternative splicing occurs on a similar scale (van Kan, unpublished data).

Secreted class I hydrophobins can self-assemble into amphipathic monolayers on fungal surfaces and form a rodlet layer (Wösten, 2001). Previous studies by Doss et al. (1997) and Mosbach et al. (2011) have not provided any evidence for the existence of a rodlet layer on the conidia or hyphae of *B. cinerea*. In this study we investigated the formation of a rodlet layer on the surface of sclerotia and apothecia. Rough fibrillar structures were found to cover the surface of wild type sclerotia, whereas a smooth layer was found to cover the surface of wild type apothecia. The surface layers in *B. cinerea* are distinct from the typical basket-weave rodlet layers produced by fungi such as *A. nidulans* and *N. crassa* (Doss et al., 1997). We conclude that sclerotia and apothecia of *B. cinerea* do not produce a rodlet layer.

This study in *B. cinerea* provides the first example that both class I and class II hydrophobins can be involved in proper fruiting body development. This situation differs from other ascomycota fungi. In *Cryphonectria parasitica*, only class II hydrophobin genes are required for pycnidium and perithecium development (Kazmierczak et al., 2005). It is well established for many Basidiomycota that hydrophobins are required for fruiting bodies development, but Basidiomycota only contain class I hydrophobin genes. It is difficult to envisage how a class I and a class II hydrophobin protein can reciprocally compensate for loss of function. The two classes of hydrophobins differ in their physico-chemical properties, such as solubility. While aggregated class I hydrophobins are insoluble in aqueous solutions and can only be released from aggregates by treatment with pure formic acid or TFA, class II hydrophobins can be readily solubilized in hot SDS or 60% ethanol. It seems plausible that the properties of the *B. cinerea* Bhp1 and Bhp2 proteins are distinct, yet the mutant analysis suggest that the proteins can functionally complement one another. This is especially remarkable because the genes are expressed in such unequal ratio. The levels of *Bhp*2 mRNA are approximately 1000-fold lower than those of *Bhp1* in all stages of apothecium development (Figure 2), yet the single *Bhp1* knockout mutant forms apothecia of normal appearance, for reasons that remain unexplained.

Supporting information

Supplementary Figure S1a, Supplementary Figure S1b, Supplementary Figure S2.

References

Bayry, J., Aimanianda, V., Guijarro, J.I., Sunde, M., Latgé, J.-P., (2012) Hydrophobins - Unique fungal proteins. PLoS Pathogens 8, e1002700.

Beever, R.E., Dempsey, G.P., (1978) Function of rodlets on the surface of fungal spores. Nature 272: 608-610.

Beever, R.E., Redgwell, R.J., Dempsey, G.P., (1979) Purification and chemical characterization of the rodlet layer of *Neurospora crassa* conidia. Journal of Bacteriology 140: 1063-1070.

Benito, E.P., ten Have, A., van 't Klooster, J., van Kan, J.A.L., (1998) Fungal and plant gene expression during synchronized infection of tomato leaves by *Botrytis cinerea*. European Journal of Plant Pathology 104: 207-220.

Bullock, S., Willetts, H.J., Ashford, A.E., (1983) The structure and histochemistry of sclerotia of *Sclerotinia minor*. Changes in ultrastructure and loss of reserve materials during carpogenic germination. Protoplasma 117: 214-225.

de Vocht, M.L., Reviakine, I., Wösten, H.A.B., Brisson, A., Wessels, J.G.H., Robillard, G.T., (2000) Structural and functional role of the disulfide bridges in the hydrophobin SC3. Journal of Biological Chemistry 275: 28428-28432.

Del Sol, R., Armstrong, I., Wright, C., Dyson, P., (2007) Characterization of changes to the cell surface during the life cycle of *Streptomyces coelicolor*: atomic force microscopy of living cells. Journal of Bacteriology 189: 2219-2225.

Dempsey, G.P., Beever, R.E., (1979) Electron microscopy of the rodlet layer of *Neurospora crassa* conidia. Journal of Bacteriology 140: 1050-1062.

Doss, R.P., Christian, J.K., Potter, S.W., Soeldner, A.H., Chastagner, G.A., (1997) The conidial surface of *Botrytis cinerea* and several other *Botrytis* species. Canadian Journal of Botany 75: 612-617.

Dyer, P.S., (2002) Hydrophobins in the lichen symbiosis. New Phytologist 154: 1-4.

Faretra, F., Antonacci, E., Pollastro, S., (1988) Sexual behaviour and mating system of *Botryotinia fuckeliana*, teleomorph of *Botrytis cinerea*. Journal of General Microbiology. 134, 2543-2550.

Gardner, J.S., Hess, W.M., Tripathi, R.K., (1983) Surface rodlets of *Tilletia indica* teliospores. Journal of Bacteriology 154: 502-504.

Hektor, H.J., Scholtmeijer, K., (2005) Hydrophobins: proteins with potential. Current Opinion in Biotechnology 16: 434-439.

Kazmierczak, P., Kim, D.H., Turina, M., Van Alfen, N.K., (2005) A hydrophobin of the chestnut blight fungus, *Cryphonectria parasitica*, is required for stromal pustule eruption. Eukaryotic Cell 4: 931-936.

Klimes, A., Dobinson, K.F., (20060 A hydrophobin gene, VDH1, is involved in microsclerotial development and spore viability in the plant pathogen *Verticillium dahliae*. Fungal Genetics and Biology 43: 283-294.

Li, M., Rollins, J.A., (2009) The development-specific protein (Ssp1) from *Sclerotinia sclerotiorum* is encoded by a novel gene expressed exclusively in sclerotium tissues. Mycologia 101: 34-43.

Linder, M.B., (2009) Hydrophobins: proteins that self assemble at interfaces. Current Opinion in Colloid & Interface Science 14: 356-363.

Livak, K.J., Schmittgen, T.D., (2001) Analysis of relative gene expression data using Real-Time Quantitative PCR and the $2^{-\Delta\Delta CT}$ method. Methods 25: 402-408.

Macindoe, I., Kwan, A.H., Ren, Q., Morris, V.K., Yang, W., Mackay, J.P., Sunde, M., (2012) Self-assembly of functional, amphipathic amyloid monolayers by the fungal hydrophobin EAS. Proceedings of the National Academy of Sciences USA. 104: 20908–20913.

Mankel, A., Krause, K., Kothe, E., (2002) Identification of a hydrophobin gene that is developmentally regulated in the ectomycorrhizal fungus *Tricholoma terreum*. Applied and Environmental Microbiology 68: 1408-1413.

McGuire, A., Pearson, M., Neafsey, D., Galagan, J., (2008) Cross-kingdom patterns of alternative splicing and splice recognition. Genome Biology 9: R50.

Mosbach, A., Leroch, M., Mendgen, K., Hahn, M., (2011) Lack of evidence for a role of hydrophobins in conferring surface hydrophobicity to conidia and hyphae of *Botrytis cinerea*. BMC Microbiology 11: 10.

Paananen, A., Vuorimaa, E., Torkkeli, M., Penttilä, M., Kauranen, M., Ikkala, O., Lemmetyinen, H., Serimaa, R., Linder, M.B., (2003) Structural hierarchy in molecular films of two class II hydrophobins. Biochemistry 42: 5253-5258.

Staats, M., van Kan, J.A.L., (2012) Genome update of *Botrytis cinerea* strains B05.10 and T4. Eukaryotic Cell 11: 1413-1414.

Stajich, J.E., Wilke, S.K., Ahrén, D., Au, C.H., Birren, B.W., Borodovsky, M., Burns, C., Canbäck, B., Casselton, L.A., Cheng, C., (2010) Insights into evolution of multicellular fungi from the assembled chromosomes of the mushroom *Coprinopsis cinerea* (*Coprinus cinereus*). Proceedings of the National Academy of Sciences USA. 107: 11889

Sunde, M., Kwan, A.H.Y., Templeton, M.D., Beever, R.E., Mackay, J.P., (2008) Structural analysis of hydrophobins. Micron 39: 773-784.

Talbot, N.J., Kershaw, M.J., Wakley, G.E., De Vries, O., Wessels, J., Hamer, J.E., (1996) MPG1 encodes a fungal hydrophobin involved in surface interactions during infection-related development of *Magnaporthe grisea*. Plant Cell 8: 985-999.

Torkkeli, M., Serimaa, R., Ikkala, O., Linder, M., (2002) Aggregation and self-assembly of hydrophobins from *Trichoderma reesei*: low-resolution structural models. Biophysical Journal 83: 2240-2247.

van der Vlugt-Bergmans, C.J.B., Brandwagt, B.F., van't Klooster, J.W., Wagemakers, C.A.M., van Kan, J.A.L., (1993) Genetic variation and segregation of DNA polymorphisms in *Botrytis cinerea*. Mycological Research 97: 1193-1200.

van Wetter, M.A., Wösten, H.A.B., Wessels, J.G.H., (2000) SC3 and SC4 hydrophobins have distinct roles in formation of aerial structures in dikaryons of *Schizophyllum commune*. Molecular Microbiology 36: 201-210.

Wessels, J., (1994) Developmental regulation of fungal cell wall formation. Annual Review of Phytopathology 32: 413-437.

Wessels, J.G.H., (1996) Fungal hydrophobins: proteins that function at an interface. Trends in Plant Science 1: 9-15.

Wessels, J., de Vries, O., Asgeirsdottir, S.A., Schuren, F., (1991a) Hydrophobin genes involved in formation of aerial hyphae and fruiting bodies in *Schizophyllum*. Plant Cell 3: 793-799.

Wessels, J.G.H., de Vries, O.M.H., Ásgeirsdóttir, S.A., Springer, J., (1991b) The thn mutation of *Schizophyllum commune*, which suppresses formation of aerial hyphae, affects expression of the Sc3 hydrophobin gene. Journal of General Microbiology 137: 2439-2445.

Whetzel, H.H., (1945) A synopsis of the genera and species of the Sclerotiniaceae, a family of stromatic inoperculate Discomycetes. Mycologia 37: 648-714.

Wösten, H.A.B., (2001) Hydrophobins: multipurpose proteins. Annual Review of Microbiology 55: 625-646.

Wösten, H.A.B., de Vries, O.M.H., Wessels, J.G.H., (1993) Interfacial self-assembly of a fungal hydrophobin into a hydrophobic rodlet layer Plant Cell 5: 1567-1574.

Wösten, H.A.B., de Vocht, M.L. (2000) Hydrophobins, the fungal coat unravelled. Biochimica et Biophysica Acta 1469 (2):79-86

Wösten, H.A.B., de Vries, O., van der Mei, H., Busscher, H.J., Wessels, J., (1994a) Atomic composition of the hydrophobic and hydrophilic membrane sides of self-assembled SC3p hydrophobin. Journal of Bacteriology 176: 7085-7086.

Wösten, H.A.B., Schuren, F., Wessels, J., (1994b) Interfacial self-assembly of a hydrophobin into an amphipathic protein membrane mediates fungal attachment to hydrophobic surfaces. EMBO Journal 13: 5848-5854

Wu-Yuan, C.D., Hashimoto, T., (1977) Architecture and chemistry of microconidial walls of *Trichophyton mentagrophytes*. Journal of Bacteriology 129: 1584-1592.

Zampieri, F., Wösten, H.A.B., Scholtmeijer, A.K., (2010) Creating surface properties using a palette of hydrophobins. Materials 3: 4607-4625.

Zhang, L., van Kan, J.A.L., (20130 *Botrytis cinerea* mutants deficient in D-galacturonic acid catabolism have a perturbed virulence on *Nicotiana benthamiana* and *Arabidopsis*, but not on tomato. Molecular Plant Pathology 14: 19-29.

Zhang, L., Villalon, D., Sun, Y., Kazmierczak, P., Van Alfen, N., (1994) Virus-associated down-regulation of the gene encoding cryparin, an abundant cell-surface protein from the chestnut blight fungus, *Cryphonectria parasitica*. Gene 139: 59-64.

Zhao, C., Waalwijk, C., de Wit, P.J.G.M., Tang, D., van der Lee, T., (2013) RNA-Seq analysis reveals new gene models and alternative splicing in the fungal pathogen *Fusarium graminearum*. BMC Genomics. 14, 21.

Zickler, D., (2006) Meiosis in mycelial fungi. In: Kües U, Fischer R (eds) Growth, Differentiation and Sexuality, vol 1. The Mycota, 2nd edn. Springer Berlin Heidelberg, pp 415-438.

Supporting information

Supplementary Figure S1a

Differential splicing of the *Bhp1* gene. Both splice variant gene models are displayed at the top; below is a plot of the cumulative read coverage across all RNAseq datasets (dark blue); the bottom panel shows reads mapped on the genome sequence (in turquoise) with experimentally validated introns marked by a red box.
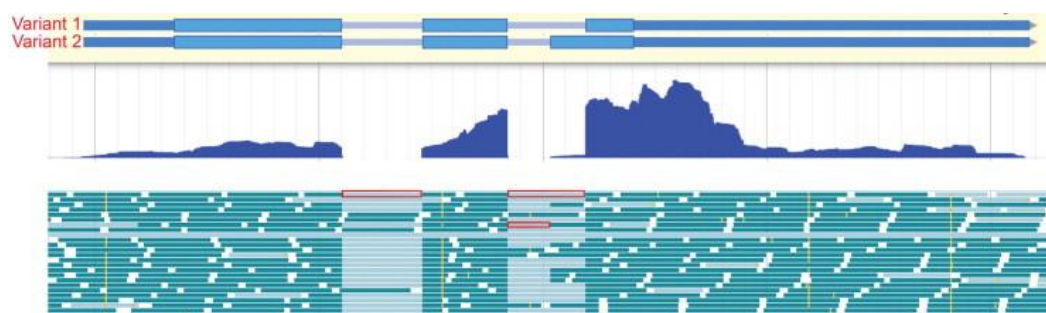
Supplementary Figure S1b

Reverse Transciptase PCR validation of splicing variants of *Bhp1* transcripts in sclerotia and different stages of apothecium development.
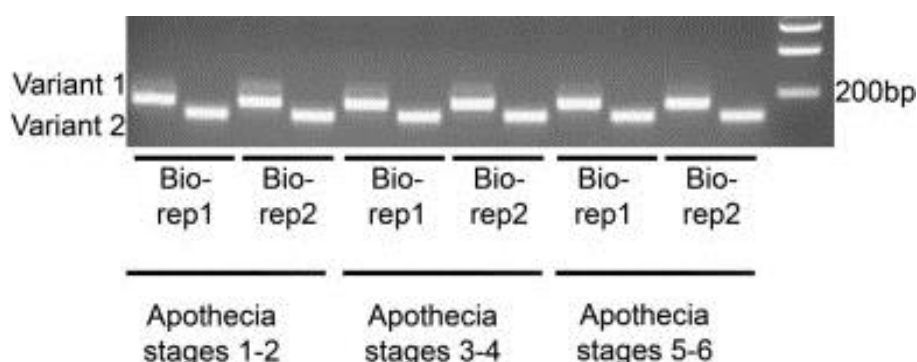
Supplementary Figure S2

Alignment of both *Botrytis cinerea* Bhp1 protein variants with orthologs in *Sclerotinia sclerotiorum* (gene ID SS1G_11895, Genbank accession EDN97370) and *S. borealis* (Genbank accession ESZ95445). The signal peptide is marked with a box. Cysteine residues are highlighted in bold case. Disulfide bridges based on the model of de Vocht et al. (2000) are indicated; alternative options for the 4th disulfide bridge in the longest splice variant are indicated by dotted lines.

Chapter 4

Mating type and sexual fruiting body of *Botrytis elliptica*, the causal agent of fire blight in lily

Abstract

Botrytis elliptica is a necrotrophic pathogen that specifically infects *Lilium* species. Previous records show that *B. elliptica* collected in the field can successfully develop apothecia in *vitro,* however, there are no formal descriptions of apothecia of *B. elliptica*. The aim of this study was to analyse the sequence of the mating type loci of *B. elliptica* and produce apothecia in the laboratory in order to describe their morphology. The sequences of both *MAT* alleles (*MAT1-1* or *MAT1-2*) of *B. elliptica* were determined and compared to the sister taxa, *Botrytis cinerea* and *Sclerotinia sclerotiorum*. Two strains of each mating type were used in crosses under controlled conditions to produce apothecia. Primordium rupture from sclerotial tissue occurred 74 days after fertilization and a mature apothecium formed within 1 month after rupture. The apothecia are 7 to 12 mm in height with a disk of 3 to 4 mm in diameter and 0.5 to 1 mm in thickness. The apothecial disk is usually umbilicate, depressed to funnel and rounded in shape. The number of apothecia growing on a sclerotium was one to nine. Asci are long, cylindrical with a size of 208 × 14 µm, thin walled and bearing eight ascospores. Ascospores are hyaline in colour, ellipsoidal with rounded ends, usually 18 to 24 µm in length and 6 to 10 µm in width (mean 19.5 × 8 µm). Ascospores were infectious on lily leaves.

Introduction

There are various modern lily cultivars on the market which originate from the genus *Lilium* of the family Liliaceae. The genus *Lilium* comprises about 100 species and was classified into seven sections, of which three comprise important hybrid cultivars for breeding: Asiatic, Oriental and Longiflorum (MacRae 1998; Shahin et al. 2012). Lilies are the second largest flower bulb crop in the Netherlands, and the largest flower bulb product in the world (Kamenetsky and Okubo 2012). Fire blight, also known as leaf blight is a major threat to lily production worldwide. The disease poses a major economic threat and has been recorded in Argentina, China, Korea, Italy, Japan, Netherlands, Taiwan, United Kingdom, and the United States (Bastiaansen et al. 1997; Chiou and Wu 2001; Doss et al. 1988; Furukawa et al. 2005; Hwang 2001; Mansfield and Hutson 1980; Migheli et al. 1990). During the growing season, fire blight may affect numerous lily species such as *Lilium candidum*, *Lilium longiflorum*, *Lilium auratum,* and *Lilium speciosum* (Bastiaansen et al. 1997; Doss et al. 1988; Fang Hsieh et al. 2001; Furukawa et al. 2005). The disease is caused by *Botrytis elliptica* (Berk) Cooke, a necrotrophic pathogen that only infects lilies. Host specificity of *B. elliptica* was proposed to be caused by the production of an as yet unidentified, secreted necrosis-inducing protein that causes programmed cell death (van Baarlen et al. 2004) and therefore presumably serves as a host-specific necrotrophic effector (Vleeshouwers and Oliver 2014). Symptoms such as necrotic spots on leaves and petals are the early signs of infection. The necrotic lesions develop and expand quickly under favourable environmental conditions (Chiou and Wu 2001; Hwang 2001; van Baarlen et al. 2004). Control measures using fungicides for *B. elliptica* are common practice worldwide, however, it has been reported that *B. elliptica* acquires resistance to several fungicides including benzimidazoles, dicarboximides, diethofencarb, and two sterol biosynthesis inhibitors (Chastagner and Riley 1990; Migheli et al. 1990).

Fruiting bodies of species in the genus *Botrytis*, called apothecia, are rarely found in the field. Apothecia are ascomas with an open cup shape, on top of a stipe, and brown in colour (Whetzel 1945). Apothecia develop from sclerotia and act as a platform to discharge ascospores from the asci (Pöggeler et al. 2006). Apothecia of the genus *Botrytis* vary in size depending on the species, ranging from 2 to 25 mm in height and 1 to 6 mm in diameter of the apothecial disk. Several studies have shown that sclerotia must be fertilized with

microconidia in order to develop apothecia (Beever and Parkes 1993; Faretra and Antonacci 1987;Fukumori et al. 2004; Groves and Loveland 1953). Mature *Botrytis* apothecia can normally be observed 2 months after fertilization (Faretra and Antonacci 1987; Hennebert 1973; Terhem and van Kan 2014).

Most members of the genus *Botrytis* are typically designated as having heterothallic mating systems. However, some species in the genus are reported to have homothallic reproductive mating systems, i.e. *Botrytis porri* and *Botrytis globosa* (Buchwald 1953; Elliott 1964). *B. elliptica* is believed to have a heterothallic mating system, requiring a cross between different alleles to undergo sexual development and form apothecia (van den Ende and Pennock-Vos 1996). The mating type locus in the genus *Botrytis* is designated as *MAT*, with two alleles defined as *MAT1-1* and *MAT1-2*. As is common in Ascomycota, the *MAT* alleles lack sequence similarity but are flanked by identical genes, i.e., *APN2* and *SLA2* (Pöggeler et al. 2006). The presence of both *MAT* alleles will activate sexual development. Two decades ago, efforts were made to generate apothecia from *B. elliptica*, but complete apothecia failed to form. The apothecia failed to expand the apothecial disk which resulted in empty asci and ascospores (Chastagner et al. 1992). Some years later, van den Ende and Pennock-Vos (1996) managed to collect apothecia in a lily production field in Lisse, the Netherlands and successfully performed crosses with *B. elliptica* strains, but a formal description of the apothecia of *B. elliptica* was not provided. Staats et al. (2007) could not detect apothecia of *B. elliptica* during a field survey; however, they performed AFLP analysis to study the genetic diversity in the population. Over 60 % of haplotypes of *B. elliptica* were unique to a single isolate and only 2 % of all pairwise haplotype comparisons differed by less than four markers. Furthermore, haplotypes that were prominent in one growing season were not found again in the next year. These data collectively provided strong evidence for the occurrence of sexual reproduction in the field (Staats et al. 2007). Also field surveys in North America and Taiwan failed to reveal the presence of apothecia of *B. elliptica* in the field (Huang et al. 2001). Currently, there is no documentation or description of apothecia of *B. elliptica* available to the public. The aim of this study was to analyse the sequence of the MAT loci of *B. elliptica* and to produce apothecia in the laboratory in order to describe their morphology.

Materials and methods

Strains

Six *B. elliptica* strains (Be9601, Be9605, Be9610, Be9612, Be9623, Be0004) collected in a lily production field in Lisse, the Netherlands in the years 1996 and 2000, were provided by dr. J. van Doorn (PPO Lisse). Strains were plated on malt extract agar (MEA) and incubated at 20 °C with continuous exposure to near-UV light and white light until cultures sporulated.

B. elliptica genome sequence

Genomic DNA was isolated from strain Be9601 using a Gentra Puregene DNA purification kit (Qiagen, Venlo, the Netherlands), and used for whole genome sequencing by DNAvision in Liège, Belgium. The library containing inserts with an average length of 157 bp was sequenced on an Illumina Hiseq2000 platform by paired-end sequencing with a read length of 100 bp. A total of 33.2 million reads (yielding a dataset of >5 Gb) were assembled using Velvet 1.2.05 (Zerbino and Birney 2008) with a k-mer value of 43. The Be9601 assembly consisted of 7,860 contigs (N50 = 32,840) and had a total length of 47.6 Mbp.

Identification of mating type alleles

Freeze-dried mycelium was used for genomic DNA extraction using a Gentra Puregene DNA purification kit (Qiagen). The entire *MAT* locus could be amplified from strains with either of the *MAT* alleles, using primers annealing in the regions flanking the locus: BOTMAT5 (GTGACTGTAAAACGACGGCCAGTTCCGTATTCACAATCCATCC) and BOTMAT3 (GTGACCAGGAAACAGCTATGACCACATACTCGCATTAGTGGAAC). PCR performed on 10–50 ng DNA with Expand polymerase (Roche) and primer pair BOTMAT5/BOTMAT3 in a 25 µl reaction volume yielded a fragment of ~4.3 kb. Amplification conditions were: 95 °C 5 min, then 30 cycles of 94 °C for 30 s, 55 °C for 30 s and 72 °C for 5 min, followed with a final extension of 72 °C for 7 min. The amplicon from *B. elliptica* strain Be9623 was cloned in a TOPO-XL PCR plasmid (Life Technologies) and entirely sequenced by Baseclear (Leiden, The Netherlands) using a primer walking strategy.To identify the *MAT* alleles of strains or single ascospore progeny cultures by PCR, primer pairs were used that are specific for either of the alleles: MAT1-1 F (TGGTGTAAAAAGATTCCGTATCCG) and MAT1-1R (CACCATATGCATTCTGAGTGGAAG); or MAT1-2 F (ATCACGGCACTGTCCTCGAAAC) and MAT1-

2R (GAAGAGGTTCCAGACACAGATTG). PCRs were performed with GoTaq polymerase (Promega, Leiden, The Netherlands), according to the manufacturer's instructions. Amplification conditions were: 95 °C 5 min, then 35 cycles of 94 °C for 30 s, 52 °C for 30 s and 72 °C for 2 min, followed with a final extension of 72 °C for 5 min.

Sexual crosses

To obtain sclerotia, strains were plated on MEA and incubated in complete darkness at 15 °C for 4 weeks, followed by incubation at 0 °C for 4 weeks. Sexual crosses were set up in a reciprocal way using a standard protocol for crosses in *B. cinerea* (Faretra et al. 1988; van der Vlugt-Bergmans et al. 1993). In total, 24 sclerotia were used in one microtiter plate of six wells. Every well contained four sclerotia (maternal parent) that were fertilized with 3 ml of microconidia (paternal parent) of the mating partner. The microtiter plate was then sealed and incubated at 12 °C under neon light with a 12-h photoperiod. Non-spermatized sclerotia in sterile MilliQ water were used as a negative control. All crosses were set up with two strains of opposite mating types.

Sampling of ascospores and production of single ascospore progeny

To obtain ascospores, an apothecium was gently grinded with a mortar and pestle, followed by the addition of sterile MilliQ water, and mixed. The homogenate containing complete asci, ascospores and hymenium debris was filtered over glasswool fibre in a 5 ml pipette tip. The flowthrough contained predominantly ascospores, with little contamination by asci and hymenium tissue. Ascospores were counted using a haemocytometer. To obtain single ascospore progeny cultures, ascospores were plated on MEA at low density, up to 30 ascospores per plate, and incubated at 20 °C. After 2 days of incubation, germlings emerging from single ascospores were transferred to fresh MEA plates. At least 15 single ascospore cultures were collected from each individual apothecium. Genomic DNA was extracted from single ascospore cultures after 4 days of growth on MEA. PCR was performed as described above to identify their*MAT* allele. A chi-square test for the segregation of *MAT* alleles in the progeny was performed with a confidence level $P = 0.05$.

Light microscopy

Transverse sections of apothecia were mounted on a slide with filter-sterile MilliQ water. Observations were made with a Nikon Eclipse 90i (Nikon Instruments, Badhoevedorp, the Netherlands) compound microscope attached with a Nikon DS-5MC camera. Measurements were performed using N.I.S-Elements AR 2.30 software (Nikon Instruments, Badhoevedorp, the Netherlands). At least 40 ascospores, asci, hymenia, pharaphyses, ectal excipulum, and medullary excipulum were measured. The mean, standard deviation, and 95 % confidence intervals were calculated.

Infection assay

Ascospores were collected from a mixture of 10 apothecia using the method described above. The ascospore suspension was adjusted to 1×10^6 ml^{-1} in potato dextrose broth (12 g/l). 6–12 droplets of 3 µl of ascospore suspension were inoculated on the lower sides of lily leaves freshly cut from mature plants. Inoculated leaves were stored in a box with high relative humidity, > 95 %, and placed at room temperature. The infection assay was performed with 3–5 leaves per treatment and was repeated three times.

Results

The mating type locus of *Botrytis elliptica*

As in most Ascomycota, the mating type (*MAT*) locus in *Sclerotiniaceae* is flanked by two highly conserved genes, *APN*2 (a homologue of the *Saccharomyces cerevisiae APN*2 gene encoding a *DNA* lyase) and *SLA*2 (a homologue of the *S. cerevisiae SLA*2 gene encoding a cytoskeleton assembly protein) (Amselem et al. 2011). The draft genome sequence of *B. elliptica* isolate Be9601 was determined (van Kan and Staats, unpublished). Nucleotide alignment was performed to identify the region that is homologous to the *MAT* locus of *B. cinerea* (Amselem et al. 2011). The *MAT* locus of Be9601 (Figure 1) appeared to contain the *MAT1-1* allele, which includes the *MAT1-1-1* gene (encoding the MAT-alpha domain) and the *MAT1-1-5* gene, in the same configuration as in *B. cinerea* strain B05.10 (Amselem et al. 2011). Using primers BOTMAT5 and BOTMAT3 on DNA of *B. elliptica* Be9623, a fragment was amplified that contains the *MAT1-2* allele, which includes the *MAT1-2-1* gene (encoding

a high mobility group domain protein) and the *MAT1-2-4* gene (Figure 1), in the same configuration as in *B. cinerea* strain T4 (Amselem et al. 2011). The four *MAT* genes in *B. elliptica* were >90 % similar to their orthologs in *B. cinerea* and >75 % similar to their orthologs in *Sclerotinia sclerotiorum* (Table 1; Supplemental Figure 1). Alike in the *MAT* loci in *B. cinerea*, there was a truncated fragment of the *MAT1-2-1* gene in the *MAT1-1* locus and a truncated fragment of the *MAT1-1-1* gene in the *MAT1-2* locus (Figure 1). Both gene fragments lack start codons as well as their typical DNA-binding domain and thus appear non-functional. The sequences of both *MAT* alleles were deposited in Genbank under accession numbers KM219113 (MAT1-1) and KM243314 (MAT1-2).

Characterization of strains

Four different *B. elliptica* strains were analyzed by PCR for their *MAT* allele. Two strains carried the *MAT1-1* allele and another two strains carried the *MAT1-2* allele. To analyse the production of sclerotia, these strains were plated on MEA plates and incubated in a 15 °C incubator in darkness. All strains formed sclerotia, except for Be9610 (*MAT1-1*). Approximately 30 sclerotia were produced in one plate. Fully developed sclerotia were observed in the MEA plate after 30 days. Table 2 shows the characterization of strains.

Sexual crosses

To analyse the ability of *B. elliptica* to develop apothecia, the *MAT1-1* strains were crossed with the *MAT1-2* strains in all possible combinations. Because of the failure of Be9610 to produce sclerotia, this strain could only be used as paternal parent (microconidia). Of the nine crosses that were set up, four crosses were fertile and resulted in the formation of apothecia. The crosses that produced apothecia were all set up from *MAT1-2* strains as the maternal parent (sclerotia). No apothecia formed from crosses that used *MAT1-1* strain Be9612 as the maternal parent. As a control, sclerotia from the *MAT1-1* strain or the *MAT1-2* strain that were incubated in sterile MilliQ water did not produce apothecia. Table 3 displays the results of the sexual crosses. The experiment was performed three times with identical results.
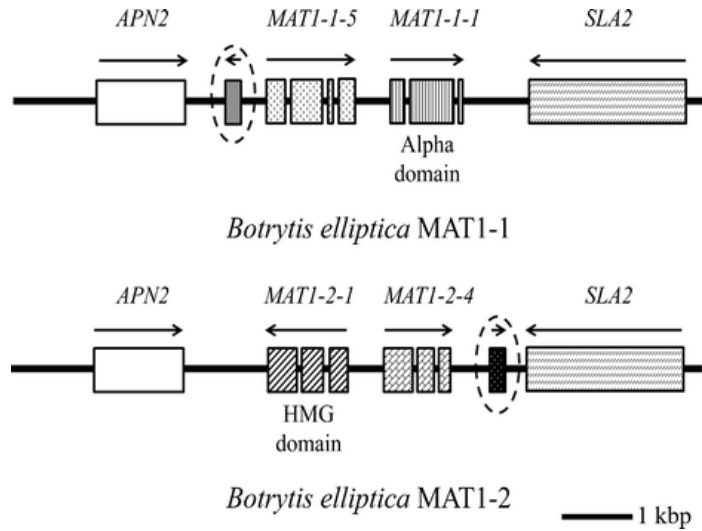
Figure 1: Structure of the MAT locus in *B.elliptica.* Top panel: *MAT1-1* allele of strain Be9601; bottom panel: *MAT1-2*allele of strain Be9623. MAT alleles are non-homologous in DNA sequence, but are flanked by identical genes, *APN*2 and *SLA*2. Introns in the *MAT* genes are indicated by lines connecting the exons (indicated by boxes). The boxes marked with dotted circles represent truncated fragments of the *MAT1-2-1* gene (in the *MAT1-1* locus in the top panel) and the *MAT1-1-1* gene (in the *MAT1-2* locus in the bottom panel), respectively. The direction of transcription is indicated by arrows.

Table 1: Homology of *B. elliptica MAT* genes to orthologs in other Sclerotiniaceae

B. elliptica gene	Protein length	Homology to *B. cinerea* ortholog		Homology to *S. sclerotiorum* ortholog	
		Identity	Similarity	Identity	Similarity
MAT1-1–1	353 aa	96	97	81	84
MAT1-1–5	376 aa	86	92	75	87
MAT1-2–1	376 aa	94	96	78	86
MAT1-2–4	279 aa	82	90	63	76

Table 2: Morphological and molecular characterization of *B. elliptica* strains

Strain	Microconidia	Macroconidia	Sclerotia	Mating type allele
Be9610	Yes	Yes	No	*MAT1-1*
Be9612	Yes	Yes	Yes	*MAT1-1*
Be9605	Yes	Yes	Yes	*MAT1-2*
Be0004	Yes	Yes	Yes	*MAT1-2*

Table 3: Results of sexual crosses

Cross	Sclerotia	Microconidia	Replicates[a]	# Repeats[b]	Apothecia
1	Be9612	Be0004	3	3	−
2	Be0004	Be9612	3	3	+
3	Be9612	Be9605	3	3	−
4	Be9605	Be9612	3	3	+
5	Be0004	Be9610	3	3	+
6	Be9605	Be9610	3	3	+
7	Be9612	Sterile MilliQ water	3	3	−
8	Be0004	Sterile MilliQ Water	3	3	−
9	Be9605	Sterile MilliQ Water	3	3	−

[a] number of biological replicates within an experiment

[b] number of repeated experiments

Apothecia were sampled from two different fertile crosses, and at least 15 single ascospore progeny were cultured from three independent apothecia of each. To identify the *MAT* alleles in the progeny, amplification of genomic DNA was performed by PCR with *MAT*-allele-specific primers. Table 4 shows that the *MAT* alleles segregated almost 1:1 in progeny. In one of the three experiments, the segregation was skewed, with the *MAT1-1* allele being dominant for reasons that remain unexplained. A chi-square test indicated that, over the entire set of three biological repeats, the segregation ratio between the *MAT* alleles did not significantly deviate from 1:1 ($P < 0.05$, Table 4).

Table 4: Segregation of *MAT* alleles in the progeny

Cross	Sclerotia	Microconidia	Apothecium (biological replicates)	Mating types		Total no. of ascospores	Chi square value
				MAT1-1	*MAT1-2*		
1	Be0004	Be9612	1	11	13	24	0.09[*]
			2	7	8	15	0.02[*]
			3	18	2	20	5.28
			Total	36	23	59	2.86[*]
2	Be9605	Be9612	1	11	10	21	0.02[*]
			2	7	9	16	0.09[*]
			3	16	2	18	4.45
			Total	34	31	55	3.07[*]

[*] no significant deviation from 1:1 segregation in the progeny ($P < 0.05$)

Morphological description of sclerotia and apothecia

Morphological structures of apothecia of *B. elliptica* were described based on the general descriptions by Whetzel (1945). Sclerotia are plano-convex, black, with irregular shape, and sometimes firmly attached to each other. Sclerotia range in size from 3 to 14 mm, and are frequently concave or hollow on the inward. Optimal conditions for development of sclerotia are in malt extract agar in darkness, in a temperature range between 15 °C and 20 °C. From 74 days after fertilization onwards, primordia ruptured from the surface of sclerotia and sometimes from the bottom (Figure 2a). The primordia develop into a stipe in 7 to 10 days after emergence. The stipe is cylindrical and erected (Figure 2b, c). The stipe surface is pubescent, scabrous, light brown in colour, 7 to 12 mm in height, and 1.5 to 2 mm in width. One to nine (mean = four) apothecia emerged on a sclerotium. The apothecial disk is umbilicate, depressed to funnel and round in shape, usually 3 to 4 mm in diameter and 0.5 to 1 mm thick. It is slightly shallow, cup-shaped and becomes flat when mature; light brown in colour, becoming dark brown at maturity (Figure 2d, e). Apothecia are mature 94 to 104 days after fertilization. At first the margin of the disk is entire, becoming serrate to irregular (not shown). Asci formed in the apothecial disk were long and cylindrical in shape with an average dimension of 200 × 14 µm (*n* = 40) (Figure 2f). An apical pore was not clearly observed in the ascus tip. The ascus has a thin wall and bears eight ascospores (Figure 2f). The ascospores are hyaline, ellipsoidal with rounded ends, usually 18.5 - 24 µm in length (mean 19.5 ± 1.3 µm, *n* = 40) and 6 - 10 µm in width (8.1 ± 0.8 µm, *n* = 40) (Figure 2g). The medullary excipulum ranges in shape between textura globosa and textura angularis, with a thickness 240 - 344 µm (*n* = 40) (Figure 2h). The underside of the apothecial disk is pubescent. Ectal excipulum is in the shape of textura globosa with a thickness of 59 to 87 µm (*n* = 40) (Figure 2i). The hymenium ranges from 87 to 106 µm in height (*n* = 40) and the subhymenium from 100 to 124 µm (*n* = 40). The size of paraphyses ranges from 197 µm to 291 µm (*n* = 40).

Infectivity of ascospores

Droplets of ascospore suspensions were inoculated on the lower side of lily leaf surfaces. As a control, suspensions of asexual conidia were inoculated at the same density. Symptom development became visible at 20–24 h post inoculation (hpi) and was indistinguishable between the ascospores and conidia (not shown). The infected area turned brown in colour

and necrotic spots developed at the infection site. At 24 hpi, the lesion was approximately 1 mm in diameter, equivalent to the size of the inoculation droplet. Hyphae were growing on the infected area and could be examined under the light microscope. The lesions expanded to 2–4 mm in diameter at 36 hpi and lesions were circular to oval in shape (Figure 3). At 48 hpi, the first botryose clusters of spores could be observed in some infected areas. At 4 weeks post inoculation, sclerotia formed on lily leaves and had a typical appearance of *B. elliptica* sclerotia (not shown)
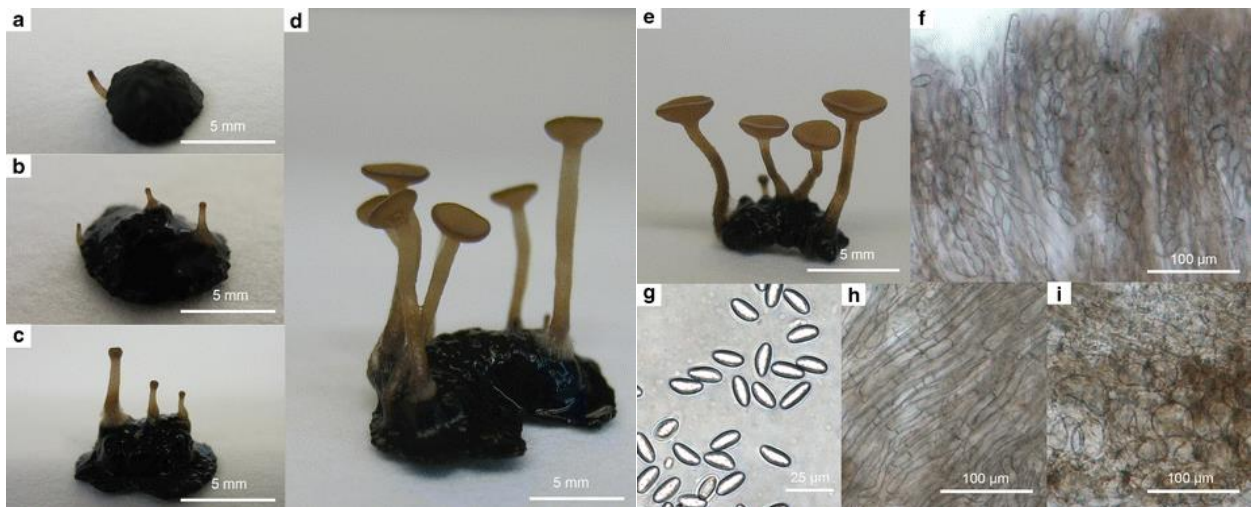
Figure 2: Morphology of sexual structures ob B. elliptica. a,b primordia. c, stipe. d,e mature apothecia. f, ascospores in asci. g, ascospores. h, mendullary excipulum. i, ectal excipulum.

Figure 3: Disease symptoms of *B. elliptica* on lily leaves, 36 hpi. a. inoculation with ascospores, b. inoculation with conidia

Discussion

In this study we confirmed that *B. elliptica* has a heterothallic mating system with two alleles: *MAT1-1* and MAT1-2. Apothecia of *B. elliptica* can be produced in the laboratory after sexual crosses of two strains of opposite mating types, using a standard protocol developed for *B. cinerea* (Faretra et al. 1988; van der Vlugt-Bergmans et al. 1993) although *B. elliptica* apothecia took significantly longer to develop than those of *B. cinerea*.

The *MAT1-1-1* and *MAT1-2-1* genes in *B. elliptica* are orthologous to the alpha-domain protein and the HMG-domain protein, respectively, which are conserved in all Ascomycota studied thus far. These two proteins jointly act as master regulators of the initiation of sexual fruiting body development, when expressed together in a dikaryotic cell (Pöggeler et al. 2006). The *MAT1-1-5* and *MAT1-2-4* genes in *B. elliptica* are orthologous to the *MAT1-1-5* and *MAT1-2-4* genes in *B. cinerea* and have no homologues outside the family Sclerotiniaceae (Amselem et al. 2011). Deletion of either the *B. cinerea MAT1-1-5* gene or the *MAT1-2-4* gene results in a defect in sexual reproduction, specifically in the developmental transition from stipe to apothecial disk (Chapter 2). Whether the *B. elliptica MAT1-1-5* and *MAT1-2-4* genes have a similar function in apothecial disk development remains to be established.

Alike in *B. cinerea*, the *MAT* alleles of *B. elliptica* both contain a truncated *MAT* gene fragment derived from the opposite allele (i.e., a non-functional fragment of the *MAT1-2-1* gene in the *MAT1-1* locus and a non-functional fragment of the *MAT1-1-1* gene in the *MAT1-2* locus). The lengths and positions of the non-functional *MAT* gene fragments are nearly identical between *B. cinerea* and *B. elliptica* (van Kan, unpublished observations). This configuration suggests that contemporary *MAT* loci of *B. cinerea* and *B. elliptica* have both evolved from an ancestral, homothallic locus, by two separate deletion events. Amselem et al. (2011) proposed an evolutionary scenario for the *B. cinerea MAT* locus, in which deletion of the *MAT1-1-5* gene as well as a large part of the *MAT1-1-1* gene resulted in the emergence of a heterothallic *MAT1-2* allele, whereas deletion of the *MAT1-2-4* gene and the major part of the *MAT1-2-1* gene yielded the heterothallic *MAT1-1* allele. The configuration of the *B. elliptica MAT* alleles is in full agreement with the occurrence of such a scenario in a common ancestor of *B. cinerea* and *B. elliptica.*

The morphology of *B. elliptica* apothecia is in agreement with the general description of apothecia in the genus *Botrytis* (Whetzel 1945). The apothecia of *B. elliptica* range between 7 and 12 mm in height and the apothecial disks range from 3 to 4 mm in diameter and 0.5 to 1 mm in thickness. *B. elliptica* apothecia are similar in size to those of *Botrytis ranunculi*, but smaller than apothecia of *B. cinerea*, which can reach up to 25 mm in height (Bergquist and Lorbeer 1972; Faretra and Antonacci 1987). The ascospores of *B. elliptica* (23 × 10 μm) are substantially larger than those of *B. cinerea* (13 × 8 μm). The earliest primordia ruptured from the sclerotium in *B. elliptica* 74 days after fertilization; which is more than 7 weeks later than in *B. cinerea* (Faretra and Antonaci, 1987; Terhem and van Kan 2014). Whether the slow development of *B. elliptica* apothecia is due to conditions employed here, or is intrinsically slower than in *B. cinerea* remains unknown. *B. elliptica* apothecia are brown in colour and become darker when mature, alike typical characteristics of apothecia of the genus *Botrytis* (Whetzel 1945).

When comparing *B. elliptica* apothecia with *B. cinerea* side by side, we noticed that *B. elliptica* apothecia in a young stage appear slightly more yellow-greyish as compared to the yellow-brown appearance of *B. cinerea*. The apothecia of *B. elliptica* are thicker and more deeply cup-shaped than those of *B. cinerea.* Furthermore, the stipes of *B. elliptica* are uniform in width, whereas stipes of *B. cinerea* are tapered to a narrow base (not shown).

Apothecia only developed in crosses with *MAT1-2* strains acting as the maternal parent, but not in crosses of *MAT1-1* strain Be9612 as the maternal parent, in spite of several attempts in multiple replicates. The reasons for the unsuccessful development of apothecia in the crosses with Be9612 as the maternal parent is unclear, but a similar feature was reported for certain *B. cinerea* strains (van der Vlugt-Bergmans et al. 1993). The observation that apothecia were never produced when sclerotia were incubated in sterile water indicates that the *B. elliptica* strains tested are not homothallic. Individual ascospores collected from *B. elliptica* apothecia were analysed for the segregation of mating type alleles. The analysis of segregation showed that the MAT loci segregate nearly 1:1 in two independent experiments (Table 4). In a third experiment, a skewed segregation was observed, the reason of which remains unexplained. Nevertheless, in the total dataset, the segregation ratio did not significantly deviate from 1:1.

The four strains of *B. elliptica* used in these crosses were obtained from a field in which there was apparently a potential for sexual reproduction, as indicated by the presence of opposite mating types at the same location. Van den Ende and Pennock-Vos (1996) collected apothecia of *B. elliptica* on plant debris in the same fields as the strains used in this study, and they were the first to succeed in inducing production of apothecia of *B. elliptica* in vitro. They also tested the ascospores produced from apothecia by inoculating them on lily leaves. In the present study, inoculation of ascospores of *B. elliptica* on lily leaves caused similar symptoms as described by van den Ende and Pennock-Vos (1996). Disease development and lesion outgrowth was indistinguishable between inoculation with ascospores or conidia of *B. elliptica.* In view of the detection of *B. elliptica* apothecia in plant debris at the end of the winter (van den Ende and Pennock-Vos 1996), a high genetic diversity in the *B. elliptica* population that is indicative of extensive sexual reproduction (Staats et al. 2007) and our observation that ascospores are equally infectious as conidia, we propose that ascospores make an important contribution in the epidemiology of *B. elliptica*, by infecting young lily shoots emerging in early spring.

Supporting information

Supplementary Figure S1

Acknowledgements

References

Amselem, J., Cuomo, C. A., van Kan, J. A. L., Viaud, M., Benito, E. P., Couloux, A., et al. (2011) Genomic analysis of the necrotrophic fungal pathogens *Sclerotinia sclerotiorum* and *Botrytis cinerea*. PLoS Genetics *7*, e1002230.

Bastiaansen, C., Koster, A. T. J., Van der Meer, L., van den Ende, J. E., Pennock, I., & Buurman, F. (1997) A disease-forecasting system of botrytis blight ('fire') in lily. Acta Horticulturae 430: 657–660.

Beever, R. E., & Parkes, S. L. (1993). Mating behaviour and genetics of fungicide resistance of *Botrytis cinerea* in New Zealand. New Zealand Journal of Crop and Horticultural Science 21: 303–310.

Bergquist, R. R., & Lorbeer, J. W. (1972) Apothecial production, compatibility and sex in *Botryotinia squamosa.* Mycologia 64: 1270–1281.

Buchwald, N. (1953). *Botryotinia* (*Sclerotinia*) *globosa* sp. n. on *Allium ursinum*, the perfect stage of *Botrytis globosa* Raabe. Phytopathologische Zeitschrift 20: 241–254.

Chastagner, G. A., & Riley, K. (1990) Occurrence and control of benzimidazole and dicarboximide resistant *Botrytis* spp on bulb crops in Western Washington and Oregon. Acta Horticulturae 266: 437–446.

Chastagner, G. A., Riley, K., & Doss, R. P. (1992) An attempt to produce an apothecial state of *Botrytis elliptica* in vitro. Acta Horticulturae 325: 689–694.

Chiou, A., & Wu, W. (2001) Isolation, identification and evaluation of bacterial antagonists against *Botrytis elliptica* on lily. Journal of Phytopathology 149: 319–324.

Doss, R. P., Christian, J. K., & Chastagner, G. A. (1988). Infection of Easter lily leaves from conidia of *Botrytis elliptica.* Canadian Journal of Botany 66: 1204–1208.

Elliott, M. E. (1964). Self-fertility in *Botryotinia porri.* Canadian Journal of Botany 42: 1393–1395.

Fang Hsieh, T., Wen Huang, J., & Hsiang, T. (2001) Light and scanning electron microscopy studies on the infection of oriental lily leaves by*Botrytis elliptica.* European Journal of Plant Pathology 107: 571–581.

Faretra, F., & Antonacci, E. (1987) Production of apothecia of *Botryotinia fuckeliana* (de Bary) Whetz. under controlled environmental conditions.Phytopathologia Mediterranea 26: 29–35.

Faretra, F., Antonacci, E., & Pollastro, S. (1988) Sexual behaviour and mating system of *Botryotinia fuckeliana*, teleomorph of *Botrytis cinerea.* Journal of General Microbiology 134: 2543–2550.

Fukumori, Y., Nakajima, M., & Akutsu, K. (2004) Microconidia act the role as spermatia in the sexual reproduction of *Botrytis cinerea.* Journal of General Plant Pathology 70: 256–260.

Furukawa, T., Ushiyama, K., & Kishi, K. (2005) Botrytis blight of Taiwanese toad lily caused by *Botrytis elliptica* (Berkeley) Cooke. Journal of General Plant Pathology 71: 95–97.

Groves, J. W., & Loveland, C. A. (1953) The connection between *Botryotinia fuckeliana* and *Botrytis cinerea.* Mycologia 45: 415–425.

Hennebert, G. L. (1973) *Botrytis* and *Botrytis*-like genera. Persoonia 7: 183–204.

Huang, J., Hsieh, T. F., Chastagner, G. A., & Hsiang, T. (2001) Clonal and sexual propagation in *Botrytis elliptica.* Mycological Research 105: 833–842.

Hwang, B. K. (2001) Gray mold of day lily (*Hemerocallis fulva* L.) caused by *Botrytis elliptica* in Korea. The Plant Pathology Journal 17: 305–307.

Kamenetsky, R., & Okubo, H. (2012) *Ornamental geophytes: from basic science to sustainable production*. London: CRC Press.

MacRae, E. A. (1998) *Lilies : a guide for growers and collectors*. Portland: Timber Press.

Mansfield, J., & Hutson, R. (1980) Microscopical studies on fungal development and host responses in broad bean and tulip leaves inoculated with five species of *Botrytis.* Physiological Plant Pathology 17: 131–136.

Migheli, Q., Aloi, C., & Gullino, M. (1990) Resistance of *Botrytis elliptic*a to fungicides. Acta Horticulturae 266: 429–436.

Pöggeler, S., Nowrousian, M., & Kück, U. (2006) Fruiting-body development in ascomycetes. In U. Kües, R. Fischer, S. Pöggeler, M. Nowrousian, & U. Kück (Eds.), *Growth, Differentiation and sexuality* (pp. 325–355). Berlin Heidelberg: Springer.

Shahin, A., van Kaauwen, M., Esselink, D., Bargsten, J., van Tuyl, J., Visser, R. G., et al. (2012) Generation and analysis of expressed sequence tags in the extreme large genomes *Lilium* and *Tulipa.* BMC Genomics. 13, 640.

Staats, M., van Baarlen, P., & van Kan, J. A. L. (2007) AFLP analysis of genetic diversity in populations of *Botrytis elliptica* and *Botrytis tulipae*from the Netherlands. European Journal of Plant Pathology 117: 219–235.

Terhem, R. B., & van Kan, J. A. L. (2014) Functional analysis of hydrophobin genes in sexual development of *Botrytis cinerea.* Fungal Genetics and Biology 71: 42–51.

van Baarlen, P., Staats, M., & van Kan, J. A. L. (2004) Induction of programmed cell death in lily by the fungal pathogen *Botrytis elliptica.* Molecular Plant Pathology 5: 559–574.

van den Ende, J., & Pennock-Vos, M. (1996) Primary sources of inoculum of *Botrytis elliptica* in lily. Acta Horticulturae 430: 591–596.

van der Vlugt-Bergmans, C. J. B., Brandwagt, B. F., van't Klooster, J. W., Wagemakers, C. A. M., & van Kan, J. A. L. (1993) Genetic variation and segregation of DNA polymorphisms in *Botrytis cinerea.* Mycological Research 97: 1193–1200.

Vleeshouwers, V. G. A. A., & Oliver, R. P. (2014) Effectors as tools in disease resistance breeding against biotrophic, hemibiotrophic, and necrotrophic plant pathogens. Molecular Plant-Microbe Interactions 27: 196–206.

Whetzel, H. H. (1945) A synopsis of the genera and species of the Sclerotiniaceae, a family of stromatic inoperculate Discomycetes. Mycologia 37: 648–714.

Zerbino, D. R., & Birney, E. (2008) Velvet: algorithms for de novo short read assembly using de Bruijn graphs. Genome Research 18: 821–829.

Supporting information

Supplementary Figure S1

Alignment of *B.elliptica* MAT genes to their orthologs in *B.cinerea* and *S.sclerotiorum*

```
BeMAT1-2-1    MSLSSLRLGKWVPHHGTVLETPLANVPYPAVDTTPVEAYMIPGLTKEIYNAMRNFINELD 60
BcMAT1-2-1    MSLSSLRLGKWVPHHGTVLETPLANVPYPAVDTTPVESYMIPGLTKEIYNSMRNFINELD 60
SsMAT1-2-1    MSLSTLRLGKWVPHRGTILETPLADVPYPAVDITPVEAYGIPGLSKEIYDAMRTFFNELD 60
              ****:*********:**:******:******* ****:* ****:****::**.*:****

BeMAT1-2-1    LYNALDINPWCELQDYEYMSIGTPERQILLHFYQQHTDRKGVFVRDAYINRMFLAPLDEF 120
BcMAT1-2-1    LYNALDINPWCELRDHEYMSIGTPERQILLHFYQQHTDRKGVFVRDAYINRMFLAPLDEF 120
SsMAT1-2-1    LYNALDINPWCELKDSQYLGIGTPERQILLHFYEQHTDRKGVFVRDAYVSRIFLAPLDEF 120
              *************:* :*:.*************:***************:.*:********

BeMAT1-2-1    EHKQMLAVAGFANLCLEPLQIEQRRMMNGSWDENGSILPQNTGATPCSTPEKNHLASSSI 180
BcMAT1-2-1    EHKQMLAVAGFANLCLEPLQIEQRRMMNGSWDENSSILPQNAGATPCSTPGKNHLASSSM 180
SsMAT1-2-1    EDKQMLAVAGFTNLCLEPLNVEHRRMMNGSWDENCTILPTNVGVTLCSGSGSGKKHLSP-SL 179
              *.*********:*******::*:*********** :*** *.*.* ** . *:**:. *:

BeMAT1-2-1    PTGLKPKIPRPANEWILYRADNHLPIKKAYPGITNNEISSIIAGMWAAETPERRLKYKIR 240
BcMAT1-2-1    PTGLKPKIPRPANEWILYRADNHLPIKKAYPGITNNEISSIIAGMWAAETPERRLKYKIR 240
SsMAT1-2-1    PAALKPKIPRPANEWILYRADNHIPIKKAYPGITNNEISSIIAGMWAAETPERRLKYKIR 239
              *:.*************************:********************************

BeMAT1-2-1    ADLLKEAHKKAYPTYKYAPRKPSEKKRRVSKKTLNKSSANQLSQNINSNTTTTASS---- 296
BcMAT1-2-1    ADLLKEAHKKAYPTYKYAPRKPSEKKRRVSKKTLNKSTANQLSQNFNSTTISTESSTESS 300
SsMAT1-2-1    ADLLKEAHKKAYPTYKYAPRKPSEKKRRASKKTLTKPTTNQLSHNINTTTS-------S 291
              ****************************.*****.*.::****:*:*:.*        *

BeMAT1-2-1    INYPLLNHDSTDDTSMGTMSTFGLNIHMDHSNLLEQQLQPEHCRLSYGDEPVGMNFAPTE 356
BcMAT1-2-1    INYPILNHDSIDDTIMGTMGTFGLNIHMDHSNVLEQQLQPEHYRLSYSDEAMGMNFAPTE 360
SsMAT1-2-1    ISFPIANNNSIDNS---DLNTFGLNIHINHSNITEQQLQSENSRLTYNDQSIGMNFTSTE 348
              *.:*: *::* *:: :.*******::***: *****.*: **:*.*::*****:.**

BeMAT1-2-1    AWQTVQQQDLYTFFSPQQQY                         376
BcMAT1-2-1    AWQTVQQQDLYTFFSPQQQY                         380
SsMAT1-2-1    SWQMVQQQDLYDFFSPRQITLGATESDNVQICQGSSSDMCWKRTDI 394




BeMAT1-2-4    MQPQAKADGDVETSFRRPKINAADALNYMKDFSQEFQRPGSNTITQHAVSEINPIVYDVD 60
BcMAT1-2-4    MQPQAEANGDVETSTRRPKVNAAHVLSCMKDFSHEFRRLDSYTTTQHAVPEMNPIVYDVD 60
SsMAT1-2-4    MQPQAGANAGAETSTGRSQINAMYVLNHMNDFSRDFKRPGSKTTTPQPFLGIAPIVYDVN 60
              ***** *:...***  *.::**  .*. *:***::*:* .* * * :..  : ******:

BeMAT1-2-4    YTVMHNSSQGTGG-EGHIRKDKMTTEQRHSQRDLSNVVRHGNSLANSFMKIETGLLGLRF 119
BcMAT1-2-4    YTVIHNPSQETGG-EGNIRTDKMTTEQRHSQRELSDVVRYGNSLANSFMKIETGLLGLRF 119
SsMAT1-2-4    YTVIHDSLQWIGGDERQLLKPKVTTEQRQSQRELSNVVRHTNNLANSFMKLETGLLNLRF 120
              ***:*:. *  ** * :: . *:*****:***:**:**: *.*******:*****.***

BeMAT1-2-4    DGRGSASFREKIAAGQRIALRIYIQNEIKRRAADLGLVKLGSCETSLIRDVAKRIVERGR 179
BcMAT1-2-4    DGRGSASFREKLAAGQRISLRIYIQNEIKRLAADLGLVKLGICETLLIKDVAKRIVERRR 179
SsMAT1-2-4    DKQGSAPLIRQLAAGQRIALRIYLQNEITKQAADLGLVKLGECETLAIRDVVKSMVDRRR 180
              * :***.: .::******:****:****.: ********** ***  *:**.* :*:* *

BeMAT1-2-4    TMTQAEGNMFADDIFQREFKPDVEDESGVGYIEPFLKR-------ISELIWNLQFDRTFA 232
BcMAT1-2-4    TMTQAEGNMFADDIFQREFKLDVDDASGVGYAYIKPFLER-------VSELIWNLQFDRTFA 232
SsMAT1-2-4    TITQAEGNVFADEIFENEFDFDNGDESGEAHIEAYLKRSEEIRNEISDLIWNLQFDRTFA 240
              *:*****:***:***:.**. *  * ** .:*:.:*:* :*:***********

BeMAT1-2-4    RTMSHLLPLNYNSWAKEKTIPKGLIKRKRLRKIKRERGLHGYHWVEL 279
BcMAT1-2-4    RTMSHLFPLNYDSWAKETT-PKGLRKRRRMRRIKRERVSEGHHWVEL 278
SsMAT1-2-4    RTMSHLLPLNYDSWKEKIITPTSIRKRRCMRRIKRVESAGG------ 281
              ******:****:** ::   *..: **: :*:*** .    *
```

Mating type and sexual fruiting body of *Botrytis elliptica*, the causal agent of fire blight in lily

```
BeMAT1-1-1    MTAPFKTTMKHTHKRQQRKLTTTQYRVSKPATKCRRANDAMQSLTYHSAPFISEAEGGMQ 60
BcMAT1-1-1    MTAPFKTTMKHTYKRQQKKLTTTQYRVSKPAAKCRRANDAMQSLTYHSAPFISEAEGGMQ 60
SsMAT1-1-1    MTTPFKTTMKHTMKRQQRKLTTTQYRVSKPATKCRRANDSIQPLTYHTAPFIGEIEGGIQ 60
              **:********* ****:************:*******::*.****:****.* ***:*

BeMAT1-1-1    HVAMNERQTAWVEAPRRSVNSYILFRTFYMILTVLGNIPQKYKSAILSVLWGRDPFHAKW 120
BcMAT1-1-1    HVAMNERQTAWVEAPRRSVNSYILFRTFYMILTVLGNIPQKYKSAILSVLWGRDPFHAKW 120
SsMAT1-1-1    HVAMNTRQIGWVEAPRRSVNSYILFRTFYMILNVLGNIPQKYKSAILSVLWGRDPFHAKW 120
              ***** ** .*********************.***************************

BeMAT1-1-1    SIIARAYTLMRDAGVKRSVSEFLALVCPHIGILTVDDYLSDLNWTFETNEEGTVCLRQTS 180
BcMAT1-1-1    SIIARAYTLMRDAGVRRSVSEFLALVCPHIGILTVDDYLSDLNWTFETNEEGTVCLRQTS 180
SsMAT1-1-1    SILARAYTLMRDTNVRRTVSEYLALVCPYIGILAVNDYLTDLNWIFETNEEGIVCLRQTS 180
              **:**********:.*:*:***:*******:****:*:***:**** ******* *******

BeMAT1-1-1    PPEIGSFPPHIARTLLTDLDIITFCGAQGYLPAATAASIVQGWNRVHPMANMAIQGTLPV 240
BcMAT1-1-1    PPEIGSFPAHIARTLLTDLDIITFCGTQGYLPVATAASIVQGWNRVHPMANMAIQGTLPV 240
SsMAT1-1-1    PSDIRSFPAHIARTTLTDLDVITFCGSQGYLPAATAAGIVQGWNRMHPNANMAIQGTLPV 240
              *.:* ***.***** *****:*****.***** .****.*******:** ***********

BeMAT1-1-1    TQHIASTQNAYGAWEMPSGVIVAPPPKPAFDQPLAYTPPALIPGATGSLTGSLPPPPPWS 300
BcMAT1-1-1    TQHIASTQNAYGAWEMPSGVIVAPPPKPAFDQPIAYTPPALVPGATASLTGSLPPPPPWS 300
SsMAT1-1-1    TQHIASTQNAYGAWEMPKGVIVAPPPKPAFDHPLTYTLSTPLP------TGTLPPPPPWS 294
              *****************.*************:*:::**  .: :*     **:********

BeMAT1-1-1    TGMMAGYWGHDSGTIDLSALDTRFDQFNPTSLADAGGLYMPDDAPSPPLFADF 353
BcMAT1-1-1    TGMMAGYWGHDSGTIDLSALHTQFDQFNPTSLTDAGGLYMPEDVPSPPLFADF 353
SsMAT1-1-1    TGMMAGYWSQDNGSIDLNGLENQFDQFNPTSLGDANSLYVPGDISPPSDLTDS 347
              ********.:*.*:***..*..:********** **..**:* * ..*. ::*


BeMAT1-1-5    MKARTRLRIRQEGYRRKRSSRGNKHRSAREVPLNAIRNWKRDRIDTQDPSNFSDATFVEL 60
BcMAT1-1-5    MKVRTRLQIRREACRRKRILLGNKHRSAREVPLNAIRTWKRDKINTQDPSNFLDATLIEL 60
SsMAT1-1-5    MKVNTAIQMRREAFLRRKYLWGIKLHSARYIRPCALRTWKRDEVNTLDPSTFPDATPVEL 60
              **..* :::*:*.  *::    * * :*** :   *:*.****.::* ***.* *** :**




BeMAT1-1-5    AAALGKGELLTGMKMGGSSVSLTYSRYNPGVEATANAPGTPCDPAFLDALVTDCCVLIWE 120
BcMAT1-1-5    AAALEKGELLTDRGTGDSSVSLTYSRFNAGVEATANVPGIPCDPAFLDALVTDCCVLIWE 120
SsMAT1-1-5    AAALERDELLTGVEVGYNPISLTSDRFDPGVEATADTPGKPCEPAFLDALVTDCCVLIWE 120
              **** :.****.   * ..:*** .*::.******:.** **:*****************

BeMAT1-1-5    FCSLYRHTDFNSMHDLLPTKYADIFHDLNTVFGQCRRLKKSPELFSTLAQERQFIAKMSR 180
BcMAT1-1-5    FHSLYRHTDLDSIDDPLPTKYANIFHDLNTVFGECRRLKKSPELFSTLVQERQFTSKMSR 180
SsMAT1-1-5    FRSLYRYTDFNSMDDPLPTKYADIFYDLNTVFTQCRRLKKSPELFSTLVQERQFMEKMSR 180
              * ****:**::*:.* ******:**:****** :**************.*****  ****

BeMAT1-1-5    IAEIVDHLREVIVLKNDGKLAQNKMREKEKELARDLPFFYPGRADGKHPWTRWLENSSPV 240
BcMAT1-1-5    IAEIVDHLRDVIVLKNEGKLTRKKMRKKEKELSKDLPFFYPGRADGKHPWTRWLENSSPV 240
SsMAT1-1-5    IAEIVDHLRDVIVLKNDSKLARNEMRKKERELAKCLPFFYPGRADGRHPWTRWLENSSPV 240
              *********:******.**:::.**:**.**:: ************:.*************

BeMAT1-1-5    MPPGWVGIQQKIPHIGDNIIRRITTMYELYERQFRVEKLIDSKVNDTLDDFPAPGEAFEH 300
BcMAT1-1-5    MPPGWVGIQQKIPHIGDNIIRRITTMYELYERQFRIEKLTDSKVNDTLDDFPAPGEAFEH 300
SsMAT1-1-5    MPPGWLGIQQKIPHIGDNIIRRITTMYELYERQFRIEGLIDRKVNDTLEDFPAPGEAFEH 300
              *****:**************************.:* * * ******:.************

BeMAT1-1-5    MNYSRFSTLAVNYVQYKTGDRPATDKNGMLRIEKLTEAVQRSFRWQENPVITGNANVPYH 360
BcMAT1-1-5    MEYSRFSTLAVNYVQYKTGDRPETDKNGILRIEKLTEAVQRSFRWQENPVITGNANIPYH 360
SsMAT1-1-5    MAYSKFSTMAVNYVQYRSGDRSESDQNGILRIEKLAEAVQRSFRRQENPVIAKNANIPYH 360
              * **:***:*******::***. .:*:**:*******:******* ******: ***:***

BeMAT1-1-5    RFMMGYKIEVLNEEVS 376
BcMAT1-1-5    RFMMGYKIETMNEEVP 376
SsMAT1-1-5    RFMMGYKVETLNGDVQ 376
              *******:*.:* :*
```

129

Chapter 5

A novel *Botrytis* species is associated with a newly emergent foliar disease in cultivated *Hemerocallis*

Abstract

Foliar tissue samples of cultivated daylilies (*Hemerocallis* hybrids) showing the symptoms of a newly emergent foliar disease known as 'spring sickness' were investigated for associated fungi. We isolated repeatedly a fungal species which proved to be member of the genus *Botrytis*, based on immunological tests. DNA sequence analysis of these isolates, using several phyogenetically informative genes, indicated that they represent a new *Botrytis* species, most closely related to *B. elliptica* (fire blight) which is a major pathogen of cultivated Lilium. The distinction of the isolates was confirmed by morphological analysis of asexual sporulating cultures. Pathogenicity tests on *Hemerocallis* demonstrated that this new species was able to induce lesions and rapid tissue necrosis. We infer that this new species, described as *B. deweyae,* is an important contributor to the development of 'spring sickness' symptoms. The emergence of this disease is suggested to have been triggered by breeding-related changes in cultivated hybrids, particularly the erosion of genetic diversity.

Introduction

The emergence of new fungal pathogens in cultivated and wild plants is a major cause for concern (Fisher et al., 2012) and many factors influence such patterns of emergence and establishment. Interspecific hybridisation between different fungal species may be a major contributor to the evolution of novel diversity (Schardl and Carven, 2003). In plant pathogens, it has been demonstrated that rapid genome evolution and host shifts may occur after hybridisation events. For example, establishment of a new species of *Zymoseptoria, Z. pseudotritici,* exhibiting an expanded host range on grasses took place within just a few hundred generations of a hybridisation event between *Z. tritici* and an unidentified species (Stukenbrock et al., 2012). There is also considerable evidence that the commensal endophytic state and a parasitic, pathogenic state can be highly plastic (Schardl and Craven, 2003; Schulz, 2005). Indeed, there is confirmation that several fungal diseases of plants can exist as a symptomless, endophytic infection – as, for instance, in the necrotrophic generalist *Botrytis cinerea* (grey mould) (Barnes and Shaw, 2003; Sowley at al., 2010) and obligate biotrophic *Albugo* species (Ploch and Thines 2011). Anthropogenic change to natural environments is also likely to be a major factor in promoting the emergence of new pathogens (Fisher et al., 2012). Important issues such as climate change, degradation of natural environments (such as forest clearance and loss of genetic diversity in natural plant populations), dispersal of plants and their associated fungi to new areas and dependence on agricultural monoculture systems are likely to enhance the probability of new diseases emerging, establishing and spreading. The initial emergence events are likely to go unreported not only because of their low frequency, but also because the damage resulting from a new pathogen could be attributed to other microbial species or to abiotic stress-induced damage.

The genus *Hemerocallis* (daylily) of the family Hemerocallidaceae in the order Asparagales has been cultivated for thousands of years (Rodriguez-Enriquez and Grant-Downton, 2012). This small genus of petaloid monocotyledons has been valued as a food crop, as a medicinal plant and as an ornamental. The native range extends from eastern Asia, with a centre of diversity in Japan, Korea and China, possibly as far west as central Europe. Widespread cultivation has led to naturalisation of the genus in many parts of the world (Rodriguez-Enriquez and Grant-Downton, 2012). Cultivated *Hemerocallis* in North America, where the

numerous hybrids are popular ornamental garden plants, were recently challenged by the accidental introduction of a genus-specific biotrophic rust pathogen, *Puccinia hemerocallidis* (daylily rust) (Williams-Woodward et al., 2001; Hernández et al., 2002). This pathogen caused a rapidly-spreading epidemic. The lack of resistance amongst hybrid cultivars - with one study showing only a minority of the cultivars tested exhibiting any resistance to even a single *P. hemerocallidis* isolate - demonstrated the susceptibility of cultivated varieties that have been bred outside of their native range in the absence of any pressure from this specific pathogen (Muller et al., 2003). Other emerging threats to cultivated daylily include infection by the *Armillaria* genus (Schnabel et al., 2005; Blaedow et al., 2010). Both in the West and in China, anthracnose diseases caused by *Colletotrichum* species have been identified and a new species of *Colletotrichum, C. hemerocallidis*, was recently described in China (Yang et al., 2012).

However, the etiology of one emerging disease of cultivated *Hemerocallis* in Western gardens has remained elusive. 'Spring sickness' describes a group of disease symptoms that primarily affect the emergent post-winter foliar growth of the plant, causing distortion, stunting, chlorosis, ragged leaf edges and necrotic lesions (Bergeron, 2001). These symptoms not only disfigure the foliage but also weaken the plant, resulting in reducing flowering, and -in severe cases - the affected growing point dies. The first reports of this disease come from the U.S.A. in the 1970s (Wooten, 1972) and widespread notification of these symptoms has occurred only over the past 20 years. To date, there has not been a report in peer-reviewed literature of filamentous fungal species being isolated from *Hemerocallis* material showing such symptoms. Nevertheless, there is considerable speculation that fungal pathogens may be responsible or contribute to disease development (Bergeron, 2001; Wooten, 1972; Bergeron and Somers, 2010). Here, we report the isolation of a new species of *Botrytis* from foliar material of *Hemerocallis* from the United Kingdom that showed a range of symptoms that correspond to 'spring sickness'. We demonstrate that this new species is distinct at the molecular and morphological level from its closest relative, *B. elliptica* (fire blight), and that the two species have diverged in their host range. Our data shows that cryptic fungal species and fungal diseases can be identified from common cultivated plants outside of their natural range, suggesting that there may be a significant reservoir of fungal diversity from which new diseases may emerge.

Materials and Methods

Isolation from plant material

Samples were collected from collections of hybrid *Hemerocallis* growing in gardens in England, from Oxfordshire, Wiltshire and Somerset. Pieces of asymptomatic and symptomatic leaf tissue, each approximately 6 mm^2, were surface-sterilized by immersing in 30% (v/v) sodium hypochlorite-based domestic bleach containing detergent (Parazone; Jeyes, Cambridge, UK) for 30 sec followed by 4×5 min washes in sterile distilled water. Surface-sterilized leaf pieces were plated out on 2% (w/v) malt extract agar (MEA) (Oxoid, Basingstoke, UK) and grown under natural ambient light. The 6 isolates, labelled B1, B2, B4, B5, B6 and P1, were routinely grown on 2% MEA and stock cultures were maintained at 4°C in the dark. Stocks were also preserved as excised mycelial material in sterile 50% (v/v) glycerol at −80°C.

Immunological tests of fungal isolates and plant extracts for *Botrytis* antigens

Plate cultures of fungal isolates were washed with 5 ml phosphate buffered saline, pH 7.4 (Sigma) plus 0.05% Tween 20 (Sigma) (PBST). 1 ml was removed by suction, centrifuged briefly at 13,000×g in a microcentrifuge and 400 µl of the supernatant tested with Botrytis QuickStixs (EnviroLogix, Portland, Maine, USA) which employs the anti-*Botrytis*-monoclonal antibody, BC-12.CA4, raised and employed in previous studies (Meyer and Dewey, 2000; Dewey et al., 2008; Dewey et al., 2013). Tests were performed by incubating a QuickStix in the supernatant for 10 minutes, the lower pad was then removed and the intensity of the test line (signal intensity, SI) was determined using an EnviroLogix Quickstix reader (Dewey et al., 2008, ; Dewey et al., 2013). Extracts of leaf tissues were made by crushing leaf material in an extraction bag (Noegen, UK) with PBST, 1:5 (w/v). 400 µl of the resulting non-particulate extract was tested with EnviroLogix *Botrytis* QuickStix system as above.

DNA extraction, PCR amplification and sequencing

Genomic DNA was extracted from plugs of cultured mycelial material that were frozen and ground in liquid nitrogen. DNA was purified from tissue powder using the DNEasy kit (Qiagen, Manchester, UK) and quantified using a Nanodrop spectrophotometer. PCRs were performed using approximately 4–12 ng genomic DNA at in a 50 µl reaction using the proof-

reading Phusion polymerase kit (Finnzymes, Thermo Scientific, UK) according to the manufacturer's instructions. Cycling conditions for the amplifications were as follows: 98°C for 1 minute; 10 cycles of 98°C for 10 seconds, primer-specific annealing temperature 1 for 30 seconds, extension at 72°C for 45 seconds; 15 cycles of 98°C for 10 seconds, primer-specific annealing temperature 2 for 30 seconds, extension at 72°C for 45 seconds; final extension at 72°C for 5 minutes.

The 18S rRNA sequence was amplified using *ITS1* primers previously described (Staats et al., 2005) (Supplementary Table S1). The primer-specific annealing temperatures 1 and 2 were 60°C and 56°C respectively. The amplification of the *G3PDH, HSP60* and *RPB2* sequences was achieved using primers for the genus *Botrytis* described in (Staats et al., 2005) (Supplementary Table S1). Primer-specific annealing temperatures 1 and 2 were 62°C and 60°C respectively for *G3PDH* and *HSP60*, and 60°C and 56°C respectively for *RPB2*. *NEP1* was amplified using primers NEP1for and NEP1revB (Staats et al., 2007) (Supplementary Table S1) with primer-specific annealing temperatures 1 and 2 of 62°C and 60°C respectively. *NEP2* was amplified using primers NEP2forE and NEP2revE (Staats et al., 2007) (Supplementary Table S1) with primer-specific annealing temperatures 1 and 2 of 62°C and 60°C respectively. PCRs were run on 1.5% (w/v) agarose gels, the bands were cut out with a clean razor and extracted using Qiaex II kit (Qiagen, Manchester, UK). Purified PCR fragments were then cloned into pJET sequencing vector (CloneJET PCR cloning kit; Thermo Scientific, UK) and transformed into *E. coli* DH5α competent cells. Transformants were selected on LB-ampicillin plates (with 100 μg ampicillin per ml of medium) and colonies with inserts identified by PCR screening. Plasmid DNA was extracted from selected colonies using GeneJET Plasmid Miniprep Kit (Thermo Scientific, UK) and sequenced by Source Biosciences (Nottingham, UK).

Genomic DNA was extracted from leaf material showing symptoms and from leaf material of the same cultivar without symptoms, collected on the same day. Leaf material was derived from the cultivars 'Gerda Brooker' and 'Free Bird'. Small sections of leaf material approximately 2×2 cm were ground to a fine powder in liquid nitrogen. DNA was purified from tissue powder using the DNEasy kit (Qiagen, Manchester, UK) and quantified using Nanodrop spectrophotometer. PCRs were performed using approximately 100 ng genomic

DNA as template at in a 50 μl reaction using the proof-reading Phusion polymerase kit (Finnzymes, Thermo Scientific, UK) according to the manufacturer's instructions. *NEP1* primers that amplify the promoter to 3' end - NEP1(−207for) and NEP1(+1124rev) - (Staats et al., 2007) (Supplementary Table S1) were used in a primary PCR with cycling as follows.

98°C for 1 minute; 10 cycles of 98°C for 20 seconds, 64°C for 30 seconds, extension at 72°C for 45 seconds; 10 cycles of 98°C for 20 seconds, 60°C for 30 seconds, extension at 72°C for 45 seconds; 15 cycles of 98°C for 20 seconds, 58°C for 30 seconds, extension at 72°C for 45 seconds; final extension at 72°C for 5 minutes. A 2 μl aliquot of primary PCR was then used as a template in a 50 μl reaction with NEP1for and NEP1revB primers (Staats et al., 2007) (Supplementary Table S1) as follows: 98°C for 1 minute; 15 cycles of 98°C for 10 seconds, 64°C for 30 seconds, extension at 72°C for 20 seconds; 15 cycles of 98°C for 10 seconds, 60°C for 30 seconds, extension at 72°C for 20 seconds; final extension at 72°C for 5 minutes. PCRs were run on 1.5% (w/v) agarose gels, the PCR fragments were then removed, purified, cloned and sequenced as described above.

Phylogenetic analysis

Sequences of *Botrytis* genes were obtained from GenBank (www.ncbi.nlm.nih.gov/genbank) and aligned with newly sequenced genes from the six isolates using MUSCLE (Edgar, 2004). Phylogenies for single gene and combined datasets were reconstructed using a maximum-likelihood inference conducted with RAxML version 7.2.6 (Stamatakis, 2006) via the raxmlGUI interface (Silvestro and Michalak, 2012). We conducted five independent runs from different starting points to assess convergence within two likelihood units of the best tree, which was consistently selected. The parameters of partition were allowed to vary independently under the GTRGAMMA model of evolution as implemented in RAxML. Maximum-likelihood nodal support was calculated by analysing 1000 bootstrap replicates.

Induction of sporulation and sclerotia formation

To determine whether presence of host material stimulated macroconidia production, 1% water agar on which surface-sterilized pieces of greenhouse-grown *Hemerocallis* 'Jurassic Spider' young leaf tissue had been placed. Plates were also made with 1% water agar with

0.5 ml plant extract added. The plant extract was made by thoroughly crushing young leaf tissue in an extraction bag (Neogen, Ayr, UK) with PBST at 1:5 (w/v). The extract was passed through a 0.25 micron filter (Millipore) attached to a syringe for sterilisation before addition to molten agar. To attempt to stimulate production of macroconidia, MEA plates were incubated without light and under a mixture of day light and near UV light at room temperature (~20°C) for 7 to 10 days. Plates were also incubated in the dark except for a continuous near-UV light source. Isolates were also grown on oatmeal agar (OMA) (Difco, Becton Dickinson BV, Breda, The Netherlands), potato dextrose agar (PDA) (Oxoid, Basingstoke, UK), Czapeks Dox medium (Oxoid, Basingstoke, UK), V8 agar (prepared with 200 ml V8 vegetable juice (Campbell Soup Company, Camden, NJ, USA), 20 g agar, 800 ml water, pH adjusted to 6.0 with NaOH).

Light microscopy

Sporulating structures were mounted on slides with filter-sterilised MilliQ water. Observations were made with a Nikon Eclipse 90i (Nikon Instruments, Badhoevedorp, The Netherlands) compound microscope with a Nikon DS-5MC camera attached. Measurements were performed using N.I.S. Elements AR 2.30 software (Nikon Instruments, Badhoevedorp, The Netherlands).

Electron microscopy

Spores were removed from the edges of mature cultures of B2 and B4 using a sticky pad mounted in a SEM stub. Samples were directly coated with gold/palladium in a Polaron SC7640 sputter coating unit (Quorum Technologies, Ashford, UK). Spores were also trapped using poly-lysine coated slides and subsequently treated in osmium tetroxide vapour for 3 hours, followed by 4% paraformaldehyde in phosphate buffer for 3 hours, dehydrated then subsequently sputter coating as described. Images were taken using a JEOL JSM-5510 scanning electron microscope unit (JEOL, Welwyn Garden City, UK) operating at 15 kV.

Pathogenicity assays

Pathogenicity tests were carried out using detached leaves of the following plants: *Alstroemeria* hybrid; *Tricyrtis formosana*; *Lilium* Oriental hybrid; *Hemerocallis fulva* and *Hemerocallis* 'Jurassic Spider'. Leaves were placed on 0.3% water agar in large Petri

dishes. Four replicates were made with the leaf adaxial and abaxial sides upwards. The exposed surfaces were inoculated with a 5 mm mycelial plug from MEA cultures of isolates B1, B2 and B4. The Petri dishes were sealed and incubated at 25°C under 12 hours light and monitored for up to 14 days. As a control, plugs of *B. elliptica* (isolate 9601), grown on MEA agar under identical conditions, were used. A sterile MEA agar control was also performed. Macroconidia of B1, B4 and B5 from sporulating plates were collected in sterile potato dextrose broth (1.2 g/l) and adjusted to concentrations 1×10^6 ml^{-1}. Excised *Hemerocallis* leaves on water agar were inoculated with 3 µl droplets of spore suspensions on their upper sides and three replicates performed for each. The material was sealed in a plastic box with a >90% humidity at 25°C and monitored for up to 10 days after inoculation.

Pathogenicity tests were also carried out on axenic plantlets of *Hemerocallis* 'Jurassic Spider' as follows. Previously established cultures of *Hemerocallis* 'Jurassic Spider' were maintained at 4°C on a 0.6% agarose growth medium composed of Murashige and Skoog macroelements (Murashige and Skoog, 1962) with Heller's microelements (Heller, 1953) and 5 ml/litre of 1% ferric ammonium citrate solution, adjusted to pH 5.5 before autoclaving. The clumps of shoots were divided, with the leaves and roots trimmed. The plantlets derived from division were grown in Magenta boxes containing sterilised 100 ml vermiculite plus 80 ml liquid growth medium (as above, but lacking the 0.6% agarose). In each box, 5 divisions were planted and chilled at 4°C in the dark for 2 weeks, then removed in a well-lit growth room at 20°C with 16 hour photoperiod for 2 weeks to allow wound healing and establishment prior to inoculation. Individual plantlets were inoculated with a 5 mm mycelial plug from a plate culture of one of the fungal isolates (B1, B2, B4) and incubated at 25°C under 16 hours direct light in a growth room for up to 10 days. For controls, *B. elliptica* (isolate 9601) and sterile MEA plugs were used. For each fungal isolate and for each control, three replicate Magenta boxes were inoculated.

To confirm *Botrytis* infection of *Hemerocallis* tissue, extracts of plant tissues were made by crushing sections of aerial material in an extraction bag (Neogen, UK) with PBST, 1:5 (w/v). 400 µl of the resulting non-particulate extract was tested with EnviroLogix *Botrytis* QuickStix system as above. To determine if pathogenicity varied depending on the host cultivar that was challenged, plantlets of a range of cultivars were tested using the same method except

that one plantlet per Magenta box was used. Two replicates were performed for each plant genotype. These pathogenicity assays were all performed with the B1 isolate. The 15 cultivars were as follows: 'Running Late', 'Lavender Curls', 'Dark Mosaic', 'Heavenly Flight of Angels', 'Golden Chimes', 'Barbara', 'Party Array', 'Rococo', 'Bo Knows', 'Cayenne', 'Corky', 'Miss Jessie', 'flava clone 3', 'Persian Pattern', 'Jellyfish Jealousy'.

Identification of mating types and sexual crosses

Five isolates were analysed (B1, B2, B4, B5 and P1) to identify the mating type alleles. Gentra Puregene DNA purification kit (Qiagen, Venlo, The Netherlands) was used for DNA extraction from freeze-dried mycelia following the manufacturer's instructions. 10–50 ng genomic DNA was used in 25 μl reaction volume. PCRs were performed with GoTaq polymerase (Promega) according to manufacturer's instructions. Primers used were *MAT1-1* forward/reverse and *MAT1-2* forward/reverse (Supplementary Table S1). Amplification conditions were as follows: 95°C 5 minutes, then 35 cycles of 94°C for 30 seconds, 52°C for 30 seconds and 72°C for 2 minutes, followed with a final extension of 72°C for 5 minutes. PCR products were visualised on gel to determine the mating type of each isolate. Crosses were set up between isolates carrying different mating types (Faretra et al., 1998). Isolates B1 and B5 (each of the *MAT1-1* mating type) were mated with isolates B2 and B4 (each of the *MAT1-2* mating type). To develop sclerotia, strains were plated on oatmeal agar and incubated in darkness for 1 month at 15°C, followed by incubation at 0°C in darkness for 1 month. For mating, sclerotia were sampled from the plates, rinsed in water with a soft toothbrush and place in a 6-well microtitre plate. Mycelial cultures were flooded with sterile water and a suspension of mycelial fragments and microconidia was obtained by gently rubbing the surface with a spatula. The sclerotia were fertilised by addition of this suspension at 3 ml per well. Reciprocal crosses were set up in this manner, with each partner as a female (sclerotial) or male (microconidial) parent. As a control, sclerotia that were not exposed to microconidia and kept in sterile water were used. The microtitre plates were sealed and incubated at 12°C in normal artificial light with a 12 hour photoperiod.

Results

Isolations and preliminary identification

Over a period of 4 years, leaf samples of *Hemerocallis* cultivars that showed symptoms typical of 'spring sickness' such as necrotic patches, necrotic lesions, distortion and chlorosis (Figure 1a,b) were found to be associated with an unidentified filamentous fungus after the material was rigorously surface-sterilised and plated on malt extract agar (MEA). Occasionally, fungal growth was visible on the symptomatic plant material in the form of dense, short mycelia producing microconidia (Figure 1c,d) suggesting that a filamentous fungus triggers symptom development. However, no macroconidia could be observed on the plant material. In total, 6 independent isolates were collected (Table 1). Vegetative growth at 25°C with ambient light and supplemental near-UV light was rapid, but significant macroconidial sporulation did not occur. Although microconidia were readily identified, only a small number of macroconidia could be found on older cultures at the edges of the Petri dish in two isolates (B2 and B4). The overall hyphal morphology and appearance of melanised sclerotia in older cultures (Figure 1e) suggested that the isolates are members of the genus *Botrytis* and prompted further investigations and DNA analyses. The immunological tests of surface washings of cultures of the isolates using the *Botrytis*-specific monoclonal antibody BC-12. CA4 (Meyer and Dewey, 2000; Dewey et al., 2008; Dewey et al., 2013) gave strong positive results (Table 1) indicating that they are all members of the genus *Botrytis*.
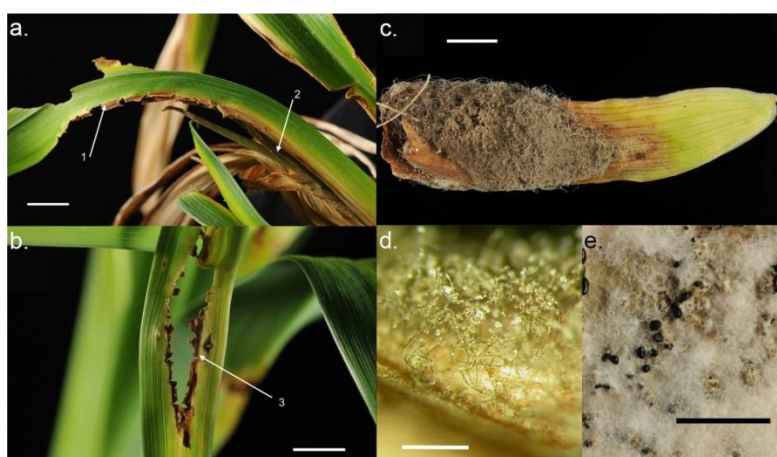
Figure 1: a,b, Spring foliage of *Hemerocallis* cultivars showing symptoms typical of 'spring sickness' disease, c, sporulating fungus on young leaf, d, close up of sporulating fungus *B. deweyae*, e, melanised sclerotia growing on medium

Table 1: Table of fungal isolates identified in this study

Isolate	Host name	Host symptoms	Date of isolation	Culture S.I.
B1	Hemerocallis 'Jurassic Spider'	Developing necrosis, distortion and chlorosis of young foliage	30 November 2009	42
B2	Hemerocallis 'Lola Branham'	Severe necrosis, distortion and chlorosis of young and maturing foliage	19 February 2010	35
B4	Hemerocallis unnamed tetraploid hybrid	Necrosis of mature outer leaves just above soil level	9 June 2010	11
B5	Hemerocallis 'Gerda Brooker'	Severe necrosis of young and mature foliage	15 April 2011	50
P1	Hemerocallis 'Free Bird'	Severe necrosis, distortion and chlorosis of aerial parts; eventual death of tissues back to rhizome	15 April 2011	55
B6	Hemerocallis 'Ruby Storm'	Severe necrosis and chlorosis of leaves emerging from dormancy	12 March 2012	53

Host name, host symptoms and the date of isolation are described. The post-isolation fungal culture signal intensity (S.I.), from tests of PBST suface washings of fungal cultures, with EnviroLogix Botrytis QuickStix using the anti-Botrytis-monoclonal antibody BC-12.CA4, is shown.

Sequence analyses and phylogenetic tree

To determine their identity, all 6 isolates were subjected to DNA sequence analysis. Sequencing of the *ITS* region confirm they all represent *Botrytis* species. Interestingly, all 6 isolates shared a unique polymorphism, an indel, in the highly conserved *ITS* sequence (Figure 2). BLAST analysis of Genbank data showed that no other known member of the genus *Botrytis* possesses this sequence variant.

EU519207 *Botrytis elliptica*   CCAAAACCCAAATTTTTCTATGGTT

EU519208 *Botrytis squamosa*   CCAAAACCCAAATTTTTCTATGGTT

EU093077 *Botrytis aclada*   CCAAAACCCAAATTTTTCTATGGTT

FJ914712 *Botrytis byssoidea*   CCAAAACCCAAATTTTTCTATGGTT

EU519206 *Botrytis porri*   CCAAAACCCAAATTTTTCTATGGTT

HM989942 *Botrytis cinerea*   CCAAAACCCAAATTTTTCTATGGTT

Botrytis deweyae **B1**   CCAAAACCCAAA-TTTTCTATGGTT

Botrytis deweyae **B2**   CCAAAACCCAAA-TTTTCTATGGTT

Botrytis deweyae **B4**   CCAAAACCCAAA-TTTTCTATGGTT

Botrytis deweyae **B5**   CCAAAACCCAAA-TTTTCTATGGTT

Botrytis deweyae **B6**   CCAAAACCCAAA-TTTTCTATGGTT

Botrytis deweyae **PI**   CCAAAACCCAAA-TTTTCTATGGTT

Figure 2: Alignment of a region of partial ITS sequence from various *Botrytis* species. The aligned region shows the indel identified in all 6 examined isolates of *B. deweyae*.

ITS sequence does not permit sufficient resolution to the species level. To further resolve the relationships of these isolates to other species in the genus *Botrytis*, analysis of nuclear protein-coding gene sequences that are known to be phylogenetically informative to the species level was undertaken. Five genes previously used to build phylogenies of the genus *Botrytis* (Staats et al., 2005; Staats et al., 2007) were used. Three were single-copy housekeeping genes - encoding glyceraldehyde-3-phosphate dehydrogenase (*G3PDH*), a heat-shock protein (*HSP60*) and a DNA-dependent RNA polymerase subunit II protein (*RPB2*) (Staats et al., 2005) and two were single-copy genes encoding phytotoxic proteins (*NEP1* and *NEP2*) (Staats et al., 2007).

Combined phylogenetic analysis of these 5 sequences confirmed the distinction between isolate B1 and previously described *Botrytis* species (Figure 3). The genes encoding phytotoxic proteins *NEP1* (Figure 4) and *NEP2* (Figure 5) provided higher resolution between B1 and other members of *Botrytis*.

The *HSP60* sequence was found to be identical to *B. elliptica* and the other sequences were also close to this species, suggesting that its nearest relative was *B. elliptica* (not shown). Phylogenetic analysis confirmed that this isolate was most closely related to *B. elliptica* and formed a monophyletic group with *B. elliptica* and *B. squamosa* (Figure 3). Divergence at synonymous sites between the new isolate and *B. elliptica* and *B. squamosa* was 1.1±0.32%, while divergence at synonymous sites between *B. elliptica* and *B. squamosa* was 1.0±0.31%.
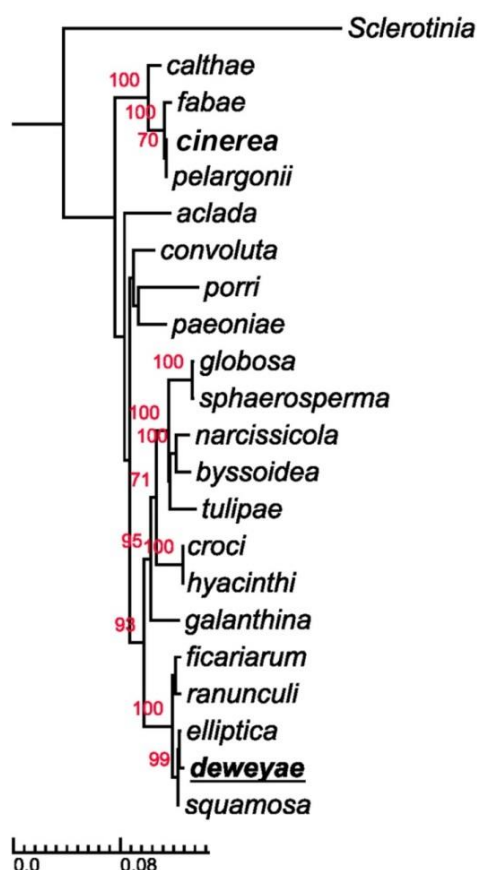
Figure 3: Phylogeny of *Botrytis* species based on the combined analysis of 5 different genes. Sequences of *G3PDH*, *HSP60*, *RPB2*, *NEP1* and *NEP2* were used. The phylogenetic position of *B. deweyae* (B1 isolate, type) is underlined. The phylogeny was constructed using the genus *Sclerotinia* as the outgroup.

The presence of a polymorphism in the *ITS1* sequence (Figure 2), as well as multiple sequence differences at other genes, strongly suggests that they represent an undescribed species (Schubert et al., 2007). *G3PDH*, *NEP1* and *ITS* sequences from all six isolates were identical confirming genetic similarity of isolates. Genetic similarity of isolates together with significant divergence between the new isolates and *B. elliptica* and *B. squamosa* strongly suggests that the new isolates represent an undescribed species.

Further supporting our notion that this species may be involved in development of 'spring sickness', PCR amplification and sequencing of a *NEP1* fragment from DNA extracts of six distinct samples of symptomatic leaf material generated sequences identical to this phylogenetic group (not shown), while PCR amplification on DNA extracts from asymptomatic leaf material did not yield a *NEP1* fragment. Sequences from fungal specimens were submitted to the Genbank database with accession numbers HG799518-HG799538.

Morphological analyses

Non-sporulating colonies are smooth to slightly fluffy and occasionally form aerial mycelia; colonies typically whitish to pale brown in colour on malt extract agar (Figure 6 a,b,c,d). The distance between septa ranges from 38.5 μm to 127. Typically, sclerotium development is seen only as cultures mature; formation varies between isolates and depending on environmental conditions (Figure 6e). Growth in darkness promotes sclerotia formation. On oatmeal agar, sclerotia are formed within 4 weeks at 15°C in darkness. Sclerotia are hemispherical convex in shape and with a concave surface, sometimes hollow in the centre. Sclerotia are black with size ranging from 2 to 6 mm (average 3 mm) in diameter.

The initial absence of significant macroconidial development upon isolation indicates that such conditions are sub-optimal for promotion of asexual sporulation. Exclusion of light and exposure to supplemental near-UV light in the presence of daylight individually fails to trigger sporulation. Surface-sterilised host leaf material and sterile, crude extracts of host leaf material also do not stimulate sporulation. Sporulation (Figure 6f) is more reliably initiated after a minimum of 7 days exposure to near-UV light in the absence of other light sources, though this varies with the isolate and the medium (Supplementary Table S2). One isolate, B2, does not appear to sporulate under these conditions. The dependence on specific environmental conditions is a contrast to *B. elliptica* and *B. cinerea* which efficiently initiate macroconidia formation even when plates are exposed to daylight. The optimum temperature for sporulation of these isolates is 20°C. Conidiophores are erect, septate, opposite branched and slightly swollen at the top (Figure 7a). Figure 7b shows different shapes of macroconidia and Figure 7c shows a scanning electron micrograph of microconidia.
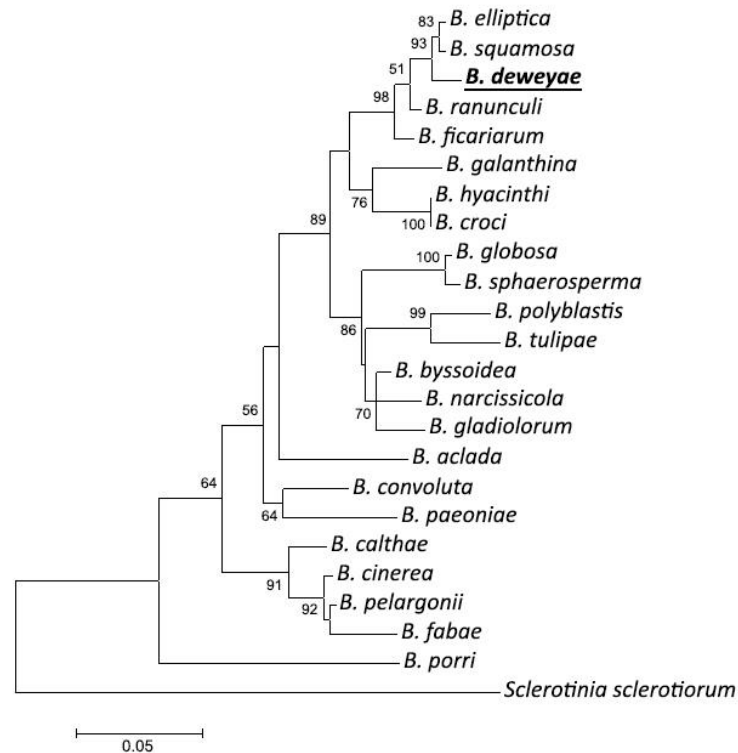
Figure 4: Phylogeny of *Botrytis* species based on the combined analysis of *NEP1* gene. The phylogenetic position of *B. deweyae* (B1 isolate, type) is underlined. The phylogeny was constructed using *Sclerotinia sclerotiorum* as the outgroup.
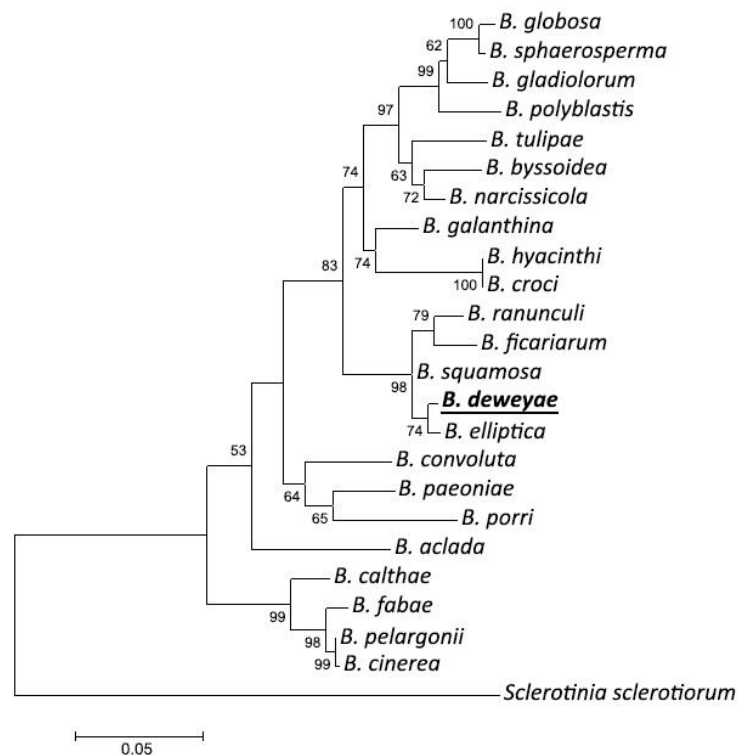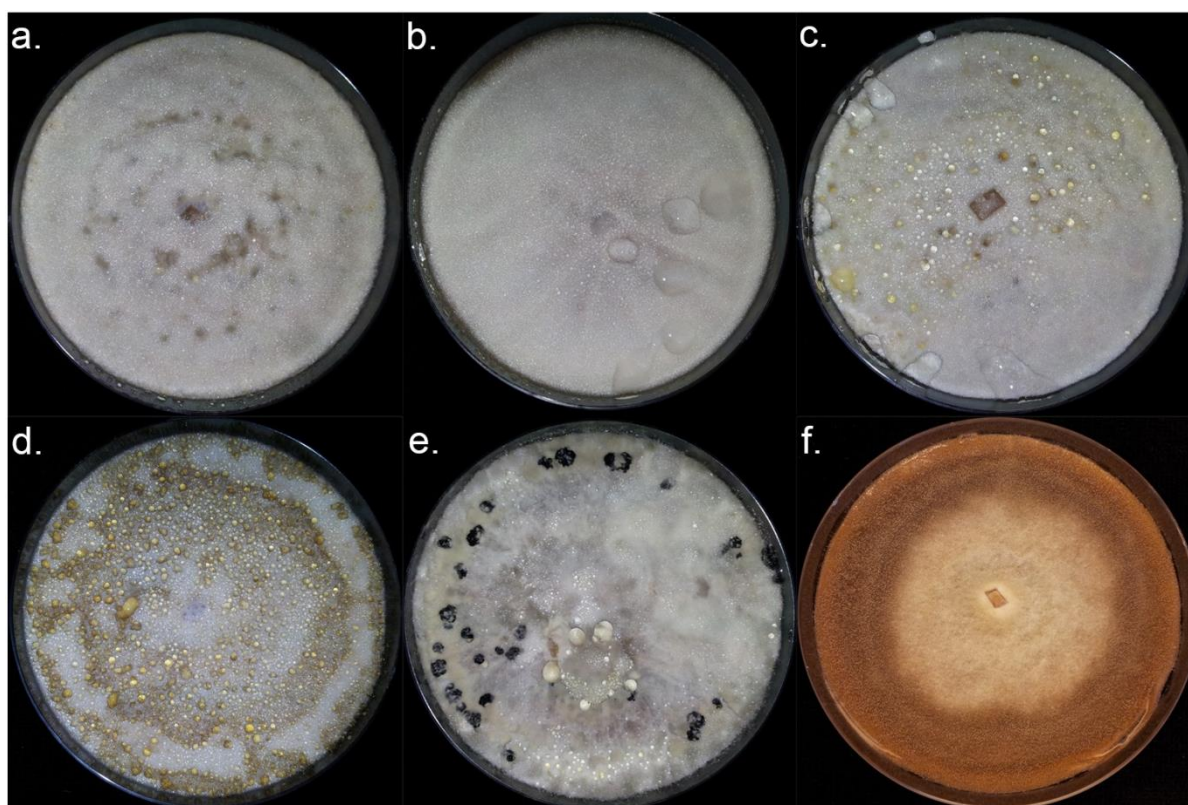

Figure 5: Phylogeny of *Botrytis* species based on the combined analysis of *NEP2* gene. The phylogenetic position of *B. deweyae* (B1 isolate, type) is underlined. The phylogeny was constructed using *Sclerotinia sclerotiorum* as the outgroup.

Figure 6:a, b,c,d non sporulating isolates. e, sclerotial formation in OMA medium. f sprolating isolate.
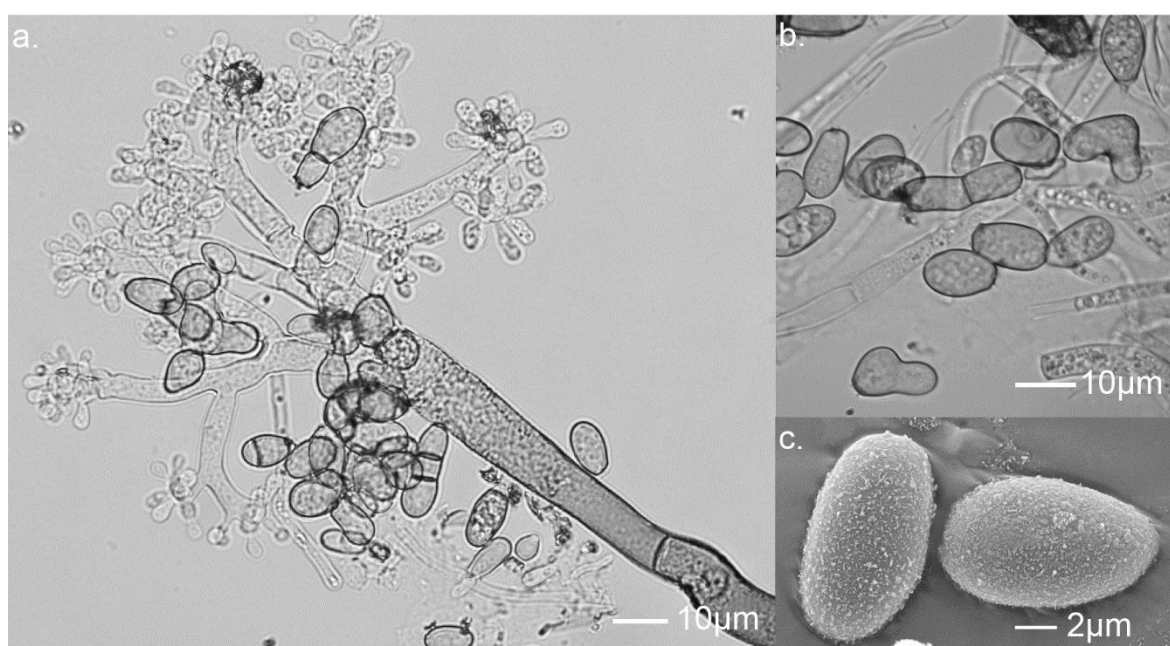
Figure 7: a, development of *Botrytis deweyae* showing production of conidiophores and macroconidia. b, macroconidia in different shapes. c, scanning electron micrograph of the typical macroconidia.

Formal description

Based on the molecular, morphological and host specificity data presented herein, this fungal isolate from *Hemerocallis* represents a new species:

Botrytis deweyae *van Kan, Terhem & Grant-Downton, sp. nov. MycoBank MB804656; Myconame ID 512235.*

Conidiophores erect, septate, medium brown, smooth, mostly unbranched, with slightly swollen basal and apical cells, 3–4 µm × 10–20 µm. *Conidiogenous cells* predominantly terminal, pale brown, giving rise to botryose clusters of conidia. *Conidia* ellipsoid to ovoid, becoming oblong and 1-septate with age, or irregular and somewhat distorted, hyaline to medium brown, smooth, apex obtuse, base with small flattened abscission scar, 6.5–18 µm × 3.5–11 µm (*av.* = 12.5×7 µm, n = 50). No sporulation observed on leaf tissue. *Sclerotia* hemispherical, convex, sometimes hollow in the center, with concave surface; black, 2–6 mm (av. 3 mm) diam. Sclerotia develop in oatmeal agar within four weeks of incubation at 15°C in the dark. Sclerotia are scattered; cultures normally develop 25–30 sclerotia per plate.

Culture characteristics: Colonies incubated in the dark on MEA, optimal growth at 25°C, minimum at 4°C, maximum at 37°C. Colony growth rate 0.4–15.8 mm/d; surface dirty white to pale brown, reverse ochreous (Rayner 1970), with moderate to abundant aerial mycelium, creating fluffy appearance. Colonies also sporulate on MEA under near-ultraviolet light at 20°C.

Typus: UK, Oxford, from host plant *Hemerocallis* 'Jurassic Spider', Robert Grant-Downton, 30th November 2009, holotype CBS H-21133; culture ex-type CBS 134650.

Distribution and host range.

Known only from cultivated specimens of *Hemerocallis* from the UK but likely to be widespread on *Hemerocallis* in cultivation and possibly in the wild due to the cryptic nature of this species and its broad temperature tolerance.

Etymology.

Named after Dr. Molly Dewey in recognition of her outstanding contributions to plant pathology and mycology, in particular relating to the genus *Botrytis*.

Pathogenicity assays

To determine whether *Botrytis* isolates induce the symptoms of the plant material from which they were originally isolated, basic assays were performed using excised surface-sterilised leaf material of *Hemerocallis* on plates. Inoculation of Hemerocallis leaf material with conidial suspensions did not result in necrosis, though the conidia germinated and grew out into hyphae which after 10 days had covered the leaf surface (Figure 8a). Inoculation of mycelial plugs onto the leaf surfaces did not cause any disease symptoms. Instead after several days of incubation, the fungus formed sclerotia on the leaf surface (Figure 8b). Inoculation of *Hemerocallis* plantlets from *in vitro* culture demonstrated that these isolates had the capacity to cause severe necrosis and death of plantlets. Within 10–14 days of inoculation, plantlets showed chlorosis, necrosis, collapse and death of leaf tissue (Figure 9), although the roots and meristematic region were comparatively intact. Tests on plant material extracts after inoculation with B1, B2 and B4 isolates using the *Botrytis*-specific monoclonal antibody BC-12.CA4 (Meyer and Dewey, 2000; Dewey et al., 2008; Dewey et al., 2013) gave strong positive results with signal intensity values ranging between 34 and 46 whilst the control plant tissue without fungal inoculation gave a signal intensity value of 0. B1 isolates appeared to be the most virulent, rapidly causing complete necrosis and collapse of all inoculated plant material within 14 days (Figure 9). Although microconidia could be found developing on leaf tissue, typical conidiophores producing macroconidia are not produced on the host under these conditions. Plantlets representing a range of different *Hemerocallis* cultivars were tested to determine if there may be easily recognised resistance to infection with isolate B1. All the tested cultivars developed similar symptoms of tissue necrosis, collapse and death within 14 days of inoculation (not shown). Testing the isolates from *Hemerocallis* on the leaves of several other monocots such as *Lilium* did not produce lesions, indicating that the host range may be restricted. However, *B. elliptica* did induce similar lesions on *Lilium* material but not on *Hemerocallis* or any other species tested.
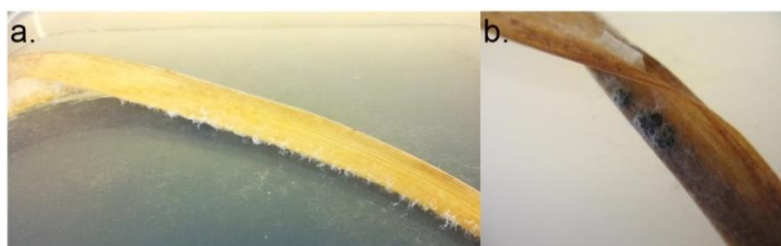
Figure 8: a, hypae growing out of the leaf. b, sclerotia forming on leaf.

Figure 9: Effect of inoculation of *Hemerocallis* plantlets with *Botrytis deweyae*. a, control *Hemerocallis* 'Jurassic Spider' plantlets (uninoculated) (left) and *Hemerocallis* 'Jurassic Spider' plantlets infected with *B. deweyae* (right) after inoculation with B1 isolate, shown 10 days after inoculation. The plant material was excised from sterile vermiculite. Scale indicates 10 cm. b, close-up of tissue necrosis on the basal portion of a *Hemerocallis* 'Jurassic Spider' plantlet following *B. deweyae* infection, following colonisation of leaf bases.

Mating type and sexual crosses

PCR analysis of the mating type locus, *MAT1*, of *Botrytis* revealed that different isolates had different alleles (Table 2). Reciprocal crosses between pairs of strains of opposite mating types, using a method well established for *B. cinerea* (Faretra et al., 1998; van der Vlugt-Bergmans et al., 1993), in all cases failed to result in the development of apothecia. Possibly this was due to the developmental condition of the sclerotia that had developed on plates and were used in the attempted sexual crosses in this study.

Table 2: MAT1 alleles in different *Botrytis deweyae* isolates

Isolate	B1	B2	B4	B5	P1
MAT locus	*MAT1-1*	*MAT1-2*	*MAT1-2*	*MAT1-1*	*MAT1-2*

Discussion

We report the discovery of a new species of the Ascomycota fungal genus *Botrytis* from cultivated material of *Hemerocallis* (commonly known as the daylily) showing a range of symptoms corresponding to those reported for a mysterious disease, 'spring sickness'. Recently, several new species of *Botrytis* have been reported, such as *B. sinoallii* from China which is pathogenic on *Allium* crops (Zhang et al., 2010a), *B. fabiopsis* from central China which is pathogenic on broad bean (Zhang et al., 2010b) and *B. caroliniana* from North America which is pathogenic on blackberry fruits and broad bean leaves (Li et al., 2012). Other as yet undescribed pathogenic *Botrytis* species are likely to interact with cultivated plants, for example a foliar pathogen of *Hosta* (also in the order Asparagales) that is closely related to *B. tulipae* (Laudon, 1978). This new species, *B. deweyae*, represents the first novel and morphologically distinctive species to be identified in Europe for many years, as compared with recently described *B. pseudocinerea* that is genetically but not morphologically distinct from *B. cinerea* (Walker et al., 2011). It is likely that *B. deweyae* has evaded detection as 1) the critical diagnostic morphological feature of macroconidia do not seem to develop on infected plant material nor are they produced from laboratory cultures except under a specific environmental regime, 2) isolation from infected material has not employed sufficiently stringent surface sterilization to prevent overgrowth from less systemic/pathogenic fungi, 3) the disease symptoms are relatively subtle, have a short temporal manifestation and can easily be attributed to another causative agent, and 4) it is probable that this species has a highly restricted host range.

There have been some reports of investigations of 'spring sickness' disease by specialist growers of *Hemerocallis* (Bergeron, 2001; Bergeron and Somers, 2010), yet the causative agent had not been identified although other fungal species, such as the yeast-like *Aureobasidium microstictum* (daylily leaf streak) have been implicated (Begeron and Somers, 2010). The rigorous surface-sterilisation procedure we employed in isolations is likely to have been an important factor in finding this new species, as other opportunistic microbial species colonising damaged tissue more superficially would have been removed. In our studies, *B. deweyae* was repeatedly isolated from diseased material over a 4 year period. Whilst our pathogenicity assays using detached leaf material and plantlets *in vitro* under laboratory conditions cannot fully replicate mature plants growing in gardens in the colder

months of the year, the rapid development of similar leaf tissue necrosis suggests this species has the capacity to be the major contributor to initiating symptom development. Other microbial species, such as *A. microstictum*, may opportunistically infect as secondary colonisers and aggravate disease development. The rapidity with which plantlet destruction took place was surprising but this is likely to have been enhanced by the absence of any other microbial flora in these cultures. Numerous microbial species have been shown to act antagonistically to *Botrytis* infections of plants (reviewed in Elad and Stewart, 2004). For instance, infection of *Lilium* by *B. elliptica* can be antagonised by specific bacteria (Chiou and Wu, 2001). Our hypothesis that *B. deweyae* is the main agent of 'spring sickness' disease development is supported by a report of its closest relative, *B. elliptica*, infecting spring growth of *Hemerocallis fulva* in Korea (Chang et al., 2001). In this case, symptoms were similar with necrosis and death of young leaf tissue, but it was accompanied by significant production of macroconidia. Tests *in vitro* indicated that *B. elliptica* was only capable of infecting *Hemerocalis* tissue after physical damage to the plant (Chang et al., 2001); this suggests that *B. elliptica* lacks the capacity to infect uninjured *Hemerocallis* tissues. There have been no other reports of *B. elliptica* infecting *Hemerocallis*.

The infection of *Hemerocallis* with *B. elliptica* demonstrates that although this species has been most commonly associated with infections of bulbous true lily (Lilium, Liliaceae *sensu stricta*) - where it is a major disease of cultivated lily bulb crops (Lorbeer et al., 2004) - it is also capable of infecting other distantly related petaloid monocots such as *Hemerocallis* (Hemerocallidaceae) and *Tricytris* (Convallariaceae) (Chang et al., 2001; Furukawa et al., 2005). There is also evidence that *B. elliptica* can infect dicotyledonous hosts (Tompkin and Hansen, 1950; Harrison and Williamson, 1986), albeit under unnatural conditions. Whether *B. deweyae* is an emergent pathogen that has evolved from a *B. elliptica* population that has undergone a host-shift to *Hemerocallis* is a matter that remains open for further study. The significant morphological and DNA sequence divergences from any described *B. elliptica* strain suggest that this would not have been a recent event. As 2 mating loci (*MAT1*) alleles are present in just 5 tested isolates, recent and rapid sympatric speciation from *B. elliptica* would appear unlikely. To date, only cultivated material from Britain has been examined but it is almost certain that *B. deweyae*, like its closest relative *B. elliptica* (Lorbeer et al., 2004; Huang et al., 2001), is cosmopolitan and will be

detected in cultivated populations of hybrid *Hemerocallis* elsewhere in the world and perhaps also in native and naturalised *Hemerocallis* populations in nature.

Given the lack of any report of this species from indigenous *Hemerocallis* populations, its morphology and the nature of disease development, it is plausible that *B. deweyae* may be an endophyte that is undergoing the transition to a more aggressive pathogenic state. There was apparent variation in pathogenicity amongst three isolates tested on plantlets, with the isolate B1 being the most pathogenic. Endophytic *Botrytis* have been identified using sequencing methods from naturalised populations of *Centaurea stoebe* (Shipunov et al., 2008), clearly demonstrating that outside of their native range plant species can retain or acquire endophytic *Botrytis* species. Five putative new endophytic species were discovered in this study alone. Intriguingly, there is also evidence that pathogenic *B. cinerea* (grey mould) can exist as a systemic endophyte without causing pathogenesis in plants (Barnes and Shaw, 2003; Sowley et al., 2010). By some mechanism, *B. cinerea* must be capable of substantially down-regulating gene expression responsible for aggressive, necrotrophic pathogenesis thereby permitting it to co-exist and grow within plant tissues without damaging them or even triggering defence responses. In the case of *B. deweyae* the absence of identifiable macroconidia in nature, after growth on the host *in vitro* and even the absence of sporulation on plates (except under specific conditions) suggests that this development is usually highly suppressed, as might be expected of an endophytic lifestyle (Schulz and Boyle, 2005). In common with other specialised *Botrytis* species that infect petaloid monocotyledons (Lorbeer et al., 2004), additional studies are required to identify the precise details of the life cycle. Whether, as in *B. elliptica* (Huang et al., 2001; Staats et al., 2007), sexual reproduction is important in natural populations of *B. deweyae* requires further investigations.

As this disease has become prevalent only in the past 20 years, one factor that may be precipitating the evolution of pathogenesis is the increasing loss of genetic diversity in the host plant through in-breeding of the cultivated hybrid lines, as demonstrated by an AFLP study (Tomkins et al., 2001). It is known from studies of *Colletotrichum* that the ability for a fungal isolate to exhibit pathogenic or mutualistic behaviour can depend on the host genotype (Redman et al., 2001). The emergence of in-breeding depression and loss of vigour

amongst *Hemerocallis* hybrids may favour the emergence of strains that are able to effectively take advantage of weakened resistance systems in the plant and hence exploit the host in a more parasitic manner. In hybrid daylily, it is conceivable that the effects of combining divergent genomes followed by multiple generations of in-breeding and selection for novel traits have compromised the effectiveness of mechanisms that regulate pathogen resistance and endophyte activity *in planta*. Such a biotic environment may facilitate the emergence of new diseases, including transitions from endophytes to parasites and host shifts.

Other factors may have assisted the emergence of this disease. The clonal propagation of cultivars by division, which creates large wounds, and the tendency to plant *Hemerocallis* as monocultures or near-monocultures by enthusiasts may assist spread of strains with emerging pathogenic tendencies. A role for bulb mites (for example members of the genus *Rhizoglyphus*) in spreading fungal material such as mycelium fragments to new infection sites appears plausible (Bergeron and Somers, 2007; Gray et al., 1975; Diez et al., 2000). Anecdotal reports suggest that both treatment by both acaricides and fungicides may reduce the incidence of 'spring sickness', supporting this view (Bergeron et al., 2001). Young, emerging leaf tissues in late winter and spring may be particularly vulnerable to pathogenesis not only due to injury by fluctuating environments (such as tissue damage by freezing weather) but also due to rapid mobilisation of stored compounds from the tuberous roots to sustain new growth. Both factors may tip the balance in favour of fungal development.

Our discovery suggests that other potentially important pathogenic fungi could be easily overlooked and many are likely to remain unknown to science. The large reservoirs of endophytic fungi residing in plants (Arnold et al., 2000), for example those found in wild grasses (Poaceae) (Schardl et al., 2004), may be a source of important biological diversity for the evolution of new plant pathogens, especially with continued erosion of genetic diversity in cultivated plants and in fragmented natural habitats (Fisher et al., 2012). As threats from emerging pathogens to crop and wild plant resources continue to grow, investment in surveillance and detection systems for new plant diseases should be made a priority. This case in particular demonstrates that diagnostic tools using immunological and DNA

sequencing methods, in combination with more conventional morphological and pathology assays, will need to work together in the future if other new plant diseases are to be identified effectively. Widespread 'cryptic' diseases of this kind with a small detrimental impact on the host may be important indicators of host and pathogen groups in which more virulent diseases are likely to be emergent.

Supporting Information

Supplementary Table S1 and Supplementary Table S2

Acknowledgments

References

Arnold E, Maynard Z, Gilbert G, Coley PD, Kursar TA (2000) Are tropical fungal endophytes hyperdiverse? Ecology Letters 3: 267–274.

Barnes SE, Shaw ME (2003) Infection of commercial hybrid *Primula* seed by *Botrytis cinerea* and latent disease spread through the plants. Phytopathology 93: 573–578.

Bergeron S (2001) Spring sickness. The Daylily Journal 56: 434–440.

Bergeron S, Somers K (2010) An update on spring sickness. The Daylily Journal 65: 16–19.

Blaedow KE, Baumgartner K, Cox KD, Schnabel G (2010) Natural infection of an herbaceous host by *Armillaria*: a case study on *Hemerocallis*. Canadian Journal of Plant Pathology 32: 351–360.

Chang SW, Kim SK, Hwang BK (2001) Gray mould of daylily (*Hemerocallis fulva* L.) caused by *Botrytis elliptica* in Korea. Plant Pathology Journal 17: 305–307.

Chiou AL, Wu WS (2001) Isolation, identification and evaluation of bacterial antagonists against *Botrytis elliptica* on lily. Journal of Phytopathology 149: 319–324.

Dewey FM, Hill M, De Scenzo R (2008) Quantification of *Botrytis* and laccase in wine grapes. American Journal of Enology and Viticulture 59: 47–54.

Dewey FM, Steel CC, Gurr SJ (2013) Lateral flow devices to rapidly determine levels of stable *Botrytis* antigens in table and dessert wines. American Journal of Enology and Viticulture 62(2):291-295.

Diez A, Okabe K, Eckenrode CJ, Villani MG, O'Connor BM (2000) Biology, ecology and management of the bulb mites of the genus *Rhizoglyphus.* Experimental and Applied Acarology 24: 85–113.

Edgar RC (2004) MUSCLE: multiple sequence alignment with high accuracy and high throughput. Nucleic Acids Research 32: 1792–97.

Elad Y, Stewart A (2004) Microbial control of Botrytis spp. In: Elad Y, Williamson B, Tudzynski P, Delen N, eds. Botrytis: Biology, Pathology and Control. Dordrecht: Springer 223–241.

Furukawa T, Ushimaya K, Kishi K (2005) Botrytis blight of Taiwanese toad lily caused by *Botrytis elliptica* (Berkley) Cooke. Journal of General Plant Pathology 71: 95–97.

Faretra F, Antonacci E, Pollastro S (1988) Sexual behaviour and mating system of *Botryotinia fuckeliana,* teleomorph of *Botrytis cinerea*. Microbiology 134: 2543–2550.

Fisher MC, Henk DA, Briggs CJ, Brownstein JS, Madoff LC, et al. (2012) Emerging fungal threats to animal, plant and ecosystem health. Nature 484: 186–194.

Gray EC, Shaw MW, Shiel RS (1975) The role of mites in the transmission of smoulder in Narcissus. Plant Pathology 24: 105–107.

Harrison JG, Williamson B (1986) *Botrytis* spp. on red raspberry: survival in fruits and infection of canes. Transactions of the British Mycological Society 86: 171–173.

Heller R (1953) Recherches sur la nutrition minérale des tissues végétaux cultivés in vitro. Annales des Sciences Naturelles Botanique et Biologie Végétale 14: 1–233.

Hernández JR, Palm ME, Castlebury LA (2002) *Puccinia hemerocallidis*, cause of daylily rust, a newly introduced disease in the Americas. Plant Disease 86: 1194–1198.

Huang J, Hsieh T-F, Chastagner GA, Hsiang T (2001) Clonal and sexual propagation in *Botrytis elliptica*.. Mycological Research 105: 833–842.

Laundon GF (1978) New host records of plant disease fungi in New Zealand. New Zealand Journal of Agricultural Research 21: 705–707.

Li X, Kerrigan L, Chai W, Schnabel G (2012) *Botrytis caroliniana*, a new species isolated from blackberry in South Carolina. Mycologia 104: 650–658.

Lorbeer JW, Seyb AM, de Boer M, van den Ende JE (2004) Botrytis species on bulb crops. In: Elad Y, Williamson B, Tudzynski P, Delen N, eds. Botrytis: Biology, Pathology and Control. Dordrecht: Springer. 273–294.

Meyer U, Dewey FM (2000) Efficacy of different immunogens for raising monoclonal antibodies to *Botrytis cinerea*. Mycological Research 104: 979–987.

Mueller DS, Williams-Woodward JL, Buck JW (2003) Resistance of daylily cultivars to the daylily rust pathogen, *Puccinia hemerocallidis*. Hortscience 38: 1137–1140.

Murashige T, Skoog F (1962) A revised medium for rapid growth and bioassays with tobacco tissue cultures. Physiologia Plantarum 15: 473–497.

Ploch S, Thines M (2011) Obligate biotrophic pathogens of the genus *Albugo* are widespread as asymptomatic endophytes. Molecular Ecology 20: 3692–3699.

Rayner RW (1970) A mycological colour chart. Commonwealth Mycological Institute (Kew). London.

Redman RS, Dunigan DD, Rodriguez RJ (2001) Fungal symbiosis from mutualism to parasitism: who controls the outcome, host or invader? New Phytologist 151: 705–716.

Rodriguez-Enriquez MJ, Grant-Downton RT (2012) A new day dawning: *Hemerocallis*(daylily) as a future model organism. AoB Plants pls055.

Tompkins CM, Hansen HN (1950) Flower blight of *Stephanotis floribunda*, caused by *Botrytis elliptica*, and its control. Phytopathology 40: 780–781.

Tomkins JP, Wood TC, Barnes LS, Westman A, Wing RA (2001) Evaluation of genetic variation in the daylily (*Hemerocallis* spp.) using AFLP markers. Theoretical and Applied Genetics 102: 489–496.

Schardl CL, Craven KD (2003) Interspecific hybridization in plant-associated fungi and oomycetes: a review. Molecular Ecology 12: 2861–2873.

Schardl CL, Leuchtmann A, Spiering MJ (2004) Symbioses of grasses with seedborne fungal endophytes. Annual Review of Plant Biology 55: 315–340.

Schnabel G, Bussey KE, Bryson PK (2005) First report of *Armillaria gallica* causing Armillaria root rot in daylily in South Carolina. Plant Disease 89: 683.

Schubert K, Groenewald JZ, Braun U, Dijiksterhuis J, Starink M, et al. (2007) Biodiversity in the *Cladosporium herbarum* complex (*Davidiellaceae, Capnodiales*), with standardisation of methods for *Cladosporium* taxonomy and diagnostics. Studies in Mycology 58: 105–156.

Schulz B, Boyle C (2005) The endophytic continuum. Mycological Research 109: 661–686.

Silvestro D, Michalak I (2012) raxmlGUI: a graphical front-end for RAxML. Organisms Diversity and Evolution 12: 335–337.

Shipunov A, Newcombe G, Raghavendra AKH, Anderson CL (2008) Hidden diversity of endophytic fungi in an invasive plant. American Journal of Botany 95: 1096–1108.

Sowley ENK, Dewey FM, Shaw MW (2010) Persistent, symptomless, systemic and seed-borne infection of lettuce by *Botrytis cinerea.* European Journal of Plant Pathology 126: 61–71.

Staats M, van Baarlen, P, van Kan JAL (2005) Molecular phylogeny of the plant pathogenic genus *Botrytis* and the evolution of host specificity. Molecular Biology and Evolution 22: 333–346.

Staats M, van Baarlen P, Schouten A, van Kan JAL, Bakker FT (2007a) Positive selection in phytotoxic protein-encoding genes of *Botrytis* species. Fungal Genetics and Biology 44: 52–63.

Staats M, van Baarlen P, van Kan JAL (2007b) AFLP analysis of genetic diversity in populations of *Botrytis elliptica* and *Botrytis tulipae* from the Netherlands. European Journal of Plant Pathology 117: 219–235.

Stamatakis A (2006) RAxML-VI-HPC: maximum likelihood-based phylogenetic analyses with thousands of taxa and mixed models. Bioinformatics 22: 2688–2690.

Stukenbrock EH, Christiansen FB, Hansen TT, Dutheil JY, Schierup MH (2012) Fusion of two divergent fungal individuals led to the recent emergence of a unique widespread pathogen species. Proceedings of the National Academy of Sciences USA 109: 10954–10959.

Walker A-S, Gautier A, Confais J, Martinho D, Viaud M, et al. (2011) *Botrytis pseudocinerea*, a new cryptic species causing gray mould in French vineyards in sympatry with *Botrytis cinerea*. Phytopathology 101: 1433–1445.

Williams-Woodward JL, Hennen JF, Parda KW, Fowler JM (2001) First report of daylily rust in the United States. Plant Disease 85: 1121.

Wooten J (1972) Performance of modern, named daylilies in South Florida. Proceedings of the Florida State Horticultural Society 85: 438–440.

van der Vlugt-Bergmans CJB, Brandwagt BF, vant't Klooster JW, Wagemakers CAM, van Kan JAL (1993) Genetic variation and segregation of DNA polymorphisms in *Botrytis cinerea*. Mycological Research 97: 1193–1200.

Yang Y, Liu Z, Cai L, Hyde KD (2012) New species and notes of *Colletotrichum* on daylilies (*Hemerocallis* spp.) Tropical Plant Pathology 37: 165–174.

Zhang J, Zhang L, Li G-Q, Yang L, Jiang D-H, et al. (2010a) *Botrytis sinoallii* – a new species of the grey mould pathogen on *Allium* crops in China. Mycoscience 51: 421–431.

Zhang J, Wu M-D, Li G-Q, Yang L, Yu L, et al. (2010b) *Botrytis fabiopsis*, a new species causing chocolate spot of broad bean in central China. Mycologia 102: 1114–1126.

Supporting information

Supplementary Table S1

Table S1: List of primers employed in PCRs in this study.

Primer name	Primer sequence (5' to 3')
G3PDH for	ATTGACATCGTCGCTGTCAACGA
G3PDH rev	ACCCCACTCGTTGTCGTACCA
HSP60 for	CAACAATTGAGATTTGCCCACAAG
HSP60 rev	GATGGATCCAGTGGTACCGAGCAT
ITS for	TCCGTAGGTGAACCTGCGG
ITS rev	TCCTCCGCTTATTGATATGC
RPB2 for	GATGATCGTGATCATTTCGG
RPB2 rev	CCCATAGCTTGCTTACCCAT
NEP1(−207)for	CACCTTGTGGGAGATTGTATGGGTGGATATACATC
NEP1(+1124)rev	GGTCACCTAATTTTGGCTTTCAGGGTC
NEP1for	CCAACGCAAAATTCCTTTCTATCC
NEP1revB	GTTGGCGAAGTTGTGGTCATTGAA
NEP2forE	TCATCATGGTTGCCTTCTCAAGAT
NEP2revE	AAGTAGCAGCTGCAAGATTGTTTG
MAT 1-1 F	CCAGCAGTAAATGCAGAAGAGCCAA
MAT 1-1 R	CATCATACCAGTGGACCAAGGAGG
MAT 1-2 F	GACTAGGAAAATGGGTACCGCATC
MAT 1-2 R	GAATGTGTAGAGATCCTGTTGTTG

Supplementary Table S2

Table S2: Production of macroconidia (sporulation) from isolates of *Botrytis deweyae* grown on different media. Colonies were grown at 20°C in darkness except for a UV light source, and examined for sporulation at 6 days and 12 days.

Medium	Days of exposure to UV in darkness	B1 isolate	B2 isolate	B4 isolate	B5 isolate
Oatmeal agar	6	No sporulation	No sporulation	Sporulation	No sporulation
Czapek Dox	6	No sporulation	No sporulation	Sporulation	No sporulation
V8 juice agar	6	No sporulation	No sporulation	Sporulation	No sporulation
Oatmeal agar	12	No sporulation	No sporulation	Sporulation	Sporulation
Czapek Dox	12	No sporulation	No sporulation	Sporulation	No sporulation
V8 juice agar	12	Sporulation	No sporulation	Sporulation	No sporulation

Chapter 6

General discussion

General discussion

Sex in fungi

Most fungal taxa have both asexual and sexual modes of reproduction. Fungi which lack sexual reproduction, or for which it was never reported, have long been considered to form a separate phylum (Deuteromycota), which became obsolete with the discovery that this phylum was paraphyletic. The loss of the capacity of sexual reproduction has been considered an evolutionary dead-end because of the reduced capacity of asexual organisms to adapt to changing environments. This view is, however, increasingly challenged by the observation of tremendous genetic flexibility and genome dynamics in several asexual fungi including *Fusarium oxysporum* (Rep and Kistler 2010; Ma et al. 2010) and *Verticillium dahliae* (de Jonge et al. 2013; Seidl and Thomma 2014).

Sex in fungi is complex and costly, as it involves many processes that are required to fulfil the different steps at cellular level (plasmogamy, karyogamy and meiosis) as well as the differentiation of the cell types and tissues that make up the fruiting body structure in which the sexual progeny develops (Idnurm 2011; Nelson and Metzenberg 1992). Yet, the advantages conferred by the capacity of sexual reproduction (maintenance of genetic diversity in the population, facilitating adaptation to adverse conditions) makes the costs affordable. Fungi have been attractive model systems for studies on sexual development because of the ease of cultivation, short generation times and large population sizes.

Fungi have evolved two sexual reproduction systems: heterothallism and homothallism. Fungi with a heterothallic sexual reproduction system require two partners of opposite mating type for mating to occur, whereas fungi with a homothallic reproduction system are able to self-fertilize, although they also remain capable of outcrossing (Ni et al. 2011). Whether a species is heterothallic or homothallic is determined by genes in the mating type (*MAT*) locus. In heterothallic fungi, isolates of opposite mating types have distinct, non-homologous alleles of the *MAT* locus, i.e. *MAT1-1* and *MAT1-2*, and the presence of both alleles in a single (dikaryotic) cell is required for sexual development to occur. By contrast, most homothallic fungi have a *MAT* locus in which all genes required for sexual development are present in a gene cluster, and it is the environment that determines whether or not the

fungus will start sexual development. Homothallic sexual reproduction is in fact similar to clonal reproduction which does not result in recombinant progeny. The advantage of such a reproduction system, however, might be the formation of ascospores which serve as survival structures or propagules for dispersal and infection of plants.

The mating type locus and its functions

The first description of the organization of the *MAT* locus in the genus *Botrytis* was from *B. cinerea* (Amselem et al. 2011). The two alleles of the *B. cinerea MAT* locus are designated as either *MAT1-1* or *MAT1-2*, and each is flanked by the *APN2* gene on the 5'-end and the *SLA2* gene on the 3'-end. The *MAT1-1* locus contains two genes: the *MAT1-1-1* gene encoding a protein with an alpha domain and the *MAT1-1-5* gene. The *MAT1-2* locus also contains two genes: the *MAT1-2-1* gene encoding a protein with a high mobility group domain and the *MAT1-2-4* gene. **Chapter 4** describes the organization and sequence of the *MAT* locus of *B. elliptica*. Both alleles of the *MAT* locus in *B. elliptica* are also flanked by the *APN2* gene and the *SLA2* gene, similar to *B. cinerea*. In addition the *MAT1-1* and *MAT1-2* loci of *B. elliptica* each contain the same two genes, orthologous to their counterparts in *B. cinerea*, in identical organization. *B. cinerea* and *B. elliptica* are distant taxa within the genus, clustering in different clades (Staats et al., 2005). If the organization of the *MAT* locus in these two species is representative for their respective clades, it suggests that the organization of the *MAT* loci is conserved in the genus. Amselem et al. (2011) suggested a scenario for the evolution of the heterothallic *MAT* locus in *B. cinerea* from an ancestral, homothallic locus by two inversion events and a deletion. This scenario might have occurred in the common ancestor of the genus and the locus organization was therefore retained in all *Botrytis* species.

In **Chapter 2**, functional analysis by targeted deletion showed that the genes in the *MAT* locus play different roles in sexual development of *B. cinerea*. The *MAT1-1-1* (alpha domain) and *MAT1-2-1* (HMG domain) genes are the key regulatory genes that control the initiation of sexual development in *B. cinerea*, while the *MAT1-1-5* and *MAT1-2-4* genes are essential to control the development of an apothecial disk. I propose that the orthologous genes in mating type loci of other *Botrytis* species have an identical function.

Chapter 5 describes a new *Botrytis* species, *B. deweyae* which appeared to be a sister taxon of *B. elliptica*. The *MAT1-1* and *MAT1-2* mating type alleles are present in the different strains of *B. deweyae* that were available. However, *B. deweyae* apothecia were never observed even though several trials of sexual crosses were performed. It appears that all *B. deweyae* strains used in this study were infertile under the tested conditions (**Chapter 5)**, which are routinely conducive for sexual reproduction in both *B. cinerea* and *B. elliptica* (**Chapters 2, 3 and 4**). Infertile strains are not only observed in *B. deweyae*, but also in *B. elliptica* (**Chapter 4**) and in *B. cinerea* (Van Der Vlugt-Bergmans et al. 1993). Different experimental approaches might be needed to produce apothecia and ascospores in *B. deweyae*. Firstly, more strains need to be tested; this would require more extensive sampling from *Hemerocallis* hybrids showing typical symptoms of 'spring sickness'. In fact, in this study only five strains were available of which one produced sclerotia, which, however, looked distinct from those of other *Botrytis* species. *B. deweyae* sclerotia had a lighter color, they did not dehydrate and shrink during long term cold storage, as is usually observed for sclerotia of other *Botrytis* species when they mature. As a consequence, the *B. deweyae* sclerotia were fragile and broke easily during manipulation in sexual crosses. It is important to obtain sclerotia that mature in a similar way as those those of other species. In addition to testing more strains, different media and temperature regimes need to be tested.

Hydrophobins and the rodlet layer

Hydrophobins are small secreted proteins present in almost all Ascomycota and Basidiomycota. Hydrophobins can be divided into Class I and Class II based on their properties (Wösten and Scholtmeijer 2015; Wösten 2001; Wessels 1994). Hydrophobins play different roles in fungi, either during development or the infection of host plants. Several studies have shown that hydrophobins are present in so-called rodlet layers (Zhang et al. 2011; Wösten 2001; Van Wetter et al. 2000; Talbot et al., 1996; Stringer and Timberlake 1995). In **Chapter 3** we demonstrate that *B. cinerea* hydrophobins are expressed mainly during sclerotium and apothecium development. In *Aspergillus nidulans,* a mutant lacking the hydrophobin gene *rodA* did not produce rodlet layers while a mutant lacking the *dewA* gene was not affected in rodlet layer formation (Stringer and Timberlake, 1994). Rodlet layer formation in *B. cinerea* has also been investigated in macroscopic structures of wild type and mutant strains in which one or several hydrophobin genes were deleted; a rodlet layer was

never observed, neither in wild type nor in any of the mutant strains. These findings are in agreement with earlier observations by Mosbach et al. (2011) and Doss et al. (1997). **Chapter 3** demonstrated that *B. cinerea* expresses hydrophobin genes to very high transcript levels during sclerotium and apothecium development. The aberrant surface morphology of hydrophobin mutants clearly demonstrated that the *B. cinerea* hydrophobins are important in conferring surface integrity in the wild type, apparently without the need of being deposited in a rodlet layer. We also provided the first evidence in Ascomycota fungi for the existence of a splice variant in a hydrophobin gene transcript. The *Bhp*1 gene produced two types of transcripts that differed by the presence of an additional stretch of 13 amino acid residues (including one cysteine residue) resulting from intron retention. Further study is required to investigate the biological functions of both hydrophobin variants in *B. cinerea*.

Transcriptome analysis of apothecium development

Fungi in the phylum Ascomycota produce different types of fruiting bodies: cleistothecia, perithecia, apothecia or pseudothecia. Until now, several studies have focused on investigating the mechanisms involved in ascocarp development, mainly in model species, such as *Neurospora crassa* (Nowrousian 2009)*, Aspergillus nidulans* (Dyer and O'Gorman 2012) and *Sordaria macrospora* (Teichert et al. 2012). Apothecia produced by *B. cinerea* are better suited for transcriptome analysis in ascoscarp development than Ascomycota species forming perithecia, cleistothecia or pseudothecia. This is due to the fact that different developmental stages of apothecia can be sampled more easily without being contaminated by mycelia or other somatic tissue than those of other ascocarps. In addition, the genome of *B. cinerea* is well assembled without gaps (van Kan et al., unpublished) which is not the case for many other fungi.

In earlier studies on gene expression in fungal ascocarp development, EST sequencing and microarray hybridization were used. Both methods have their limitations; the EST analysis generally has a low sequencing depth, whereas microarrays often provide low signals and only provide information about the genes present on the array. The quality of the data in earlier studies was also influenced by contamination of the ascocarp tissue with mycelium or other somatic tissue, especially in the young stages of development. Cleistothecia, perithecia and pseudothecia are small (< 500 µm for the mature ascocarp), and it is difficult to sample

clean ascocarp tissue (Teichert et al. 2012). In many studies such as those by Nelson et al. 1997; Qi et al. 2006; Hallen et al. 2007, ascocarps were sampled by removing or scraping developing structures from a solid agar plate. Teichert et al. (2012) used laser microdissection to excise *Sordaria macrospora* ascocarp tissue with minimal mycelial contamination, and used these samples for RNAseq analysis. They analyzed young perithecia (protoperithecia) that were grown on special membrane slides covered with a thin layer of agar. However, even by using laser microdissection, the ascocarps still contained small quantities of mycelium that grew across the fruiting bodies, as concluded from the observation that the data showed overlap of reads with data obtained from mycelia. In spite of the difficulties in obtaining clean RNAseq data from young perithecia by laser microdissection, the data obtained by RNAseq analysis were much better than those obtained by EST sequencing and microarray hybridization (Teichert et al., 2012).
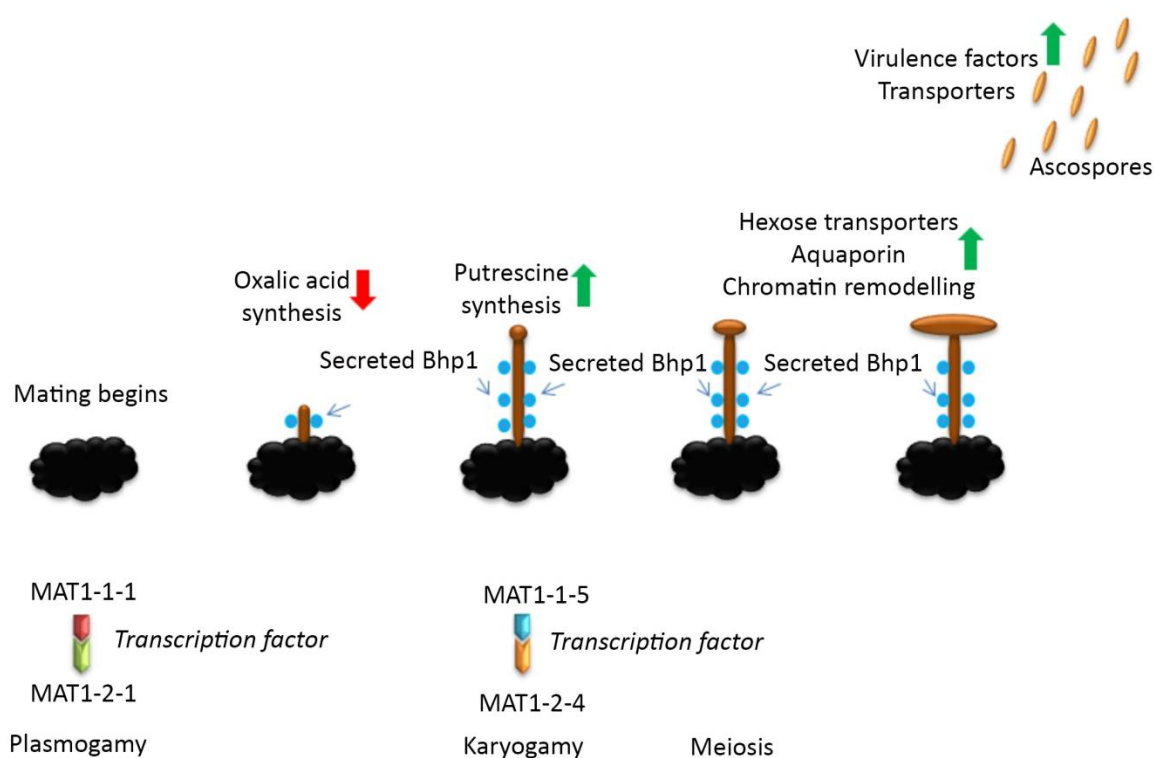
Figure 1: Schematic overview of processes occurring during apothecium development and the role of *MAT* genes. Red arrow indicates down-regulated genes, green arrows indicate up-regulated genes.

Chapter 2 describes the use of RNA sequencing to study the transcriptome during apothecium development of *B. cinerea*. The data were analysed in different ways. Differential expression analysis was used to examine the changes in gene expression

between two consecutive stages of apothecium development, while cluster analysis was used to identify the genes that were co-expressed at specific stages. The data provide detailed information on the transcriptional changes during apothecium development and on the requirement of *MAT* genes for this process. Figure 1 illustrates different stages of *B. cinerea* apothecium development and some of the physiological processes that occur based on transcriptional changes during these transitions. Firstly the initiation of sexual development requires plasmogamy between microconidia of the paternal parent and receptive cells within the sclerotium of the maternal parent, through a fertilization process that is poorly studied. Plasmogamy gives rise to dikaryotic cells that express both the *MAT1-1-1* gene (alpha domain) and *MAT1-2-1* gene (HMG domain). These MAT proteins likely dimerize to act as a transcriptional regulator that enables initiation of sexual development. Once the primordium of a stipe ruptures from the sclerotium, the hydrophobin gene *Bhp1* is very highly expressed and the secreted Bhp1 protein assembles at the outer surface during stipe elongation. The hydrophobin is continuously synthesized enabling to strengthen the elongating stipe until mature apothecia develop. During the early stages of stipe formation, polyketide synthase gene *BcPKS15* and the neighboring genes belonging to this cluster are specifically expressed but the bioactive polyketide that they produce is still unknown. In nature, a *B. cinerea* apothecium will develop in the top layer of soil in early spring. The polyketide produced by the *BcPKS15* gene cluster might function as a bioactive compound that protects a fruiting body from colonization by antagonistic bacteria and fungi or from predation by insects. Once stipe elongation is complete, the *MAT1-1-5* and *MAT1-2-4* genes produce a heterodimeric transcription factor which activates the genes that are important for apothecial disk development. At this stage the karyogamy process is likely to begin. During apothecial disk development, another (zinc finger) transcription factor will be activated, which might be under direct control of the MAT1-1-5/MAT1-2-4 transcription factor complex. Many of the genes that are expressed specifically in apothecial disks have no homologs outside the genus *Botrytis* or the family of *Sclerotiniaceae*, hence their function remains elusive. The main biological function of the apothecial disk is to produce asci loaded with ascospores. The data in **Chapter 2** present, to our knowledge, the first analysis of the transcriptome of ascospores ever. We observed a remarkable change in gene expression between the apothecial disks and the ascospores, with ~5000 genes being differentially expressed. Among the genes that were specifically expressed in ascospores, were several

genes encoding potential virulence factors such as pectinolytic enzymes, proteolytic enzymes, monosaccharide transporters and ABC transporters that might participate in the efflux of antimicrobial plant defense compounds. The ascospore transcriptome data clearly suggest that they are primed to infect host plants.

Dual mating behavior

In the early 1990s several studies reported that unusual mating behavior may occur in *B. cinerea* (Beever and Parkes 1993; Van Der Vlugt-Bergmans et al. 1993; Faretra et al. 1988). This unusual behavior is referred to as 'dual mater', and it describes a strain able to mate both with a partner of opposite mating type and a partner of similar mating type but unable to self-fertilize. Faretra et al. (1988) were the first to describe dual mater behavior in *B. cinerea*. In their study, 213 field strains were crossed with tester strains (SAS56 of the *MAT1-1* type and SAS405 of the *MAT1-2* type). Of the 213 field strains 187 behaved as heterothallics and 34 strains as dual maters (Faretra et al. 1988). van der Vlugt-Bergmans et al. (1993) crossed 8 strains isolated from tomato, rose or gerbera with the same tester strains, of which 5 strains behaved as heterothallics and 3 strains as dual maters. Finally, Beever and Parkes (1993) crossed the same tester strains with 50 field strains and found 41 strains to behave as heterothallics and 9 strains as dual maters. In further studies, Faretra and Pollastro (1996) showed that sexual crosses between two heterothallic strains could yield single ascospore progeny that behaved as dual maters, at a frequency of 6%. No further studies were performed to characterize the progeny from successful crosses from the dual mater strains that were described by Faretra et al., (1988), van der Vlugt-Bergmans et al., (1993) and Beever and Parkes (1993). From a cross between SAS56 (*MAT1-1*, Benomyl-sensitive, Vinclozolin-sensitive) and SAS405 (*MAT1-2*, Benomyl-resistant, Vinclozolin-resistant), performed by van der Vlugt-Bergmans et al. (1993), 81 progeny were sampled from one apothecium. I identified the mating type alleles of the 81 progeny by PCR and observed that they segregated normally (*MAT1-1* = 38, *MAT1-2* = 43). The progeny was tested for presence of fungicide resistance markers (Table 1), which are genetically unlinked (Faretra and Pollastro 1991). The segregation of fungicide resistance markers did not significantly deviate from a normal distribution.

Table 1: Segregation of fungicide resistance in the progeny of cross SAS56(*MAT1-1*) x SAS405 (*MAT1-2*).

	Vinclozolin-sensitive	Vinclozolin- resistant
Benomyl-sensitive	27 progeny (11 *MAT1-1*, 16 *MAT1-2*)	13 progeny (6 *MAT1-1*, 7 *MAT1-2*)
Benomyl-resistant	11 progeny (7 *MAT1-1*, 4 *MAT1-2*)	30 progeny (13 *MAT1-1*, 17 *MAT1-2*)

SAS56: Benomyl-sensitive and Vinclozolin-sensitive
SAS405: Benomyl-resistant and Vinclozolin- resistant

To identify dual mater strains in this progeny, each isolate of the 81 progeny was back-crossed to their parents SAS56 (*MAT1-1*) and SAS405 (*MAT1-2*), and self-fertilized. One single ascospore progeny isolate, named RS26 (carrying a *MAT1-2* allele), produced apothecia when sclerotia derived from RS26 were incubated in water under apothecium development-promoting conditions and was thus considered homothallic. A sibling from the same cross between SAS56 and SAS405, the isolate named RS11 (carrying a *MAT1-2* allele), was able to mate with both its parents, SAS56 and SAS405, but was not homothallic and was thus considered to show dual mater behavior. The sequences of *MAT1-2* alleles of RS26 and RS11 were identical to that of SAS405 (not shown).

I used a genetic approach to study the aberrant sexual behavior in isolates RS26 (homothallism with a *MAT1-2* allele) and RS11 (dual mating with a *MAT1-2* allele), assuming that these traits are controlled by a single Mendelian locus, and considering the following possible scenarios:

1. If homothallic strains produce an apothecium, ascospores are formed but there is clonal propagation because meiosis occurs between two identical genotypes. Progeny obtained from an apothecium produced by a homothallic strain should be identical to its parent.

2. If dual mating is genetically controlled by the *MAT* locus itself or by a different, closely linked locus, dual mating behavior should occur in half the progeny from a cross of a dual mater with any other strain. Furthermore, the dual mating behavior should co-segregate with the *MAT* allele derived from the dual mater parent.

3. Crossing RS11 with a different strain carrying a *MAT1-2* allele should result in progeny carrying exclusively *MAT1-2* alleles, of which half would behave as dual maters and the other half as normal heterothallic strains, only able to mate with *MAT1-1* strains).

4. If dual mating is genetically determined by a locus unlinked to the *MAT* locus, it should be possible to transmit the dual mating behavior from the genetic background of a *MAT1-2* strain into a *MAT1-1* strain, for example by back-crossing RS11 (*MAT1-2*) to its parent SAS56 (*MAT1-1*), and testing the progeny with a *MAT1-1* allele for dual mating behavior.

Figure 2 illustrates the experimental design that was used to study the dual mater behavior in *B. cinerea* and it summarizes the results obtained. Details of the experiments and the results are provided in the following paragraphs.
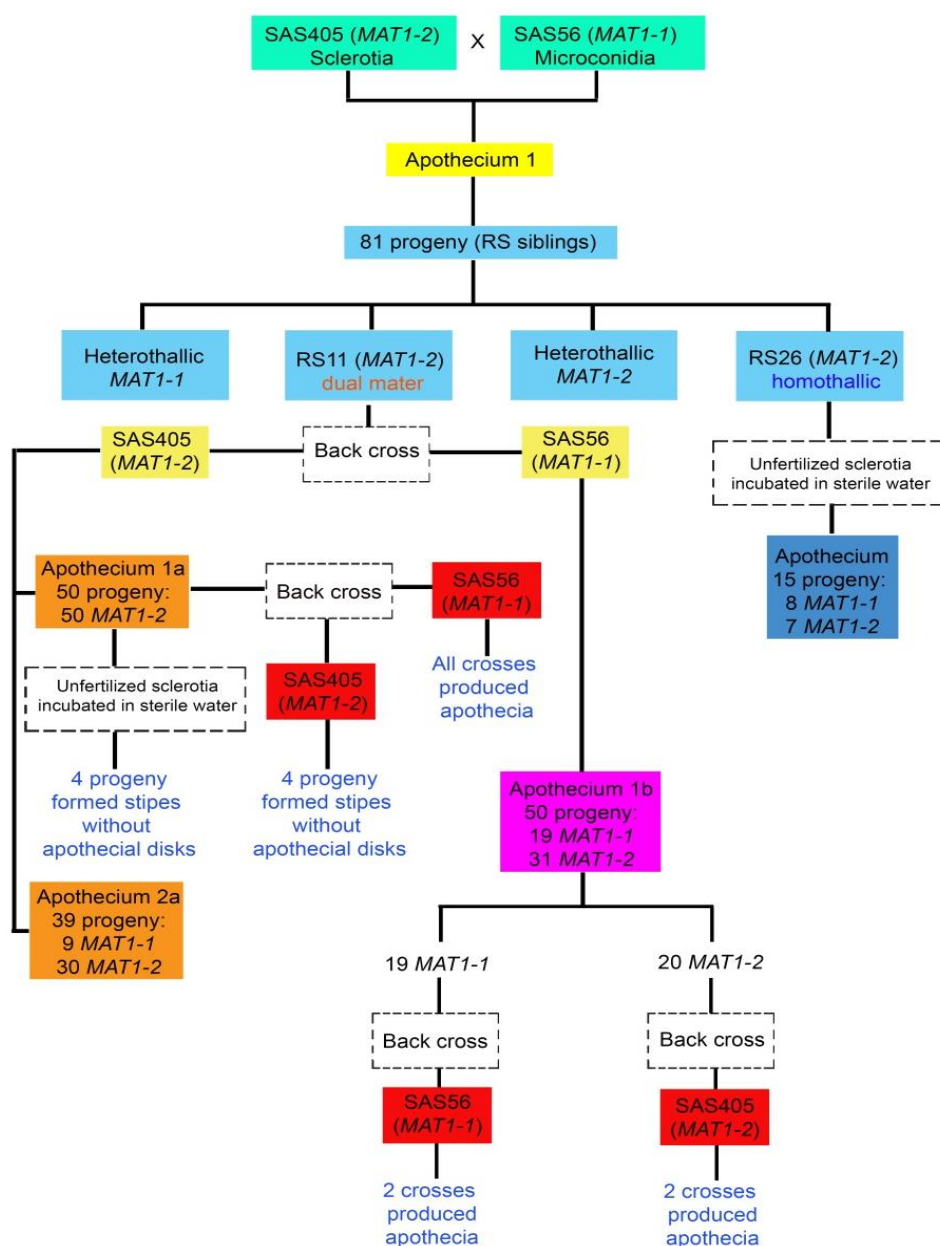
Figure 2: Schematic approach followed to study the genetics of dual mater behavior in *B. cinerea.* Details are explained in the text.

Self-fertilization of homothallic strain RS26 (carrying the *MAT1-2* allele) resulted in the production of apothecia, from which 15 single ascospore progeny were sampled and analysed for the segregation of fungicide resistance markers and *MAT* alleles (Table 2). All 15 progeny were resistant to both benomyl and vinclozolin, like their parent RS26, suggesting that they could have been derived from homothallic sexual reproduction. Remarkably, however, it appeared that eight of the 15 progeny contained a *MAT1-1* allele, while only seven carried a *MAT1-2* allele alike their parent RS26. Six out of the 15 progeny were also tested for the segregation of alleles of microsatellite markers developed for *B. cinerea* by Fournier et al. (2002). All progeny tested carried the parental RS26 alleles of markers BC1 (Figure 3), BC4 and BC10 (not shown), as was expected. For marker BC2, however, only one of the six progeny analyzed carried the parental allele, while the remaining 5 progeny carried an alternative allele (Figure 3).

Table 2: Segregation of *MAT* alleles and fungicide resistance in progeny of self-fertilized strain RS26 (*MAT1-2*).

	Mating types	Benomyl (10ug/ml)	Vinclozolin (5ug/ml)
RS26 (Parent)	*MAT1-2*	+	+
Progeny from selfing			
32-1	*MAT1-2*	+	+
32-2	*MAT1-2*	+	+
32-3	*MAT1-1*	+	+
32-4	*MAT1-2*	+	+
32-5	*MAT1-2*	+	+
32-6	*MAT1-1*	+	+
32-7	*MAT1-1*	+	+
32-8	*MAT1-1*	+	+
32-9	*MAT1-2*	+	+
32-10	*MAT1-2*	+	+
32-11	*MAT1-1*	+	+
32-12	*MAT1-1*	+	+
32-13	*MAT1-2*	+	+
32-14	*MAT1-1*	+	+
32-15	*MAT1-1*	+	+
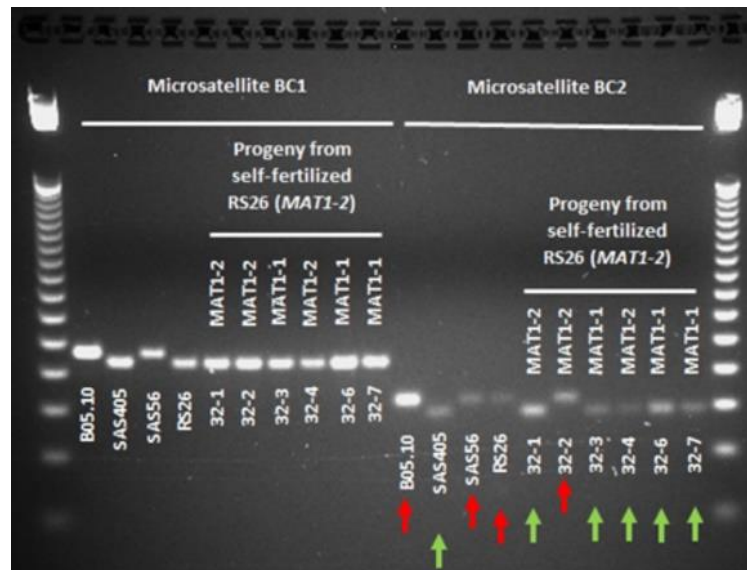
Figure 3: Segregation of microsatellite markers BC1 and BC2 (Fournier et al., 2002) in six progeny from homothallic strain RS26. Markers used are indicated at the top. Strains analyzed are the parental isolates B05.10, SAS405, SAS56, the homothallic strain RS26 and the progeny from self-fertilized RS26 (32-1 until 32-7), as indicated at the bottom of the lanes. All progeny tested have the same allele for microsatellite marker BC1 as their parent RS26. For marker BC2, progeny isolate 32-2 has the same allele as its parent RS26 and isolates B05.10 and SAS56 (indicated by red arrows), while the other five progeny have the same allele as isolate SAS405 (indicated by green arrows).

Based on the analysis of microsatellite markers (Figure 3), progeny produced from self-fertilization of RS26 probably resulted from contamination. Therefore, RS26 was excluded for further study.

The dual mater strain RS11 (carrying a MAT1-2 allele) is able to mate with both its parents SAS56 and SAS405 but is not homothallic. RS11 was sensitive to benomyl and resistant to vinclozolin, whereas its parents were either sensitive (SAS56) or resistant (SAS405) to both fungicides, thus validating that RS11 is a sexual recombinant of these two strains. However the alleles for six microsatellite markers (Fournier et al. 2002) in RS11 were all identical to the alleles of its parent SAS405, while RS11 contained none of the alleles derived from SAS56 (not shown).

Two separate apothecia were sampled from a cross between RS11 (*MAT1-2*) and SAS405 (*MAT1-2*) and a total of 50 (from apothecium 1a) and 39 (from apothecium 2a) progeny were sampled from these apothecia, respectively. All 50 progeny from apothecium 1a (Figure 2) possessed a *MAT1-2* allele. To analyse whether the progeny were sexual recombinants of these parents, the segregation of fungicide resistance markers in the progeny was analyzed (Table 3). The progeny were all sensitive to benomyl, even though parental strain SAS405 was resistant to benomyl. Also, half of the progeny was sensitive to vinclozolin although both parents were resistant to this fungicide. The results of fungicide resistance segregations were in disagreement with the phenotypes of the parents, and this observation could not be explained. When sclerotia from 30 of the 50 progeny from apothecium 1a were incubated in water under apothecium-inducing conditions, four progeny showed the emergence of apothecial stipes which, however, failed to develop into disks. When the same 30 progeny were tested in backcrosses to SAS56 and SAS405, all behaved as regular heterothallic strains.

In apothecium 2a from the same cross, it was observed that 9 out of 39 progeny carried a *MAT1-1* allele whereas both parents in this cross carried a *MAT1-2* allele (Figure 2). The presence of the *MAT1-1* allele in this progeny cannot be explained.

Table 3: Segregation of fungicide resistance in the progeny of cross RS11 (*MAT1-2*) x SAS405 (*MAT1-2*) sampled from apothecium 1a.

	Vinclozolin-sensitive	Vinclozolin- resistant
Benomyl-sensitive	26 progeny (all *MAT1-2*)	24 progeny (all *MAT1-2*)
Benomyl-resistant	0	0

RS11: Benomyl-sensitive and Vinclozolin-resistant
SAS405: Benomyl-resistant and Vinclozolin- resistant

Dual mater strain RS11 was also backcrossed to SAS56, in order to examine whether the dual mating behavior could be transmitted to a genotype with a *MAT1-1* allele (Figure 2). From apothecium 1b, I sampled 50 progeny and observed that 19 contained a *MAT1-1* allele and 31 a *MAT1-2* allele. To test for dual mating behavior of this progeny, all isolates with the *MAT1-1* allele were backcrossed to SAS56 and 20 isolates with the *MAT1-2* allele were

backcrossed to SAS405 (Figure 2). For both sets of backcrosses, two produced apothecia, suggesting that ~10% of the progeny in apothecium 1b behaved as dual maters.

Altogether, the results of the genetic analysis of dual mating behavior were puzzling. In some cases, results clearly indicated contamination, for example if a cross between two strains with identical *MAT* alleles yielded progeny with the opposite *MAT* allele. After the first indication of contamination, I took technical measures to reduce the chance of contamination in cultures and crosses. Even after taking such measures, some of the results remained difficult to interpret. It was impossible to reconstruct at which stage of the process the contamination might have occurred, over the five months period that is required for a cross to be completed. I decided not to include these data in an experimental chapter in the thesis but rather include them in the general discussion section.

Endophytic fungi with necrotrophic capability

Fungi are often classified into necrotrophs, hemi-biotrophs, biotrophs or endophytes based on their interaction with their host plant. Necrotrophs are pathogens obtaining nutrients by triggering programmed cell death in their host (Mengiste 2012). Biotrophs are pathogens that cause minimal damage to their host plant and disease symptoms usually occur as a result of nutrient depletion (Spoel et al. 2007; Glazebrook 2005; Hancock and Huisman 1981). Endophytic fungi colonize plant tissues without causing visible symptoms of disease or stress (Delaye et al. 2013; Rodriguez et al. 2009; Purahong and Hyde 2011), and endophytes are often considered to protect plants from drought, or attack by pathogens and pests, by their ability to produce antimicrobial secondary metabolites.

The 29 species described in the genus *Botrytis* are all considered to be necrotrophic pathogens, except for *B. deweyae,* which grows as an endophyte in *Hemerocallis* species and only under particular conditions can cause disease (**Chapter 5**). Fungi with such behavior are also referred to as "latent pathogens" (Hyde and Soytong 2008; Álvarez-Loayza et al. 2011; Eaton et al. 2011; Delaye et al. 2013). Other examples of endophytes known to be latent pathogens are *Phomopsis citri*, *Fusicoccum aesculi*, *Ladiodiplodia theobromae* (Wright 1998) and *Phomopsis viticola* (Mostert et al. 2000). There is no information on the mechanisms that control the switch in behavior from endophyte to pathogen. Sieber (2007) proposed

that endophytes have co-evolved with their hosts and can thus not be highly virulent, and symptoms are observed only very rarely and to a limited extent. The occasional pathogenic behavior of endophytes may be influenced by abiotic or biotic factors (Sieber 2007). Our observation that *B. deweyae* can grow as an endophyte inside *Hemerocallis* but may also cause very severe necrotic lesions on young leaves, leading to total destruction of the plant, argues against the hypothesis by Sieber (2007) that endophytes cannot be highly virulent. Further arguments against this hypothesis are provided by several reports that even *B. cinerea* (Barnes and Shaw, 2003; Sowley et al., 2010) is able to grow as an endophyte in host plants without causing disease symptoms and yet such isolates can be highly aggressive in infection experiments (Sowley et al., 2010; van Kan et al., unpublished observations). The capacity of *Botrytis* species to act as devastating necrotrophic pathogens, but also display an endophytic lifestyle suggests that the classification of fungi into pathogens or endophytes might need reconsideration. For a better understanding of the lifestyle of *B. deweyae,* analysis of its genome and its gene expression profile during endophytic and necrotrophic growth on *Hemerocallis* is needed. Studies on the endophytic fungus *Pestalotiopsis fici* using genomic and transcriptomic approaches revealed that the genome of *P. fici* contains up to 74 gene clusters related to secondary metabolite production, including 27 polyketide synthase genes (Wang et al. 2015). This number of secondary metabolite gene clusters is much higher as compared to *B. cinerea* and *Sclerotinia sclerotiorum* with a necrotrophic lifestyle (each ~40 secondary metabolite gene clusters) and to *Neurospora crassa* with a saprotrophic lifestyle (31 gene clusters). Many studies have revealed that endophytic fungi can be interesting resources for production of novel bioactive compounds (Li et al. 1996; Zou et al. 2000; Silva et al. 2005; Phongpaichit et al. 2007; Lösgen et al. 2007; Gu et al. 2007; Bérdy 2005). It will be interesting to study whether also *B. deweyae* contains more polyketide synthase genes than the 20 *PKS* genes present in *B. cinerea* (Kroken et al. 2003).

Perspectives

Fruiting bodies of fungi are attractive and useful for human beings, not only for their beauty or their nutritional value and culinary quality, they are also a source of natural products with beneficial properties. Metabolites from fungal fruiting bodies, or their chemical derivatives, are exploited as medicine or food additives. Many of these compounds are called "secondary metabolites". Genome sequences of fungi have revealed the enormous potential

of fungi to produce secondary metabolites, of which only some have been identified and chemically characterized. *Botrytis cinerea* is no exception to this rule: of the 43 putative secondary metabolite gene clusters, the products are identified for less than 10 of them. The polyketide produced in *B. cinerea* primordial stipes by the secondary metabolite gene cluster, including the *Bcpks15* gene is just one of the examples of unknown and unexplored metabolites with potentially interesting properties. Other examples of secondary metabolite gene clusters that are exclusively expressed in fungal fruiting bodies were reported in *Sordaria macrospora* (Nowrousian 2009; Schindler and Nowrousian 2014), and *Coprinopsis cinerea* (Plaza et al. 2014).

A different perspective of the insights into *B. cinerea* fruiting body development might be in disease control. *B. cinerea* apothecia have rarely been detected in the field, yet studies on the population genetics of *B. cinerea* (Giraud et al. 1997) have revealed that sexual reproduction occurs much more frequently than previously assumed. However, sexual reproduction not only maintains or increases genetic diversity, the sclerotia also act as overwintering structures and in early spring, ascospores act as propagules for dispersal and infection on newly emerging plant tissues. By understanding the mechanisms that control sexual development in *B. cinerea*, it might be feasible to identify a step in apothecium development as a target for control this ubiquitous, devastating pathogen.

References

Álvarez-Loayza P, White JF, Jr., Torres MS, Balslev H, Kristiansen T, Svenning J-C, Gil N (2011) Light Converts Endosymbiotic Fungus to Pathogen, Influencing Seedling Survival and Niche-Space Filling of a Common Tropical Tree, *Iriartea deltoidea*. PLoS ONE 6 (1):e16386.

Amselem J, Cuomo CA, van Kan JAL, Viaud M, Benito EP, Couloux A, Coutinho PM, de Vries RP, Dyer PS, Fillinger S, Fournier E, Gout L, Hahn M, Kohn L, Lapalu N, Plummer KM, Pradier J-M, Quévillon E, Sharon A, Simon A, ten Have A, Tudzynski B, Tudzynski P, Wincker P, Andrew M, Anthouard V, Beever RE, Beffa R, Benoit I, Bouzid O, Brault B, Chen Z, Choquer M, Collémare J, Cotton P, Danchin EG, Da Silva C, Gautier A, Giraud C, Giraud T, Gonzalez C, Grossetete S, Güldener U, Henrissat B, Howlett BJ, Kodira C, Kretschmer M, Lappartient A, Leroch M, Levis C, Mauceli E, Neuvéglise C, Oeser B, Pearson M, Poulain J, Poussereau N, Quesneville H, Rascle C, Schumacher J, Ségurens B, Sexton A, Silva E, Sirven C, Soanes DM, Talbot NJ, Templeton M, Yandava C, Yarden O, Zeng Q, Rollins JA, Lebrun M-H, Dickman M (2011) Genomic Analysis of the Necrotrophic Fungal Pathogens *Sclerotinia sclerotiorum* and *Botrytis cinerea*. PLoS Genetics 7 (8):e1002230.

Barnes SE, Shaw ME (2003) Infection of commercial hybrid *Primula* seed by *Botrytis cinerea* and latent disease spread through the plants. Phytopathology 93: 573–578.

Beever RE, Parkes SL (1993) Mating behaviour and genetics of fungicide resistance of *Botrytis cinerea* in New Zealand. New Zealand Journal of Crop and Horticultural Science 21 (4):303-310.

Bérdy J (2005) Bioactive microbial metabolites, a personal view. Journal of Antibiotics 58 (1):1-26

de Jonge R, Bolton MD, Kombrink A, van den Berg GCM, Yadeta KA, Thomma BPHJ (2013) Extensive chromosomal reshuffling drives evolution of virulence in an asexual pathogen. Genome Research 23 (8):1271-1282.

Delaye L, García-Guzmán G, Heil M (2013) Endophytes versus biotrophic and necrotrophic pathogens—are fungal lifestyles evolutionarily stable traits? Fungal Diversity 60 (1):125-135.

Doss RP, Christian JK, Potter SW, Soeldner AH, Chastagner GA (1997) The conidial surface of *Botrytis cinerea* and several other *Botrytis* species. Canadian Journal of Botany 75 (4):612-617.

Dyer PS, O'Gorman CM (2012) Sexual development and cryptic sexuality in fungi: insights from *Aspergillus* species. FEMS Microbiology Reviews 36 (1):165-192.

Eaton CJ, Cox MP, Scott B (2011) What triggers grass endophytes to switch from mutualism to pathogenism? Plant Science 180 (2):190-195.

Faretra F, Antonacci E, Pollastro S (1988) Sexual behaviour and mating system of *Botryotinia fuckeliana*, teleomorph of *Botrytis cinerea*. Journal of General Microbiology 134 (9):2543-2550.

Faretra F, Pollastro S (1991) Genetic basis of resistance to benzimidazole and dicarboximide fungicides in *Botryotinia fuckeliana* (*Botrytis cinerea*). Mycological Research 95 (8):943-951.

Faretra F, Pollastro S (1996) Genetic studies of the phytopathogenic fungus *Botryotinia fuckeliana* (*Botrytis cinerea*) by analysis of ordered tetrads. Mycological Research 100 (5):620-624.

Fournier E, Giraud T, Loiseau A, Vautrin D, Estoup A, Solignac M, Cornuet JM, Brygoo Y (2002) Characterization of nine polymorphic microsatellite loci in the fungus *Botrytis cinerea* (Ascomycota). Molecular Ecology (3):253-255.

Giraud T, Fortini D, Levis C, Leroux P, Brygoo Y (1997) RFLP markers show genetic recombination in *Botryotinia fuckeliana* (*Botrytis cinerea*) and transposable elements reveal two sympatric species. Molecular Biology and Evolution 14 (11):1177-1185.

Glazebrook J (2005) Contrasting mechanisms of defense against biotrophic and necrotrophic pathogens. Annual Review of Phytopathology 43 (1):205-227.

Gu W, Ge H, Song Y, Ding H, Zhu H, Zhao X, Tan R (2007) Cytotoxic benzo [j] fluoranthene metabolites from Hypoxylon truncatum IFB-18, an endophyte of Artemisia annua. Journal of Natural Products 70 (1):114-117.

Hallen HE, Huebner M, Shiu S-H, Güldener U, Trail F (2007) Gene expression shifts during perithecium development in *Gibberella zeae* (anamorph *Fusarium graminearum*), with particular emphasis on ion transport proteins. Fungal Genetics and Biology 44 (11):1146-1156.

Hancock JG, Huisman OC (1981) Nutrient movement in host-pathogen systems. Annual Review of Phytopathology 19 (1):309-331.

Idnurm A (2011) Sex determination in the first-described sexual fungus. Eukaryotic Cell 10 (11):1485-1491

Kroken S, Glass NL, Taylor JW, Yoder O, Turgeon BG (2003) Phylogenomic analysis of type I polyketide synthase genes in pathogenic and saprobic ascomycetes. Proceedings of the National Academy of Sciences 100 (26):15670-15675.

Li J-y, Strobel G, Sidhu R, Hess W, Ford EJ (1996) Endophytic taxol-producing fungi from bald cypress, *Taxodium distichum*. Microbiology 142 (8):2223-2226.

Lösgen S, Schlörke O, Meindl K, Herbst-Irmer R, Zeeck A (2007) Structure and biosynthesis of chaetocyclinones, new polyketides produced by an endosymbiotic fungus. European Journal of Organic Chemistry 2007 (13):2191-2196.

Ma L-J, van der Does HC, Borkovich KA, Coleman JJ, Daboussi M-J, Di Pietro A, Dufresne M, Freitag M, Grabherr M, Henrissat B, Houterman PM, Kang S, Shim W-B, Woloshuk C, Xie X, Xu J-R, Antoniw J, Baker SE, Bluhm BH, Breakspear A, Brown DW, Butchko RAE, Chapman S, Coulson R, Coutinho PM, Danchin EGJ, Diener A, Gale LR, Gardiner DM, Goff S, Hammond-Kosack KE, Hilburn K, Hua-Van A, Jonkers W, Kazan K, Kodira CD, Koehrsen M, Kumar L, Lee Y-H, Li L, Manners JM, Miranda-Saavedra D, Mukherjee M, Park G, Park J, Park S-Y, Proctor RH, Regev A, Ruiz-Roldan MC, Sain D, Sakthikumar S, Sykes S, Schwartz DC, Turgeon BG, Wapinski I, Yoder O, Young S, Zeng Q, Zhou S, Galagan J, Cuomo CA, Kistler HC, Rep M (2010) Comparative genomics reveals mobile pathogenicity chromosomes in *Fusarium*. Nature 464 (7287):367-373.

Mengiste T (2012) Plant Immunity to Necrotrophs. Annual Review of Phytopathology 50 (1):267-294.

Mosbach A, Leroch M, Mendgen K, Hahn M (2011) Lack of evidence for a role of hydrophobins in conferring surface hydrophobicity to conidia and hyphae of *Botrytis cinerea*. BMC Microbiology 11 (1):10

Mostert L, Crous P, Petrini O (2000) Endophytic fungi associated with shoots and leaves of Vitis vinifera, with specific reference to the *Phomopsis viticola* complex. Sydowia 52 (1):46-58.

Nelson MA, Kang S, Braun EL, Crawford ME, Dolan PL, Leonard PM, Mitchell J, Armijo AM, Bean L, Blueyes E, Cushing T, Errett A, Fleharty M, Gorman M, Judson K, Miller R, Ortega J, Pavlova I, Perea J, Todisco S, Trujillo R, Valentine J, Wells A, Werner-Washburne M, Yazzie S, Natvig DO (1997) Expressed sequences from conidial, mycelial, and sexual stages of *Neurospora crassa*. Fungal Genetics and Biology 21 (3):348-363.

Nelson MA, Metzenberg RL (1992) Sexual development genes of *Neurospora crassa*. Genetics 132 (1):149-162.

Ni M, Feretzaki M, Sun S, Wang X, Heitman J (2011) Sex in fungi. Annual Review of Genetics 45:405.

Nowrousian M (2009) A novel polyketide biosynthesis gene cluster is involved in fruiting body morphogenesis in the filamentous fungi *Sordaria macrospora* and *Neurospora crassa*. Current Genetics 55 (2):185-198.

Phongpaichit S, Nikom J, Rungjindamai N, Sakayaroj J, Hutadilok-Towatana N, Rukachaisirikul V, Kirtikara K (2007) Biological activities of extracts from endophytic fungi isolated from *Garcinia* plants. FEMS Immunology & Medical Microbiology 51 (3):517-525.

Plaza D, Lin C-W, van der Velden NS, Aebi M, Kunzler M (2014) Comparative transcriptomics of the model mushroom *Coprinopsis cinerea* reveals tissue-specific armories and a conserved circuitry for sexual development. BMC Genomics 15 (1):492

Purahong W, Hyde K (2011) Effects of fungal endophytes on grass and non-grass litter decomposition rates. Fungal Diversity 47 (1):1-7.

Qi W, Kwon C, Trail F (2006) Microarray analysis of transcript accumulation during perithecium development in the filamentous fungus *Gibberella zeae* (anamorph *Fusarium graminearum*). Molecular Genetics and Genomics 276 (1):87-100.

Rep M, Kistler HC (2010) The genomic organization of plant pathogenicity in *Fusarium* species. Current Opinion in Plant Biology 13 (4):420-426.

Rodriguez RJ, White Jr JF, Arnold AE, Redman RS (2009) Fungal endophytes: diversity and functional roles. New Phytologist 182 (2):314-330.

Schindler D, Nowrousian M (2014) The polyketide synthase gene pks4 is essential for sexual development and regulates fruiting body morphology in *Sordaria macrospora*. Fungal Genetics and Biology 68:48-59.

Seidl MF, Thomma BPHJ (2014) Sex or no sex: Evolutionary adaptation occurs regardless. BioEssays 36 (4):335-345.

Sieber TN (2007) Endophytic fungi in forest trees: are they mutualists? Fungal Biology Reviews 21:75-89.

Silva GH, Teles HL, Trevisan HC, Bolzani VdS, Young M, Pfenning LH, Eberlin MN, Haddad R, Costa-Neto CM, Araújo ÂR (2005) New bioactive metabolites produced by *Phomopsis cassiae*, an endophytic fungus in *Cassia spectabilis*. Journal of the Brazilian Chemical Society 16:1463-1466.

Sowley ENK, Dewey FM, Shaw MW (2010) Persistent, symptomless, systemic and seed-borne infection of lettuce by *Botrytis cinerea.* European Journal of Plant Pathology 126: 61–71.

Spoel SH, Johnson JS, Dong X (2007) Regulation of tradeoffs between plant defenses against pathogens with different lifestyles. Proceedings of the National Academy of Sciences 104 (47):18842-18847.

Staats M, van Baarlen, P, van Kan JAL (2005) Molecular phylogeny of the plant pathogenic genus *Botrytis* and the evolution of host specificity. Molecular Biology and Evolution 22: 333–346.

Stringer MA, Timberlake WE (1994) dewA encodes a fungal hydrophobin component of the *Aspergillus* spore wall. Molecular Microbiology 16 (1):33-44.

Talbot NJ, Kershaw MJ, Wakley GE, De Vries O, Wessels J, Hamer JE (1996) MPG1 encodes a fungal hydrophobin involved in surface interactions during Infection-related development of *Magnaporthe grisea*. The Plant Cell 8 (6):985-999.

Teichert I, Wolff G, Kück U, Nowrousian M (2012) Combining laser microdissection and RNA-seq to chart the transcriptional landscape of fungal development. BMC Genomics 13 (1):511

van Der Vlugt-Bergmans CJB, Brandwagt BF, Vant't Klooster JW, Wagemakers CAM, van Kan JAL (1993) Genetic variation and segregation of DNA polymorphisms in *Botrytis cinerea*. Mycological Research 97 (10):1193-1200.

van Wetter MA, Wösten HAB, Wessels JGH (2000) SC3 and SC4 hydrophobins have distinct roles in formation of aerial structures in dikaryons of *Schizophyllum commune*. Molecular Microbiology 36 (1):201-210.

Wang X, Zhang X, Liu L, Xiang M, Wang W, Sun X, Che Y, Guo L, Liu G, Guo L (2015) Genomic and transcriptomic analysis of the endophytic fungus *Pestalotiopsis fici* reveals its lifestyle and high potential for synthesis of natural products. BMC Genomics 16 (1):28

Wessels J (1994) Developmental regulation of fungal cell wall formation. Annual Review of Phytopathology 32 (1):413-437.

Wösten HAB, Scholtmeijer K (2015) Applications of hydrophobins: current state and perspectives. Applied Microbiology and Biotechnology:1-11.

Wösten HAB (2001) Hydrophobins: multipurpose proteins. Annual Reviews in Microbiology 55 (1):625-646.

Wright JG (1998) The role of endophytes in citrus stem end rots. PhD Thesis.

Zhang S, Xia YX, Kim B, Keyhani NO (2011) Two hydrophobins are involved in fungal spore coat rodlet layer assembly and each play distinct roles in surface interactions, development and pathogenesis in the entomopathogenic fungus, *Beauveria bassiana*. Molecular Microbiology 80(3):811-26.

Zou W, Meng J, Lu H, Chen G, Shi G, Zhang T, Tan R (2000) Metabolites of *Colletotrichum gloeosporioides*, an endophytic fungus in *Artemisia mongolica*. Journal of Natural Products 63 (11):1529-1530.

Summary

The genus *Botrytis* comprises 29 species, predominantly necrotrophic pathogens that infect a single host plant species with two exceptions: *Botrytis cinerea,* which can infect more than 200 host plants, and *Botrytis pseudocinerea* which causes disease on several unrelated host plants.

Chapter 1 introduces the genus *Botrytis*, its molecular phylogeny and its asexual and sexual stages, followed by a description of the organization and function of mating type loci in *Ascomycota* and an outline of the thesis.

Chapter 2 describes a genome-wide expression analysis of apothecium development in *B. cinerea* and the function of mating type genes in this process. First, the transcript levels of *B. cinerea* orthologs of *Aspergillus nidulans* and *Sordaria macrospora* genes known to be involved in sexual development were examined. Secondly, differential expression analysis was performed to compare transcriptional changes occurring at distinct stages of apothecium development. Thirdly, cluster analysis identified genes that were co-expressed in specific stages, particularly in sclerotia, three developmental stages of apothecia and mature ascospores. Functional analyses by targeted knockout mutagenesis revealed that the *MAT1-1-1* gene and the *MAT1-2-1* gene are both required for the initiation of sexual development. Deletion mutants in either of these genes failed to produce any sexual structures. Deletion of the *MAT1-1-5* gene or the *MAT1-2-4* gene resulted in normal development of stipes which, however, were defective in the formation of an apothecial disk, asci and ascospores. In addition, comparative gene expression profiling was performed for a *MAT1-1-5* deficient mutant blocked at the transition from stipes to apothecial disk formation and wild type apothecial disks.

Chapter 3 describes possible roles of hydrophobin genes in development of *B. cinerea,* especially in sclerotia and apothecia. The *Bhp1*, *Bhp2* and *Bhp3* genes are required for both sclerotium and apothecium development. Deletion of *Bhp1* and *Bhp3* affected the surface hydrophobicity of sclerotia, while deletion of *Bhp1* and *Bhp2* affected apothecium development. The DNA proportion and RNA expression of hydrophobin genes in apothecia was quantified to determine the proportion of maternal and paternal contribution to

apothecium tissue. Nearly 99% of the apothecial tissue appeared to be derived from the maternal parent.

Chapter 4 describes the mating type gene organization in *B. elliptica*, which is highly similar to that in *B. cinerea*. The *B. elliptica MAT1-1* locus contains the *MAT1-1-1* gene and the *MAT1-1-5* gene, whereas the *MAT1-2* locus contains the *MAT1-2-1* gene and the *MAT1-2*-4 gene. Apothecia were developed from a cross that was set up between a *MAT1-1* and a *MAT1-2* strain, which proved that *B. elliptica* is a heterothallic species. Mature apothecia developed approximately three months after fertilization. Ascospores were infectious on lily leaves and able to induce necrotic symptoms two days after inoculation.

Chapter 5 describes *Botrytis deweyae,* a novel species that can grow as an endophyte in cultivated *Hemerocallis* hybrids, but in certain conditions can cause disease referred to as 'spring sickness'. Between 2009 and 2012, *B. deweyae* isolates were collected from several *Hemerocallis* hybrids in the greenhouse. The morphology of *B. deweyae* is described. Molecular phylogenetic analyses based on three housekeeping genes and two virulence genes revealed that *B. deweyae* is closely related to the lily pathogen *B. elliptica.* Infection experiments confirmed that *B. deweyae* is able to cause necrosis on *Hemerocallis* leaves.

Chapter 6 discusses the results presented in this thesis. A model of processes and mechanisms involved in apothecium development is proposed. A detailed discussion of the phenomenon known as dual mating behavior in *B. cinerea* is also provided.

Acknowledgements

10 September 2011 marked my life as I began my journey to the Netherlands to pursue my dream in obtaining a PhD degree. After four years of studying, researching and working, I finally succeeded in completing my PhD. During these years, there were many people that contributed to my success in completing this journey, hence I would like to convey my gratitude to them here.

To my parents, who brought me to this world and nurtured me, Mak and Opak, this success is for you. Your unconditional love for me kept me on track and inspired me. For my late father who is no longer here to share this moment, I know your prayers are always with me.

My sincere gratitude goes to my supervisor and co-promotor, Dr Jan van Kan. Thank you so much for accepting me to be your PhD student. You provided an excellent supervision and guidance for me. I appreciated your suggestions and critics on the research. With your assistance, I managed to complete my experiments on time. Thank you for your time and patience in reading my manuscripts, correcting grammar and sentences until they became a complete thesis. Thank you for letting me attend conferences abroad. It is still fresh in my mind: the first conference I attend with you in Lyon although I had just arrived in Netherlands. I gained so much from all the conferences that we attend together like in Bari and Asilomar, when you introduced me to the Botrytis community around the world and other scientists. Thank you for training me to be an expert in sexual development of Botrytis especially in seting up crosses for Botrytis. I really enjoyed sharing the knowledge and experiments with others during the conferences. With so many opportunities you gave me, I have no more words to portray my gratitude towards you except you are the most wonderful supervisor I ever had.

I would like to extend my gratitude towards my promotor Prof Pierre de Wit for all the useful discussions on my PhD progress and for critical comments on my thesis writing and propositions.

I am thankful to Prof Matthias Hahn (University of Kaiserslautern Germany) for providing mutant strains for my experiments, and for the discussions and suggestions for my hydrophobin experimental chapter.

Jimmy, Ya-Fen, the Teo sisters, Siew Ling, Loo Wee the potlucks, makan-makan, talking and watching football together all brought laughter and relieved our longing for Malaysia . Together with all of you, we created a little Malaysia here. And for my best friends, Zul and Sham in Cardiff, thank you for sharing ideas and motivation.

I am thankful to my siblings and my in-laws family for all the support they gave me during all these years.

Finally I am grateful towards my family my wife the most important person in my life Norazilah Burhanudin and my cat Mimi who always be there for me. Thank you for your support, the idea, patience and endless love. Thank you for making my dream come true.

Curriculum Vitae

Razak Bin Terhem was born on the 25th of May 1985 in Sarawak Malaysia. He started his Bsc study in Forestry in the Universiti Putra Malaysia in 2006. His Bsc thesis was entitled Sexual development of *Dinoderus minutus*. In 2009, he continued with his MSc study in Plant Protection at the University of Queensland Australia. For his MSc thesis, he did research on Sexual development of *Cochliobolus* species and fungal flora on palm trees under the supervision of Dr Roger G Shivas and Dr Elizabeth Aitken. In September 2011, he started his PhD project entitled Sexual development of *Botrytis* species in the Laboratory of Pytopathology at Wageningen University, under the supervision of Dr. Jan van Kan and Prof. Pierre de Wit. Starting 1st of October 2015 he is a Lecturer at the Faculty of Forestry, Universiti Putra Malaysia.

Razak bin Terhem

Department of

Forest Management,

Faculty of Forestry,

Universiti Putra Malaysia,

43400 Serdang Selangor,
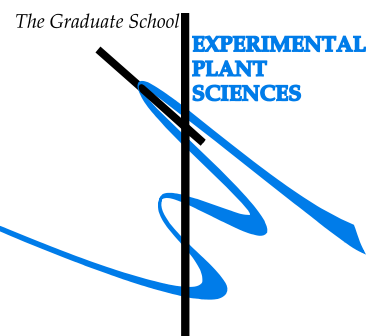
Malaysia.

razakterhem@upm.edu.my

List of publications

Terhem RB, van Kan JAL (2014) Functional analysis of hydrophobin genes in sexual development of *Botrytis cinerea*. Fungal Genetics and Biology 71:42-51.

Grant-Downton RT, **Terhem RB**, Kapralov MV, Mehdi S, Rodriguez-Enriquez MJ, Gurr SJ, van Kan JAL, Dewey FM (2014) A Novel *Botrytis* Species Is Associated with a Newly Emergent Foliar Disease in Cultivated *Hemerocallis*. PLoS ONE 9 (6):e89272.

Hyde K, Nilsson RH, Alias SA, Ariyawansa H, Blair J, Cai L, de Cock AAM, Dissanayake A, Glockling S, Goonasekara I, Gorczak M, Hahn M, Jayawardena R, van Kan JL, Laurence M, Lévesque CA, Li X, Liu J-K, Maharachchikumbura SN, Manamgoda D, Martin F, McKenzie EC, McTaggart A, Mortimer P, Nair PR, Pawłowska J, Rintoul T, Shivas R, Spies CJ, Summerell B, Taylor PJ, **Terhem R**, Udayanga D, Vaghefi N, Walther G, Wilk M, Wrzosek M, Xu J-C, Yan J, Zhou N (2014) One stop shop: backbones tree for important phytopathogenic genera: I (2014). Fungal Diversity 67 (1):21-125.

Terhem R, Staats M, van Kan JL (2015) Mating type and sexual fruiting body of *Botrytis elliptica*, the causal agent of fire blight in lily. European Journal of Plant Pathology: 142: 615-624.

Terhem RB, Rodenburg YA, Stassen JHM, van Kan JAL. Transcriptome and functional analysis of fruiting body development in *Botrytis cinerea*- in preparation.

Education Statement of the Graduate School

Experimental Plant Sciences

Issued to:	**Razak Bin Terhem**
Date:	**14 September 2015**
Group:	**Laboaratory of Phytopathology**
University:	**Wageningen University & Research Centre**

1) Start-up phase	*date*
► **First presentation of your project**	
Sexual development of Botrytis species	Jun 22, 2012
► **Writing or rewriting a project proposal**	
Sexual development of Botrytis species	Nov 2012
► **Writing a review or book chapter**	
► **MSc courses**	
► **Laboratory use of isotopes**	

	Subtotal Start-up Phase	*7.5 credits**

2) Scientific Exposure	*date*
► **EPS PhD Student Days**	
EPS PhD Student days, University of Amsterdam	Feb 10, 2012
EPS PhD Student days, Get 2 Gether Stay Okay, Soest	Jan 29-30, 2015
► **EPS Theme Symposia**	
EPS Theme 2 symposium 'Interactions between Plants and Biotic Agents, Wageningen University	Feb 10, 2012
EPS Theme 2 symposium 'Biointeractions between Plants and Biotic Agents, Utrecht University	Feb 10, 2015
► **NWO Lunteren days and other National Platforms**	
NWO-ALW meeting 'Experimental Plant Sciences', Lunteren, The Netherlands	Apr 01-02, 2012
ALW Platform Molecular Genetics Annual Meeting, Lunteren, The Netherlands	Oct 04-05, 2012
NWO-ALW meeting 'Experimental Plant Sciences', Lunteren, The Netherlands	Apr 22-23, 2013
ALW Platform Molecular Genetics Annual Meeting, Lunteren, The Netherlands	Oct 09-10, 2014
► **Seminars (series), workshops and symposia**	
Dr. Duncan Grieg (Wees Seminar)	Jun 21, 2012
Prof. Dr. Ralph Panstruga Comparative pathogenomics of powdery mildew fungi: chasing the molecular secrets of obligate biotrophy and fungal pathogenesis	Dec 04, 2012
Prof. Tom Mitchell-olds, Biology Department, Duke Univeristy, Durham North Carolina, USA., Strong selection on the genes controlling complex traits in complex enviroments	Dec 10, 2012
Prof. Dr Howard Judelson, Universiy of California, Riverside USA	May 07, 2013
Dr. Rays H.Y. Jiang, Harvard School of Public Health, Boston MA USA	May 07, 2013
Theo van der Lee and Miriam Kooman, The use of Next generation sequencing in diagnostics and detection of plant pathogens	Feb 11, 2014
Dr. Jeroen Mesters, From protein solution to single crystal X-ray diffraction: Chitin binding by LysM domains at atomic resolution	Mar 31, 2014
Dr. Pierre Rouzé, VIB, Gent, The many novel mobile introns in green algae : is intron invasion really an old story ?	May 12, 2014

►	**Seminar plus**	
►	**International symposia and congresses**	
	Botrytis-Sclerotinia Post-genome Workshop, Lyon, France	Sep 15-17, 2011
	XVI International Botrytis Symposium, Bari Italy	Jun 23-28, 2013
	XI International Fungal Biology Conference Karlhsruhe Germany	Sep 29-Oct 03, 2013
	12th European Conference on Fungal Genetics, Seville Spain	Mar 23- 27, 2014
	EPS PhD Retreat, University of Amsterdam	Jul 01-04, 2014
	The 10th International Mycological Congress, Bangkok,Thailand	Aug 03-08, 2014
►	**Presentations**	
	NWO-ALW meeting 'Experimental Plant Sciences', Lunteren, The Netherlands (poster)	Apr 22-23, 2013
	XVI International Botrytis Symposium, Bari Italy (talk and poster)	Jun 23-28, 2013
	XI International Fungal Biology Conference Karlhsruhe Germany (poster)	Sep 29-Oct 03, 2013
	12th European Conference on Fungal Genetics, Seville Spain (poster)	Mar 23-27, 2014
	The 10th International Mycological Congress, Bangkok,Thailand (talk)	Aug 03-08, 2014
	ALW Platform Molecular Genetics Annual Meeting, Lunteren, The Netherlands (talk)	Oct 09-10, 2014
►	**IAB interview**	
	Meeting with a member of the International Advisory Board of EPS	Sep 29, 2014
►	**Excursions**	
	Subtotal Scientific Exposure	*19.5 credits**

3) In-Depth Studies		*date*
►	**EPS courses or other PhD courses**	
	Host-Microbe Interactomics, Wageningen University, The Netherlands	Nov 01-02, 2011
	Phyto Path Trainning, European Bioinformatic Hixton Cambridge UK	Sep 19-20, 2012
	The power of RNA Seq, Wageningen University Netherlands	Jun 05-07, 2013
	Bioinformatic- User's Approach, Wageningen University Netherlands	Aug 26-30, 2103
►	**Journal club**	
►	**Individual research training**	
	Subtotal In-Depth Studies	*3.9 credits**

4) Personal development		*date*
►	**Skill training courses**	
	Interpersonal Communication for PhD Students (ICPS), Wageningen University	Dec 12-13, 2011
	Data Management, Wageningen University	Feb 24, 2014
	Voice Matters - Voice and Presentation , Wageningen University	Apr 01 & 15, 2014
	Techniques for Writing and Presenting a Scientific Paper (TWP), Wageningen University	Apr 07,08,10 and 11, 2014
	Information Literacy including EndNote Introduction (ILP), Wageningen University	Feb 17-18, 2015
►	**Organisation of PhD students day, course or conference**	
►	**Membership of Board, Committee or PhD council**	
	Subtotal Personal Development	*3.2 credits**

TOTAL NUMBER OF CREDIT POINTS*	**34.1**

Herewith the Graduate School declares that the PhD candidate has complied with the educational requirements set by the Educational Committee of EPS which comprises of a minimum total of 30 ECTS credits

* A credit represents a normative study load of 28 hours of study.